

INFORMATION TO USERS

This manuscript has been reproduced from the microfilm master. UMI films the text directly from the original or copy submitted. Thus, some thesis and dissertation copies are in typewriter face, while others may be from any type of computer printer.

The quality of this reproduction is dependent upon the quality of the copy submitted. Broken or indistinct print, colored or poor quality illustrations and photographs, print bleedthrough, substandard margins, and improper alignment can adversely affect reproduction.

In the unlikely event that the author did not send UMI a complete manuscript and there are missing pages, these will be noted. Also, if unauthorized copyright material had to be removed, a note will indicate the deletion.

Oversize materials (e.g., maps, drawings, charts) are reproduced by sectioning the original, beginning at the upper left-hand corner and continuing from left to right in equal sections with small overlaps. Each original is also photographed in one exposure and is included in reduced form at the back of the book.

Photographs included in the original manuscript have been reproduced xerographically in this copy. Higher quality 6" x 9" black and white photographic prints are available for any photographs or illustrations appearing in this copy for an additional charge. Contact UMI directly to order.

UMI

A Bell & Howell Information Company
300 North Zeeb Road, Ann Arbor MI 48106-1346 USA
313/761-4700 800/521-0600



UNIVERSITY OF OKLAHOMA
GRADUATE COLLEGE

**Impurity Scattering in a Two-Dimensional
Electron Gas Subject to a Perpendicular
Magnetic Field**

A Dissertation
SUBMITTED TO THE GRADUATE FACULTY
in partial fulfillment of the requirements for the
degree of
Doctor of Philosophy

By
J. Timothy Kwiatkowski
Norman, Oklahoma
1998

UMI Number: 9914397

Copyright 1998 by
Kwiatkowski, John Timothy

All rights reserved.

UMI Microform 9914397
Copyright 1999, by UMI Company. All rights reserved.

This microform edition is protected against unauthorized
copying under Title 17, United States Code.

UMI
300 North Zeeb Road
Ann Arbor, MI 48103

© by J. Timothy Kwiatkowski 1998
All Rights Reserved.

Impurity Scattering in a Two-Dimensional Electron Gas Subject to a Perpendicular Magnetic Field

A Dissertation APPROVED FOR THE
Department of Physics

By

David A. Chen
Pat M. C
Robert A. Ferguson
Walter J. ...
...

Dedication

This work is dedicated to my grandfather, Alfred Kershaw and my mother, Carolyn Kwiatkowski, without whom I would not have the ability or motivation to look out upon this universe with such wonder.

The years of anxious searching in the dark, with their intense longing, their alternations of confidence and exhaustion and the final emergence into light -- only those who have experienced it can understand it. -- Albert Einstein

Acknowledgements

As this work has spanned what seems like a lifetime, it is difficult to enumerate all who have made some contribution to this work. Yet, I will try to acknowledge those in recent memory.

I would first like to thank my advisor, Dr. Bruce Mason, for putting up with my idiosyncrasies and faults through this whole process. He has given me the guidance and the insight into many-body theory which was needed to address this task.

I would also like to thank Dr. John Furneaux, for directing me down this path in the first place. His interest in the correlation of Shubnikov-de Haas oscillations with other experimental observations certainly paved the way for this work.

My work with Dr. Chuck Hembree has definitely influenced this work as well. He also played a profound role in luring me back into the world of scientific computing.

In a more general sense, I would like to thank Dr. Jack Cohn and Dr. Ron Kantowski for their excellent discussions and for being excellent instructors.

Dr. Lakshmiarahan provided me with the background in large scale scientific computing which proved invaluable in the completion of this research.

Last, I would like to thank my wife Gayla for the motivation and the confidence she has provided me. I would also like thank Anthony and Acacia Kohn who give me inspiration and hope for the next generation.

Contents

Dedication	iv
Acknowledgements	v
List Of Figures	ix
Abstract	xii
1 Introduction	1
1.1 GaAs/GaAlAs Heterostructures	3
1.2 The Basics	4
1.3 Moving Forward	7
2 The Green's Function Approach	8
2.1 Impurity Scattering	8
2.2 The Meaning of $G_N(E)$	13
2.3 Combining $G_N(E)$ with Impurity Scattering	19
3 Standard Methods for Calculating the Density of States	24
3.1 The Self Consistent Born Approach	24
3.2 The Single-Site Approximation	29
3.3 The Many-Site Approximation	31
4 The Models and Approximations	33
4.1 Our First Model	34
4.2 The Second Model	40
4.3 The Inclusion of Electron Spin	44
5 Living a Non-Static World	46
5.1 What's Wrong With Static?	46
5.2 The Non-static Polarizability	47
5.3 Magneto-plasmons	48
5.4 Our Very Own Non-static Model	50

6	The Calculations	57
6.1	Design Decisions	57
6.2	Numerical Techniques	58
6.3	Convergence	59
6.4	Dynamic	61
6.5	Calculation Times	62
7	The Results	63
7.1	A Road Map for the Discussion of the Results	63
7.2	The Statically Screened Models	64
7.3	Including Electron-Electron Effects	81
8	Conclusions	103
8.1	Conclusions	103
8.2	Extensions and Enhancements	104
Appendix A		
	The Electron in a Magnetic Field	106
A.1	Landau Gauge	106
A.2	Symmetric Gauge	109
Appendix B		
	The Matrix Elements	117
B.1	Calculation of the Matrix Elements	117
B.2	A Look at $\delta^*(q - p)$	119
Appendix C		
	Feynman Diagrams for a 2DEG in a Magnetic Field	122
Appendix D		
	Hermite Polynomials and Their Integrals	124
Appendix E		
	Kramers-Krönig and $\Pi(\omega, q)$	130
Appendix F		
	Calculating the Fourier Potential	133
F.1	Proof of the Bessel function identity	134
F.2	The second integral	135
Appendix G		
	Program Listings	138
G.1	besselj0.f90	138
G.2	besstab.f90	141

G.3	bigw.f90	142
G.4	chempot.f90	144
G.5	densos.f90	146
G.6	findener.f90	147
G.7	findwidth.f90	149
G.8	fourpot.f90	151
G.9	geneps.f90	153
G.10	greens.f90	158
G.11	greens2.f90	161
G.12	jelem.f90	164
G.13	laguerre.f90	167
G.14	llcouple.f90	169
G.15	main.f90	171
G.16	melem.f90	184
G.17	mix.f90	185
G.18	pmix.f90	186
G.19	polarize.f90	187
G.20	refineef.f90	189
G.21	scondo_consts.f90	192
G.22	scondo_control.f90	193
G.23	scondo_interfaces.f90	194
G.24	scondo_spin.f90	201
G.25	selfe_corr.f90	202
G.26	selfener.f90	209
G.27	selfener2.f90	213
G.28	taconst.f90	217
G.29	vertpol.f90	219
G.30	Makefile	222
G.31	runparam.in	224

List Of Figures

7.1	The density of states in terms of the individual Landau Levels as output from the basic model without spin and without the vertex correction. ($a = 50\text{\AA}$)	65
7.2	As we get many closely spaced levels the individual levels begin to take on an almost Lorentzian shape. Here we have calculate 20 spin degenerate levels and filling factor $\nu = 35$)	66
7.3	The density of states and the Fermi energy plotted as a function of magnetic field.	68
7.4	The Landau Level widths vs. magnetic field without the vertex correction or spin included in the calculation.	69
7.5	The Landau Level widths vs. Landau Level index.	70
7.6	The Landau Level widths vs. mobility for $\nu = 6$ without the vertex correction.	71
7.7	The Landau Level widths vs. mobility for $\nu = 7$ without the vertex correction.	71
7.8	The Landau Level widths vs. the impurity plane distance a	73
7.9	A comparison of the density of states with and without the vertex correction at $\nu = 35$. ($\mu = 200.000$)	74
7.10	A comparison of the static polarizability with and without the vertex correction at $\nu = 35$. ($\mu = 200.000$)	74
7.11	A comparison of the static polarizability with and without the vertex correction at $\nu = 35$ at a lower mobility. ($\mu = 100.000$)	75
7.12	A comparison of the density of states with and without the vertex correction at $\nu = 4$	76
7.13	A comparison of the static polarizability with and without the vertex correction at $\nu = 4$	76
7.14	A comparison of the density of states with and without the vertex correction at $\nu = 5$	77
7.15	A comparison of the static polarizability with and without the vertex correction at $\nu = 5$	77
7.16	The Landau Level widths vs. mobility for $\nu = 6$ with the vertex correction.	79

7.17	The Landau Level widths vs. mobility for $\nu = 7$ with the vertex correction.	79
7.18	The density of states for the non-vertex model with and without spin plotted as a function of magnetic field.	80
7.19	$\text{Im}\frac{1}{\epsilon(q,E)}$ as calculated from the Green's functions resulting from the static impurity model. ($N_s = 2 \times 10^{11} \text{cm}^{-2}$, $\mu = 100,000 \text{cm}^2/\text{V}\cdot\text{s}$, $T = 4.2\text{K}$, $a = 50\text{\AA}$, $B = 1.378\text{T}$)	82
7.20	A comparison between the output of the static and non-static models. Here the Fermi Energies have been aligned at $E = 0$	83
7.21	The individual contributions of the Landau levels to the density of states in the non-static model.	84
7.22	The dielectric response for our system with 12 calculated Landau levels. ($N_s = 2 \times 10^{11} \text{cm}^{-2}$, $T = 4.2\text{K}$, $\mu = 50,000 \text{cm}^2/\text{V}\cdot\text{s}$, $a = 50\text{\AA}$, $B = 0.390\text{T}$)	86
7.23	By identifying the peaks in the response functions, we see that this result is consistent with the zero field plasmon theory. ($N_s = 2 \times 10^{11} \text{cm}^{-2}$, $T = 4.2\text{K}$, $\mu = 50,000 \text{cm}^2/\text{V}\cdot\text{s}$, $a = 50\text{\AA}$, $B = 0.390\text{T}$)	87
7.24	Increasing the mobility produces well defined levels in the density of states. Here all Fermi Energies are aligned at $E = 0$	88
7.25	The density of states plotted for different electron sheet densities. (Again all Fermi energies are aligned at $E = 0$.)	89
7.26	The dielectric response function for $N_s = 2 \times 10^{11} \text{cm}^{-2}$, $T = 4.2\text{K}$, $\mu = 10,000 \text{cm}^2/\text{V}\cdot\text{s}$, $a = 50\text{\AA}$, $B = 0.390\text{T}$	90
7.27	The dielectric response function for $N_s = 2 \times 10^{11} \text{cm}^{-2}$, $T = 4.2\text{K}$, $\mu = 30,000 \text{cm}^2/\text{V}\cdot\text{s}$, $a = 50\text{\AA}$, $B = 0.390\text{T}$	91
7.28	The dielectric response function for $N_s = 2 \times 10^{11} \text{cm}^{-2}$, $T = 4.2\text{K}$, $\mu = 80,000 \text{cm}^2/\text{V}\cdot\text{s}$, $a = 50\text{\AA}$, $B = 0.390\text{T}$	92
7.29	The dielectric response function for $N_s = 2 \times 10^{11} \text{cm}^{-2}$, $T = 4.2\text{K}$, $\mu = 100,000 \text{cm}^2/\text{V}\cdot\text{s}$, $a = 50\text{\AA}$, $B = 0.390\text{T}$	93
7.30	The dielectric response function for $N_s = 1 \times 10^{11} \text{cm}^{-2}$, $T = 4.2\text{K}$, $\mu = 50,000 \text{cm}^2/\text{V}\cdot\text{s}$, $a = 50\text{\AA}$, $B = 0.195\text{T}$	94
7.31	The dielectric response function for $N_s = 4 \times 10^{11} \text{cm}^{-2}$, $T = 4.2\text{K}$, $\mu = 50,000 \text{cm}^2/\text{V}\cdot\text{s}$, $a = 50\text{\AA}$, $B = 0.780\text{T}$	95
7.32	The density of states at $\nu = 3$. ($N_s = 2 \times 10^{11} \text{cm}^{-2}$, $\mu = 50,000 \text{cm}^2/\text{V}\cdot\text{s}$, $T = 4.2\text{K}$, $a = 50\text{\AA}$, $B = 2.757\text{T}$)	97
7.33	The density of states at $\nu = 6$. ($N_s = 2 \times 10^{11} \text{cm}^{-2}$, $\mu = 50,000 \text{cm}^2/\text{V}\cdot\text{s}$, $T = 4.2\text{K}$, $a = 50\text{\AA}$, $B = 1.378\text{T}$)	98
7.34	The dielectric response function at $\nu = 3$. ($N_s = 2 \times 10^{11} \text{cm}^{-2}$, $T = 4.2\text{K}$, $\mu = 50,000 \text{cm}^2/\text{V}\cdot\text{s}$, $a = 50\text{\AA}$, $B = 1.378\text{T}$)	99
7.35	The dielectric response function at $\nu = 6$. ($N_s = 2 \times 10^{11} \text{cm}^{-2}$, $\mu = 50,000 \text{cm}^2/\text{V}\cdot\text{s}$, $T = 4.2\text{K}$, $a = 50\text{\AA}$, $B = 2.757\text{T}$)	100

7.36	The density of states at $\nu = \frac{3}{2}$. ($N_s = 2 \times 10^{11} \text{cm}^{-2}$, $\mu = 50,000 \text{cm}^2/\text{Vs}$, $T = 4.2 \text{K}$, $a = 50 \text{\AA}$, $B = 5.514 \text{T}$)	101
7.37	The dielectric response function at $\nu = \frac{3}{2}$. ($N_s = 2 \times 10^{11} \text{cm}^{-2}$, $\mu = 50,000 \text{cm}^2/\text{Vs}$, $T = 4.2 \text{K}$, $a = 50 \text{\AA}$, $B = 5.514 \text{T}$)	102

Abstract

We have calculated the Landau level (projected) Green's functions and the density of states of a two-dimensional electron gas in a perpendicular magnetic field as effected by impurity scattering using several different approximations. The material parameters which we choose correspond to GaAs/GaAlAs heterostructures. At the simplest level we include the effects of Landau level mixing. An approximation to the vertex correction is then added to the calculation, and the results are compared. Finally we add the electron-electron interaction to the model in place of the vertex correction. In all cases, the electron spin is considered. We find that the vertex correction over-compensates for the screening and yields unreasonable results. In addition, we find the dynamic electron-electron screening to be a dominant factor in determining the properties of the system and bridges the gap between low and high magnetic field behavior.

Chapter 1

Introduction

The goal of this work is to examine the energy states of a perfect two-dimensional electron gas (2DEG) in a perpendicular magnetic field as they are affected by an external potential provided by "impurities". The results presented here are the results of several numerical models all of which would not be realistically possible to solve without the aid of large computers.

Why study this type of system in the first place? We live in a three dimensional houses, eat three dimensional food, and wear three dimensional clothes. The truth is we also live in a world of constraints. There are forces which for the most part limit our movement to a quasi-two dimensional space. Gravity constrains our movement more or less to the surface of the earth. Strangely enough, we also live in a quantum mechanical world where energies have strangely discrete values. (It is just that these values are so closely spaced that we can not usually discern them from one another so that we think that we live in a continuum.)

The key to this is quantum confinement. In the system we wish to study, electrons are constrained to move in a two dimensional space which is provided by quantum effects. So we can effectively produce a two dimensional electron gas. We will be studying semi-conductor devices in which this is the case although other systems such as liquid Helium interfaces offer this same quantum confinement.

It was postulated by Shrieffer in 1957 that the electrons confined in the inversion layer of a MOS structure (Metal Oxide Semiconductor) would not behave classically. However, if the interface between the two materials is not "smooth" enough, the scattering from the interface would mask the quantum effect. The quantum signature

was not seen until the work of Fowler, Fang, Howard, and Stiles (1966) via magneto-conductance measurements. Subsequently, much of the early experimental work in this area was performed using silicon MOSFETs (Metal Oxide Semiconductor Field Effect Transistors.) Later, engineering processes produced better and better samples as driven by the electronics industry. Other similar systems were studied using newer more promising materials (for ever faster electronic devices.) Processes such as MBE (Molecular Beam Epitaxy) and MOVCD (Metal Organic Chemical Vapor Deposition) produced clean devices with controllable doping parameters and sharp interfaces. Several of the III-V semiconductors are very closely lattice matched and provide a rich field of study.

We will be primarily interested in the Gallium Arsenide/Aluminum Gallium Arsenide (GaAs/AlGaAs) heterostructures. Growth processes are such that this system may be fabricated so that the interface is very nearly atomically smooth between the two extremely pure materials. In addition, there are several aspects of the silicon MOSFET that we wish to ignore such as the valley degeneracy of silicon. Gallium arsenide is a direct gap semi-conductor with a conduction band which is virtually parabolic at low energy or temperature. This will allow us to approximate the system as a perfect 2DEG. The only differences which are meaningful to our model between a perfect 2DEG and the real world GaAs/AlGaAs are the effective electron mass, the dielectric constant and the effective Landé g -factor. (i.e. some slightly modified physical constants.) Since we can't live in a perfect world, we will throw in some "impurities" to model the dopants of the material which provide the extra electrons in the conduction band. Yet, we will limit them to an infinitely thin sheet parallel to the 2DEG. We could account for a more realistic distribution of impurities which varies over a finite region in the third dimension by multiplying by the appropriate form factor or by explicitly integrating the potential over the distribution along the z axis. This adds unneeded computational complexity and does not significantly affect the results.

1.1 GaAs/GaAlAs Heterostructures

Before we continue with our theoretical description of the perfect two dimensional electron gas, let us stop and look a bit closer at the properties of the physical system which we are using as the basis for this model.

Typically some material from the fourth row of the periodic table is added to the material with the wider band gap (GaAlAs) to provide extra electrons which will accumulate at the interface. It is typical to use silicon. The GaAs is left undoped. This layer of electrons forms a *quasi*-2DEG which is confined by the sharp potential well formed at the discontinuity. Typically these electron donors are separated from the interface by an undoped GaAlAs “spacer” layer in order to reduce the scattering effects in the interface. Subsequently carrier mobilities of up to $15 \times 10^6 \text{cm}^2/\text{Vs}$ can be achieved at liquid helium temperatures. It is in these materials that the Integer Quantum Hall Effect (IQHE) and particularly the Fractional Quantum Hall Effect (FQHE) have been studied.

As such, this is not strictly a 2DEG but rather a *quasi*-2DEG since typically more than one bound state exists in the potential well. However, due to the sharp narrow triangular shape, there are typically two or three widely spaced states. If we are careful not to over-fill the lowest of these energy levels (“subbands”) and maintain low temperatures, then we will find that the system does behave much like a true 2DEG.

Such effects (IQHE and FQHE) provided the original motivation of this work which was to correlate the low magnetic field Shubnikov-deHaas oscillations to the observed properties in the high magnetic field IQHE and FQHE regime. Extracting information from these magneto-resistance measurements lead to a detailed interest into the form of the density of states (DOS) of this 2DEG. As such we will concentrate on the form of the DOS in this system. However, we will additionally talk about the enhanced Landé g-factor and the magneto-plasmon response functions as they apply to this system.

1.2 The Basics

We will be studying specifically the system where a magnetic field is applied perpendicularly to the interface. Classically this is the electron in a magnetic field problem where the electron feels the force given by:

$$\vec{F} = \frac{e}{c} \vec{v} \times \vec{B} \quad (1.1)$$

in Gaussian units where we have $\vec{B} = B\hat{z}$. The electron obeys Newton's Law such that we have:

$$\dot{v}_x = \frac{eB}{mc} v_y \quad (1.2)$$

$$\dot{v}_y = -\frac{eB}{mc} v_x \quad (1.3)$$

where we have ignored the z direction. The solution to this set of equations is a circular orbit with angular frequency

$$\omega_c = \frac{eB}{mc} \quad (1.4)$$

where m is the mass of the electron. B is the magnetic field in Gauss. e is the electron charge in esu's and c is the speed of light in cm/s^2 . This is the characteristic frequency of the system. (The cyclotron energy in GaAs $\approx 0.17meV/T$.)

In the quantum case this system is described by the Hamiltonian:

$$H = \frac{1}{2m} \left(\hat{p} + \frac{e}{c} \vec{A} \right)^2 \quad (1.5)$$

where \vec{A} is the vector potential such that

$$\nabla \times \vec{A} = \vec{B} \quad (1.6)$$

It turns out that the vector potential is not unique. There are two common choices. The first is the "Landau Gauge" which has

$$\vec{A} = Bx\hat{y} \quad (1.7)$$

and the second is the “symmetric gauge” where

$$\vec{A} = \frac{B}{2}(-y\hat{x} + x\hat{y}) \quad (1.8)$$

They each yield the same physical result as we should hope. Each has its advantages for different calculations. The Landau gauge as we have written it will end up quantizing the y-momentum of the electron while the symmetric gauge will quantize the z component of the angular momentum. Therefore they each yield a set of basis wavefunctions which may be translated in to the other. For the most part we will be using the Landau gauge in our discussion unless we wish to make use of the cylindrical symmetry of the symmetric gauge.

The quantum mechanical view of this system is essentially the same as the classical in that the characteristic frequency of the system is still ω_c . The solution to the the wave equation gives us the result that the energies are quantized by

$$E_n = (n + \frac{1}{2})\hbar\omega_c, \quad \text{where } n = 0. 1. 2. 3. \dots \quad (1.9)$$

with the wavefunctions

$$\psi_{N,p} = (L\pi^{\frac{1}{2}}2^N N!l)^{-\frac{1}{2}} H_N(x/l - pl)e^{-\frac{x/l - pl}{2}} e^{ipq} \quad (1.10)$$

in the Landau gauge. L is the length of the sample (using periodic boundary conditions). $l = \sqrt{\frac{\hbar}{eB}} = \sqrt{\frac{\hbar c}{eB}}$ is the “magnetic length” and p are the quantized y-momententa given by

$$p = \frac{2\pi\nu}{L}, \quad \text{where } \nu = 1. 2. 3. 4. \dots \quad (1.11)$$

and the $H_N(x)$ are the Hermite polynomials. In the symmetric gauge the wave functions are given by:

$$\phi_{N,m} = \left(\frac{N!}{2\pi l^2 (N+m)!} \right)^{\frac{1}{2}} \left(\frac{r^2}{2l^2} \right)^{\frac{m}{2}} L_N^m \left(\frac{r^2}{2l^2} \right) e^{-\frac{r^2}{4l^2}} e^{-im\theta} \quad (1.12)$$

where $m \geq 0$ is an integer which represents the quantization of the z-component of the angular momentum and the $L_Y^m(x)$ are generalized Laguerre polynomials. Both of these results are calculated in Appendix A.

In a large system of non-interacting electrons the density of states of this system would be a series of large delta function spikes. Each of these “Landau levels” will contain a density of electrons for each spin given by the Landau degeneracy

$$g_L = \frac{1}{2\pi l^2} \quad (1.13)$$

This is a massively degenerate system as $\frac{q_L}{B} \approx 2.418 \times 10^{10} \text{cm}^{-2} \text{T}^{-1}$. This relation may be obtained most easily from (1.10) by considering a finite width of the sample. W . If we use the fact that $x/l - pl \geq 0$ we can obtain an expression as follows:

$$\begin{aligned} W/l - p_{max}l &= 0 \\ \frac{p_{max}}{W} &= \frac{1}{l^2} \\ g_L &= \frac{\nu_{max}}{W L} = \frac{1}{2\pi l^2} \end{aligned} \quad (1.14)$$

since $\frac{\nu_{max}}{W L}$ simply describes the maximum density of the Landau level.

Of course in a real system the electrons are interacting with each other and any external potentials. Under these conditions, each of these Landau levels will broaden to a finite width. Then we can consider that the conductivity of the 2DEG is going to be proportional to the density of states at the Fermi Energy. If we then perform an experiment where we measure the conductivity (or the resistivity) of the sample we will find that the conductivity oscillates as the magnetic field is increased due to the increasing Landau level degeneracy which alters the number of occupied Landau Levels. These oscillations are called “Shubnikov-de Haas” oscillations and are clearly observed. There is actually much more to the calculation of the conductivities of the 2DEG, but the essential features do correlate directly with the shape of the density of states.

1.3 Moving Forward

With some of the basics in hand, we are about to move into the world of many body Green's function techniques. Before, we embark on this journey, let us state exactly what we will be doing.

We are going to treat our system as a perfect two-dimensional electron gas with a magnetic field applied perpendicularly to the electron sheet. The electrons will scatter from impurities which are in a plane parallel to the 2DEG separated by a distance, a . We are going to assume that the impurities are singly charged, randomly distributed with a two dimensional density, N_i , and interact with the electrons via the Coulomb force. Since we are targeting our model toward GaAs/AlGaAs heterostructures with a parabolic band structure, we will be using the effective mass approximation with $m^* = 0.067m_e$. Additionally, the dielectric constant for the bare material will be taken as $\kappa = 12.8$ and the effective Landé g -factor will be taken as $g^* = -0.44$.

With some of these details out of the way, let us make a small disclaimer before attacking the Green's function techniques. Making sense of the discussions on this topic in the journals can be very frustrating if one wants to keep track of the details. Since a relatively small group of researchers is working on this topic, there seems to be a general understanding of the basic assumptions and formulations by this small group. We will *attempt* to remedy a bit of this. Obviously, a comprehensive treatment of Green's functions techniques cannot be covered here. Therefore, we assume that the audience is somewhat familiar with these techniques or at least has access to the basic texts [17, 13, 14] on this subject. Now, let us proceed.

Chapter 2

The Green's Function Approach

2.1 Impurity Scattering

Starting with the Hamiltonian:

$$H = \psi^\dagger \hat{h}_0 \psi + \sum_i^{N_i} \psi^\dagger V(\vec{r} - \vec{R}_i) \psi \quad (2.1)$$

where h_0 is the Hamiltonian for the non-interacting electron and the corresponding Green's function as given by the expansion in terms of the unperturbed Green's functions $G_0(\vec{r}_2, t_2; \vec{r}_1, t_1)$:

$$\begin{aligned} G(\vec{r}_2, t_2; \vec{r}_1, t_1) &= G_0(\vec{r}_2, t_2; \vec{r}_1, t_1) \\ &+ \int d\vec{r}'_1 dt'_1 G_0(\vec{r}_2, t_2; \vec{r}'_1, t'_1) U(\vec{r}'_1) G_0(\vec{r}'_1, t'_1; \vec{r}_1, t_1) \\ &+ \dots \end{aligned} \quad (2.2)$$

we will look at the formal concepts of impurity scattering.

For brevity, let us write this expansion in the form

$$\begin{aligned} G(1, 2) &= G_0(1, 2) + \int d1' G_0(1, 1') U(1') G(1', 2) \\ &+ \int d1' d2' G_0(1, 1') U(1') G(1', 2') U(2') G(2', 2) + \dots \end{aligned} \quad (2.3)$$

where we have used the notation $1'$ to represent the particle's position, \vec{r}'_1 , and time, t'_1 .

Since the arrangement of the impurities will be different in every sample and many measurements such as transport measurements give averaged properties, what we are truly interested in is the average of the Green's function over all possible impurity distributions. Now, exactly what do we mean by "averaging over all possible impurity distributions?" We shall define it as:

$$\langle f\{R_i\}\rangle_I = \frac{1}{\mathcal{V}^{N_i}} \int d\vec{R}_1 \dots d\vec{R}_{N_i} f\{\vec{R}_i\} \quad (2.4)$$

where \mathcal{V} is the dimensional volume of the sample. (This would actually be an area in a two dimensional system.) Using this definition, we will now continue to look at the impurity average of the Greens' function.

$$\begin{aligned} \langle G(2,1)\rangle_I &= G_0(1,2) + \langle \int d1' G_0(2,1') U(1') G(1',1)\rangle_I \\ &+ \langle \int d1' d2' G_0(1,1') U(1') G(1',2') U(2') G(2',2)\rangle_I \\ &+ \dots \end{aligned}$$

Since G_0 is independent of the impurities we see that

$$\langle G_0(1,2)\rangle_I = G_0(1,2) \quad (2.5)$$

so that we have

$$\begin{aligned} \langle G(1,2)\rangle_I &= \langle G_0(1,2)\rangle_I \\ &+ \int d1' G_0(1,1') G_0(1',2) \langle U(1')\rangle_I \\ &+ \int d1' d2' G_0(1,1') G_0(1',2') G_0(2',2) \langle U(1') U(2')\rangle_I \\ &+ \dots \end{aligned} \quad (2.6)$$

So now we only have to deal with terms of the form $\langle U(1')\rangle_I$, $\langle U(1') U(2')\rangle_I$, etc. Now, the first of these averages is given by:

$$\langle U(1')\rangle_I = \frac{1}{\mathcal{V}^{N_i}} \int d\vec{R}_1 \dots d\vec{R}_{N_i} \sum_i^{N_i} V(\vec{r}_1 - \vec{R}_i) \quad (2.7)$$

In order to make this more manageable we will expand the potentials in terms of their Fourier transforms as:

$$\begin{aligned}
\langle U(1') \rangle_I &= \frac{1}{\mathcal{V}^{N_i}} \int d\vec{R}_1 \dots d\vec{R}_{N_i} \sum_i \int \frac{d\vec{k}_1}{(2\pi)^3} v(\vec{k}_1) e^{-i\vec{k}_1 \cdot (\vec{r}'_1 - \vec{R}_i)} \quad (2.8) \\
&= \int \frac{d\vec{k}_1}{(2\pi)^3} v(\vec{k}_1) \sum_i \frac{1}{\mathcal{V}^{N_i}} \int d\vec{R}_1 \dots d\vec{R}_{N_i} e^{-i\vec{k}_1 \cdot (\vec{r}'_1 - \vec{R}_i)} \\
&= \frac{1}{\mathcal{V}} \int \frac{d\vec{k}_1}{(2\pi)^3} v(\vec{k}_1) \sum_i \delta(\vec{k}_1) e^{-i\vec{k}_1 \cdot \vec{r}'_1} \\
&= \frac{N_i}{\mathcal{V}(2\pi)^3} v(0) = \frac{n_i}{(2\pi)^3} v(0)
\end{aligned}$$

This first term is just proportional to the spatial average of $V(\vec{r})$. Since the average is just a constant energy offset, we can adjust the potential so that $v(0) = 0$ and therefore $\langle U(1') \rangle_I = 0$. We will see that this greatly simplifies our calculation.

Continuing, our next major contribution then comes from $\langle U(1')U(2') \rangle_I$. Again we shall write the potentials in terms of their Fourier transforms to obtain:

$$\begin{aligned}
\langle U(1')U(2') \rangle_I &= \frac{1}{\mathcal{V}^{N_i}} \int d\vec{R}_1 \dots d\vec{R}_{N_i} \quad (2.9) \\
&\quad \times \sum_{i,j} V(\vec{r}'_1 - \vec{R}_i) V(\vec{r}'_2 - \vec{R}_j) \\
&= \frac{1}{\mathcal{V}^{N_i}} \int d\vec{R}_1 \dots d\vec{R}_{N_i} \sum_i \int \frac{d\vec{k}_1}{(2\pi)^3} \frac{d\vec{k}_2}{(2\pi)^3} \\
&\quad \times v(\vec{k}_1) v(\vec{k}_2) e^{-i\vec{k}_1 \cdot (\vec{r}'_1 - \vec{R}_i)} e^{-i\vec{k}_2 \cdot (\vec{r}'_2 - \vec{R}_j)} \\
&= \int \frac{d\vec{k}_1}{(2\pi)^3} \frac{d\vec{k}_2}{(2\pi)^3} v(\vec{k}_1) v(\vec{k}_2) \\
&\quad \times \sum_i \frac{1}{\mathcal{V}^{N_i}} \int d\vec{R}_1 \dots d\vec{R}_{N_i} e^{-i\vec{k}_1 \cdot (\vec{r}'_1 - \vec{R}_i)} e^{-i\vec{k}_2 \cdot (\vec{r}'_2 - \vec{R}_j)}
\end{aligned}$$

We now have to consider two cases. $i = j$ and $i \neq j$. Let us look at the second case. If $i \neq j$, then the impurity average separates so that

$$\begin{aligned}
&\frac{1}{\mathcal{V}^{N_i}} \int d\vec{R}_1 \dots d\vec{R}_{N_i} e^{-i\vec{k}_1 \cdot (\vec{r}'_1 - \vec{R}_i)} e^{-i\vec{k}_2 \cdot (\vec{r}'_2 - \vec{R}_j)} = \quad (2.10) \\
&= \left[\frac{1}{\mathcal{V}} \int d\vec{R}_i e^{-i\vec{k}_1 \cdot (\vec{r}'_1 - \vec{R}_i)} \right] \left[\frac{1}{\mathcal{V}} \int d\vec{R}_j e^{-i\vec{k}_2 \cdot (\vec{r}'_2 - \vec{R}_j)} \right]
\end{aligned}$$

$$= \frac{1}{\mathcal{V}^2} \delta(\vec{k}_1) e^{i\vec{k}_1 \cdot \vec{r}'_1} \delta(\vec{k}_2) e^{i\vec{k}_2 \cdot \vec{r}'_2}$$

For case where $i = j$ we have

$$\begin{aligned} & \frac{1}{\mathcal{V}^{N_i}} \int d\vec{R}_1 \dots d\vec{R}_{N_i} e^{-i\vec{k}_1 \cdot (\vec{r}'_1 - \vec{R}_1)} e^{-i\vec{k}_2 \cdot (\vec{r}'_1 - \vec{R}_1)} = \\ &= \frac{1}{\mathcal{V}} \int d\vec{R}_i e^{-i\vec{k}_1 \cdot (\vec{r}'_1 - \vec{R}_i)} e^{-i\vec{k}_2 \cdot (\vec{r}'_1 - \vec{R}_i)} \\ &= \frac{1}{\mathcal{V}} \int d\vec{R}_i e^{-i(\vec{k}_1 + \vec{k}_2) \cdot \vec{R}_i} e^{-i(\vec{k}_1 \cdot \vec{r}'_1 - \vec{k}_2 \cdot \vec{r}'_1)} \\ &= \frac{1}{\mathcal{V}} \delta(\vec{k}_1 + \vec{k}_2) e^{i\vec{k}_1 \cdot (\vec{r}'_2 - \vec{r}'_1)} \end{aligned} \quad (2.11)$$

Thus equation (2.9) becomes

$$\begin{aligned} \langle U(1')U(2') \rangle_t &= \\ &= \sum_{i \neq j}^{N_i} \int \frac{d\vec{k}_1}{(2\pi)^3} \frac{d\vec{k}_2}{(2\pi)^3} v(\vec{k}_1) v(\vec{k}_2) \frac{1}{\mathcal{V}^2} \delta(\vec{k}_1) e^{i\vec{k}_1 \cdot \vec{r}'_1} \delta(\vec{k}_2) e^{i\vec{k}_2 \cdot \vec{r}'_2} \\ &+ \sum_i^{N_i} \int \frac{d\vec{k}_1}{(2\pi)^3} \frac{d\vec{k}_2}{(2\pi)^3} v(\vec{k}_1) v(\vec{k}_2) \frac{1}{\mathcal{V}} \delta(\vec{k}_1 + \vec{k}_2) e^{i\vec{k}_1 \cdot (\vec{r}'_2 - \vec{r}'_1)} \\ &= \frac{N_i(N_i - 1)}{\mathcal{V}^2(2\pi)^6} [v(0)]^2 + \frac{N_i}{\mathcal{V}(2\pi)^3} \int \frac{d\vec{k}_1}{(2\pi)^3} v(\vec{k}_1) v(-\vec{k}_1) e^{i\vec{k}_1 \cdot (\vec{r}'_2 - \vec{r}'_1)} \end{aligned} \quad (2.12)$$

Because we have chosen $v(0) = 0$ this becomes

$$\langle U(1')U(2') \rangle_t = \frac{n_i}{(2\pi)^3} \int \frac{d\vec{k}_1}{(2\pi)^3} |v(\vec{k}_1)|^2 e^{i\vec{k}_1 \cdot (\vec{r}'_2 - \vec{r}'_1)} \quad (2.13)$$

where we have used the fact that for a real potential $v(-\vec{k}) = v^*(\vec{k})$.

Now let us create a more general expression for these impurity averages. We could have written (2.9) as

$$\begin{aligned} \langle U(1')U(2') \rangle_t &= N_i \frac{1}{\mathcal{V}} \int d\vec{R} V(\vec{r}'_1 - \vec{R}) V(\vec{r}'_1 - \vec{R}) \\ &+ N_i(N_i - 1) \left[\frac{1}{\mathcal{V}} \int d\vec{R} V(\vec{r}'_1 - \vec{R}) \right] \left[\frac{1}{\mathcal{V}} \int d\vec{R} V(\vec{r}'_1 - \vec{R}) \right] \\ &= N_i \langle V(1')V(2') \rangle + N_i(N_i - 1) \langle V(1') \rangle \langle V(2') \rangle \end{aligned} \quad (2.14)$$

Using this notation and continuing with this process, we can see that

$$\begin{aligned}
\langle U(1')U(2')U(3') \rangle_I &= \\
&= N_i(N_i - 1)(N_i - 2)\langle V(1') \rangle \langle V(2') \rangle \langle V(3') \rangle \\
&\quad + N_i(N_i - 1) \sum_{perm} \langle V(1') \rangle \langle V(2')V(3') \rangle \\
&\quad + N_i \langle V(1')V(2')V(3') \rangle \\
&= N_i \langle V(1')V(2')V(3') \rangle
\end{aligned} \tag{2.15}$$

and

$$\begin{aligned}
\langle U(1')U(2')U(3')U(4') \rangle_I &= \\
&= N_i(N_i - 1)(N_i - 2)(N_i - 3)\langle V(1') \rangle \langle V(2') \rangle \langle V(3') \rangle \langle V(4') \rangle \\
&\quad + N_i(N_i - 1)(N_i - 2) \sum_{perm} \langle V(1') \rangle \langle V(2') \rangle \langle V(3') \rangle \langle V(4') \rangle \\
&\quad + N_i(N_i - 1) \sum_{perm} \langle V(1') \rangle \langle V(2')V(3')V(4') \rangle \\
&\quad + N_i(N_i - 1) \sum_{perm} \langle V(1')V(2') \rangle \langle V(3')V(4') \rangle \\
&\quad + N_i \langle V(1')V(2')V(3')V(4') \rangle \\
&= N_i \langle V(1')V(2')V(3')V(4') \rangle \\
&\quad + N_i(N_i - 1) \sum_{perm} \langle V(1')V(2') \rangle \langle V(3')V(4') \rangle
\end{aligned} \tag{2.16}$$

where we can evaluate

$$\begin{aligned}
\langle V(1)V(2)\dots V(n) \rangle &= \\
&= \int \frac{d\vec{k}_1}{(2\pi)^3} \frac{d\vec{k}_2}{(2\pi)^3} \dots \frac{d\vec{k}_n}{(2\pi)^3} v(\vec{k}_1)v(\vec{k}_2)\dots v(\vec{k}_n) \\
&\quad \times \frac{1}{\mathcal{V}^n} \delta(\vec{k}_1 + \vec{k}_2 + \dots + \vec{k}_n) e^{-i\vec{k}_1 \cdot \vec{r}_1} e^{-i\vec{k}_2 \cdot \vec{r}_2} \dots e^{-i\vec{k}_n \cdot \vec{r}_n}
\end{aligned} \tag{2.17}$$

From this point, we can see that it will more practical to deal with the Fourier transform of the impurity potential.

2.2 The Meaning of $G_N(E)$

In the study of the behavior of a two dimensional electron gas in a magnetic field, we find that there are several entities that are used in the calculation of the properties of the system which are not adequately explained, if they are explained at all. In order to gain a better understanding of the approximations and the entities which we are using, we need to examine closely several of the finer details associated with these objects.

Exactly what does $G_N(E)$ represent? Assuming that we already know what a Green's function, $G(\vec{r}_1, \tau_1; \vec{r}_2, \tau_2)$ represents, how are these functions related? To answer these questions up front, let us make the statement that this is a "projection" of the Green's Function that is most like the N^{th} non-interacting Green's function representing an electron on the N^{th} Landau Level. Although this statement is a bit vague, it accurately describes the spirit of this Green's function. Why would we be interested in such an object? An analogy would be the orbital description of atoms and atomic bonds. We have a relatively "good idea" of the shapes of the electronic clouds such that we may understand bonding behavior. Here we have a "good idea" of what the highly degenerate Landau Levels represent and what it takes to excite the system from one state to another for a non-interacting electron. This will hopefully give us insight into how impurities (and the Coulomb interaction) effect the single electron excited states of the system.

With these ideas in mind let us proceed to lay out a more rigorous treatment of $G_N(E)$. The first thing to realize is that our system is time translational so that we may write:

$$G(\vec{r}_1, \tau_1; \vec{r}_2, \tau_2) = G(\vec{r}_1, \vec{r}_2; \tau_1 - \tau_2) \quad (2.18)$$

which allows us to take the Fourier Transform of the Green's Function to obtain $G(\vec{r}_1, \vec{r}_2; E)$. Of course this is not the end of the story. We still have to massage this into the entity which we will use in our calculations.

Starting with the definition of the single particle non-interacting retarded Green's function, in general we have:

$$G_0^R(\vec{r}_1, \tau_1; \vec{r}_2, \tau_2) = -i \langle [\psi_0(\vec{r}_1, t_1), \psi_0^\dagger(\vec{r}_2, t_2)] \rangle \theta(t_1 - t_2) \quad (2.19)$$

$$\begin{aligned}
&= -i \sum_n \phi_n(\vec{r}_1) \phi_n^*(\vec{r}_2) \langle 0 | [c_n(t_1), c_n^\dagger(t_2)] | 0 \rangle \theta(t_1 - t_2) \\
&= -i \sum_n \phi_n(\vec{r}_1) \phi_n^*(\vec{r}_2) e^{-iE_n t_1} e^{iE_n t_2} \theta(t_1 - t_2) \\
&= -i \sum_n \phi_n(\vec{r}_1) \phi_n^*(\vec{r}_2) e^{-iE_n(t_1 - t_2)} \theta(t_1 - t_2)
\end{aligned}$$

which we can Fourier transform to obtain:

$$\begin{aligned}
G_0^R(\vec{r}_1, \vec{r}_2; E) &= \int_{-\infty}^{\infty} dt e^{iEt} \left[-i \sum_n \phi_n(\vec{r}_1) \phi_n^*(\vec{r}_2) e^{-iE_n t} \right] \theta(t) \quad (2.20) \\
&= -i \sum_n \phi_n(\vec{r}_1) \phi_n^*(\vec{r}_2) \int_0^{\infty} dt e^{i(E - E_n)t} \\
&= \sum_n \frac{\phi_n(\vec{r}_1) \phi_n^*(\vec{r}_2)}{E - E_n}
\end{aligned}$$

where we have used the subscript n to represent each of the unique unperturbed eigenstates.

Let us now take the the expectation value of $G(\vec{r}_1, \vec{r}_2; E)$ for a given eigenstate in our system. In term of the eigenstates of the unperturbed electron in a magnetic field expressed in the Landau gauge, $|Np\rangle$, we have:

$$\begin{aligned}
\langle N_1 p_1 | G(\vec{r}_1, \vec{r}_2, E) | N_1 p_1 \rangle &= \int d\vec{r}_1 d\vec{r}_2 \phi_{N_1 p_1}^*(\vec{r}_1) G(\vec{r}_1, \vec{r}_2, E) \phi_{N_1 p_1}(\vec{r}_2) \quad (2.21) \\
&= \int d\vec{r}_1 d\vec{r}_2 \phi_{N_1 p_1}^*(\vec{r}_1) \sum_{N_2 p_2} \frac{\phi_{N_2 p_2}(\vec{r}_1) \phi_{N_2 p_2}^*(\vec{r}_2)}{E - E_{N_2}} \phi_{N_1 p_1}(\vec{r}_2) \\
&= \sum_{N_2 p_2} \frac{\delta_{N_1 N_2} \delta_{p_1 p_2}}{E - E_{N_2}} \\
&= \frac{1}{E - E_{N_1}}
\end{aligned}$$

as a result of the orthogonality of the wavefunctions. We would like however to make this object cover the entire Landau level subspace. So we will opt to sum over all of the states in the Landau Level. Now we have:

$$G_{0N_1}^R(E) = \sum_{p_1} \frac{1}{E - E_{N_1}} = \frac{gL}{E - E_{N_1}} \quad (2.22)$$

In this way we can proceed to write the non-interacting Green's function as a sum of the projections on the Landau levels.

$$G_0^R(\vec{r}_1, \vec{r}_2; E) = \frac{1}{g_L} \sum_N G_{0,N}^R(E) \sum_p \phi_{Np}^*(\vec{r}_1) \phi_{Np}(\vec{r}_2) \quad (2.23)$$

where g_L is the Landau level degeneracy for the system.

We can now see that we can separate $G_0^R(\vec{r}_1, \vec{r}_2; E)$, the non-interacting Green's function, into its Landau level projections. Can we separate the interacting Green's function in the same manner?

To begin this aspect of the discussion, let us consider this system to now be influenced by an external potential $U(\vec{r})$. We need to look at a progression of terms like:

$$T_0 = G_0^R(\vec{r}_1, \vec{r}_2; E) \quad (2.24)$$

$$T_1 = \int d\vec{r}_3 G_0^R(\vec{r}_1, \vec{r}_3; E) U(\vec{r}_3) G_0^R(\vec{r}_3, \vec{r}_2; E) \quad (2.25)$$

$$T_2 = \int d\vec{r}_3 d\vec{r}_4 G_0^R(\vec{r}_1, \vec{r}_3; E) U(\vec{r}_3) G_0^R(\vec{r}_3, \vec{r}_4; E) U(\vec{r}_4) G_0^R(\vec{r}_4, \vec{r}_2; E) \quad (2.26)$$

⋮

The first of these terms, T_0 can obviously be separated into its Landau level projections as we have just finished showing this fact. Let us then look at the second term:

$$\begin{aligned} T_1(\vec{r}_1, \vec{r}_2; E) &= \int d\vec{r}_3 G_0^R(\vec{r}_1, \vec{r}_3; E) U(\vec{r}_3) G_0^R(\vec{r}_3, \vec{r}_2; E) \quad (2.27) \\ &= \int d\vec{r}_3 \sum_{N_1 p_1} \left[\frac{\phi_{N_1 p_1}(\vec{r}_1) \phi_{N_1 p_1}^*(\vec{r}_3)}{E - E_{N_1}} \right] U(\vec{r}_3) \\ &\quad \times \sum_{N_2 p_2} \left[\frac{\phi_{N_2 p_2}(\vec{r}_3) \phi_{N_2 p_2}^*(\vec{r}_2)}{E - E_{N_2}} \right] \\ &= \sum_{N_1 p_1, N_2 p_2} \frac{\phi_{N_1 p_1}(\vec{r}_1) \phi_{N_2 p_2}^*(\vec{r}_2)}{(E - E_{N_1})(E - E_{N_2})} U_{N_1 p_1, N_2 p_2} \end{aligned}$$

Once again taking the expectation of a single state and summing over the Landau level subspace we obtain:

$$\begin{aligned}
T_{1,N}(E) &= \sum_p \langle .Np | T_1 | .Np \rangle \\
&= \sum_p \int d\vec{r}_1 d\vec{r}_2 \\
&\quad \times \sum_{N_1p_1, N_2p_2} \frac{o_{N_1p}^*(\vec{r}_1) o_{N_1p_1}(\vec{r}_1) o_{N_2p_2}^*(\vec{r}_2) o_{N_2p}^*(\vec{r}_2)}{(E - E_N)(E - E_{N_2})} \\
&\quad \times U_{N_p, N_2p_2} \\
&= \sum_p U_{N_p, N_p} \frac{1}{E - E_N} \frac{1}{E - E_N} \\
&= \sum_p U_{N_p, N_p} G_{0,N}^R(E) G_{0,N}^R(E) \tag{2.28}
\end{aligned}$$

We can also reconstruct this term as:

$$T_1 = \sum_N T_{1,N}(E) \tag{2.29}$$

Let us continue this inductive investigation by considering the next term.

$$\begin{aligned}
T_2(\vec{r}_1, \vec{r}_2; E) &= \tag{2.30} \\
&= \int d\vec{r}_3 \int d\vec{r}_4 G_0(\vec{r}_1, \vec{r}_3; E) U(\vec{r}_3) G_0(\vec{r}_3, \vec{r}_4; E) U(\vec{r}_4) G_0(\vec{r}_4, \vec{r}_2; E) \\
&= \int d\vec{r}_3 \int d\vec{r}_4 \sum_{N_1p_1} \left[\frac{o_{N_1p_1}(\vec{r}_1) o_{N_1p}^*(\vec{r}_3)}{E - E_N} \right] \\
&\quad \times U(\vec{r}_3) \sum_{N_2p_2} \left[\frac{o_{N_2p_2}(\vec{r}_3) o_{N_2p_2}^*(\vec{r}_4)}{E - E_{N_2}} \right] \\
&\quad \times U(\vec{r}_4) \sum_{N_3p_3} \left[\frac{o_{N_3p_3}(\vec{r}_4) o_{N_3p_3}^*(\vec{r}_2)}{E - E_{N_3}} \right] \\
&= \sum_{N_1p_1, N_2p_2, N_3p_3} U_{N_1p_1, N_2p_2} U_{N_2p_2, N_3p_3} \frac{o_{N_1p_1}(\vec{r}_1) o_{N_3p_3}^*(\vec{r}_2)}{(E - E_{N_1})(E - E_{N_2})(E - E_{N_3})}
\end{aligned}$$

Taking the expectation value:

$$T_{2,N}(E) = \tag{2.31}$$

$$\begin{aligned}
&= \sum_p \int d\vec{r}_1 d\vec{r}_2 \sum_{N_1 p_1, N_2 p_2, N_3 p_3} U_{N_1 p_1, N_2 p_2} U_{N_2 p_2, N_3 p_3} \\
&\quad \times \frac{\phi_{N_p}^*(\vec{r}_1) \phi_{N_1 p_1}(\vec{r}_1) \phi_{N_3 p_3}^*(\vec{r}_2) \phi_{N_p}(\vec{r}_2)}{(E - E_N)(E - E_{N_2})(E - E_{N_3})} \\
&= \sum_p \sum_{N_2 p_2} U_{N_p, N_2 p_2} U_{N_2 p_2, N_p} \frac{1}{E - E_N} \frac{1}{E - E_{N_2}} \frac{1}{E - E_N} \\
&= \sum_p \sum_{N_2 p_2} U_{N_p, N_2 p_2} U_{N_2 p_2, N_p} G_{0,N}^R(E) G_{0,N_2}^R(E) G_{0,N}^R(E)
\end{aligned}$$

Since the interacting form of the Greens function involves a sum of terms such as these, we can conclude by induction that it can be continue to be decomposed in this manner. Yet, there is one other class of terms which we would like to show is of this form which arises when an electron is temporarily excited to another state leaving an unoccupied state behind which behaves like a positively charged electron. This "electron-hole" pair is originally excited with the energy E to the state with energy α . This term is given by:

$$\begin{aligned}
T(\vec{r}_1, \vec{r}_2; E) &= \frac{1}{2\pi} \int d\alpha \int d\vec{r}_3 d\vec{r}_4 V(\vec{r}_1, \vec{r}_3) \left(\sum_{N_1 p_1} \frac{\phi_{N_1 p_1}(\vec{r}_3) \phi_{N_1 p_1}^*(\vec{r}_1)}{\alpha - E_{N_1}} \right) \\
&\quad \times \left(\sum_{N_2 p_2} \frac{\phi_{N_2 p_2}(\vec{r}_4) \phi_{N_2 p_2}^*(\vec{r}_3)}{E - \alpha - E_{N_2}} \right) V(\vec{r}_4, \vec{r}_2) \\
&= \frac{1}{2\pi} \int d\alpha \int d\vec{r}_3 d\vec{r}_4 \int \frac{d\vec{q}_1}{(2\pi)^2} V(\vec{q}_1) e^{i\vec{q}_1 \cdot (\vec{r}_1 - \vec{r}_3)} \left(\sum_{N_1 p_1} \frac{\phi_{N_1 p_1}(\vec{r}_3) \phi_{N_1 p_1}^*(\vec{r}_1)}{\alpha - E_{N_1}} \right) \\
&\quad \times \left(\sum_{N_2 p_2} \frac{\phi_{N_2 p_2}(\vec{r}_4) \phi_{N_2 p_2}^*(\vec{r}_3)}{E - \alpha - E_{N_2}} \right) \int \frac{d\vec{q}_2}{(2\pi)^2} V(\vec{q}_2) e^{i\vec{q}_2 \cdot (\vec{r}_4 - \vec{r}_2)} \\
&= \frac{1}{2\pi} \int d\alpha \sum_{N_1 p_1, N_2 p_2} \int \frac{d\vec{q}_1}{(2\pi)^2} \frac{d\vec{q}_2}{(2\pi)^2} V(\vec{q}_1) V(\vec{q}_2) e^{i\vec{q}_1 \cdot \vec{r}_1} e^{-i\vec{q}_2 \cdot \vec{r}_2} \\
&\quad \times \frac{M_{N_1 p_1, N_2 p_2}(\vec{q}_1)}{\alpha - E_{N_1}} \frac{M_{N_2 p_2, N_1 p_1}(\vec{q}_2)}{E - \alpha - E_{N_2}}
\end{aligned} \tag{2.32}$$

where

$$M_{N_1 p_1, N_2 p_2}(\vec{q}) = \langle N_1 p_1 | e^{i\vec{q} \cdot \vec{r}} | N_2 p_2 \rangle \tag{2.33}$$

Now, this is essentially the polarizability of the electron gas as it reflects the response to an external potential. We have a slightly different approach to this term since we

have the potential interaction which initiated the state and the interaction generated when the state decays. We can separate out the potential terms so that

$$\begin{aligned}
T_{pot}(E, \vec{q}) &= \frac{-1}{2\pi} \int d\alpha \sum_{N_1 p_1, N_2 p_2} \frac{M_{N_1 p_1, N_2 p_2}(\vec{q})}{\alpha - E_{N_1}} \frac{M_{N_2 p_2, N_1 p_1}(\vec{q})}{E - \alpha - E_{N_2}} \\
&= \sum_{N_1 p_1, N_2 p_2} M_{N_1 p_1, N_2 p_2}(\vec{q}) M_{N_2 p_2, N_1 p_1}(\vec{q}) \\
&\quad \times \int d\alpha G_{0, N_1}^R(\alpha) G_{0, N_2}^R(E - \alpha)
\end{aligned} \tag{2.34}$$

One of the primary advantages of using this form of the Green's function is that the spectral function $A(x)$ is just the energy density of states and is easily calculated from:

$$A(E) = \frac{1}{\pi} \int d\vec{r} \text{Im} G^R(\vec{r}, \vec{r}; E) \tag{2.35}$$

We should notice that taking the sum of the expectation values of $G^R(\vec{r}, \vec{r}; E)$ is equivalent to taking the spatial contraction of the Green's function as in the following example.

$$\int d\vec{r} G_0^R(\vec{r}, \vec{r}; E) = \int d\vec{r} \sum_{N_p} \frac{\mathcal{O}_{N_p}(\vec{r}) \mathcal{O}_{N_p}^*(\vec{r})}{E - E_N} \tag{2.36}$$

$$\begin{aligned}
&= \sum_N \left(\sum_p \frac{1}{E - E_N} \right) \\
&= \sum_N G_{0, N}^R(E)
\end{aligned} \tag{2.37}$$

Of course then we can treat

$$A_N(E) = \frac{1}{\pi} \text{Im} G_N^R(E) \tag{2.38}$$

as the effective density of states for a "Landau level" for the interacting system. These quantities are ultimately what we wish to calculate in order to get a better understanding of the density of states.

2.3 Combining $G_N(E)$ with Impurity Scattering

Now that we have looked at impurity scattering and the form of the Green's function which we are using, it is time to combine both of these principles. This final combination will result in the tools which we will use to develop our model of the two dimensional electron gas in a magnetic field. Returning to our expansion of the Green's function but this time after we Fourier transform the time dependence:

$$\begin{aligned}
 G^R(\vec{r}_1, \vec{r}_2; E) &= G_0^R(\vec{r}_1, \vec{r}_2; E) + \int d\vec{r}_3 G_0^R(\vec{r}_1, \vec{r}_3; E) U(\vec{r}_3) G_0^R(\vec{r}_3, \vec{r}_2; E) \\
 &+ \int d\vec{r}_3 d\vec{r}_4 G_0^R(\vec{r}_1, \vec{r}_3; E) U(\vec{r}_3) G_0^R(\vec{r}_3, \vec{r}_4; E) U(\vec{r}_4) G_0^R(\vec{r}_4, \vec{r}_2; E) \\
 &+ \dots
 \end{aligned} \tag{2.39}$$

Now we want to express this in terms of our $G_N(E)$, so let us expand each of the $G_0^R(\vec{r}_1, \vec{r}_2; E)$ terms as:

$$\begin{aligned}
 G_0^R(\vec{r}_1, \vec{r}_2; E) &= \sum_{N_1 p_1} \frac{\phi_{N_1 p_1}(\vec{r}_1) \phi_{N_1 p_1}^*(\vec{r}_2)}{E - E_{N_1}} \\
 &= \sum_{N_1 p_1} \phi_{N_1 p_1}(\vec{r}_1) \phi_{N_1 p_1}^*(\vec{r}_2) \frac{1}{g_L} G_{0, N_1}^R(E)
 \end{aligned} \tag{2.40}$$

where again g_L is the Landau level degeneracy. Substituting this into 2.39 we get:

$$\begin{aligned}
 G^R(\vec{r}_1, \vec{r}_2; E) &= \left(\sum_{N_1 p_1} \phi_{N_1 p_1}(\vec{r}_1) \phi_{N_1 p_1}^*(\vec{r}_2) \frac{1}{g_L} G_{0, N_1}^R(E) \right) \\
 &+ \int d\vec{r}_3 \left(\sum_{N_1 p_1} \phi_{N_1 p_1}(\vec{r}_1) \phi_{N_1 p_1}^*(\vec{r}_3) \frac{1}{g_L} G_{0, N_1}^R(E) \right) U(\vec{r}_3) \\
 &\quad \times \left(\sum_{N_2 p_2} \phi_{N_2 p_2}(\vec{r}_3) \phi_{N_2 p_2}^*(\vec{r}_2) \frac{1}{g_L} G_{0, N_2}^R(E) \right) \\
 &+ \int d\vec{r}_3 d\vec{r}_4 \left(\sum_{N_1 p_1} \phi_{N_1 p_1}(\vec{r}_1) \phi_{N_1 p_1}^*(\vec{r}_3) \frac{1}{g_L} G_{0, N_1}^R(E) \right) U(\vec{r}_3) \\
 &\quad \times \left(\sum_{N_2 p_2} \phi_{N_2 p_2}(\vec{r}_3) \phi_{N_2 p_2}^*(\vec{r}_4) \frac{1}{g_L} G_{0, N_2}^R(E) \right) U(\vec{r}_4) \\
 &\quad \times \left(\sum_{N_3 p_3} \phi_{N_3 p_3}(\vec{r}_4) \phi_{N_3 p_3}^*(\vec{r}_2) \frac{1}{g_L} G_{0, N_3}^R(E) \right)
 \end{aligned} \tag{2.41}$$

$$\begin{aligned}
& + \dots \\
& = \frac{1}{g_L} \sum_{N_1 p_1} \phi_{N_1 p_1}(\vec{r}_1) \phi_{N_1 p_1}^*(\vec{r}_2) G_{0, N_1}^R(E) \\
& + \frac{1}{g_L^2} \sum_{\substack{N_1 p_1 \\ N_2 p_2}} \phi_{N_1 p_1}(\vec{r}_1) \phi_{N_2 p_2}^*(\vec{r}_2) G_{0, N_1}^R(E) U_{N_1 p_1, N_2 p_2} G_{0, N_2}^R(E) \\
& + \frac{1}{g_L^3} \sum_{\substack{N_1 p_1 \\ N_2 p_2 \\ N_3 p_3}} \phi_{N_1 p_1}(\vec{r}_1) \phi_{N_3 p_3}^*(\vec{r}_2) G_{0, N_1}^R(E) U_{N_1 p_1, N_2 p_2} G_{0, N_2}^R(E) \\
& \quad \times U_{N_2 p_2, N_3 p_3} G_{0, N_3}^R(E) \\
& + \dots
\end{aligned} \tag{2.42}$$

Now we are ready to take the expectation value of this expression to obtain:

$$\begin{aligned}
G_N^R(E) & = \sum_p \int d\vec{r}_1 d\vec{r}_2 \phi_{Np}^*(\vec{r}_1) \phi_{Np}(\vec{r}_2) G^R(\vec{r}_1, \vec{r}_2; E) \\
& = \sum_p \frac{1}{g_L} G_{0, N}^R(E) \\
& + \sum_p \frac{1}{g_L^2} G_{0, N}^R(E) U_{Np, Np} G_{0, N}^R(E) \\
& + \sum_p \frac{1}{g_L^3} \sum_{N_2 p_2} G_{0, N}^R(E) U_{Np, N_2 p_2} G_{0, N_2}^R(E) U_{N_2 p_2, Np} G_{0, N}^R(E) \\
& + \dots
\end{aligned} \tag{2.43}$$

Note that the first term is simply given by $G_{0, N}^R(E)$ after summing over p . This is exactly what we want except that now we would like to take the average over all impurity distributions. Following the procedure that we discuss previously we form:

$$\begin{aligned}
\langle G_N^R(E) \rangle_I & = \langle G_{0, N}^R(E) \rangle_I \\
& + \sum_p \frac{1}{g_L^2} \langle G_{0, N}^R(E) U_{Np, Np} G_{0, N}^R(E) \rangle_I \\
& + \sum_p \frac{1}{g_L^3} \sum_{N_2 p_2} \langle G_{0, N}^R(E) U_{Np, N_2 p_2} G_{0, N_2}^R(E) U_{N_2 p_2, Np} G_{0, N}^R(E) \rangle_I \\
& + \dots
\end{aligned} \tag{2.44}$$

Remember that the unperturbed Green's function is independent of the impurities so we may take them out of the impurity average. Therefore we have the expression:

$$\begin{aligned}
\langle G_N^R(E) \rangle_I &= G_{0N}^R(E) \\
&+ \frac{1}{gL^2} G_{0N}^R(E) G_{0N}^R(E) \langle \sum_p U_{Np..Np} \rangle_I \\
&+ \frac{1}{gL^3} \sum_{N_2 p_2} G_{0N}^R(E) G_{0N_2}^R(E) G_{0N}^R(E) \langle \sum_p U_{Np..N_2 p_2} U_{N_2 p_2..Np} \rangle_I \\
&+ \dots
\end{aligned} \tag{2.45}$$

Now all we need to deal with are terms like $\langle \sum_p U_{Np..Np} \rangle_I$. To take care of these we will again use the Fourier representation of the potential.

$$\begin{aligned}
V_I(\vec{r}) &= \sum_{\alpha}^{N_i} V(\vec{r} - \vec{R}_{\alpha}) \\
&= \sum_{\alpha}^{N_i} \int \frac{d\vec{q}}{(2\pi)^2} v(\vec{q}) e^{i\vec{q} \cdot (\vec{r} - \vec{R}_{\alpha})}
\end{aligned} \tag{2.46}$$

The quantity $U_{N_1 p_1..N_2 p_2}$ now becomes:

$$\begin{aligned}
U_{N_1 p_1..N_2 p_2} &= \langle N_1 p_1 | \sum_{\alpha}^{N_i} \int \frac{d\vec{q}}{(2\pi)^2} v(\vec{q}) e^{i\vec{q} \cdot (\vec{r} - \vec{R}_{\alpha})} | N_2 p_2 \rangle \\
&= \sum_{\alpha}^{N_i} \int \frac{d\vec{q}}{(2\pi)^2} v(\vec{q}) \langle N_1 p_1 | e^{i\vec{q} \cdot \vec{r}} | N_2 p_2 \rangle e^{-i\vec{q} \cdot \vec{R}_{\alpha}} \\
&= \int \frac{d\vec{q}}{(2\pi)^2} v(\vec{q}) M_{N_1 p_1..N_2 p_2}(\vec{q}) \sum_{\alpha}^{N_i} e^{-i\vec{q} \cdot \vec{R}_{\alpha}}
\end{aligned} \tag{2.47}$$

where now we have used the notation

$$M_{N_1 p_1..N_2 p_2}(\vec{q}) = \langle N_1 p_1 | e^{i\vec{q} \cdot \vec{r}} | N_2 p_2 \rangle \tag{2.48}$$

We are now ready to take the impurity averages. The impurity average of the second in equation (2.45) is

$$\langle \sum_p \sum_{\alpha}^{N_i} U_{Np..Np} \rangle_I = \langle \sum_p \int \frac{d\vec{q}}{(2\pi)^2} v(\vec{q}) M_{Np..Np}(\vec{q}) \sum_{\alpha}^{N_i} e^{-i\vec{q} \cdot \vec{R}_{\alpha}} \rangle_I \tag{2.49}$$

$$\begin{aligned}
&= \sum_p \int \frac{d\vec{q}}{(2\pi)^2} v(\vec{q}) M_{N_p, N_p}(\vec{q}) \langle \sum_{\alpha}^{N_i} e^{-i\vec{q} \cdot \vec{R}_{\alpha}} \rangle_I \\
&= \sum_p \int \frac{d\vec{q}}{(2\pi)^2} v(\vec{q}) M_{N_p, N_p}(\vec{q}) \frac{N_i}{V} (2\pi)^2 \delta(\vec{q}) \\
&= \frac{N_i}{V} \sum_p v(0) M_{N_p, N_p}(0) \\
&= 0
\end{aligned}$$

since we have chosen to let the constant energy offset, $v(0)$, to be zero. Now, if we look at the third term in (2.45), we see that this one will give us something more interesting:

$$\begin{aligned}
\langle \sum_p U_{N_p, N_2 p_2} U_{N_2 p_2, N_p} \rangle_I &= \sum_p \langle \int \frac{d\vec{q}_1}{(2\pi)^2} v(\vec{q}_1) M_{N_p, N_2 p_2}(\vec{q}_1) \sum_{\alpha}^{N_i} e^{-i\vec{q}_1 \cdot \vec{R}_{\alpha}} \\
&\quad \times \int \frac{d\vec{q}_2}{(2\pi)^2} v(\vec{q}_2) M_{N_2 p_2, N_p}(\vec{q}_2) \sum_{\beta}^{N_i} e^{-i\vec{q}_2 \cdot \vec{R}_{\beta}} \rangle_I \\
&= \sum_p \int \frac{d\vec{q}_1}{(2\pi)^2} \frac{d\vec{q}_2}{(2\pi)^2} v(\vec{q}_1) v(\vec{q}_2) M_{N_p, N_2 p_2}(\vec{q}_1) M_{N_2 p_2, N_p}(\vec{q}_2) \\
&\quad \times \langle \sum_{\alpha \beta}^{N_i} e^{-i\vec{q}_1 \cdot \vec{R}_{\alpha}} e^{-i\vec{q}_2 \cdot \vec{R}_{\beta}} \rangle_I \\
&= \sum_p \int \frac{d\vec{q}_1}{(2\pi)^2} \frac{d\vec{q}_2}{(2\pi)^2} v(\vec{q}_1) v(\vec{q}_2) M_{N_p, N_2 p_2}(\vec{q}_1) M_{N_2 p_2, N_p}(\vec{q}_2) \\
&\quad \times \left(\frac{N_i(N_i - 1)}{V^2} (2\pi)^4 \delta(\vec{q}_1) \delta(\vec{q}_2) + \frac{N_i}{V} (2\pi)^2 \delta(\vec{q}_1 + \vec{q}_2) \right) \\
&= \frac{N_i(N_i - 1)}{V^2} \sum_p M_{N_p, N_2 p_2}(0) M_{N_2 p_2, N_p}(0) v(0) v(0) \\
&\quad + \frac{N_i}{V} \sum_p \int \frac{d\vec{q}_1}{(2\pi)^2} M_{N_p, N_2 p_2}(\vec{q}_1) M_{N_2 p_2, N_p}(-\vec{q}_1) v(\vec{q}_1) v(-\vec{q}_1) \\
&= \frac{N_i}{V} \sum_p \int \frac{d\vec{q}_1}{(2\pi)^2} M_{N_p, N_2 p_2}(\vec{q}_1) M_{N_2 p_2, N_p}(-\vec{q}_1) v(\vec{q}_1) v(-\vec{q}_1)
\end{aligned} \tag{2.50}$$

where again we have set the constant potential offset to zero. We can plug this expression back into equation (2.45).

$$\begin{aligned}
\langle G_N^R(E) \rangle_I &= G_{0N}^R(E) & (2.51) \\
&+ \frac{1}{gL^3} \sum_{N_2 p_2} G_{0N}^R(E) G_{0N_2}^R(E) G_{0N}^R(E) \\
&\times \frac{V_i}{V} \sum_p \int \frac{d\vec{q}_1}{(2\pi)^2} M_{Np, N_2 p_2}(\vec{q}_1) M_{N_2 p_2, Np}(-\vec{q}_1) v(\vec{q}_1) v(-\vec{q}_1) \\
&+ \dots
\end{aligned}$$

We could continue generating terms like this forever. At this point we should have a pretty good feel for the types of expansions that we are dealing with here.

Chapter 3

Standard Methods for Calculating the Density of States

3.1 The Self Consistent Born Approach

Using our Green's function techniques, we are now ready to proceed with the calculation of the density of states of a two dimensional electron gas in a magnetic field. Our first try with this will yield what we will call the Self Consistent Born approach. Essentially this involves a simple self-consistent impurity scattering as given by the following two diagrams:

$$\Sigma_N(E) = \textcircled{\Sigma_N} = \begin{array}{c} N_i \\ \times \\ | \\ i \end{array} + \begin{array}{c} N_i \\ \times \\ \text{---} \\ \text{---} \\ \text{---} \end{array} \quad (3.1)$$

$$G_N(E) = \text{---} \text{---} \text{---} = \text{---} \text{---} \text{---} + \text{---} \text{---} \text{---} \textcircled{\Sigma_N} \text{---} \text{---} \text{---} \quad (3.2)$$

In equation form, this gives us:

$$\Sigma_N(E) = \sum_{N_2 p_2 p} \frac{1}{g_L} \langle U_{Np, N_2 p_2} G_{N_2}(E) U_{N_2 p_2, Np} \rangle_I \quad (3.3)$$

$$G_N(E) = \frac{1}{E - E_N - \Sigma_N(E)} \quad (3.4)$$

where $g_L = (2\pi l^2)^{-1}$ is the Landau level degeneracy. We have dropped the first term in the self-energy since this gives just the average energy of the interaction as we did

in our general treatment of impurity scattering. Now we can substitute the second equation into the first to obtain:

$$\Sigma_N(E) = \sum_{N_2 p_2 p} \langle |U_{Np, N_2 p_2}|^2 \rangle_I \frac{1}{E - E_N - \Sigma_{N_2}(E)} \quad (3.5)$$

To simplify this a bit let us make the assignment

$$\frac{1}{4} \Gamma_{N, N_2}^2 = \frac{1}{g_L} \sum_{pp_2} \langle |U_{Np, N_2 p_2}|^2 \rangle_I \quad (3.6)$$

so that

$$\Sigma_N(E) = \sum_{N_2} \frac{1}{4} \Gamma_{N, N_2}^2 \frac{1}{E - E_N - \Sigma_{N_2}(E)} \quad (3.7)$$

Now if we assume that we are dealing with magnetic field large enough that the wave functions do not overlap significantly, the diagonal terms of $\frac{1}{4} \Gamma_{N, N_2}^2$ will dominate. Therefore we ignore all off-diagonal terms such that

$$\Sigma_N(E) = \frac{1}{4} \Gamma_{N, N}^2 \frac{1}{E - E_N - \Sigma_N(E)} \quad (3.8)$$

With a little rearrangement, the equation becomes a simple quadratic

$$[\Sigma_N(E)]^2 + (E_N - E)\Sigma_N(E) + \frac{1}{4} \Gamma_{N, N}^2 = 0 \quad (3.9)$$

with the solution

$$\Sigma_N(E) = \frac{(E - E_N) \pm \sqrt{(E - E_N)^2 - \Gamma_{N, N}^2}}{2} \quad (3.10)$$

So now we have an expression for the Green's function:

$$G_N(E) = \frac{2}{\Gamma_{N, N}^2} \left[(E - E_N) \pm \sqrt{(E - E_N)^2 - \Gamma_{N, N}^2} \right] \quad (3.11)$$

Now we notice that $G_N(E)$ has an imaginary component when the energy is within $\Gamma_{N, N}^2$ of a Landau level. In order for the Green's function to be a retarded Green's function, it needs to be analytic in the upper half of the complex plane. This requires

us to choose the solution which gives the negative imaginary part. The Landau level density of states is then given by

$$\begin{aligned}
D_N(E) &= -(2\pi^2 l^2)^{-1} \text{Im} G_N(E) \\
&= -(2\pi^2 l^2)^{-1} \frac{2}{\Gamma_{N,N}} \sqrt{1 - \left(\frac{E - E_N}{\Gamma_{N,N}}\right)^2} : |E - E_N| \leq \Gamma_{N,N} \\
&= 0 : |E - E_N| > \Gamma_{N,N}
\end{aligned} \tag{3.12}$$

where we have added in the factor of $g_L = (2\pi l^2)^{-1}$ which we have omitted in our $G_{0,N}(E)$ to account for the Landau level degeneracy. We can then see that the density of states is a series of semi-elliptic states centered around the Landau level energies. This discussion usually continues with the assumption that we have short range scatterers. We can then approximate the potential as

$$V(\vec{r}) = V_z \delta^{(2)}(\vec{r}) \tag{3.13}$$

which gives the simple result that

$$\Gamma_{N,N} = 4(2\pi l^2) n_i |V_z|^2 \tag{3.14}$$

though the derivation of this in the Landau gauge is not exactly simple. Starting with (3.6) we have

$$\begin{aligned}
\Gamma_{N,N} &= \frac{1}{g_L} \sum_{p_1 p_2} \langle \int d\vec{r}_1 d\vec{r}_2 \phi_{N p_1}^*(\vec{r}_1) V_z \delta^2(\vec{r}_1 - \vec{R}_\alpha) \phi_{N p_2}(\vec{r}_1) \\
&\quad \times \phi_{N p_2}^*(\vec{r}_2) V_z \delta^2(\vec{r}_2 - \vec{R}_\beta) \phi_{N p_1}(\vec{r}_2) \rangle_I
\end{aligned} \tag{3.15}$$

which reduces to

$$\Gamma_{N,N} = \frac{1}{g_L} V_z^2 \sum_{p_1 p_2} \langle \phi_{N p_1}^*(\vec{R}_\alpha) \phi_{N p_2}(\vec{R}_\alpha) \phi_{N p_2}^*(\vec{R}_\beta) \phi_{N p_1}(\vec{R}_\beta) \rangle_I \tag{3.16}$$

Now, remembering our discussion about impurity scattering, we will take the average over all impurities. Note that here we did not use the Fourier transform of the

potential due to the simple nature of the potential. Still we have two cases. In the first case $\alpha \neq \beta$ and, in the second case $\alpha = \beta$. Therefore we have:

$$\begin{aligned}\Gamma_{N,N} &= 4(2\pi l^2)V_z^{-2} \frac{1}{V^2} \sum_{p_1 p_2} \sum_{\alpha \neq \beta} \int d\vec{R}_\alpha d\vec{R}_\beta \phi_{N p_1}^*(\vec{R}_\alpha) \phi_{N p_2}(\vec{R}_\alpha) \phi_{N p_2}^*(\vec{R}_\beta) \phi_{N p_1}(\vec{R}_\beta) \\ &+ 4(2\pi l^2)V_z^{-2} \frac{1}{V} \sum_{p_1 p_2} \sum_{\alpha} \int d\vec{R}_\alpha \phi_{N p_1}^*(\vec{R}_\alpha) \phi_{N p_2}(\vec{R}_\alpha) \phi_{N p_2}^*(\vec{R}_\alpha) \phi_{N p_1}(\vec{R}_\alpha) \quad (3.17)\end{aligned}$$

We have already shown that this first term is removed by subtracting a suitable constant from the potential without any effect which we have done implicitly by ignoring the first contribution. Therefore we shall drop it from our expression. The remaining term may be dealt with as follows:

$$\begin{aligned}\Gamma_{N,N} &= 4(2\pi l^2)V_z^{-2} \frac{1}{V} \sum_{p_1 p_2} \sum_{\alpha} \int d\vec{R}_\alpha \phi_{N p_1}^*(\vec{R}_\alpha) \phi_{N p_2}(\vec{R}_\alpha) \phi_{N p_2}^*(\vec{R}_\alpha) \phi_{N p_1}(\vec{R}_\alpha) \\ &= 4V_z^{-2} \frac{1}{V} \sum_{p_1} \sum_{\alpha} \int d\vec{R}_\alpha \phi_{N p_1}^*(\vec{R}_\alpha) \phi_{N p_1}(\vec{R}_\alpha) \quad (3.18)\end{aligned}$$

where we have used the property of the wavefunctions that

$$\sum_p \phi_{N_1 p}^*(\vec{r}) \phi_{N_2 p}(\vec{r}) = \frac{1}{2\pi l^2} \delta_{N_1, N_2} \quad (3.19)$$

Continuing, we have

$$\begin{aligned}\Gamma_{N,N} &= 4V_z^{-2} \frac{1}{V} \sum_{p_1} \sum_{\alpha} 1 \\ &= 4V_z^{-2} \frac{N_i}{V} \sum_{p_1} 1 \\ \Gamma_{N,N} &= 4V_z^{-2} \frac{n_i}{2\pi l^2} \quad (3.20)\end{aligned}$$

which gives us the result that we have claimed.

This result bears a striking resemblance to the result obtained from the Born approximation in zero magnetic field. In this zero field case, we have for this two dimensional system:

$$\frac{1}{\tau(k_1)} = 2\pi n_i \int \frac{d^2 k_2}{(2\pi)^2} \delta(\epsilon_{k_1} - \epsilon_{k_2}) |T_{k_1 k_2}|^2$$

$$\begin{aligned}
&= (2\pi)^2 n_i \int \frac{k_2 dk_2}{(2\pi)^2} \delta(\epsilon_{k_1} - \epsilon_{k_2}) |T_{k_1 k_2}|^2 \\
&= n_i \int d\epsilon_{k_1} |T_{k_1 k_2}|^2
\end{aligned} \tag{3.21}$$

with

$$T_{k_1 k_2} = \int d\vec{r} o_{k_2}^*(\vec{r}) v_{k_1}(\vec{r}) \tag{3.22}$$

where $v_{k_1}(\vec{r})$ are the wavefunctions of the initial state and $o_{k_2}(\vec{r})$ are the wavefunctions of the final (scattered) state. For the case of a delta function potential, this yields the result

$$\frac{1}{\tau} = n_i m |V_z|^2 \tag{3.23}$$

We can now relate the two quantities by inserting

$$n_i V_z^2 = \frac{1}{m\tau} \tag{3.24}$$

into equation (3.20) obtaining the relation

$$\begin{aligned}
\Gamma_{N,N}^2 = \Gamma^2 &= 4 \frac{1}{2\pi l^2} \frac{1}{m\tau} \\
&= \frac{2 eB}{\pi m\tau} \\
&= \frac{2 \omega_c}{\pi \tau}
\end{aligned} \tag{3.25}$$

So we have a simple relation between the Landau level width and the scattering time in the zero field Born approximation. Therefore this approach is known as the ‘‘Self Consistent Born Approximation’’ (SCBA).

To summarize, if we ignore the inter-Landau level interactions in our system we obtain the result that the density of states has a semi-elliptic form. In addition, if we consider only short range scatterers, the width of these semi-elliptic states is independent of the Landau level index and can be related to the zero field scattering time in the Born approximation.

where the self-similarity yields the expression:

$$\hat{O} = 1 + \sum_{N_2 m_2} |N_2 m_2\rangle G_{N_2}(E) \langle N_2 m_2 | \hat{V}_I \hat{O} \quad (3.30)$$

which we can easily solve for \hat{O} such that

$$\hat{O} = \left[1 - \sum_{N_2 m_2} |N_2 m_2\rangle G_{N_2}(E) \langle N_2 m_2 | \hat{V}_I \right]^{-1} \quad (3.31)$$

so that we have an expression for the self energy given by:

$$\begin{aligned} \Sigma_N(E) &= 2\pi l^2 N_i \sum_m \langle N m | \left(\frac{\hat{V}_I}{1 - \sum_{N_2 m_2} |N_2 m_2\rangle G_{N_2}(E) \langle N_2 m_2 | \hat{V}_I} \right) | N m \rangle \\ &= 2\pi l^2 N_i \sum_m \langle N m | \hat{V}_I \left(\sum_{N_3 m_3} |N_3 m_3\rangle \langle N_3 m_3 | \right) \\ &\quad \times \left(\frac{1}{1 - \sum_{N_2 m_2} |N_2 m_2\rangle G_{N_2}(E) \langle N_2 m_2 | \hat{V}_I} \right) | N m \rangle \\ &= 2\pi l^2 N_i \sum_{N_3 m_3} \langle N m | \hat{V}_I | N_3 m_3 \rangle \\ &\quad \times \langle N_3 m_3 | \left(\frac{1}{1 - \sum_{N_2 m_2} |N_2 m_2\rangle G_{N_2}(E) \langle N_2 m_2 | \hat{V}_I} \right) | N m \rangle \quad (3.32) \end{aligned}$$

Here we have used the fact that the wavefunctions form a complete set in order to avoid dealing with the commutation of the \hat{V}_I and \hat{O} operators in the steps to come. Continuing.

$$\begin{aligned} \Sigma_N(E) &= 2\pi l^2 N_i \sum_{N_3 m_3} \langle N m_3 | \hat{V}_I | N m_3 \rangle \\ &\quad \times \langle N_3 m_3 | \left(\frac{1}{1 - \sum_{N_2 m_2} |N_2 m_2\rangle G_{N_2}(E) \langle N_2 m_2 | \hat{V}_I} \right) | N m \rangle \quad (3.33) \end{aligned}$$

by using the orthogonality of the wavefunctions, $\langle N_3 m_3 | N_2 m_2 \rangle = \delta_{N_3 N_2} \delta_{m_3 m_2}$.

We still cannot deal with this expression without applying our further assumption that the Landau levels do not overlap significantly. Therefore, we can ignore all of the off-diagonal Landau level terms in the sum. Again, this is a valid assumption for

high magnetic fields where the energy broadening due to scattering is much smaller than the large cyclotron energy. Proceeding,

$$\begin{aligned}\Sigma_N(E) &= 2\pi l^2 N_i \sum_{mm_3} \langle Nm | \hat{V}_I | Nm_3 \rangle \\ &\quad \times \langle Nm_3 | \left(\frac{1}{1 - |Nm_3\rangle G_N(E) \langle Nm_3 | \hat{V}_I} \right) | Nm \rangle\end{aligned}\quad (3.34)$$

Since we are using the symmetric gauge and we have a cylindrically symmetric potential, so that $\langle Nm | \hat{V}_I | Nm_3 \rangle = \delta_{m_3 m} \langle Nm | \hat{V}_I | Nm \rangle$, we may write,

$$\begin{aligned}\Sigma_N(E) &= 2\pi l^2 N_i \sum_m \langle Nm | \hat{V}_I | Nm \rangle \\ &\quad \times \langle Nm | \left(\frac{1}{1 - |Nm\rangle G_N(E) \langle Nm | \hat{V}_I} \right) | Nm \rangle \\ &= 2\pi l^2 N_i \sum_m \frac{\langle Nm | \hat{V}_I | Nm \rangle}{1 - G_N \langle Nm | \hat{V}_I | Nm \rangle}\end{aligned}\quad (3.35)$$

Additionally, we may separate out the first term in the original series so that

$$\begin{aligned}\Sigma_N(E) &= 2\pi l^2 N_i \sum_m \langle Nm | \hat{V}_I | Nm \rangle \\ &\quad + 2\pi l^2 N_i \sum_m \frac{\langle Nm | \hat{V}_I | Nm \rangle^2}{G_N^{-1} - \langle Nm | \hat{V}_I | Nm \rangle}\end{aligned}\quad (3.36)$$

One then solves this self-consistent set of equations. The result is again for high magnetic fields. The density of states in this approximation shows a large asymmetry with a sharp cutoff on the high energy side and a truncated tail on the low energy side. In addition, the solution predicts that below a certain critical density $N_i^{(p)}$, the level splits into p impurity bands each tending toward the same asymmetry. [1, pages 1525-1526] On the other hand, if the density of scatters is increased, the behavior returns to that of the self-consistent Born results.

3.3 The Many-Site Approximation

The next particular approximation in the set of approximations set forth by Ando is the Many-Site Approximation. [2, 4] This approximation naturally extends the

Single-Site Approximation to scattering many times from more than one impurity site. Once again short range scatterers are assumed and inter-Landau level interactions are ignored. The diagrams for this approximation are given by:

$$\begin{array}{c} \times \\ \parallel \\ \parallel \end{array} = \begin{array}{c} \times \\ \diagup \quad \diagdown \\ \text{---} \blacktriangleright \text{---} \\ \diagdown \quad \diagup \end{array} + \begin{array}{c} \times \\ \diagup \quad \diagdown \\ \text{---} \text{---} \text{---} \\ \diagdown \quad \diagup \end{array} + \begin{array}{c} \times \\ \diagup \quad \diagdown \\ \text{---} \text{---} \text{---} \text{---} \\ \diagdown \quad \diagup \end{array} + \dots \quad (3.37)$$

$$\Sigma_{N\sigma} = \begin{array}{c} \times \\ \parallel \\ \parallel \end{array} + \begin{array}{c} \times \quad \times \\ \diagup \quad \diagdown \quad \diagup \quad \diagdown \\ \text{---} \text{---} \text{---} \text{---} \\ \diagdown \quad \diagup \quad \diagdown \quad \diagup \end{array} + \begin{array}{c} \times \quad \times \quad \times \\ \diagup \quad \diagdown \quad \diagup \quad \diagdown \quad \diagup \quad \diagdown \\ \text{---} \text{---} \text{---} \text{---} \text{---} \\ \diagdown \quad \diagup \quad \diagdown \quad \diagup \quad \diagdown \quad \diagup \end{array} + \dots \quad (3.38)$$

Unfortunately, this approach is limited because it yields unphysical results due to a problem with the analyticity: the imaginary part of the retarded self energy becomes positive in certain regions of the solution. This is most likely a result of truncating the approximating series. However, for the case of high density weak short-range scatterers, the series may be summed to give an asymptotic expansion. [2, p.626] The asymptotic expansion is necessary since the approximate series does not converge. Ultimately, it can be shown that the result yields a shape for the Landau Levels which has high and low energy tails. These tails drop off more rapidly than for a Gaussian shaped energy level which has been conjectured as the shape of the density of states. Additionally the levels approach the semi-elliptic limit as the Landau level index increases. It can also be shown that as the density of scatterers increases the effect of multiple scattering from the same impurity decreases therefore again yielding SCBA behavior.

Chapter 4

The Models and Approximations

The starting point for these calculations is based on the work of Xie, Li and Das Sarma [24] in 1990 where they set out to develop a method to extend the simple Self Consistent Born model by including the Landau level interactions. They also extend this model by including the effect of non-linear static screening via the Random Phase Approximation (RPA). This allows for the relaxation of two of the basic assumptions in the Self Consistent Born Approximation. This approach no longer requires that the Landau levels have negligible overlap, and it allows the model potential to be the much more realistic Coulomb potential as seen by the two dimensional electron gas. Of course, this is obtained by solving self-consistently for both the scattering and the screening effects. As such we will need to rely on numerical methods to generate the results in this framework.

In the course of this odyssey, we will be looking at several different models which take Landau level mixing into account. Our approach will be slightly different than that taken by Xie, Li and Das Sarma. In the first model which we will look at, we will not include the effects of the so-called “vertex correction.” As we will see, the essential characteristics of the system can be studied without the additional computational effort required by the inclusion of the vertex correction. In our second model, we will add a vertex correction to the calculation, but we will make a different approximation than that of Xie *et al.* This will be done to provide a reasonable extension of our first model. From this point, we will add the electron spin to each of the models and explain what effects that it has on the calculations.

In our next chapter, we will introduce a model which includes non-static screening introduced via the electron-electron interaction. This enhancement will produce

results that are somewhat different than these static model. We will defer further discussion of the non-static case to the next chapter.

4.1 Our First Model

In our first treatment of this system, we will essentially follow the same procedure which we applied in the Self Consistent Born approach. However, we will include a modification to the impurity potential in the form of the static screening provided by the 2DEG. We will use the Random Phase Approximation (RPA) to self-consistently calculate a static dielectric constant for this system. In diagrammatic format this is given by:

$$\Sigma_N(E) = \text{circle with } \Sigma_N \text{ inside} = \text{triangle with } N_i \text{ at top and } \times \text{ at center} \quad (4.1)$$

$$G_N(E) = \text{double arrow} = \text{single arrow} + \text{single arrow} \rightarrow \text{circle with } \Sigma_N \text{ inside} \rightarrow \text{double arrow} \quad (4.2)$$

$$u(\vec{q}) = \text{dashed line with } \times \text{ at end} = \text{wavy line} + \text{wavy line} \rightarrow \text{shaded oval} \rightarrow \text{dashed line with } \times \text{ at end} \quad (4.3)$$

$$\Pi(\vec{q}) = \text{shaded oval} = \text{double loop} \quad (4.4)$$

For our system, we will assume that the impurities are distributed randomly in a two dimensional plane which is parallel to the 2DEG and separated by a distance a from the 2DEG. One could use a more complicated distribution for the impurities along the third dimension, but the major effect would be to modify the result with an appropriately calculated structure factor. In fact, it effectively adds more disorder to the system. Yet, the basic calculation is unchanged as noted by Xi, Li and Das Sarma (1990) We will continue in these footsteps. The two dimensional Fourier transform of the impurity potential is then given by (Appendix F):

$$V_I(\vec{q}) = \frac{2\pi e^2}{\kappa q} e^{-qa} \quad (4.5)$$

where κ is the dielectric constant of the bulk material. Therefore the screened potential given by the random-phase approximation (RPA) is

$$u(\vec{q}) = \frac{V_I(\vec{q})}{\epsilon(\vec{q})} \quad (4.6)$$

where

$$\epsilon(\vec{q}) = 1 - V_{ee}(\vec{q})\Pi(\vec{q}) \quad (4.7)$$

is the static dielectric function.

$$V_{ee}(\vec{q}) = \frac{2\pi e^2}{\kappa q} \quad (4.8)$$

is the 2D Fourier transform of the electron-electron Coulomb interaction, and $\Pi(\vec{q})$ is the irreducible static polarizability. Therefore all together our diagrammatic equation (4.3) becomes

$$u(\vec{q}) = \frac{V_I(\vec{q})}{1 - V_{ee}(\vec{q})\Pi(\vec{q})} \quad (4.9)$$

$$= \frac{\frac{2\pi e^2}{\kappa q} e^{-qa}}{1 - \frac{2\pi e^2}{\kappa q} \Pi(\vec{q})} \quad (4.10)$$

$$(4.11)$$

Now our first diagram (4.1) for the self energy is

$$\Sigma_N(E) = N_i \sum_{N_2} G_{N_2}(E) \int \frac{d\vec{q}}{(2\pi)^2} |M_{N,N_2}(\vec{q})|^2 |u(\vec{q})|^2 \quad (4.12)$$

where we should recognize this as being similar to the second term of (2.51). The difference is in this equation, we are substituting the unperturbed Greens function with the full self-consistent Green's function and the impurity potential with the screened (RPA) impurity potential. (In addition, we have used the fact that $u(-\vec{q})$ is the complex conjugate of $u(\vec{q})$ for any real potential.) We will rewrite this in a slightly different form making the assignment

$$\frac{1}{4} \Gamma_{NN_2}^2 = N_i \int \frac{d\vec{q}}{(2\pi)^2} |M_{N,N_2}(\vec{q})|^2 |u(\vec{q})|^2 \quad (4.13)$$

This will allow us to write this set of equations in a manner similar to the SCB approach.

$$\Sigma_N(E) = \sum_{N_2} \frac{1}{4} \Gamma_{NN_2}^2 G_{N_2}(E) \quad (4.14)$$

Here, the Γ_{NN_2} represent the Landau level coupling constants, and the diagonal terms may be recognized as the widths of the semi-elliptic levels in the SCB approximation.

The last diagram will require a bit more work. In order to deal with this effectively at finite temperature, we will have to use the Matsubara representation of the polarizability. (Although it is a bit confusing, we will be using the same symbols for the temperature Green's functions as we do for the retarded Green's functions. The only difference will be that the arguments of the temperature functions will contain an imaginary part. This is to reduce the number of symbols which clutter the equations.) We will then generate the familiar retarded form from our final result. To begin we have:

$$\Pi(\vec{q}, i\omega) = -\frac{g_s}{3} \sum_{i\zeta_n} \sum_{\substack{N_p \\ N_2 p_2}} M_{N_p, N_2 p_2}(\vec{q}) G_N(i\zeta_n + i\omega) G_{N_2}(i\zeta_n) M_{N_2 p_2, N_p}(-\vec{q}) \quad (4.15)$$

where here we have used the full matrix elements which also depend on the momentum. One other point to notice here is that we are starting with the non-static diagram. We will later take the limit as $\omega \rightarrow 0$ in order to obtain the static result. In order to proceed we will start by considering the sum over the Matsubara fermion frequencies ($\zeta_n = \frac{(2n+1)\pi}{3}$) represented by

$$S = -\frac{1}{3} \sum_{i\zeta_n} G_N(i\zeta_n + i\omega) G_{N_2}(i\zeta_n) \quad (4.16)$$

Since we are using the self-consistent Green's functions, we will need to write them in their spectral form,

$$G_N(i\omega) = \int_{-\infty}^{\infty} dx \frac{A_N(x)}{i\omega - x} \quad (4.17)$$

Therefore S becomes

$$S = -\frac{1}{3} \int_{-\infty}^{\infty} dx \int_{-\infty}^{\infty} dy A_N(x) A_{N_2}(y) \sum_{i\zeta_n} \frac{1}{i\zeta_n + i\omega - x} \frac{1}{i\zeta_n - y}$$

$$= \int_{-\infty}^{\infty} dx \int_{-\infty}^{\infty} dy A_N(x) A_{N_2}(y) S_2 \quad (4.18)$$

where now

$$S_2 = -\frac{1}{\beta} \sum_{i\zeta_n} \frac{1}{i\zeta_n + i\omega - x} \frac{1}{i\zeta_n - y} \quad (4.19)$$

Sums of this type are covered in many textbooks. However, due to the importance of these types of sums in this subject, we will briefly layout the way to proceed. The first thing to realize is that the poles of

$$\frac{1}{e^{\beta\zeta} + 1} \quad (4.20)$$

are at exactly the fermion frequencies. Therefore

$$\frac{1}{2\pi i} \oint d\zeta \frac{F(\omega)}{e^{\beta\zeta} + 1} = -\frac{1}{\beta} \sum_{\zeta_n} F(i\zeta_n) + \sum_{\eta_m} \frac{R_m}{e^{\beta\eta_m} + 1} \quad (4.21)$$

where the η_m are the poles of $F(\omega)$ with the residues R_m . This relation will only hold if $F(\omega)$ is analytic everywhere except the simple poles at η_m . Here, we have selected a contour whose radius tends towards infinity. This implies that we also must satisfy the condition

$$\lim_{|\omega| \rightarrow \infty} |\omega F(\omega)| = 0 \quad (4.22)$$

let us note that our sum S_2 satisfies these conditions. So, we have for our case:

$$\begin{aligned} \frac{1}{2\pi i} \oint d\zeta \left(\frac{1}{e^{\beta\zeta} + 1} \right) \left(\frac{1}{\zeta + i\omega - x} \right) \left(\frac{1}{\zeta - y} \right) &= S_2 \\ &+ \left(\frac{1}{e^{\beta(x-i\omega)} + 1} \right) \left(\frac{1}{x - i\omega - y} \right) \\ &+ \left(\frac{1}{e^{\beta y} + 1} \right) \left(\frac{1}{y + i\omega - x} \right) \\ &= 0 \end{aligned} \quad (4.23)$$

since the contour we have chosen is zero. Now, we have

$$S_2 = \left[\left(\frac{1}{e^{\beta x} e^{-i\beta\omega} + 1} \right) \left(\frac{1}{x - i\omega - y} \right) + \left(\frac{1}{e^{\beta y} + 1} \right) \left(\frac{1}{y + i\omega - x} \right) \right] \quad (4.24)$$

Since ω is a boson frequency ($\omega_\nu = \frac{2\pi\nu}{j}$) the factor

$$e^{-i\delta\omega} = e^{-2\pi i\nu} = 1 \quad (4.25)$$

so that

$$S_2 = \left[\left(\frac{1}{e^{jx} + 1} \right) \left(\frac{1}{x - i\omega - y} \right) + \left(\frac{1}{e^{jy} + 1} \right) \left(\frac{1}{y + i\omega - x} \right) \right] \quad (4.26)$$

Now we can substitute this in to (4.18) which gives us

$$\begin{aligned} S &= \int_{-\infty}^{\infty} dx \int_{-\infty}^{\infty} dy A_N(x) A_{N_2}(y) \left[\left(\frac{1}{e^{jx} + 1} \right) \left(\frac{1}{x - i\omega - y} \right) \right. \\ &\quad \left. + \left(\frac{1}{e^{jy} + 1} \right) \left(\frac{1}{y + i\omega - x} \right) \right] \\ &= \int_{-\infty}^{\infty} dx \left(\frac{1}{e^{jx} + 1} \right) A_N(x) G_{N_2}(x - i\omega) \\ &\quad - \int_{-\infty}^{\infty} dy \left(\frac{1}{e^{jy} + 1} \right) A_{N_2}(y) G_N(y + i\omega) \\ &= \int_{-\infty}^{\infty} dx n_F(x) [A_N(x) G_{N_2}(x - i\omega) + A_{N_2}(x) G_N(x + i\omega)] \quad (4.27) \end{aligned}$$

Now, if we take this result and plug it back into (4.15) we have the expression

$$\begin{aligned} \Pi(\vec{q}, i\omega) &= g_s \sum_{\substack{N_p \\ N_2 p_2}} |M_{N_p, N_2 p_2}(\vec{q})|^2 \\ &\quad \times \int_{-\infty}^{\infty} dx n_F(x) [A_N(x) G_{N_2}(x - i\omega) + A_{N_2}(x) G_N(x + i\omega)] \\ &= g_s \sum_{\substack{N_p \\ N_2 p_2}} |M_{N_p, N_2 p_2}(\vec{q})|^2 \\ &\quad \times \int_{-\infty}^{\infty} dx n_F(x) [A_N(x) G_{N_2}(x - i\omega) + A_N(x) G_{N_2}(x + i\omega)] \quad (4.28) \end{aligned}$$

where we have used the symmetry of the sum over Landau level indices in order to alter the sum in the last step. We can now perform our analytic continuation, and also let $\omega \rightarrow 0$. The first term now becomes the advanced Green's function while the second term becomes the retarded greens function. Since these are complex

conjugates of each other. we may write them solely in terms of the retarded function. Therefore. for the retarded polarizability. we now have:

$$\begin{aligned}\Pi(\vec{q}, 0) &= g_s \sum_{\substack{N_p \\ N_2 p_2}} |M_{N_p, N_2 p_2}(\vec{q})|^2 \int_{-\infty}^{\infty} dx n_F(x) A_N(x) 2\text{Re}G_{N_2}(x) \\ &= -\frac{g_s}{\pi} \sum_{\substack{N_p \\ N_2 p_2}} |M_{N_p, N_2 p_2}(\vec{q})|^2 \int_{-\infty}^{\infty} dx n_F(x) \text{Im}[G_N(x)G_{N_2}(x)]\end{aligned}\quad (4.29)$$

where we have substituted the fact that $-\frac{1}{\pi}$ times the imaginary part of the retarded Green's function is equal to the spectral function. Last. taking the sum over the momenta which essentially adds the Landau level degeneracy (See Appendix B.2). we end up with:

$$\Pi(\vec{q}) = \frac{g_s}{2\pi^2 l^2} \sum_{N, N_2} |M_{N, N_2}(\vec{q})|^2 \int_{-\infty}^{\infty} dx n_F(x) \text{Im}[G_N(x)G_{N_2}(x)]\quad (4.30)$$

Therefore in summary our model becomes the self-consistent solution of the following set of equations.

$$\Sigma_N(E) = \sum_{N_2} \frac{1}{4} \Gamma_{N, N_2}^2 G_{N_2}(E)\quad (4.31)$$

$$G_N(E) = \frac{1}{E - E_N - \Sigma_N(E)}\quad (4.32)$$

$$\frac{1}{4} \Gamma_{N, N_2}^2 = N_i \int \frac{d\vec{q}}{(2\pi)^2} |M_{N, N_2}(\vec{q})|^2 |u(\vec{q})|^2\quad (4.33)$$

$$u(\vec{q}) = \frac{V_I(\vec{q})}{1 - V_{ee}(\vec{q})\Pi(\vec{q})}\quad (4.34)$$

$$\Pi(\vec{q}) = -\frac{g_s}{2\pi^2 l^2} \sum_{N, N_2} |M_{N, N_2}(\vec{q})|^2 \int_{-\infty}^{\infty} dx n_F(x) \text{Im}[G_N(x)G_{N_2}(x)]\quad (4.35)$$

Notice that the first two of these equations may be solved self-consistently given the proper set of Γ_{N, N_2} . Since these are just a simple set of real numbers. our solution to this set of equations will be very similar even under vastly different impurity potentials. In fact. we shall see in our results that we will observe this behavior.

The third equation implies that the longer the range of the interaction the more coupling will exist between the Landau levels as we would expect. Therefore. the

coupling will be more important for our Coulomb interaction than it is for a delta function interaction as in the SCBA.

In the last equation, we have the result that the polarizability is related to the overlap of the Landau levels below the Fermi Energy. If we look at the structure of the Green's functions we will realize that this quantity is primarily negative since the low energy tail of the real part of the Green's function is mostly negative and the imaginary part is negative. Therefore the strength of the potential is reduced or "screened."

Consider the situation where the Fermi energy is well above the center of level N . The real part of the Green's functions looks approximately anti-symmetric while the imaginary part looks approximately symmetric. Their product then looks anti-symmetric about the center of the level. In this case the integral of the product will tend to zero thus making the impurity interaction larger. Therefore, we should expect the lowest filled Landau levels to have the most scattering and consequently exhibit the largest level broadening. This is what we will see.

4.2 The Second Model

The step in our progression of models is to include the effects of the vertex correction. This essentially modifies our expression for the irreducible polarizability. In terms of the Feynman diagrams this is given by:

$$\Pi(\vec{q}) = \text{Diagram 1} = \text{Diagram 2} + \text{Diagram 3} \quad (4.36)$$

As is implied by the dynamics of the diagram, here we will be taking into account the interaction of "electron-hole" pairs with the impurities in the system. Here we are talking about the "hole" left in the 2DEG after an electron is excited to another state. This interaction will shorten the effective lifetime of the "electron-hole" pairs which screen the impurity potential and reducing its effect on the electrons. The

new and improved irreducible polarizability in term of the Matsubara temperature Green's functions is therefore given by:

$$\Pi(\vec{q}, i\omega) = -\frac{1}{\beta} \frac{1}{2\pi l^2} \sum_{i\zeta_n} \sum_{\substack{N_p \\ N_2 p_2}} M_{N_2 N}(-\vec{q}) G_N(i\omega + i\zeta_n) G_{N_2}(i\zeta_n) \gamma_{N N_2}(\vec{q}, i\omega + i\zeta_n, i\zeta_n) \quad (4.37)$$

where we have taken the liberty of pre-summing over the momenta as it just yields the factor of $(2\pi l^2)^{-1}$. $\gamma_{N N_2}(\vec{q}, i\omega + i\zeta_n, i\zeta_n)$ represents the vertex correction. It is given by the expression:

$$\begin{aligned} \gamma_{N N_2}(\vec{q}, i\omega + i\zeta_n, i\zeta_n) &= M_{N N_2}(\vec{q}) + \sum_{L L_2} G_L(i\omega + i\zeta_n) G_{L_2}(i\zeta_n) \\ &\times W_{N N_2, L L_2}(\vec{q}) \gamma_{L L_2}(\vec{q}, i\omega + i\zeta_n, i\zeta_n) \end{aligned} \quad (4.38)$$

where

$$W_{N N_2, L L_2}(\vec{q}) = N_i \int \frac{d\vec{q}_2}{(2\pi)^2} u(-\vec{q}_2) u(\vec{q}_2) M_{N L}(-\vec{q}_2) M_{N_2 L_2}(\vec{q}_2) e^{i(\vec{q} \times \vec{q}_2) \cdot l^2} \quad (4.39)$$

Diagrammatically these expressions are given by:

$$\gamma_{N N_2}(\vec{q}, i\omega + i\zeta_n, i\zeta_n) = \begin{array}{c} N \\ \bullet \\ \text{---} \\ \bullet \\ N_2 \end{array} = \begin{array}{c} N_2 \\ \bullet \\ \text{---} \\ \bullet \\ N \end{array} + \begin{array}{c} N \quad L \\ \text{---} \quad \text{---} \\ \bullet \quad \bullet \\ \text{---} \quad \text{---} \\ N_2 \quad L_2 \end{array} \quad (4.40)$$

$$W_{N N_2, L L_2}(\vec{q}) = \begin{array}{c} N_1 \quad L \\ \vdots \\ \times \\ \vdots \\ N_2 \quad L_2 \end{array} \quad (4.41)$$

We will approach this problem in the same manner as in the first model. Only in this case, we now have the expression for the sum as:

$$S = -\frac{1}{\beta} \sum_{i\zeta_n} G_N(i\omega + i\zeta_n) G_{N_2}(i\zeta_n) \gamma_{N N_2}(\vec{q}, i\omega + i\zeta_n, i\zeta_n) \quad (4.42)$$

If we *assume* that the vertex correction is analytic, then after the contour integration the second sum becomes:

$$S_2 = n_F(x) \left(\frac{1}{x - i\omega - y} \right) \gamma_{N,N_2}(\vec{q}, x, x - i\omega) + n_F(y) \left(\frac{1}{y + i\omega - x} \right) \gamma_{N,N_2}(\vec{q}, y + i\omega, y) \quad (4.43)$$

which gives us the result that

$$S = \int_{-\infty}^{\infty} dx n_F(x) [A_N(x) G_{N_2}(x - i\omega) \gamma_{N,N_2}(\vec{q}, x, x - i\omega) + A_{N_2}(x) G_N(x + i\omega) \gamma_{N,N_2}(\vec{q}, x + i\omega, x)] \quad (4.44)$$

This expression is a bit trickier than in our first model. In the total expression for $\Pi(\vec{q}, i\omega)$, we can use the same technique of exchanging the indices of the symmetric sum as we did previously. If we also let $\vec{q} \rightarrow -\vec{q}$ in the integral of the second sum we end up with:

$$\begin{aligned} \Pi(\vec{q}, i\omega) &= \frac{g_s}{2\pi l^2} \sum_{N,N_2} \int_{-\infty}^{\infty} dx n_F(x) A_N(x) \\ &\times [G_{N_2}(x - i\omega) M_{N_2,N}(-\vec{q}) \gamma_{N,N_2}(\vec{q}, x, x - i\omega) \\ &+ G_{N_2}(x + i\omega) M_{N,N_2}(\vec{q}) \gamma_{N,N_2}(-\vec{q}, x + i\omega, x)] \end{aligned} \quad (4.45)$$

Although it may be difficult to see, it may be shown by the symmetry of (4.38) and (4.39), that the two terms in brackets are in fact the complex conjugates of each other. Notice, that this time we cannot simply take the imaginary part of the product of the Green's functions. Therefore we have for the polarizability in our second model.

$$\begin{aligned} \Pi(\vec{q}, i\omega) &= -\frac{g_s}{\pi^2 l^2} \sum_{N,N_2} \int_{-\infty}^{\infty} dx n_F(x) \text{Im} G_N(x) \\ &\times \text{Re} [G_{N_2}(x + i\omega) M_{N_2,N}(-\vec{q}) \gamma_{N,N_2}(\vec{q}, x + i\omega, x)] \end{aligned} \quad (4.46)$$

In its current form equation (4.38) is very difficult to deal with due to the self-consistent dependency. Even though it is possible to carry out this calculation, it would prove to be very computationally intensive. With this in light, we will opt to

make the approximation that the scattering in the vertex does not alter the Landau level indices of the electrons. In other words, we will only account for the case when

$$W_{N,N_2,LL_2} \propto \delta_{NL}\delta_{N_2L_2} \quad (4.47)$$

so that we have

$$W_{N,N_2}(\vec{q}) = \frac{V_i}{2\pi} \int q_2 dq_2 u(-\vec{q}_2) u(\vec{q}_2) M_{N,N}(\vec{q}) M_{N_2,N_2}(\vec{q}) J_0(qq_2 l^2) \quad (4.48)$$

where we have also performed the integral over the angular dependence of the momentum. (The zeroth order Bessel function can be easily verified in many mathematical references as the result of integrating over the cosine factor in the cross product.)

Notice that the terms we are ignoring are second order in the overlap of the wavefunctions, so that we expect that this will be a good approximation. After making this assumption, we have:

$$\gamma_{N,N_2}(\vec{q}, i\omega + i\zeta_n, i\zeta_n) = \frac{M_{N,N_2}(\vec{q})}{1 - G_N(i\omega + i\zeta_n) G_{N_2}(i\zeta_n) W_{N,N_2}(\vec{q})} \quad (4.49)$$

where we were able to collect the terms containing γ_{N,N_2} on one side of the equation which yields great computational savings.

We must now take the static limit of this set of equations. We have the following set of equations in terms of the retarded Green's functions which we will substitute for the simple expression for the polarizability in the previous model:

$$\begin{aligned} \Pi(\vec{q}) &= -\frac{g_s}{\pi^2 l^2} \sum_{N,N_2} \int_{-\infty}^{\infty} dx n_F(x) \text{Im} G_N(x) \\ &\times \text{Re} \left[G_{N_2}(x) M_{N_2,N}(-\vec{q}) \gamma_{N,N_2}(\vec{q}, x) \right] \end{aligned} \quad (4.50)$$

$$\gamma_{N,N_2}(\vec{q}, E) = \frac{M_{N,N_2}(\vec{q})}{1 - G_N(E) G_{N_2}(E) W_{N,N_2}(\vec{q})} \quad (4.51)$$

$$W_{N,N_2}(\vec{q}) = \frac{V_i}{2\pi} \int q_2 dq_2 u(-\vec{q}_2) u(\vec{q}_2) M_{N,N}(\vec{q}) M_{N_2,N_2}(\vec{q}) J_0(qq_2 l^2) \quad (4.52)$$

4.3 The Inclusion of Electron Spin

Once we have gotten a good grasp of the previous models, we would like to include the effects of the electron spin. This is especially important in a magnetic field due to the Zeeman effect. In the systems we are studying, there is an enhancement of the spin split energy which is very apparent in magneto-resistance measurements. We would like to be able to see if we can recreate this behavior with our models.

Inclusion of spin into these models is very straight forward. Since, we have no idea about the magnetic properties of the impurities, we will assume that they contribute no direct mechanism to alter the spin of a scattered electron. In this case, the matrix elements become diagonal in the spin indices. Therefore, the equations in our first model become:

$$\Sigma_{N\sigma}(E) = \sum_{N_2} \frac{1}{4} \Gamma_{N,N_2}^2 G_{N_2\sigma}(E) \quad (4.53)$$

$$G_{N\sigma}(E) = \frac{1}{E - E_{N\sigma} - \Sigma_{N\sigma}(E)} \quad (4.54)$$

$$\frac{1}{4} \Gamma_{N,N_2}^2 = N_i \int \frac{d\vec{q}}{(2\pi)^2} |M_{N,N_2}(\vec{q})|^2 |u(\vec{q})|^2 \quad (4.55)$$

$$u(\vec{q}) = \frac{V_I(\vec{q})}{1 - V_{ee}(\vec{q})\Pi(\vec{q})} \quad (4.56)$$

$$\Pi(\vec{q}) = -\frac{g_s}{2\pi^2 l^2} \sum_{N,N_2\sigma} |M_{N,N_2}(\vec{q})|^2 \int_{-\infty}^{\infty} dx n_F(x) \text{Im}[G_{N\sigma}(x)G_{N_2\sigma}(x)] \quad (4.57)$$

where now

$$E_{N\sigma} = N\omega_c \pm \frac{1}{2}g\mu B \quad (4.58)$$

and the spin degeneracy $g_s = 1$.

If we look closely, we will see from the first two equations that the solution, for the most part, splits into two independent spin gases. The only place that there is an interaction is indirectly via the Fermi Energy in the polarizability. There is no direct exchange energy term here although one could be added in an *ad hoc* manner. So, the only difference that we should see is in the broadening of the Landau levels. This obviously will not account for the enhanced spin splitting. However, it will

provide a “more correct” broadening result. For completeness, the vertex corrected model now has the polarizability as:

$$\begin{aligned} \Pi(\vec{q}) &= -\frac{g_s}{\pi^2 l^2} \sum_{N, N_2, \sigma} \int_{-\infty}^{\infty} dx n_F(x) \text{Im} G_{N\sigma}(x) \\ &\times \text{Re} \left[G_{N_2\sigma}(x) M_{N_2, N}(-\vec{q}) \gamma_{N, N_2, \sigma}(\vec{q}, x) \right] \end{aligned} \quad (4.59)$$

$$\gamma_{N, N_2, \sigma}(\vec{q}, E) = \frac{M_{N, N_2}(\vec{q})}{1 - G_{N\sigma}(E) G_{N_2\sigma}(E) W_{N, N_2}(\vec{q})} \quad (4.60)$$

$$W_{N, N_2}(\vec{q}) = \frac{N_i}{2\pi} \int q_2 dq_2 u(-\vec{q}_2) u(\vec{q}_2) M_{N, N}(\vec{q}) M_{N_2, N_2}(\vec{q}) J_0(qq_2 l^2) \quad (4.61)$$

Again this only slightly modifies the results. Unless there are very large magnetic fields, these two spin gases will add to yield results very close to the non-spin case. Therefore, we conclude that for static RPA, our calculations will not yield any significant difference with the inclusion of spin.

Chapter 5

Living a Non-Static World

5.1 What's Wrong With Static?

One of our original goals was to understand how spin played a part in this system. Therefore this separation of spin gases was a less than satisfactory result. There must be something more to this system. There must be something which we are missing.

Searching through the literature, there were several ways to proceed. One of the directions we could have taken would be after the calculation of Xu and Vasilopoulos [25]. They included the effects of the phonon interaction with the 2DEG. Their results seem somewhat promising in predicting the spin splitting. However, it was our feeling that the same type of result could be achieved independently of the lattice. It is obvious that we must include some type of effect which allows the spin gases to shift in energy beyond the bare Zeeman effect. Let it also be noted that the approach of Xu and Vasilopoulos although self-consistent did not include the Lande g -factor enhancement in the self-consistency.

The work of Efros, Pikus and Burnett [7] had accounted for linear and non-linear electron-electron screening in the high magnetic field limit. Their approach seemed viable but their focus is toward the high field limit and the Integer Quantum Hall Effect (IQHE). Towards this end, they chose the direction of modeling the 2D random potential and concentrating on activation energies. However, the key seemed to lie somewhere in this method.

We then turned our interest towards non-static methods. As it turns out, after several failed attempts, we realized that fixed impurities (impurities with elastic

scattering) have no method of exchanging energy. Therefore, impurity scattering by itself leads to a *static* screening model since we have the requirement that $\vec{q}_1 = -\vec{q}_2$ and $\zeta_1 = \zeta_2 = 0$ at the impurity as is demonstrated by the result in equation (4.13). This fact left us with an instinctive way to proceed. First, let us look at the non-static polarizability.

5.2 The Non-static Polarizability

Recall that in our first model, we took the polarizability to be equal to the electron-hole propagator in the full self-consistent system. That is to say,

$$\Pi(\vec{q}) = \text{Diagram} \quad (5.1)$$

which ended up giving us

$$\begin{aligned} \Pi(\vec{q}, i\omega) &= \frac{g_s}{2\pi l^2} \sum_{N, N_2} |M_{N, N_2}(\vec{q})|^2 \\ &\times \int_{-\infty}^{\infty} dx n_F(x) [A_N(x)G_{N_2}(x - i\omega) + A_N(x)G_{N_2}(x + i\omega)] \end{aligned} \quad (5.2)$$

before the we took the static limit and analytic continuation. Now, let us take the analytic continuation, letting $i\omega \rightarrow E + i\delta$. Now we have

$$\begin{aligned} \Pi(\vec{q}, E) &= \lim_{\delta \rightarrow 0} \frac{g_s}{2\pi l^2} \sum_{N, N_2} |M_{N, N_2}(\vec{q})|^2 \\ &\times \int_{-\infty}^{\infty} dx n_F(x) A_N(x) [G_{N_2}(x - E - i\delta) + G_{N_2}(x + E + i\delta)] \\ &= -\frac{g_s}{2\pi^2 l^2} \sum_{N, N_2} |M_{N, N_2}(\vec{q})|^2 \\ &\times \int_{-\infty}^{\infty} dx n_F(x) \text{Im}[G_N(x)] [G_{N_2}^*(x - E) + G_{N_2}(x + E)] \end{aligned} \quad (5.3)$$

where we have expressed our results in the final equation in terms of the retarded Greens functions and $G_N^*(E)$ is the complex conjugate of $G_N(E)$ (which also happens to be an alternative representation of the advanced Green's function).

Now, let us stop a moment and look at what we are trying to do. We are looking for collective modes of the system which will effect the overall energy structure. We

are looking for the effects of the so-called “magneto-plasmons”. So, we are really looking for the zeros of the non-static dielectric function. Once we have calculated the dynamic polarizability, this is a simple task since all we need to do is plug it back into

$$\epsilon(\vec{q}, E) = 1 - V_{ee}(\vec{q})\Pi(\vec{q}, E) \quad (5.4)$$

In reality, it is not quite that simple as the impurities add sufficient scattering to the system to damp the magneto-plasma oscillations. Instead let us use the properties of

$$\left(\frac{1}{\epsilon(\vec{q}, E)} - 1 \right) = \frac{V_{ee}(\vec{q})\Pi(\vec{q}, E)}{1 - V_{ee}(\vec{q})\Pi(\vec{q}, E)} \quad (5.5)$$

It can be seen from this equation that this entity is itself a Green’s function. In fact it actually represents the propagation of a magneto-plasmon. Therefore, if we look at the imaginary part of this entity, we will have the spectral function. We then will be able to access the properties of the magneto-plasmons in the system. Notice that we can calculate, in the first approximation, the dynamic properties from the static impurity result.

5.3 Magneto-plasmons

We will take a moment here to examine the work of Smith, MacDonald and Gumbs [20]. They produced a very nice calculation of the single particle self-energy in a 2DEG in a perpendicular magnetic field using non-static screening. The approach is similar to the plasmon pole approximation used at zero magnetic field which they call the “magneto-plasmon pole” approximation. Here the effects of the collective modes of the electrons in a magnetic field are accounted for by a single magneto-plasmon pole. The frequency of this pole is determined by using both the f -sum rule and the zero-frequency Kramers-Krönig relation. [17, 13, 14] In terms of equations this approximation is given by:

$$\left(\frac{1}{\epsilon(\vec{q}, \omega)} - 1 \right) \approx -\frac{\alpha}{\pi} \left(\frac{1}{\omega - \omega_q + i\delta} - \frac{1}{\omega + \omega_q + i\delta} \right) \quad (5.6)$$

where ω_q is the frequency (energy) of the plasmon pole and α is the pole strength which is given by

$$\alpha(q) = -\pi nq \quad (5.7)$$

The static screening result then produces

$$\omega_q^2 = \frac{\alpha(q)}{\left[\frac{1}{\epsilon(q,\omega)}\right] - 1} \quad (5.8)$$

which allows us to produce the value of plasmon pole frequency. This approximation is then used to calculate a correction to the electron self-energy. In their specific model, the self energy is calculated by

$$\Sigma_{N\sigma}^{\text{RPA}}(i\omega_\nu) = -\frac{1}{3} \int \frac{d\vec{q}}{(2\pi)^2} \sum_{N_2} M_{N_1 N_2}(q) \sum_{\zeta_n} \frac{V_{ee}}{\epsilon(q, i\zeta_n)} \frac{1}{i(\omega_\nu - \zeta_n) - \omega_{N_2\sigma}} \quad (5.9)$$

Again they use the Random Phase Approximation to account for the screening where their polarizability is given by

$$\Pi(\vec{q}, E) = \frac{1}{2\pi l^2} \sum_{N_2} |M_{N_1 N_2}(\vec{q})|^2 \left(\frac{n_F(E_{N\sigma}) - n_F(E_{N_2\sigma})}{E + i\delta + E_{N\sigma} - E_{N_2\sigma}} \right) \quad (5.10)$$

Using this framework they proceed to calculate the correlation correction to the self-energy. This is given by

$$\begin{aligned} \Sigma_{N\sigma}^{\text{corr}}(E) &= \sum_{N_2} \int \frac{d\vec{q}}{(2\pi)^2} |M_{N_1 N_2}(\vec{q})|^2 V_{ee}(\vec{q}) \\ &\times \left(\frac{f_1(\vec{q}, E_{N_2\sigma})}{E - \omega_q - E_{N_2\sigma}} + \frac{f_2(\vec{q}, E_{N_2\sigma})}{E + \omega_q - E_{N_2\sigma}} \right) \end{aligned} \quad (5.11)$$

where

$$f_1(\vec{q}, E) = -\frac{\alpha(q)}{\pi} (1 - n_F(E) + n_B(\omega_q)) \quad (5.12)$$

$$f_2(\vec{q}, E) = -\frac{\alpha(q)}{\pi} (1 - n_F(E) + n_B(-\omega_q)) \quad (5.13)$$

The total self energy is given by:

$$\Sigma_{N\sigma}(E) = \Sigma_{N\sigma}^{\text{ex}}(E) + \Sigma_{N\sigma}^{\text{corr}}(E) \quad (5.14)$$

and

$$\Sigma_{N\sigma}^{\text{ex}}(E) = -(2\pi l^2) \sum_{N, N_2} \int \frac{d\vec{q}}{(2\pi)^2} |M_{N, N_2}(\vec{q})|^2 V_{ee}(\vec{q}) n_F(E_{N_2}) \quad (5.15)$$

is the electron exchange energy.

Their findings suggest that this method gives good results for the spin split enhancements at high field. They also make the statement that in their RPA model, the correlation energy is solely dependent on *inter*-Landau level excitations as the polarizability is zero if $N = N_2$. As it turns out, if there is any impurity broadening of the Landau levels, this is not strictly the case.

After assimilating this information, we now have a framework in which to proceed. We will develop our own formulation of this problem with our own form of (5.11).

5.4 Our Very Own Non-static Model

We will develop our own formulation of this problem. We will generate a correlation correction similar to (5.11) with electron-electron effects and impurity scattering. We will also opt to ignore the "vertex correction" due to the excessive computation which would be required to handle it properly. That is to say, we will be proceeding with a non-static formulation of our first model by including non-static electron-electron effects.

Therefore the model which is proposed for study is given by the following Feynman diagrams:

$$\Sigma_N(E) = \text{circle with } \Sigma_N \text{ inside} = \text{triangle with } N_i \text{ at top} + \text{dashed semi-circle} \quad (5.16)$$

$$G_N(E) = \text{thick arrow} = \text{thin arrow} + \text{thin arrow with circle } \Sigma_N \text{ in middle} \quad (5.17)$$

$$u(\vec{q}) = \text{dashed line with } x \text{ at end} = \text{wavy line with } x \text{ at end} + \text{dashed line with shaded oval in middle and } x \text{ at end} \quad (5.18)$$

$$V_{ee}(\vec{q})/\epsilon(\vec{q}, E) = \text{dashed line} = \text{wavy line} + \text{dashed line with shaded oval in middle} \quad (5.19)$$

$$\Pi(\vec{q}, E) = \text{[Diagram: a shaded oval with a central dot]} = \text{[Diagram: an empty oval with a central dot]} \quad (5.20)$$

Notice that the polarizability and subsequently the dielectric function apply to both the impurity scattering and the electron-electron scattering, yet only the static limit ($\omega = 0$) is used in calculating the screened impurity potential due to the requirement that the impurity scattering is elastic.

Since we have already talked about the non-static polarizability, let us concentrate on the self-energy which is now given by

$$\Sigma_{N\sigma}(E) = \Sigma_{N\sigma}^{\text{imp}}(E) + \Sigma_{N\sigma}^{\text{ee}}(E) \quad (5.21)$$

where we have split the contributions of the self-energy into the impurity and electron interaction parts. The first part is just the same self-energy from our static models. The second part is the heart of our discussion.

The Matsubara temperature Green's function for the electron-electron self-energy is given by

$$\Sigma_{N\sigma}^{\text{ee}}(i\omega_\nu) = -\frac{1}{3} \int \frac{d\vec{q}}{(2\pi)^2} \sum_{N_2} |M_{N,N_2}(\vec{q})|^2 \sum_{\zeta_n} \frac{V_{ee}(\vec{q})}{\epsilon(q, i\zeta_n)} G_{N_2\sigma}(i\omega - i\zeta_n) \quad (5.22)$$

This may be broken down into two further parts as

$$\Sigma_{N\sigma}^{\text{ee}}(E) = \Sigma_{N\sigma}^{\text{eeex}}(E) + \Sigma_{N\sigma}^{\text{eec}}(E) \quad (5.23)$$

which are respectively, the exchange and correlation energies. The first of these is given by:

$$\Sigma_{N\sigma}^{\text{eeex}}(i\omega_\nu) = -\frac{1}{3} \int \frac{d\vec{q}}{(2\pi)^2} \sum_{N_2} |M_{N,N_2}(\vec{q})|^2 \sum_{\zeta_n} V_{ee}(\vec{q}) G_{N_2\sigma}(i\omega - i\zeta_n) \quad (5.24)$$

and the second is given by

$$\Sigma_{N\sigma}^{\text{eec}}(i\omega_\nu) = -\frac{1}{3} \int \frac{d\vec{q}}{(2\pi)^2} \sum_{N_2} |M_{N,N_2}(\vec{q})|^2 \sum_{\zeta_n} V_{ee}(\vec{q}) \left(\frac{1}{\epsilon(q, i\zeta_n)} - 1 \right) G_{N_2\sigma}(i\omega + i\zeta_n) \quad (5.25)$$

We have done this in order to write the second expression in terms of $\frac{1}{\epsilon(q, i\zeta_n)} - 1$ which we have stated is a Green's function itself. This will allow us to decompose this expression into its spectral form.

To handle the exchange term we need to again use our path integral techniques to evaluate the frequency sum:

$$S = -\frac{1}{\beta} \sum_{\zeta_n} G_{N_2\sigma}(i\omega + i\zeta_n) \quad (5.26)$$

$$= -\frac{1}{\beta} \int_{-\infty}^{\infty} dx \sum_{\zeta_n} \frac{A_{N_2\sigma}(x)}{i\omega + i\zeta_n - x} \quad (5.27)$$

$$(5.28)$$

which reduces to evaluation the sum

$$S_2 = -\frac{1}{\beta} \sum_{\zeta_n} \frac{1}{i\omega + i\zeta_n - x} \quad (5.29)$$

Now S_2 does not exactly meet our criteria for the path integral technique since it does not behave appropriately at the boundaries. In order to deal with this we will evaluate the contour integral (using Bose frequencies, $\frac{2\pi n}{\beta}$)

$$\begin{aligned} \lim_{\tau \rightarrow 0} \frac{1}{2\pi i} \oint d\zeta \frac{1}{e^{\beta\zeta} - 1} \frac{e^{\zeta\tau}}{i\omega + \zeta - x} \\ = -S_2 + \lim_{\tau \rightarrow 0} \frac{e^{(x-i\omega)\tau}}{e^{\beta(x-i\omega)} - 1} \\ = S_2 - \frac{1}{e^{\beta x} - 1} \\ = 0 \end{aligned} \quad (5.30)$$

giving us the results that

$$S_2 = -n_F(x) \quad (5.31)$$

$$S = -\int_{-\infty}^{\infty} dx A_{N_2\sigma}(x) n_F(x) \quad (5.32)$$

$$\Sigma_{N\sigma}^{\text{eex}}(E) = -\int \frac{d\vec{q}}{(2\pi)^2} \sum_{N_2\sigma} |M_{N,N_2}(q)|^2 V_{ee}(\vec{q}) \int_{-\infty}^{\infty} dx A_{N_2\sigma}(x) n_F(x)$$

$$= \frac{1}{\pi} \int \frac{d\vec{q}}{(2\pi)^2} \sum_{N_2} |M_{NN_2}(q)|^2 V_{ee}(\vec{q}) \int_{-\infty}^{\infty} dx \text{Im}[G_{N_2\sigma}(x)] n_F(x) \quad (5.33)$$

We will now proceed to evaluate the electron-electron correlation in the same manner. First we need to express the Green's functions in (5.25) in their spectral form. Here we will use $B(\vec{q}, y)$ to denote the spectral function for $\frac{1}{\epsilon(q, E)} - 1$. So now we wish to take the sum:

$$\begin{aligned} S &= -\frac{1}{j} \sum_{\zeta_n} \left(\frac{1}{\epsilon(q, i\zeta_n)} - 1 \right) G_{N_2\sigma}(i\omega + i\zeta_n) \\ &= -\frac{1}{j} \sum_{\zeta_n} \int_{-\infty}^{\infty} dx A_{N_2\sigma}(x) \int_{-\infty}^{\infty} dy B(\vec{q}, y) \left(\frac{1}{i\zeta_n - y} \right) \left(\frac{1}{i\zeta_n + i\omega - x} \right) \end{aligned} \quad (5.34)$$

which gives us

$$S_2 = -\frac{1}{j} \sum_{\zeta_n} \left(\frac{1}{i\zeta_n - y} \right) \left(\frac{1}{i\zeta_n + i\omega - x} \right) \quad (5.35)$$

Here we are taking the sum over Bose frequencies such that $\zeta_n = \frac{2\pi n}{j}$. Therefore we have

$$\begin{aligned} &\frac{1}{2\pi i} \oint d\zeta \frac{1}{e^{j\zeta} - 1} \left(\frac{1}{\zeta - y} \right) \left(\frac{1}{\zeta + i\omega - x} \right) \\ &= -S_2 \\ &+ \frac{1}{e^{jy} - 1} \left(\frac{1}{y + i\omega - x} \right) \\ &+ \frac{1}{e^{j(x-i\omega)} - 1} \left(\frac{1}{x - i\omega - y} \right) \end{aligned} \quad (5.36)$$

which gives us

$$\begin{aligned} S_2 &= \frac{1}{e^{jy} - 1} \left(\frac{1}{y + i\omega - x} \right) + \frac{1}{e^{jx} - 1} \left(\frac{1}{x - i\omega - y} \right) \\ &= n_B(y) \left(\frac{1}{y + i\omega - x} \right) + n_F(x) \left(\frac{1}{x - i\omega - y} \right) \\ &= \frac{n_B(y) - n_F(x)}{y + i\omega - x} \end{aligned} \quad (5.37)$$

This expression may be written in many forms due to the relations

$$n_B(-x) = -n_B(x) - 1 \quad (5.38)$$

$$n_F(-x) = 1 - n_F(x) \quad (5.39)$$

We will opt to choose the following:

$$\begin{aligned} S_2 &= \frac{n_B(y) - n_F(x)}{y + i\omega - x} \\ &= \frac{-n_B(-y) - 1 - n_F(x)}{y + i\omega - x} \\ &= -\frac{n_B(-y) + n_F(-x)}{y + i\omega - x} \end{aligned} \quad (5.40)$$

which now gives us

$$S = \int_{-\infty}^{\infty} dx A_{N_2\sigma}(x) \int_{-\infty}^{\infty} dy B(\vec{q}, y) \left(-\frac{n_B(-y) + n_F(-x)}{y + i\omega - x} \right) \quad (5.41)$$

In order to make this expression more like (5.11), we are going to let $y \rightarrow -y$ and use the symmetry of the spectral function, $B(\vec{q}, -y) = -B(\vec{q}, y)$. This gives

$$S = \int_{-\infty}^{\infty} dx A_{N_2\sigma}(x) \int_{-\infty}^{\infty} dy B(\vec{q}, y) \left(\frac{n_B(y) + n_F(-x)}{i\omega - y - x} \right) \quad (5.42)$$

which is essentially (5.11) if we were to use the spectral functions in the unperturbed case:

$$A_{N\sigma}(x) = \delta(E_{N\sigma} - x) \quad (5.43)$$

$$B(y) = \delta(\omega_p - y) - \delta(\omega_p + y) \quad (5.44)$$

To continue, S becomes:

$$\begin{aligned} S &= \int_{-\infty}^{\infty} dy B(\vec{q}, y) n_B(y) G_{N_2\sigma}(i\omega - y) \\ &+ \int_{-\infty}^{\infty} dx A_{N_2\sigma}(x) n_F(-x) \left(\frac{1}{\epsilon(\vec{q}, i\omega - x)} - 1 \right) \end{aligned} \quad (5.45)$$

where we have evaluated the appropriate spectral functions. Now, we end up with the complete expression for the correlation self-energy:

$$\begin{aligned}
\Sigma_{N\sigma}^{\text{eec}}(E) &= \sum_{N_2} |M_{N,N_2}(q)|^2 \int \frac{d\vec{q}}{(2\pi)^2} V_{ee}(\vec{q}) \\
&\times \left(\int_{-\infty}^{\infty} dy B(\vec{q}, y) n_B(y) G_{N_2\sigma}(E - y) \right. \\
&+ \left. \int_{-\infty}^{\infty} dx A_{N_2\sigma}(x) n_F(-x) \left(\frac{1}{\epsilon(\vec{q}, E - x)} - 1 \right) \right) \\
\Sigma_{N\sigma}^{\text{eec}}(E) &= -\frac{1}{\pi} \sum_{N_2} |M_{N,N_2}(q)|^2 \int \frac{d\vec{q}}{(2\pi)^2} V_{ee}(\vec{q}) \\
&\times \left(\int_{-\infty}^{\infty} dy \text{Im} \left(\frac{1}{\epsilon(\vec{q}, y)} \right) n_B(y) G_{N_2\sigma}(E - y) \right. \\
&+ \left. \int_{-\infty}^{\infty} dx \text{Im}[G_{N_2\sigma}(x)] n_F(-x) \left(\frac{1}{\epsilon(\vec{q}, E - x)} - 1 \right) \right) \quad (5.46)
\end{aligned}$$

where we have used the relationship between the spectral functions and the imaginary part of the Green's functions to simplify the total expressions.

After all is said and done, we now have a complete set of equations which may be used to calculate the density of states the 2DEG self-consistently in terms of our model. The result of our work is the following set of self-consistent equations terms of the retarded functions:

$$\Sigma_{N\sigma}(E) = \Sigma_{N\sigma}^{\text{imp}}(E) + \Sigma_{N\sigma}^{\text{eex}}(E) + \Sigma_{N\sigma}^{\text{eec}}(E) \quad (5.47)$$

$$\Sigma_{N\sigma}^{\text{imp}}(E) = \sum_{N_2} \frac{1}{4} \Gamma_{N,N_2}^2 G_{N_2\sigma}(E) \quad (5.48)$$

$$\Sigma_{N\sigma}^{\text{eex}}(E) = \frac{1}{\pi} \sum_{N_2} \int \frac{d\vec{q}}{(2\pi)^2} |M_{N,N_2}(q)|^2 V_{ee}(\vec{q}) \int_{-\infty}^{\infty} dx \text{Im} G_{N_2\sigma}(x) n_F(x) \quad (5.49)$$

$$\begin{aligned}
\Sigma_{N\sigma}^{\text{eec}}(E) &= -\frac{1}{\pi} \sum_{N_2} \int \frac{d\vec{q}}{(2\pi)^2} |M_{N,N_2}(q)|^2 V_{ee}(\vec{q}) \\
&\times \left[\int_{-\infty}^{\infty} dy \text{Im} \left(\frac{1}{\epsilon(\vec{q}, y)} \right) n_B(y) G_{N_2\sigma}(E - y) \right. \\
&+ \left. \int_{-\infty}^{\infty} dx \text{Im}[G_{N_2\sigma}(x)] n_F(-x) \left(\frac{1}{\epsilon(\vec{q}, E - x)} - 1 \right) \right] \quad (5.50)
\end{aligned}$$

$$G_{N\sigma}(E) = \frac{1}{E - E_{N\sigma} - \Sigma_{N\sigma}(E)} \quad (5.51)$$

$$\frac{1}{4}\Gamma_{N,N_2}^2 = N_i \int \frac{d\vec{q}}{(2\pi)^2} |M_{N,N_2}(\vec{q})|^2 |u(\vec{q})|^2 \quad (5.52)$$

$$u(\vec{q}) = \frac{V_i(\vec{q})}{1 - V_{ee}(\vec{q})\Pi(\vec{q})} \quad (5.53)$$

$$\begin{aligned} \Pi(\vec{q}, E) &= -\frac{g_s}{2\pi^2 l^2} \sum_{N,N_2} |M_{N,N_2}(\vec{q})|^2 \\ &\times \int_{-\infty}^{\infty} dx n_F(x) \text{Im}G_N(x) [G_{N_2}^*(x-E) + G_{N_2}(x+E)] \end{aligned} \quad (5.54)$$

At this point, all that is necessary is to perform the actual calculation using a computer. Implementing the computer model itself leads to several challenging features of this calculation.

Chapter 6

The Calculations

6.1 Design Decisions

Once we have our model equations in place, we must generate the appropriate computer program to make this calculation a reality. Although we have hinted at the computational complexity of this model, one should note that our non-static calculation requires a supercomputer class of machines. With that in mind, we are going to aim at some level of efficiency.

One of the first decisions that we made was to scale the model. Typically in these systems, one scales the calculation in atomic units where lengths are scaled in terms of the Bohr radius and the energies are scaled in terms of the energies of a hydrogenic atom (Rydbergs). We have opted to scale our system in terms of the magnetic units. Therefore lengths are scaled in terms of the magnetic length, $l = \sqrt{\frac{\hbar c}{eB}}$, and energies are scaled in terms of the cyclotron energy in the system, $\hbar\omega_c = \frac{\hbar e B}{m^* c}$. This allows us, for example, to treat factors of the Landau degeneracy as, $g_L = (2\pi)^{-1}$, etc. As a whole, this will reduce the number of multiplications and allow for easy adjustment of the calculation range. This has the added advantage of allowing for simple comparison of the results of different magnetic field strengths, but we must keep this in mind when translating to standard energy units.

Another design decision was to explicitly calculate the real and imaginary parts separately instead of using Fortran's intrinsic COMPLEX type. This was to allow us to both save on extra computations when they were not needed and to allow us to use the special significances of the real and imaginary parts of the Green's functions and self-energies.

We also followed in the footsteps of Xie, Li, and DasSarma by generating the impurity density, N_i , from the zero field mobility. [24] We do this by employing the relation

$$\frac{1}{\tau_{t,s}} = \frac{2\pi m}{\hbar^3} N_i \int \frac{d\vec{q}}{(2\pi)^2} f_{t,s}(\theta) \left| u_i \left[2k_F \sin \frac{\theta}{2} \right] \right|^2 \frac{\delta(q - k_F)}{q} \quad (6.1)$$

where

$$\begin{aligned} f_t(\theta) &= 1 - \cos \theta \\ f_s(\theta) &= 1 \end{aligned} \quad (6.2)$$

describes the transport scattering and single particle scattering angular dependence respectively. Since $\tau_{t,s}$ is inversely proportional to the impurity density, it is straightforward to generate N_i from the zero field mobility. We have used the Thomas-Fermi expression for the potential to start. Therefore, keep in mind that this should be viewed as a model *parameter* rather than an experimental mobility. Using N_i directly would probably be a better idea, except that the impurity density in these samples is not a well known quantity.

6.2 Numerical Techniques

The formulation of this problem lends itself for the most part to evaluating sets of integrals. We have not chosen to implement any special integration techniques since most of the integrals can be reduced to simple sums. The only restriction on these sums is that many of them represent improper integrals which span from $-\infty$ to ∞ . The only precaution we must take here is that we make sure that our selected range of integration is large enough to contain the parts which are significantly different from zero. Such is the case with the energy range. If we let our energy range start too close to the lowest Landau level energy, the level width may become too large and a significant amount of the imaginary part of the Green's function will be unaccounted for. This will cause the calculated Fermi energy to be too large which will in turn destabilize our whole calculation.

Additionally, we do not want our Landau level widths to become too small with respect to our numerical energy grid spacing between energy points. This will yield

a poor approximation when integrating over the density of states. As a rule, we would like at least ten energy points to span the width of the energy level.

We use a binary search method to calculate the Fermi energy at finite temperature. This is done by taking an initial guess for the Fermi energy as the midpoint of the energy range, and integrating (summing) the product of the Fermi distribution function and the density of states. If our estimate gives too many electrons, we set the top of our range to the current estimate and set the new estimate to the midpoint of this new range. If we have too few electrons we choose the upper half as our new range. This process continues until we have reached the specified tolerance. Since we calculate the Fermi energy in this way, we have a very “smooth” response to changes in electron density as compared to a zero temperature result which would give changes in multiples of the energy step size. Therefore, we use a very small but finite temperature in order to calculate zero temperature properties and maintain numerical stability. We have chosen our temperatures to reflect the temperatures of “real-world” experiments.

In certain cases where special functions were not available in the mathematical libraries, we needed to resort to calculating our versions. The Laguerre polynomials are calculated via Horner's method using the standard representations for the coefficients, and using the recursive definitions for calculating the factorials. In the case of the zeroth order Bessel function, we found that not all systems have this in their libraries. Therefore, we calculated our own by splicing the Taylor series expansion and the asymptotic expansion for this function. To avoid excessive computation of these special functions in the first place, we opted to trade off size for speed by pre-calculating the matrix elements and the Bessel functions before beginning the numerical self-consistency loop.

6.3 Convergence

Although, we have written out our various self consistent models, nothing guarantees that they will converge. In our various static calculations we have taken the following approach.

To begin, we see that equations (4.31) and (4.32) may be solved independently given a set of Γ_{N,N_2} . We have found that if we generate all the quantities in a large self

consistent loop that these two equations yield various computational discontinuities which cause no end of problems with the calculation. However, since we may attack the solution of (4.31) and (4.32) independently at each energy point, we can achieve vastly improved convergence. Essentially the problem arises at the spectral edges of the Landau levels which may take thousands of iterations to converge. This behavior is caused by the fact that the relative change of the solution between iterations is largest at the discontinuous edges. Meanwhile, the centers of the Landau levels may take as few as ten iterations to converge to our given tolerance.

Using this approach, the self consistent loop is designed as follows: Given a starting set of Green's functions and a starting potential calculated in an *ad hoc* way from the zero field mobility, we then calculate the Γ_{N,N_2} which we then use to calculate the self-energies and Greens functions. Using these new Green's functions as calculated in the method above, we then calculate the static polarizability and subsequently the new version of the Fourier transformed potential which is then used to calculate the new Γ_{N,N_2} . We use a bit of admixturing of the Green's functions (a weighted sum of the old and new solution) in an *ad hoc* fashion to help stabilize the solution. This loop is continued until the Greens functions stabilize to a given tolerance. Using this method, we can achieve excellent convergence for the static model with out the vertex correction.

For the second model, we add the vertex correction, which essentially adds a step to the calculation of the potential, which involves calculating the vertex coupling, $W_{N,N_2}(\vec{q})$, before calculating the static polarizability. Otherwise the method remains unchanged. The model which includes the vertex correction does not converge as well as the model without the vertex correction. This is due to the feedback from the vertex corrections tendency to dynamically adjust the amount of Landau level broadening. The convergence is still acceptable. It should be noted however, a very small amount of "background" static scattering is added to the system to promote stability. This takes the form of a very small but non-zero imaginary part added to the self-energy. We have determined that this does not effect our results except to hasten the convergence.

6.4 Dynamic

Originally when we performed the non-static model calculation, it was not very stable. It turned out that by enforcing the Kramers-Krönig relationship between the real and imaginary parts of the Green's function, we were able to condition our system so that we now have excellent convergence.

A few special features are employed in order to speed the calculation and improve the performance. For the most part, the spectral function (also related to the imaginary part of the Green's function) for this system is zero everywhere outside of our finite range of energies (enough to include all the Landau levels plus a little buffer). The real part typically drops off as ω^{-1} . This means that if we perform integrals (approximate sums) over all energies involving the real part of the Green's functions, we will have problems. The key to handling this is to calculate the integral over the imaginary part and then use the Kramers-Krönig relationship to generate the real part. These types of integrals occur in the polarizability and in $\frac{1}{\epsilon} - 1$. This technique allows us to obtain these quantities as accurately and quickly as possible.

Once we have the polarizability and the dielectric function, we generate the non-static electron-electron self-energy. This is calculated in a few steps in order to keep the computational complexity manageable. This involves calculating the quantity

$$K_{N_1 N_2}(x) = \int_0^\infty dq q |M_{N_1 N_2}(q)|^2 V_{ee}(q) \left(\frac{1}{\epsilon(x, q)} - 1 \right) \quad (6.3)$$

This is then used to calculate $\Sigma_{N\sigma}^{\text{eec}}(E)$ via

$$\begin{aligned} \Sigma_{N\sigma}^{\text{eec}}(E) = & -\frac{1}{2\pi^2} \sum_{N_2} \int_{-\infty}^\infty dx [\text{Im}K_{N_1 N_2}(x)] n_B(x) G_{N_2\sigma}(E-x) \\ & + \text{Im}G_{N_2\sigma}(x) [(1 - n_F(x)) K_{N_1 N_2}(E-x)] \end{aligned} \quad (6.4)$$

The same type of thing may be done for the exchange energy. Here

$$\chi_{N_1 N_2} = \int_0^\infty dq q |M_{N_1 N_2}(q)|^2 V_{ee}(q) \quad (6.5)$$

and

$$\Sigma_{N\sigma}^{\text{eex}}(E) = \frac{1}{2\pi^2} \sum_{N_2} \chi_{N_1 N_2} \left[\int_{-\infty}^\infty dx \text{Im}G_{N_2\sigma}(x) n_F(x) \right] \quad (6.6)$$

We then proceed to calculate the static impurity part of the self-energy using the non-static electron-electron interaction as part of the Green's function. This allows us once again to avoid the instability at the spectral edges in the impurity scattering term of the self energy.

6.5 Calculation Times

When we developed the initial calculation based on the work of Xie *et. al.* [24], this model took several hundred iterations and several hours on a Sun workstation. After some model refinements, we reduced this time down to several minutes to obtain an answer for the static model. On a sixteen processor Cray J90, we can obtain an answer for the non-vertex static model in a few seconds. The vertex model takes somewhat longer do to the double sum over Landau level indices. (It is proportional to the square of the number of Landau levels calculated.) This fact combined with the poor convergence properties, leads to run times of several minutes on the same Cray J90.

The dynamic model is another matter entirely. The calculation time for a converged point currently is on the order of a five to ten hours of CPU time, though on a multiprocessor machine this may take only an hour or so of wall-clock time. Therefore, this calculation would not have been able to be performed with our original computational resources.

Chapter 7

The Results

7.1 A Road Map for the Discussion of the Results

Although we have deliberately kept this system as simple as possible, we are still left with a fairly large set of parameters: Impurity density, impurity plane distance, magnetic field, electron sheet density and temperature. In addition, we have six models after we include spin. To perform a full analysis of these models could take a very long time. Therefore, we will present some of the features that characterize the basic results along with some of the more intriguing aspects. We will break up our results into two categories, those results arising from basic impurity screening without including the electron-electron interactions and the result generated with the electron-electron interaction with impurity scattering. Of course, we will examine the first category in more detail since it sticks closest to the currently accepted (self-consistent Born) view of the 2DEG in a perpendicular magnetic field, and we would like to understand the ramifications of using this approximation before introducing electron-electron interactions into the model.

In this first part we will explore the differences of the four "static" models: vertex corrected vs. uncorrected and spin vs. no spin. We will look at the basic shape of the levels, and the level widths as a function of several of the parameters. From this examination, we will try to deduce the validity of the approximations and provide insight on any practical improvements. We will also briefly look at the dielectric response function using the static model as the base calculation.

In the second part, we will provide a somewhat less comprehensive look at the dynamically screened model with spin. The primary focus of this discussion will

focus on the self-consistent dielectric response function as it seems to provide the most insight into the validity of this model. We will also discuss the features of the density of states in terms of the contributions of each of the individual Landau levels.

7.2 The Statically Screened Models

We will begin with the simplest model, the one without spin and without the additional vertex correction. Our first figure (Fig. 7.1) demonstrates the basic output of the model where each of the contributions of the the Landau levels ($-\frac{1}{\pi}\text{Im}G_N(E)$) is displayed. A single state is highlighted in order to show how the electrons for a single Landau level are distributed. The overall shape of the major component of these levels is semi-elliptic in nature keeping with the theme of SCBA. This should not be much of a surprise since there is minimal overlap of the levels.

Note that the Landau levels do share electrons and that the side peaks do have a suggestive shape. By “shared” we mean that some of the electrons have energies which overlap with other Landau levels even in the presence of an energy gap. We would expect that these “shared” electrons should contribute some interesting effects to transport calculations. This would be especially interesting if one were to strengthen the boundary conditions in order to isolate the differences between electrons with different momenta.

As levels overlap more and more, the shape of the Landau levels becomes more and more “Lorentzian” in nature as shown in figure 7.2. This is important since the assumption that the levels are Lorentzian in nature does lead to reasonable predictions for the Shubnikov-de Haas oscillations at low magnetic field. [8]

In order to get a feel for the Shubnikov-de Haas oscillations and the transport properties in general, we have plotted the Fermi energy and the density of states at the Fermi energy versus magnetic field in Figure 7.3 . Here we will consider that the conductivity is essentially proportional to the density of states in the neighborhood of the Fermi energy. This is not too bad of an assumption at low temperatures. The Fermi energy might be a bit confusing in here as it is plotted in magnetic units which change with magnetic field. If one takes this into account, they will see that the Fermi energy is relatively constant at low magnetic fields and that it responds to the

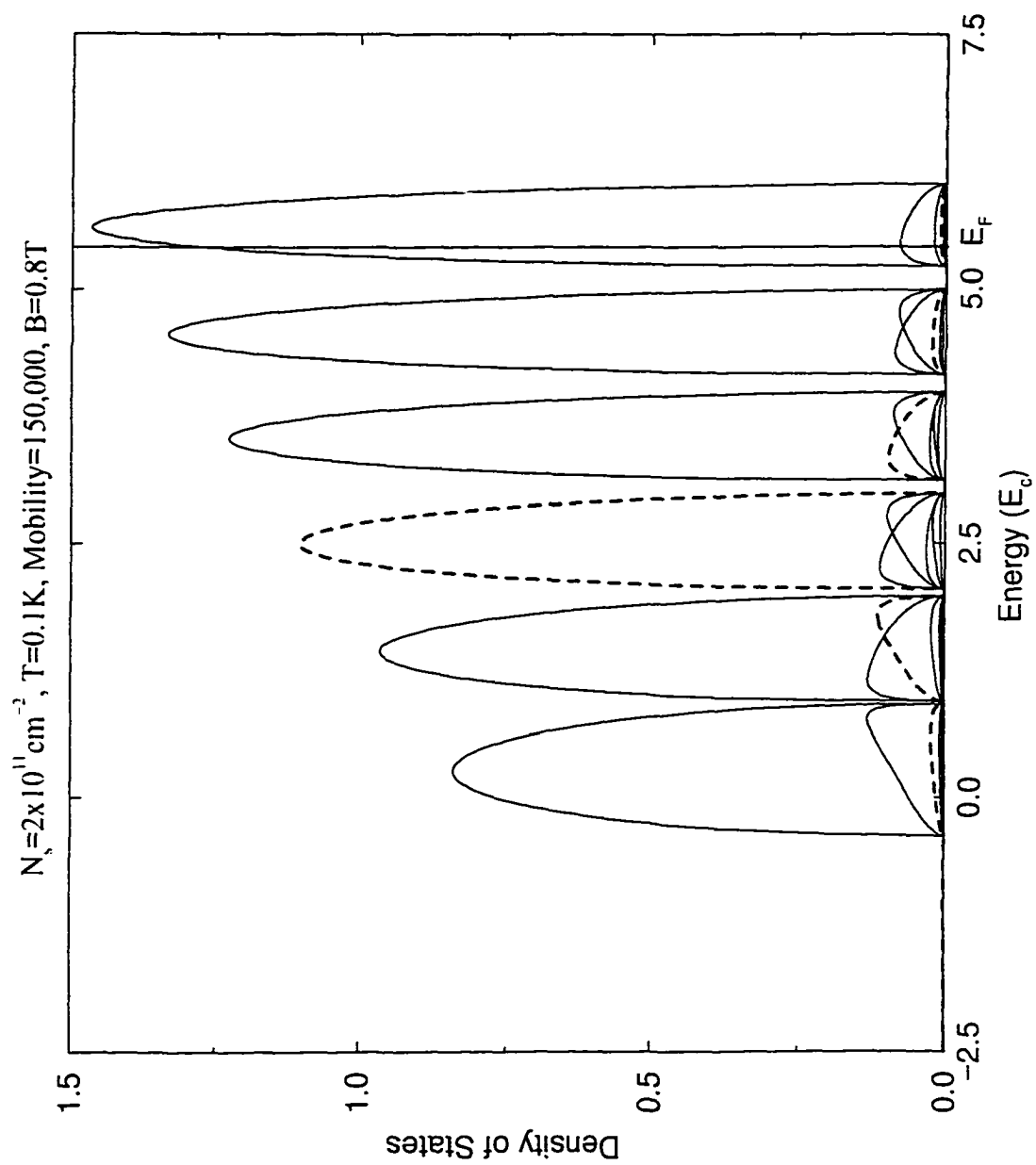


Figure 7.1: The density of states in terms of the individual Landau Levels as output from the basic model without spin and without the vertex correction. ($a = 50 \text{ \AA}$)

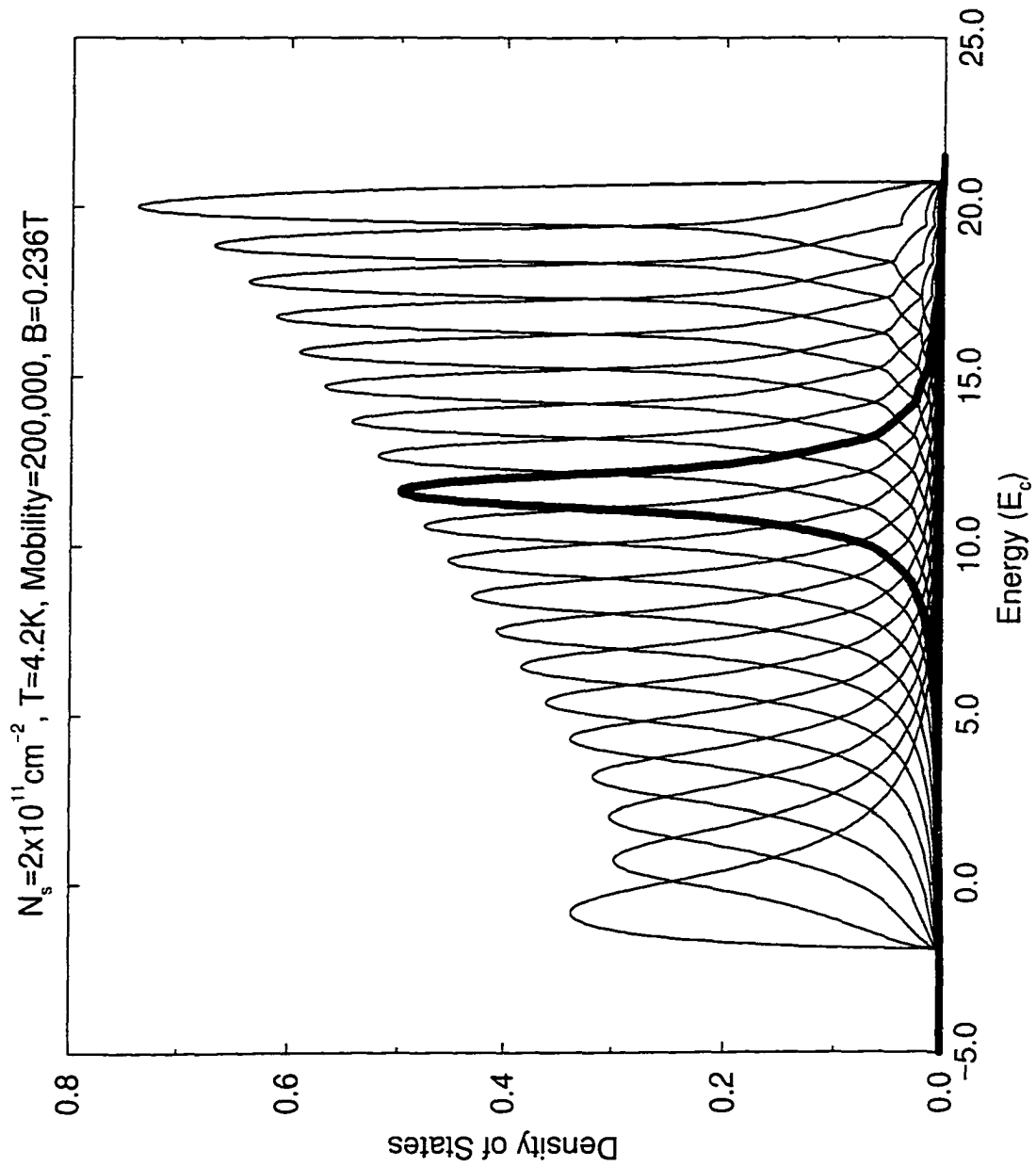


Figure 7.2: As we get many closely spaced levels the individual levels begin to take on an almost Lorentzian shape. Here we have calculate 20 spin degenerate levels and filling factor $\nu = 35$)

gaps between the Landau levels that form at higher magnetic fields. The DOS at the Fermi energy does reflect the general behavior of the Shubnikov-de Haas oscillations except for the absence of the spin split peaks which are observed at higher magnetic fields.

The widths of the Landau levels oscillate with magnetic field as indicated in Figure 7.4. When the level just above the Fermi energy is just about completely de-populated, the widths of the levels increase dramatically. This is a result of the decrease in the number electrons available for screening when a level is completely full. It is not energetically favorable for an “electron-hole pair” to form due to the large energy gap. The reduction in screening is then seen as an increase in scattering and therefore an increase in the level width. Of course, one could also view this as an attempt of the system as a whole to keep the Fermi energy as close to the zero field value as possible. The level widths of the whole system adjust accordingly.

To see some of the dependence of the level width at half the maximum value versus Landau level index, let us look at Figure 7.5. This shows the general inverse relationship between the level index and the level width for a system of many occupied Landau levels ($\nu = 35$). The anomalies at the ends are due to the sharp semi-elliptic peaks in the highest and lowest level in the calculation. Since we can not realistically calculate an infinite number of levels, we can assume this behavior continues beyond our calculated limit.

Figures 7.6 and 7.7 represent the level width versus the mobility at filling factors $\nu = 6$ and $\nu = 7$. There is a general inverse relationship between the mobility and the level width. Of course the mobility which we calculate is inversely proportional to the impurity density.

The last parameter which we will consider is the distance of the impurity plane from the 2DEG. The overall result is shown in figure 7.8 which demonstrates the inverse relationship between the impurity distance and the widths of the levels. We should be very careful about how we interpret these results as N_i , the impurity density is calculated from the “zero field mobility” using this parameter along with the electron sheet density. Therefore, the results here show the qualitative behavior which we would expect by changing the distance between the impurities and the

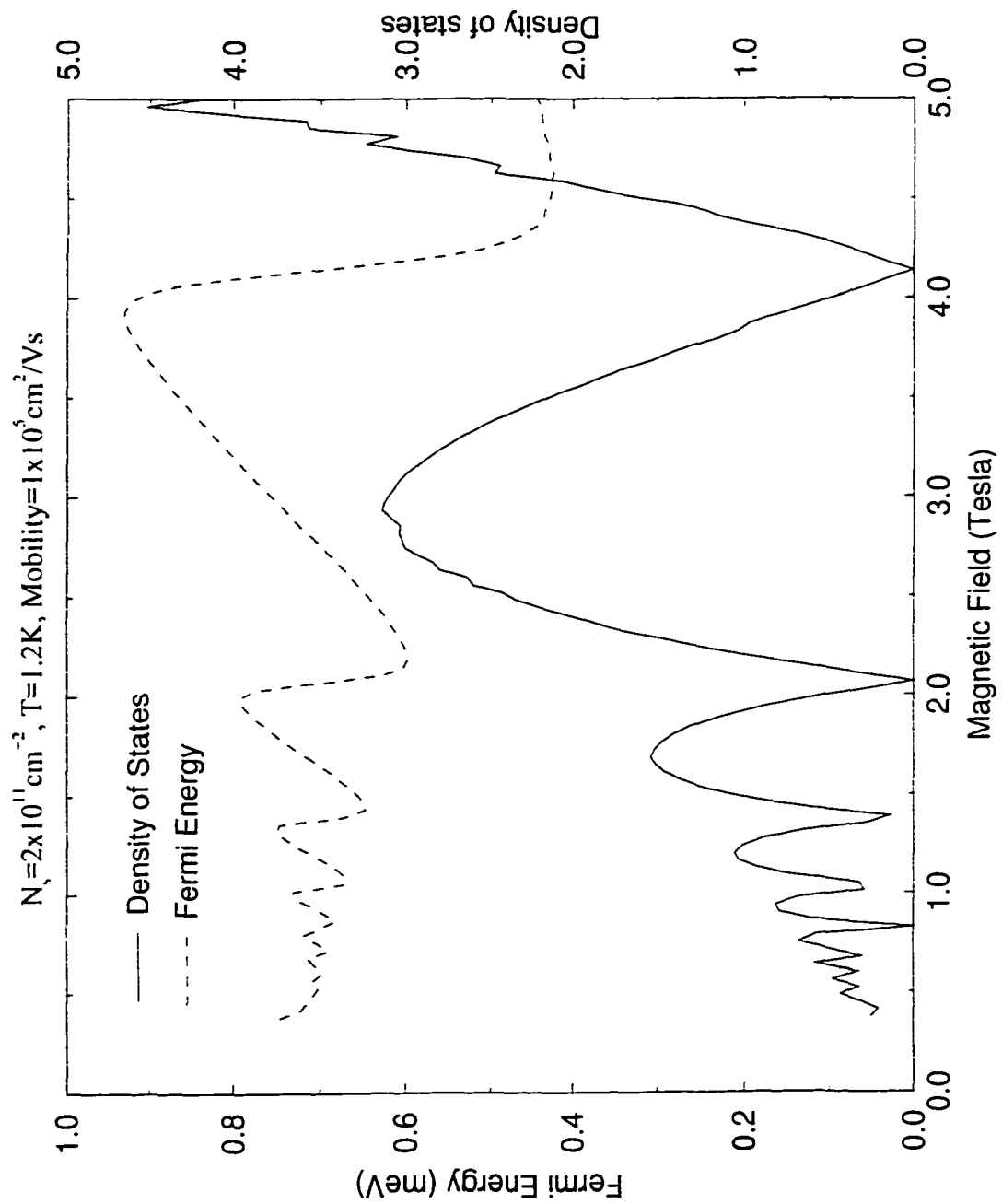


Figure 7.3: The density of states and the Fermi energy plotted as a function of magnetic field.

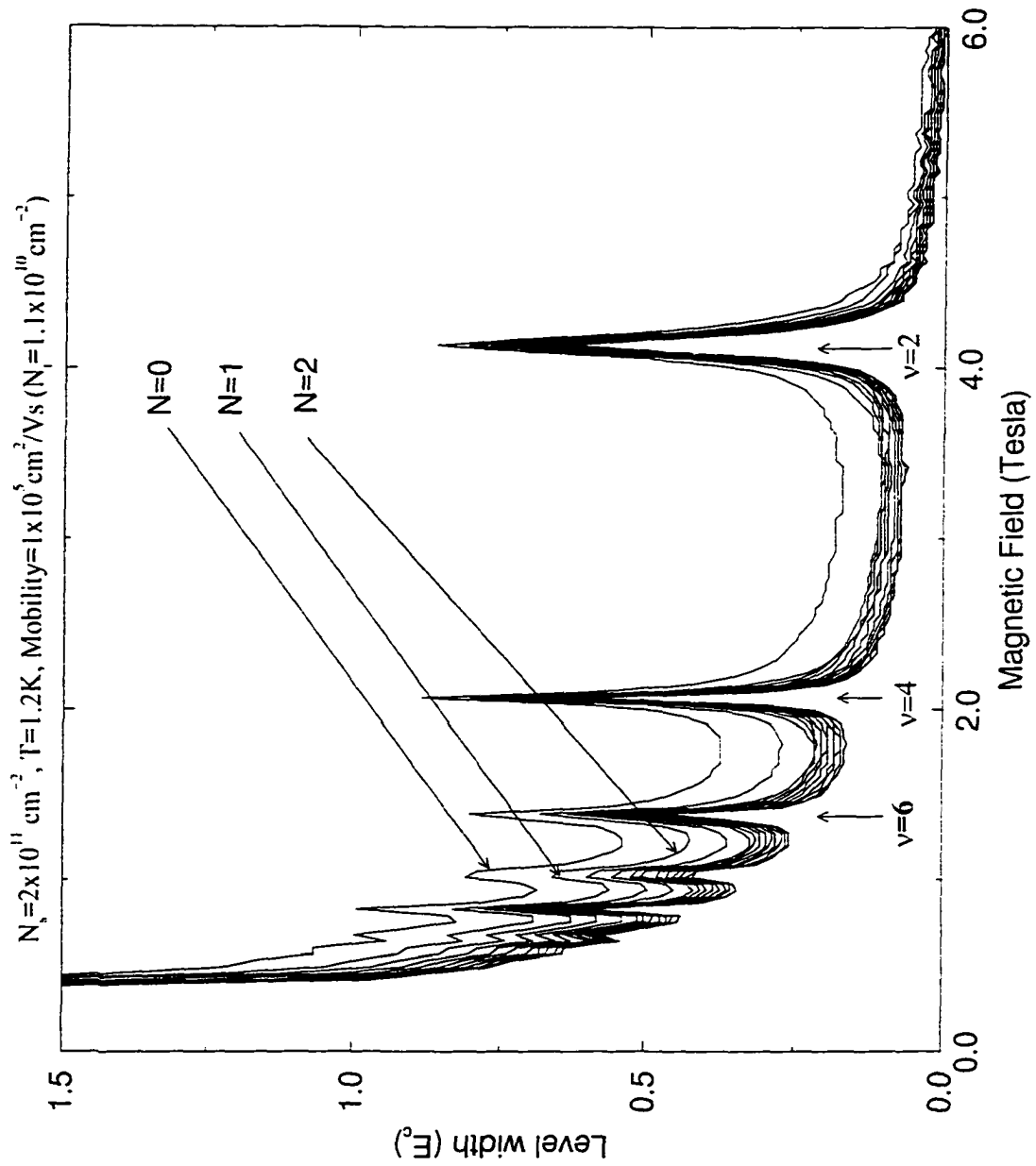


Figure 7.4: The Landau Level widths vs. magnetic field without the vertex correction or spin included in the calculation.

$N_s=2 \times 10^{11} \text{ cm}^{-2}$, $T=4.2\text{K}$, Mobility=200,000, $B=0.236\text{T}$

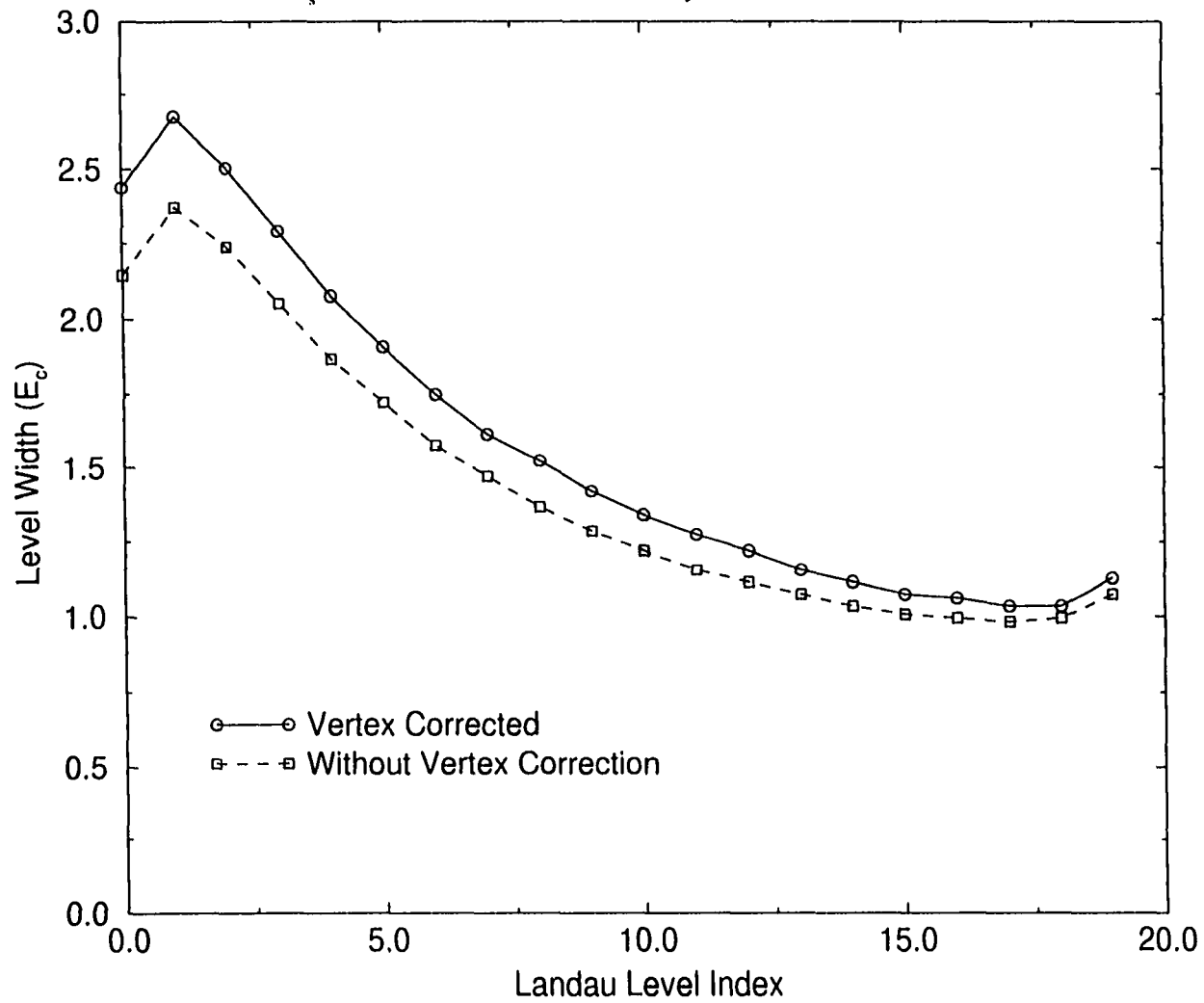


Figure 7.5: The Landau Level widths vs. Landau Level index.

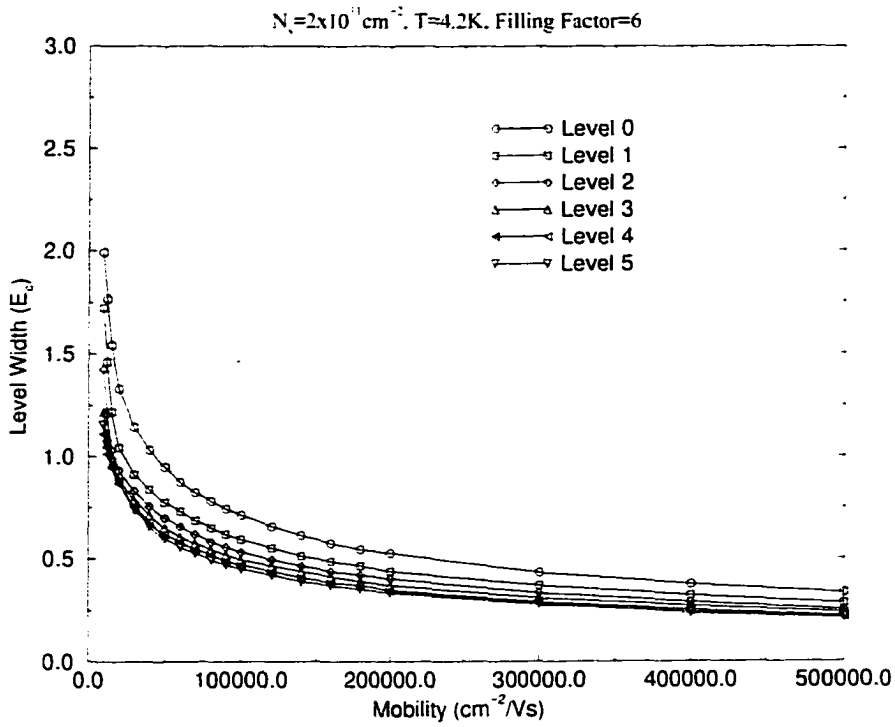


Figure 7.6: The Landau Level widths vs. mobility for $\nu = 6$ without the vertex correction.

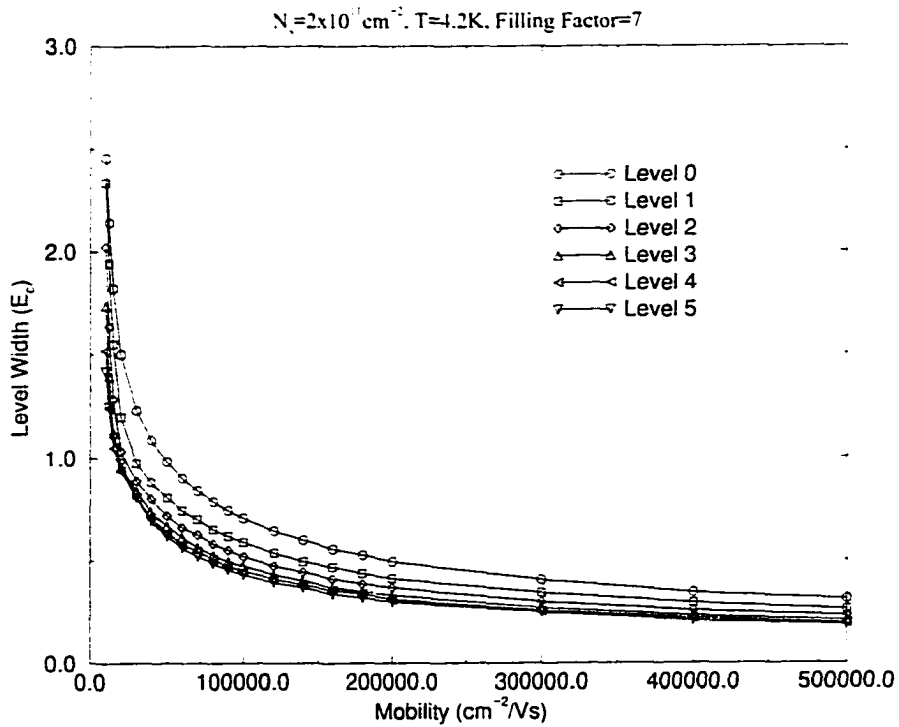


Figure 7.7: The Landau Level widths vs. mobility for $\nu = 7$ without the vertex correction.

2DEG: as the impurities get closer to the 2DEG the effective scattering time is reduced thus increasing the level width and decreasing the mobility.

This brings us to the point where we can discuss the effects that the vertex correction has on this calculation. At first glance we notice that the result produces wider Landau levels than the corresponding result without the vertex correction indicating that the screening in the system is reduced. We have already predicted that this factor would reduce the screening. The question remains about whether our specific approximation of the vertex correction has yielded reasonable results.

If we look at figure 7.9 we see that the level widths for the vertex corrected model are definitely wider. To get some insight into what causes this, let us refer to figure 7.10 where we can see that the magnitude of the polarizability is smaller for the vertex corrected model especially at low q . This tells us that the long range interaction is stronger for the vertex corrected model. At high q (short range) the two models become virtually identical. In 7.11, we see that by lowering the mobility, the polarizability of the vertex corrected model becomes more like that of the simpler model. The vertex correction reduces the strength of the polarization of the electron gas by including the effects of scattering on the polarizability. Another interesting facet of the relationship of the polarizability between the two models is the dependence on magnetic field or more accurately the filling factor. Figure 7.13 shows that at $\nu = 4$ both models display a very similar polarizability. Meanwhile at $\nu = 5$ (figure (7.15)), the polarizability displays a very different behavior. Remember that both of these results are coming from models which neglect the spin split energy, and here, we are using the filling factor from the spin model. So we are really comparing the results between a fully populated level and a half populated which lies just below the Fermi energy. We have already noted that as the scattering increases the two polarizabilities become more alike. We also see that the levels widths increase (leading to increased scattering) at even numbered filling factors.

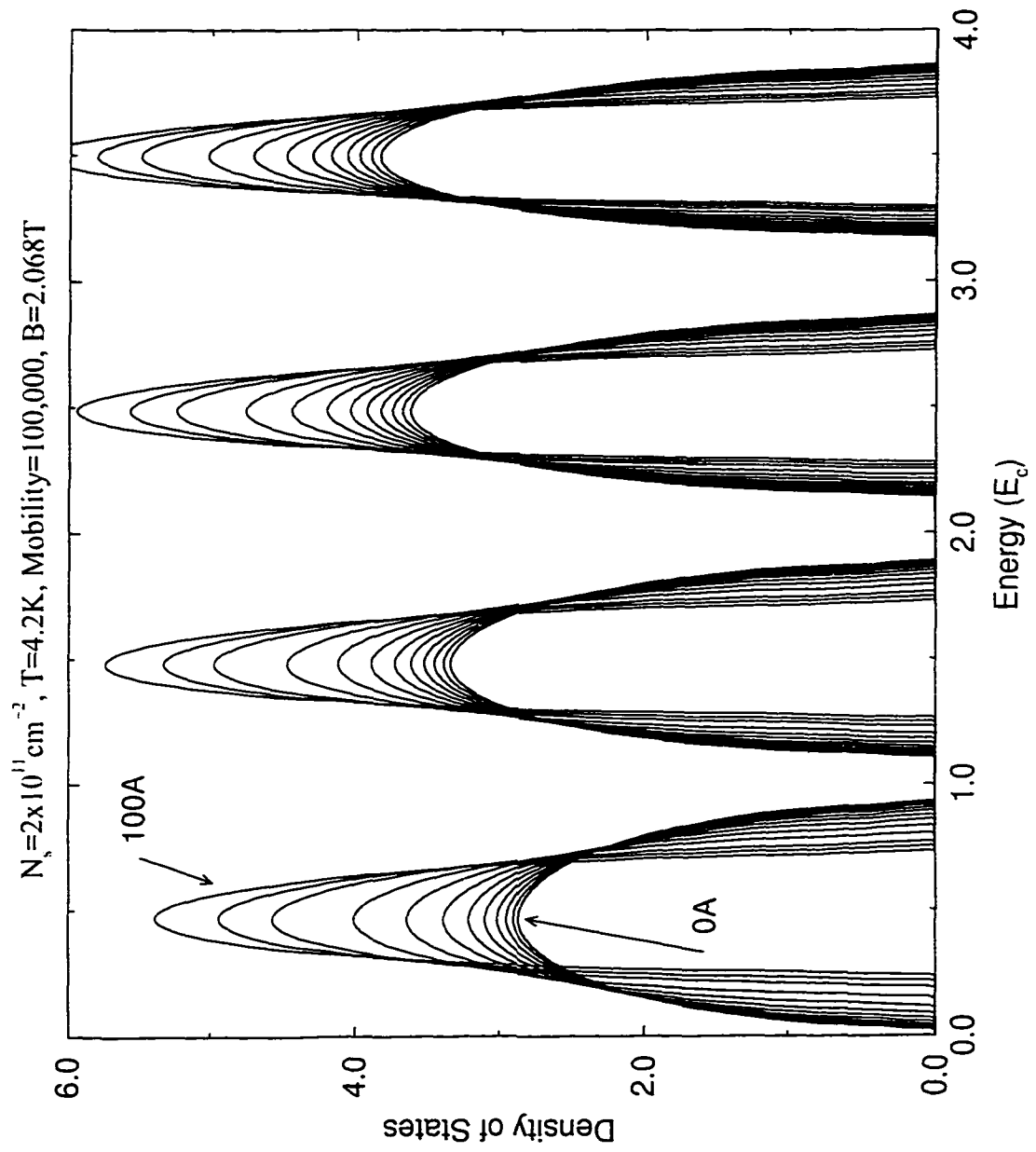


Figure 7.8: The Landau Level widths vs. the impurity plane distance a .

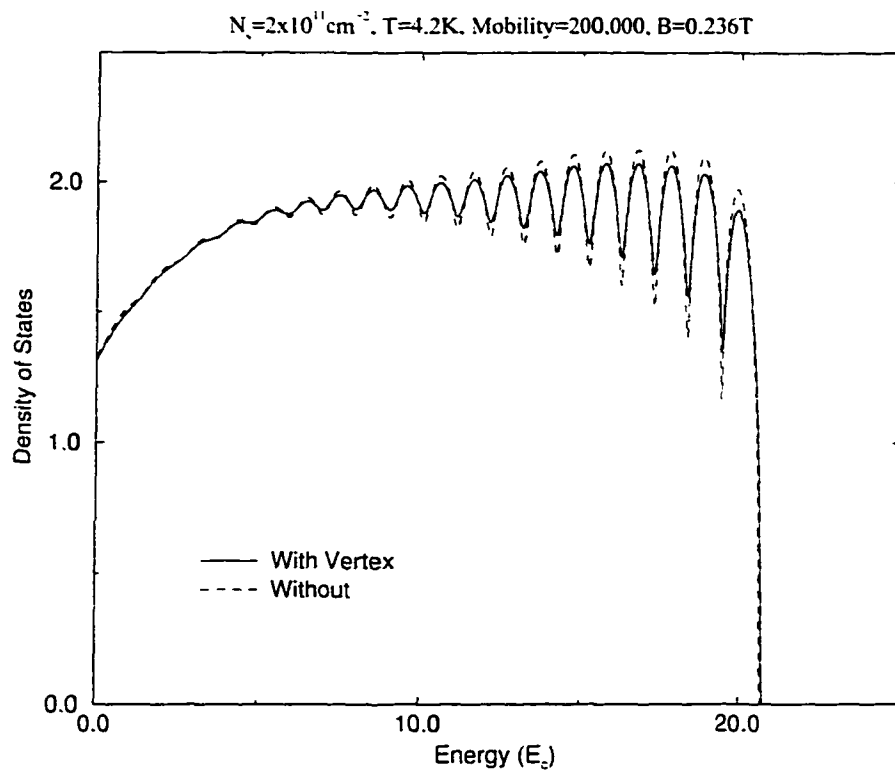


Figure 7.9: A comparison of the density of states with and without the vertex correction at $\nu = 35$. ($\mu = 200,000$)

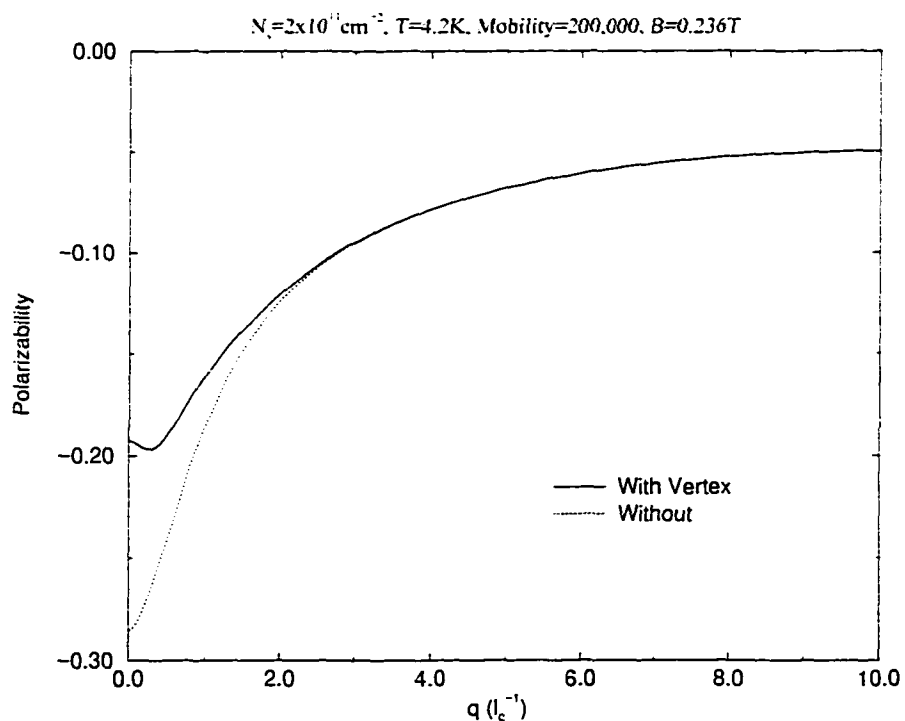


Figure 7.10: A comparison of the static polarizability with and without the vertex correction at $\nu = 35$. ($\mu = 200,000$)

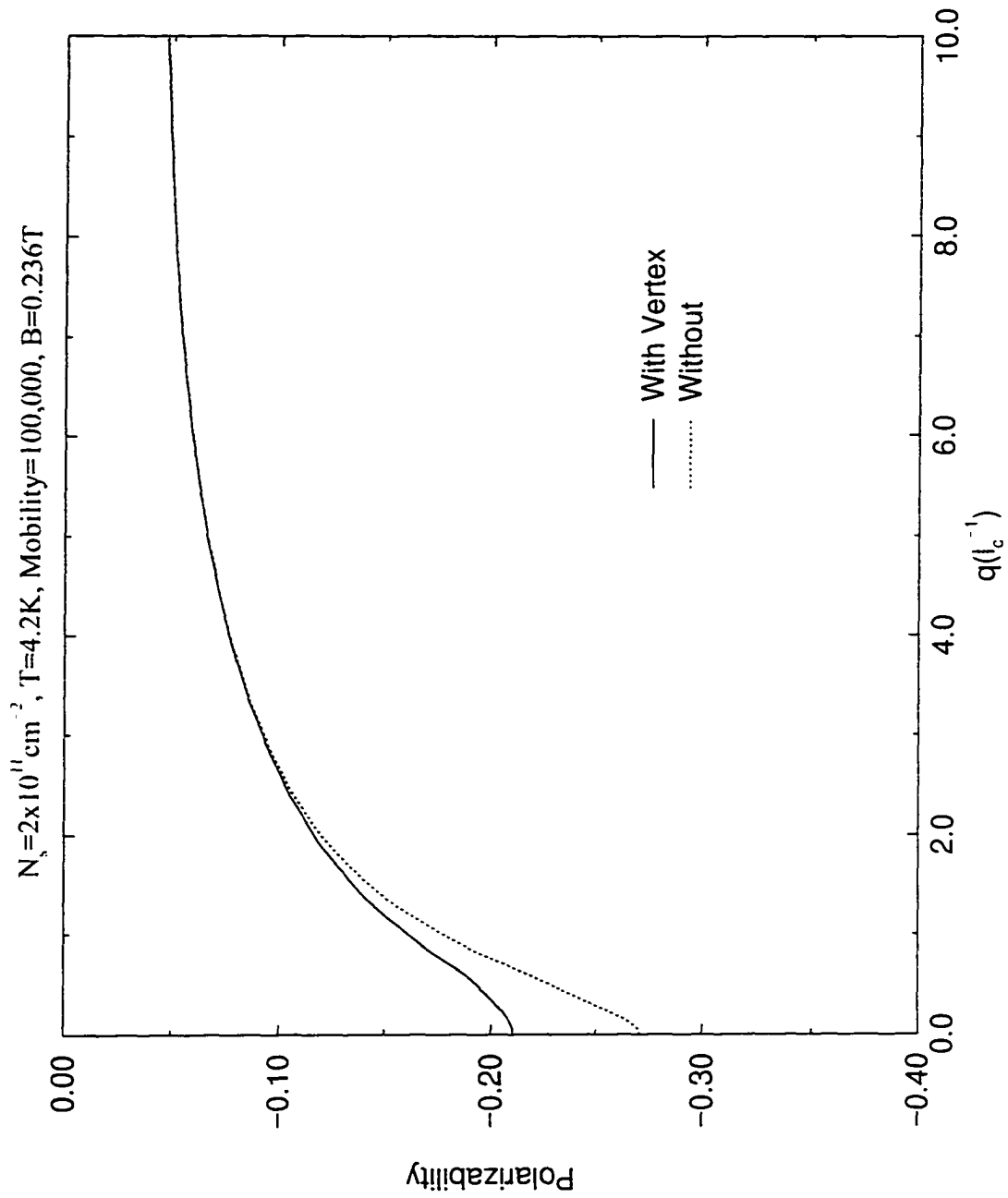


Figure 7.11: A comparison of the static polarizability with and without the vertex correction at $\nu = 35$ at a lower mobility. ($\mu = 100,000$)

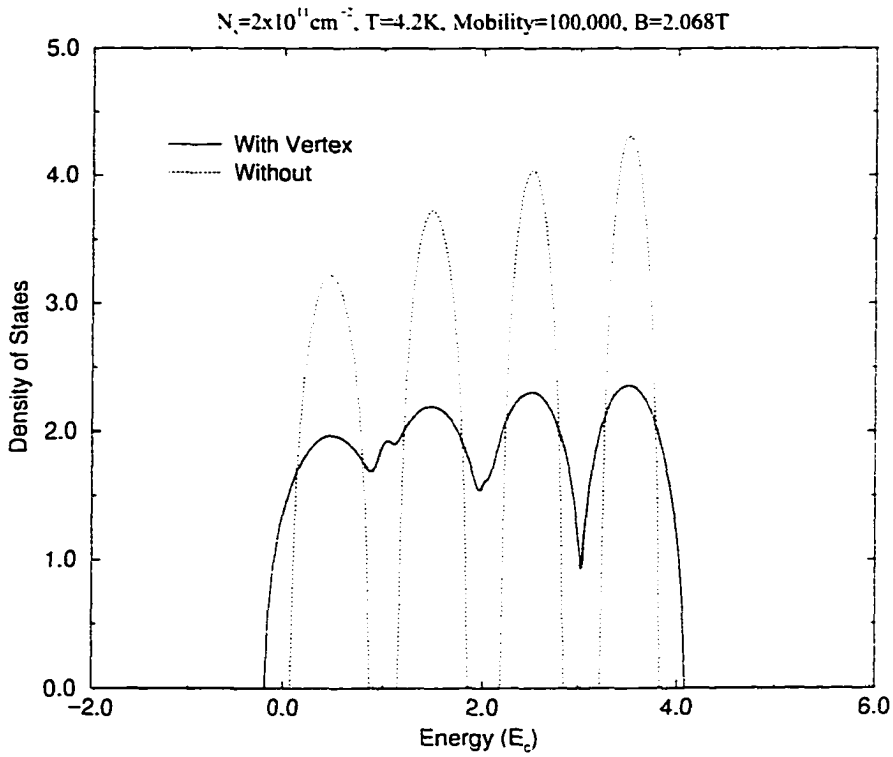


Figure 7.12: A comparison of the density of states with and without the vertex correction at $\nu = 4$.

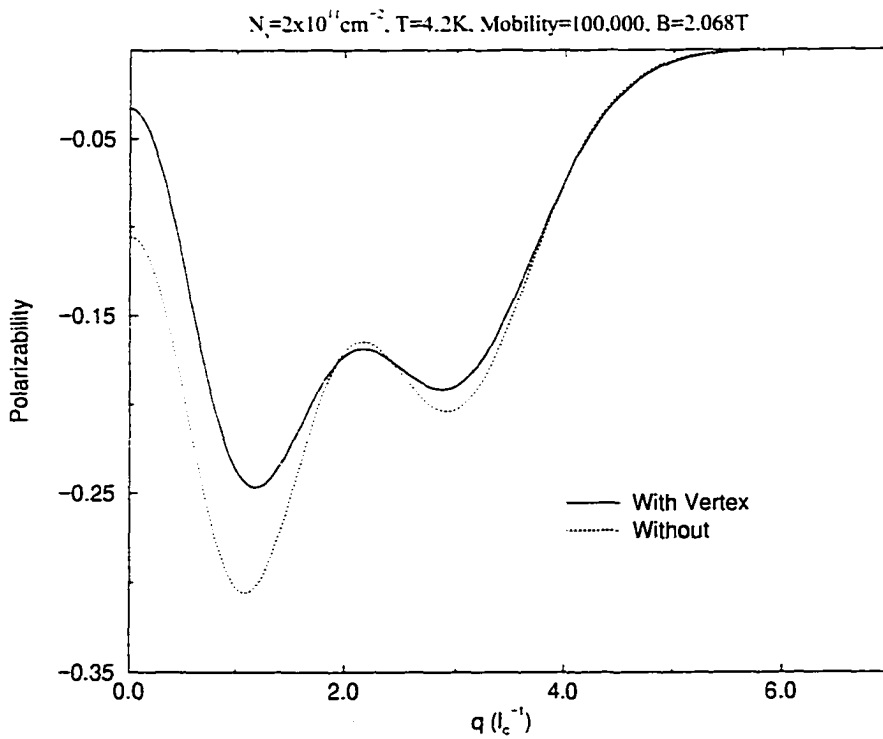


Figure 7.13: A comparison of the static polarizability with and without the vertex correction at $\nu = 4$.

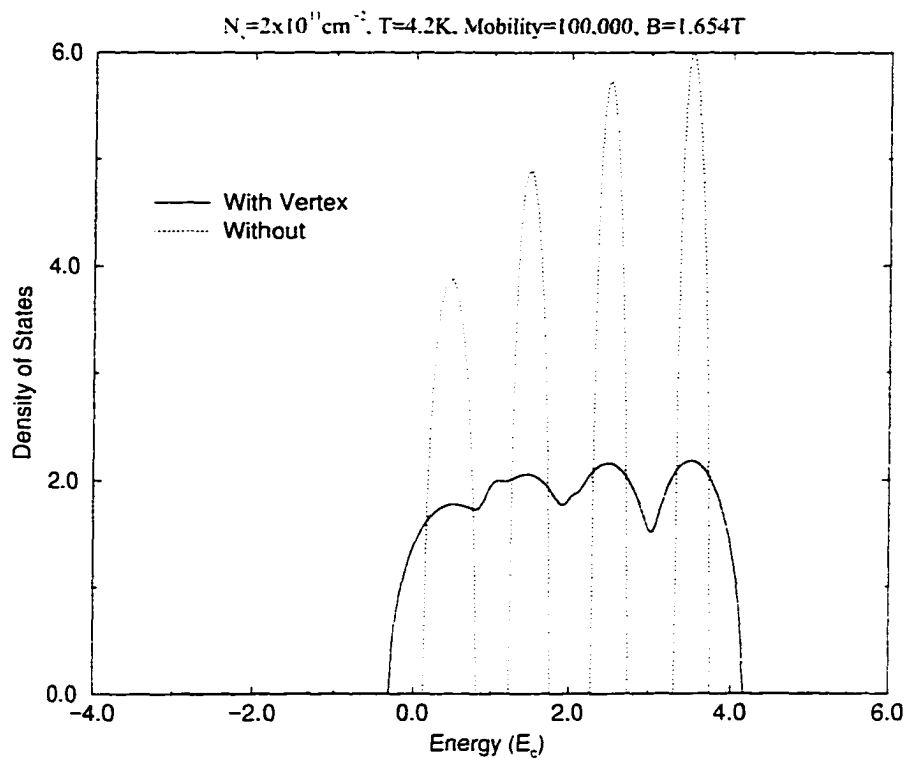


Figure 7.14: A comparison of the density of states with and without the vertex correction at $\nu = \bar{5}$.

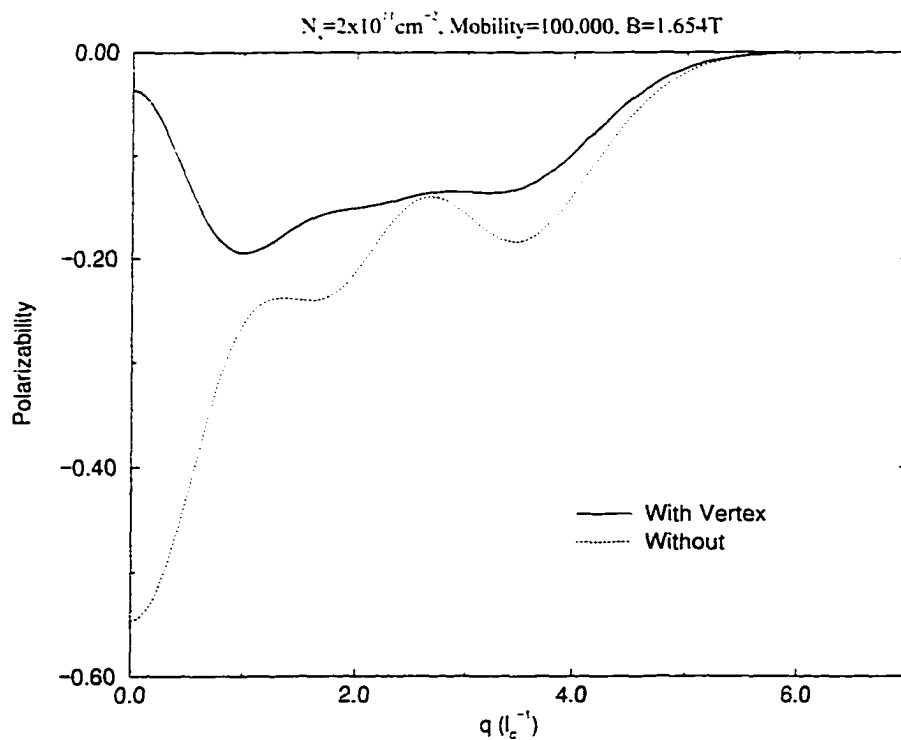


Figure 7.15: A comparison of the static polarizability with and without the vertex correction at $\nu = \bar{5}$.

The comparisons of the density of states for these cases are displayed in figures 7.12 and 7.14 where we can see the relative differences in the level widths. The artifacts which are apparent between the first and second Landau level peaks arise as a result of the overlap of two semi-elliptic states. This suggests that the vertex corrected model gives a Landau level width dependence which is closer to SCB than the uncorrected model. This can be viewed as a result of the reduction in *inter-Landau level interaction* by including the vertex. This also has the effect that the level widths do not change as much with filling factor as the uncorrected model.

The Landau level widths at half maximum versus the mobility for the vertex corrected model are shown in figures 7.16 and 7.17 as compared with the results from the model without the vertex correction presented in figures 7.6 and 7.7. In the vertex corrected model, there is a sharp saturation at $\mu = 50,000 \text{ cm}^2/\text{V}\cdot\text{s}$ where the level width does not want to decrease below $\hbar\omega_c$. In fact we actually see a slight increase in width with magnetic field which is more noticeable at $\nu = 7$. This is an odd behavior which suggests that something is “wrong” with vertex corrected model. In fact, the range of this graph is limited since the numerical results at higher mobilities do not converge. This problem seems to arise as the polarizability suddenly displays a small positive value at $q = 0$ which severely overestimates the long range interaction of the electron gas as the system gets near to a solution which then causes the numerical calculation to fail dramatically. The calculation then essentially resets itself, begins to converge, and then repeats the whole process again. This strongly suggests that our vertex correction over-estimates the reduction in screening.

So far we have not included spin in these discussions. For the calculations we have displayed the spin split energy is $1.47 \times 10^{-2} \hbar\omega_c$ which is a small fraction of these level widths. Therefore, we do not expect to see any significant difference in the results unless we are looking at high density, high magnetic fields and high mobility. Figure 7.18 which displays the density of states at the Fermi energy versus magnetic field highlights this fact using the model without the vertex correction.

We did not obtain usable results for the magnetic field runs using the vertex correction. This is as a result of the instability which we mentioned above.

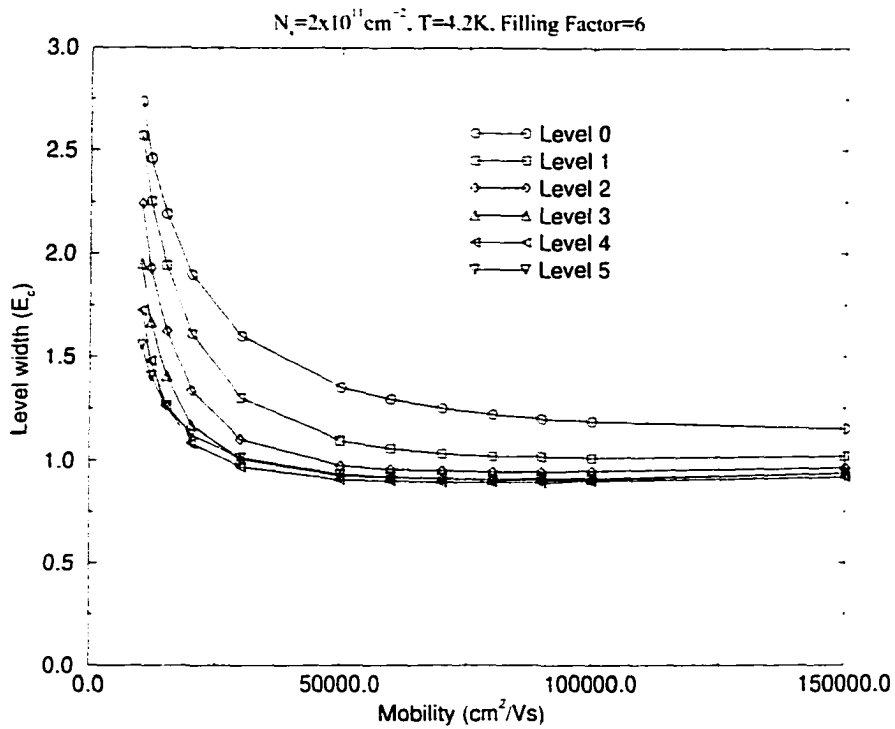


Figure 7.16: The Landau Level widths vs. mobility for $\nu = 6$ with the vertex correction.

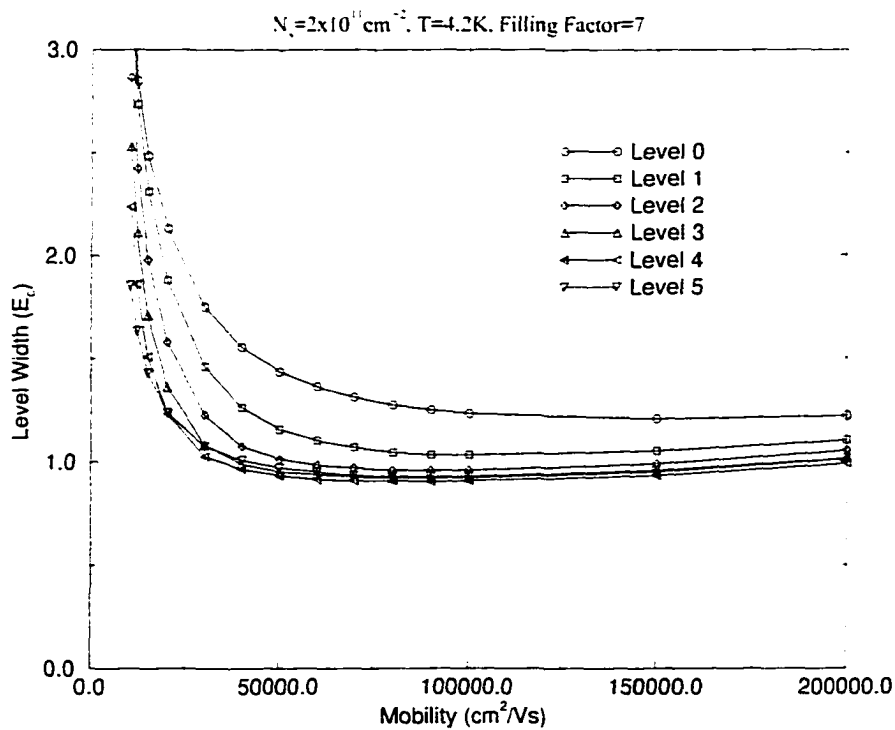


Figure 7.17: The Landau Level widths vs. mobility for $\nu = 7$ with the vertex correction.

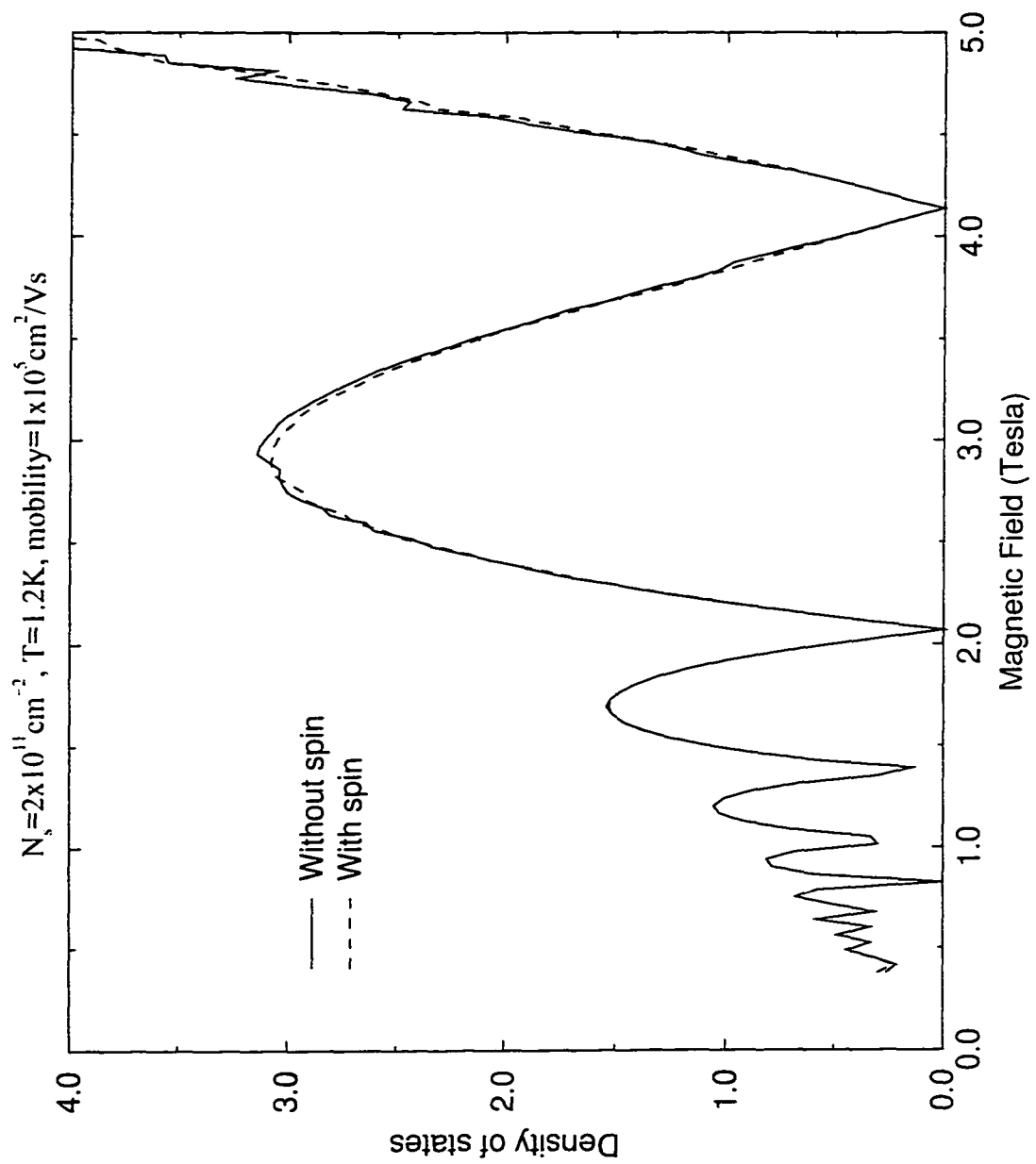


Figure 7.18: The density of states for the non-vertex model with and without spin plotted as a function of magnetic field.

In order to gain insight into our next set of calculations, let us take a brief look at the response function as a function of both momentum and energy, using the static model with spin and without the vertex correction as our starting point. Figure 7.19 demonstrates the type of peaks we develop in the response functions which are suggestive of the magneto-plasmon modes. We will see a slightly different result in our calculation which includes the dynamic electron screening.

7.3 Including Electron-Electron Effects

After looking at the statically screened impurity scattering model in some detail, it is time to focus on the output of the model which includes the electron-electron interactions which we have called the non-static model. It will become readily apparent that neglecting the collective motion of the electron gas as we did in the static model is a gross oversimplification of the system. We will find that the dynamic properties and active modification of the energy level positions and widths are key properties of this system.

To begin, we will look at a system with many Landau levels. We chose this as a starting point because a system with a large number of filled levels will not display large exchange energy effects. The basic results are shown in figure 7.20 where we are comparing the static and non-static models. In this graph, we have aligned the Fermi Energies of both models to $E = 0$ since the results of the two models are offset by the large exchange energies. (In an experimental system, typically we measure everything from the Fermi-energy anyhow, and we have already arbitrarily chosen the zero energy point anyhow.) As we can see the difference in behavior is quite large. Looking at the contribution from each of the individual levels in figure 7.21, we immediately see that most of the the levels are not semi-elliptic but instead have long negative tails. It is true that we saw this type of behavior in the static model due to the level overlap, but here even the lowest Landau level displays this feature. We will also notice that as the levels increase in energy toward the Fermi level, the shapes of the levels start to become more abrupt and begin to take on the shape found in the Many-Site Approximation.

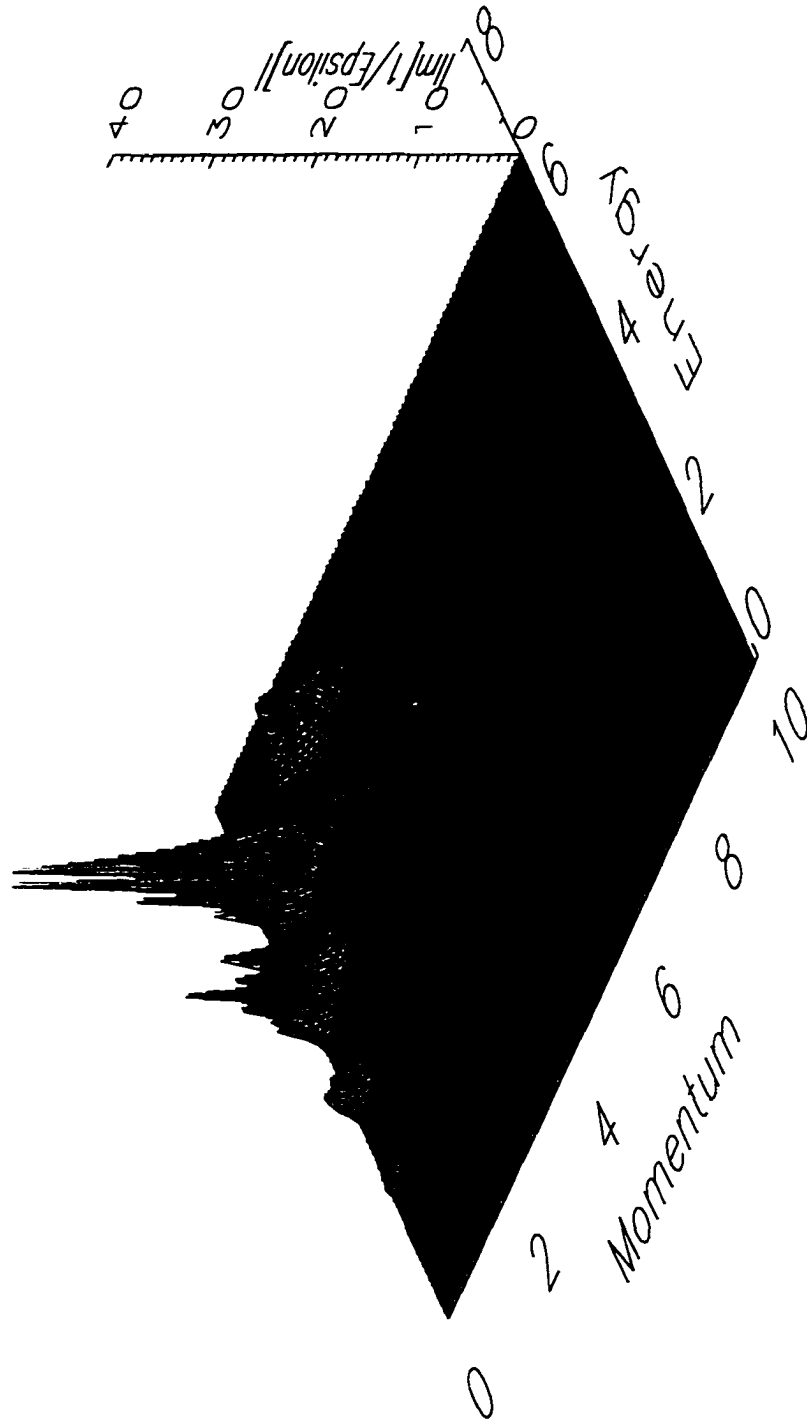


Figure 7.19: $\text{Im} \frac{1}{\epsilon(q,E)}$ as calculated from the Green's functions resulting from the static impurity model. ($N_s = 2 \times 10^{11} \text{cm}^{-2}$, $\mu = 100,000 \text{cm}^2/\text{Vs}$, $T = 4.2 \text{K}$, $a = 50 \text{\AA}$, $B = 1.378 \text{T}$)

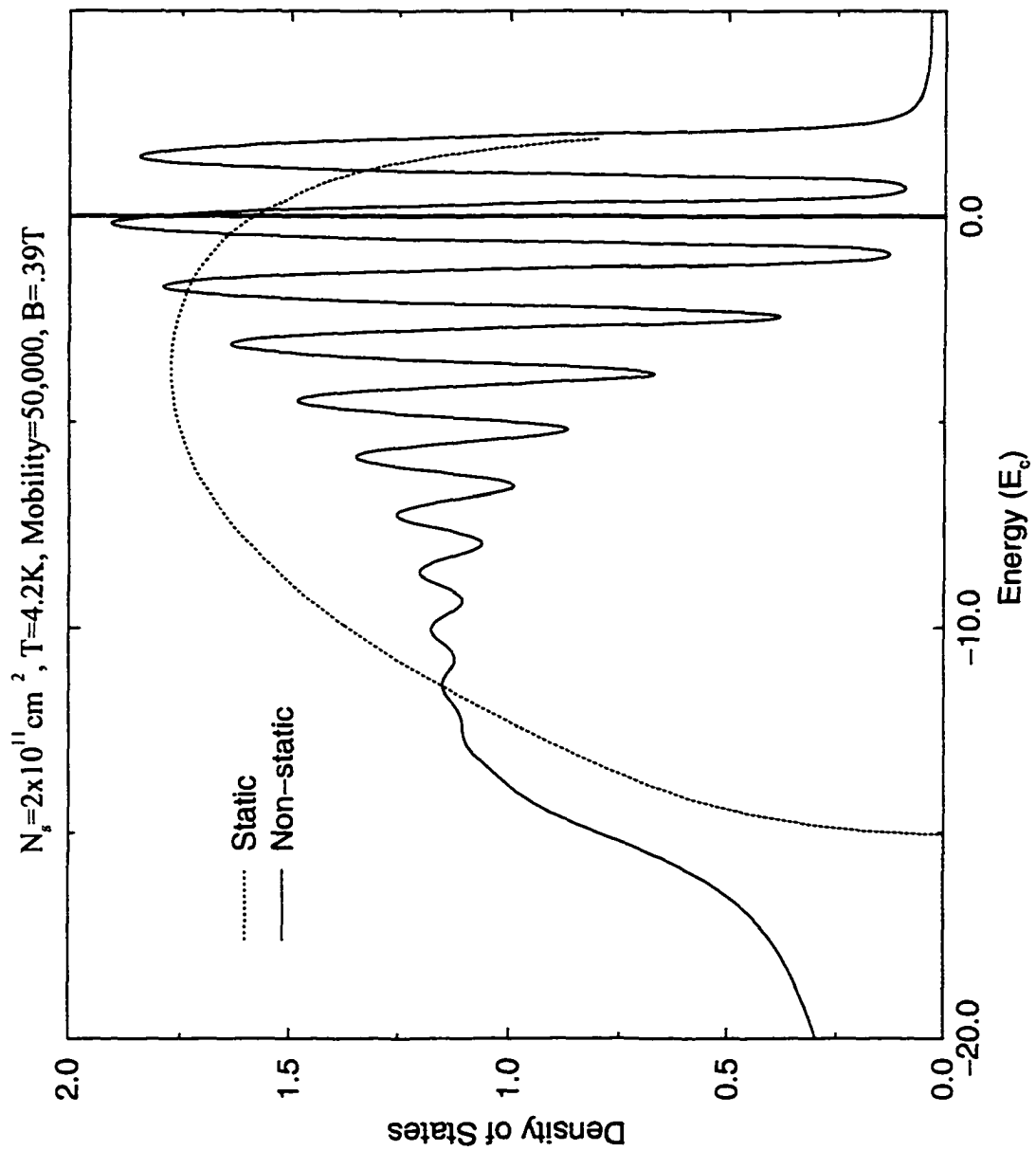


Figure 7.20: A comparison between the output of the static and non-static models. Here the Fermi Energies have been aligned at $E = 0$.

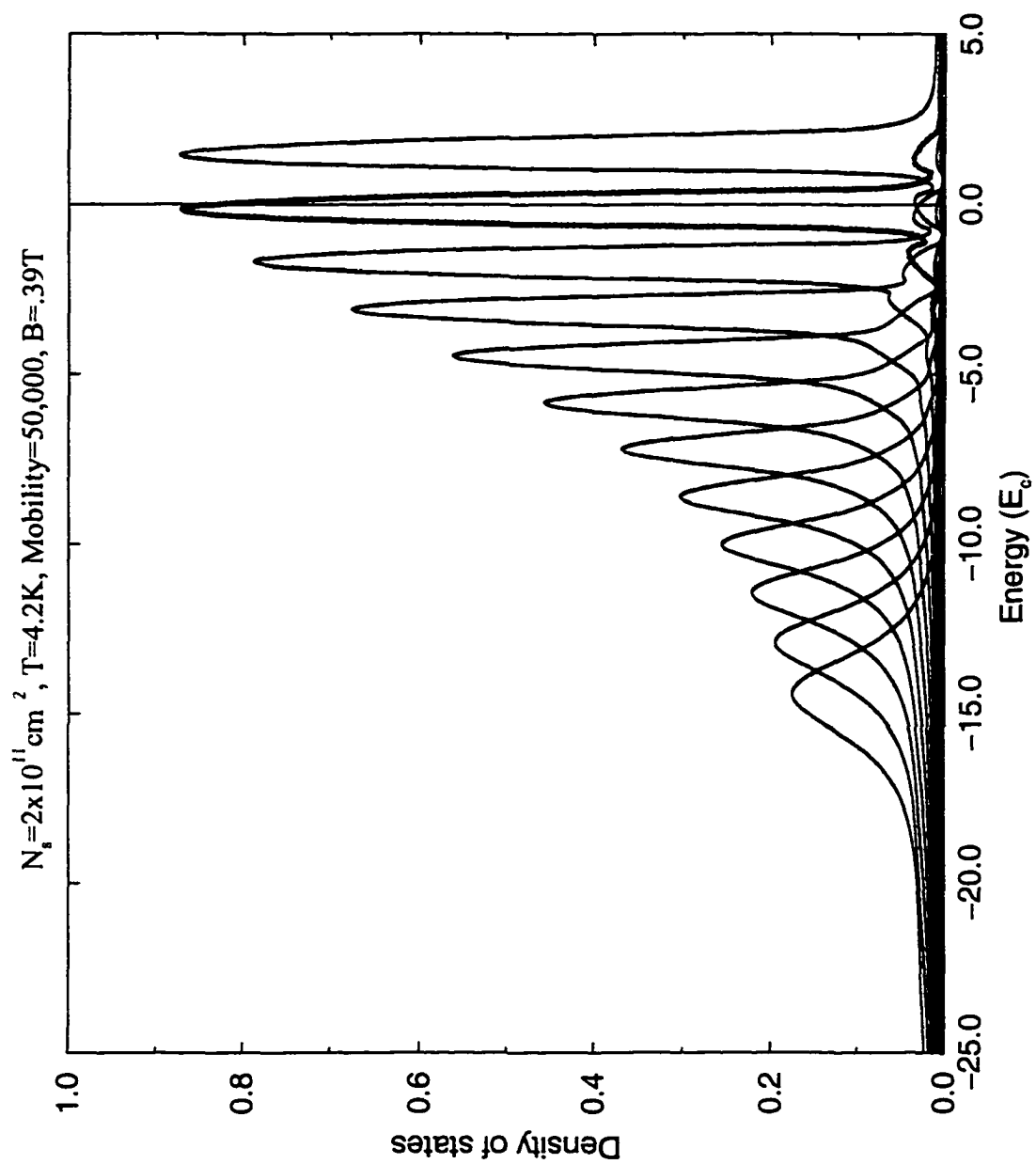


Figure 7.21: The individual contributions of the Landau levels to the density of states in the non-static model.

While developing the computational model for the non-static system, we had quite a bit of difficulty getting the system to converge. While studying the convergence, we realized that the dielectric response displayed an interesting reorganization as seen in figure 7.22. The response function, now showed some signs of the zero field plasmons. It was pointed out [15] that the result looked very much like the zero field result of Wendler and Pechstedt. [23, page 209] This can be seen more clearly in figure 7.23 which displays the peaks of $|\text{Im}[\frac{1}{\epsilon(q,E)}]|$. Here, we can see this characteristic inverted parabolic-like shape as is seen in the calculations of Wendler and Pechstedt.

The convergence problems were eventually overcome, and we were able to calculate the density of states for different mobilities and densities at various magnetic fields. Figure 7.24 shows how the density of states varies with mobility. The electron-electron effects do modify the system significantly, but the effect of impurity density still dominates the width of the Landau levels. The basic broadening due to the impurity scattering is not lost amidst large effects due only to the electron-electron scattering.

Figure 7.25 shows the effect of the electron sheet density with fixed mobility. Here we can see that we have essentially the behavior that we would expect with sharper narrower levels at higher densities.

Figures 7.26 thru 7.31 show the corresponding response functions for this system. We can see that the peaks in the response function become more defined as the Landau levels become more defined while the major parabolic feature still remains.

Up to this point, we have not talked about adding spin to the systems. In the many level solutions we have discussed above, we had actually included the spin in the model although the filling factor was chosen deliberately to minimize any spin interaction. Essentially, the results are no different for the model without spin in this regime. If we do look at higher magnetic fields, we find that the spin split enhancement due to the exchange energy can become quite large as seen by the spacing of the peaks in the density of states at the Fermi energy in figure 7.32 at filling factor $\nu = 3$. Yet, when both spins are populated evenly as in figure 7.33 where $\nu = 6$, the spin splitting is virtually given by the bare Landé g factor, and therefore we can resolve only half as many levels. We also notice how the levels

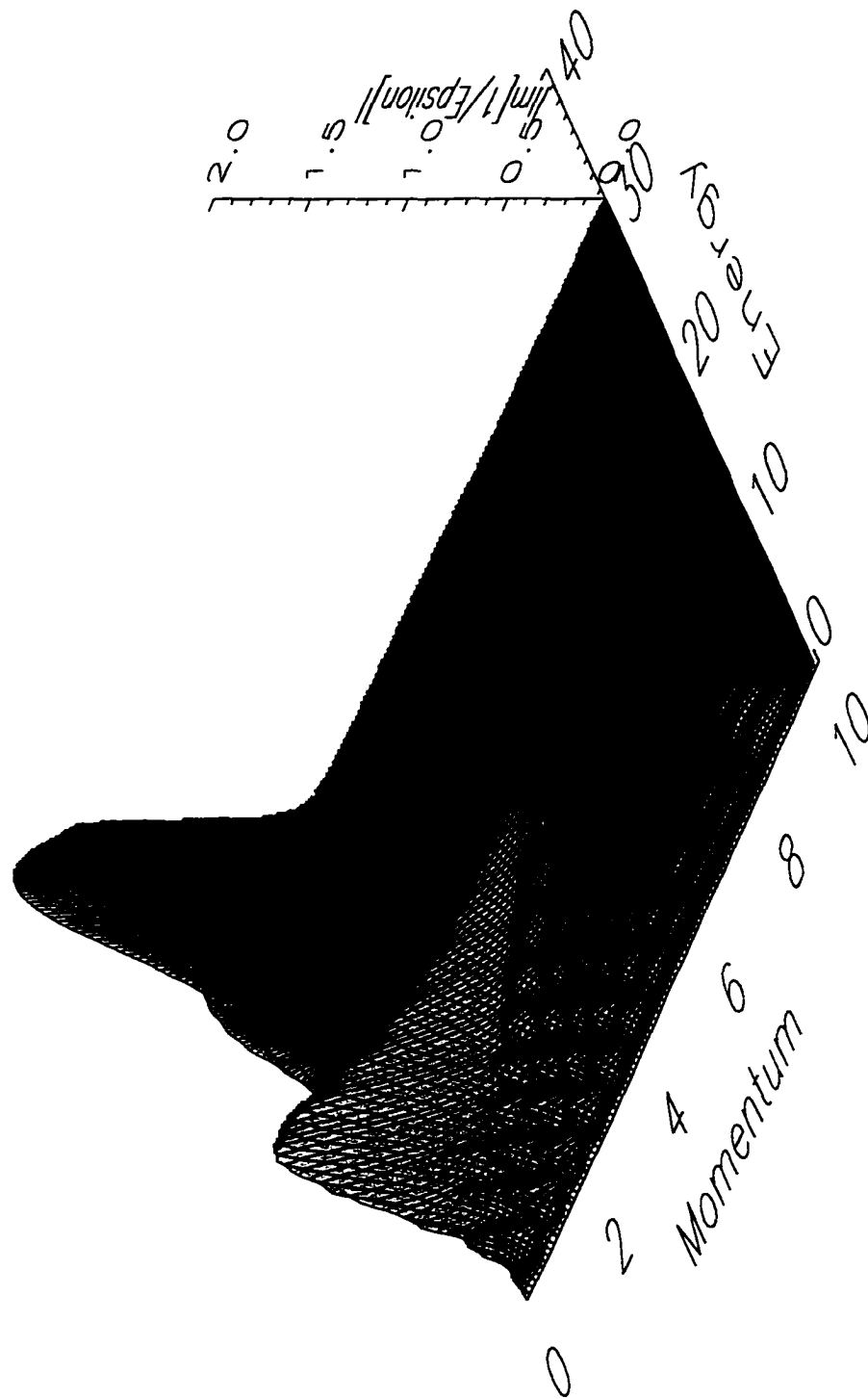


Figure 7.22: The dielectric response for our system with 12 calculated Landau levels. ($N_s = 2 \times 10^{11} \text{cm}^{-2}$, $T = 4.2 \text{K}$, $\mu = 50,000 \text{cm}^2/\text{Vs}$, $a = 50 \text{\AA}$, $B = 0.390 \text{T}$)

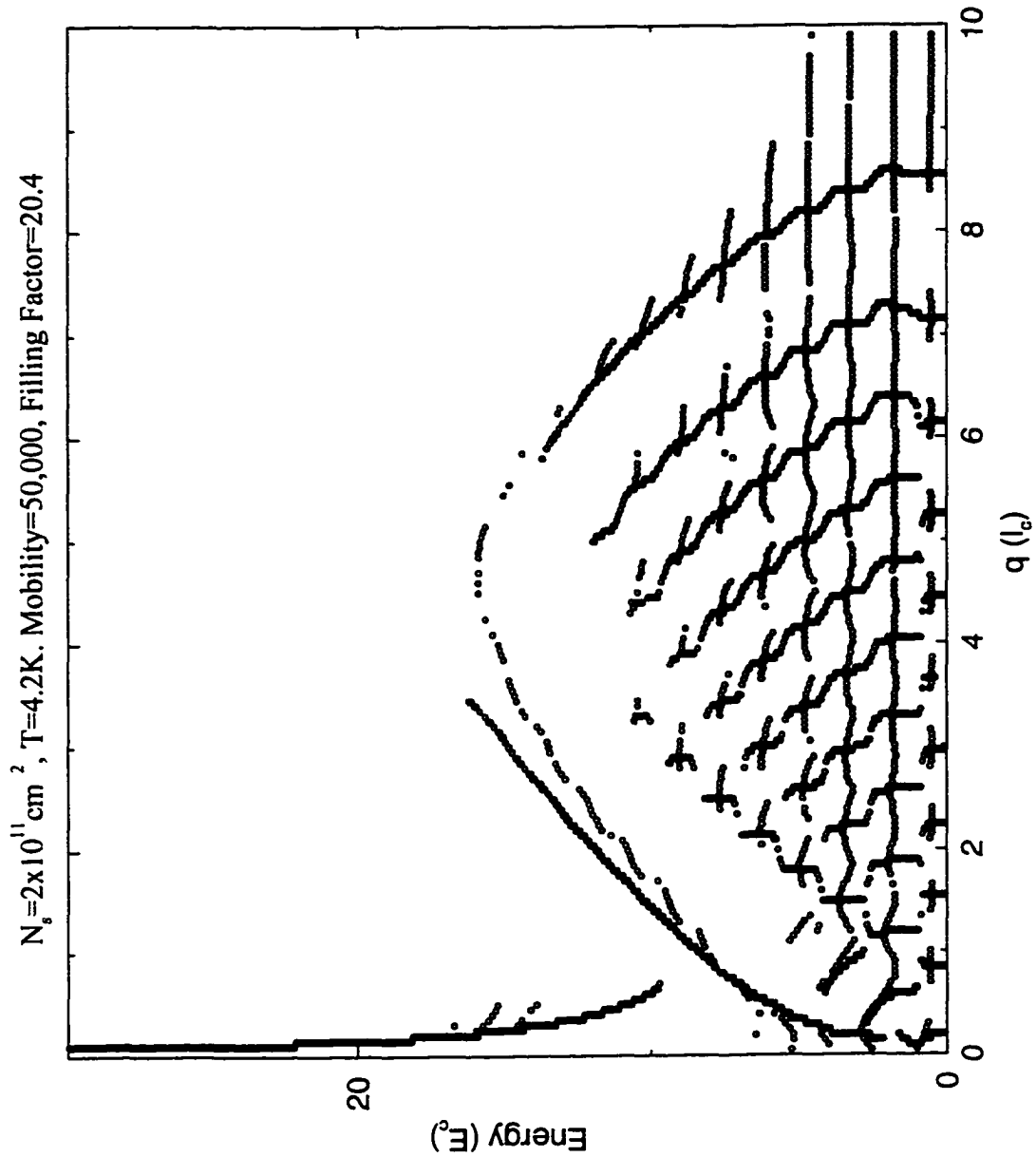


Figure 7.23: By identifying the peaks in the response functions, we see that this result is consistent with the zero field plasmon theory. ($N_s = 2 \times 10^{11} \text{ cm}^{-2}$, $T = 4.2 \text{ K}$, $\mu = 50,000 \text{ cm}^2/\text{Vs}$, $a = 50 \text{ \AA}$, $B = 0.390 \text{ T}$)

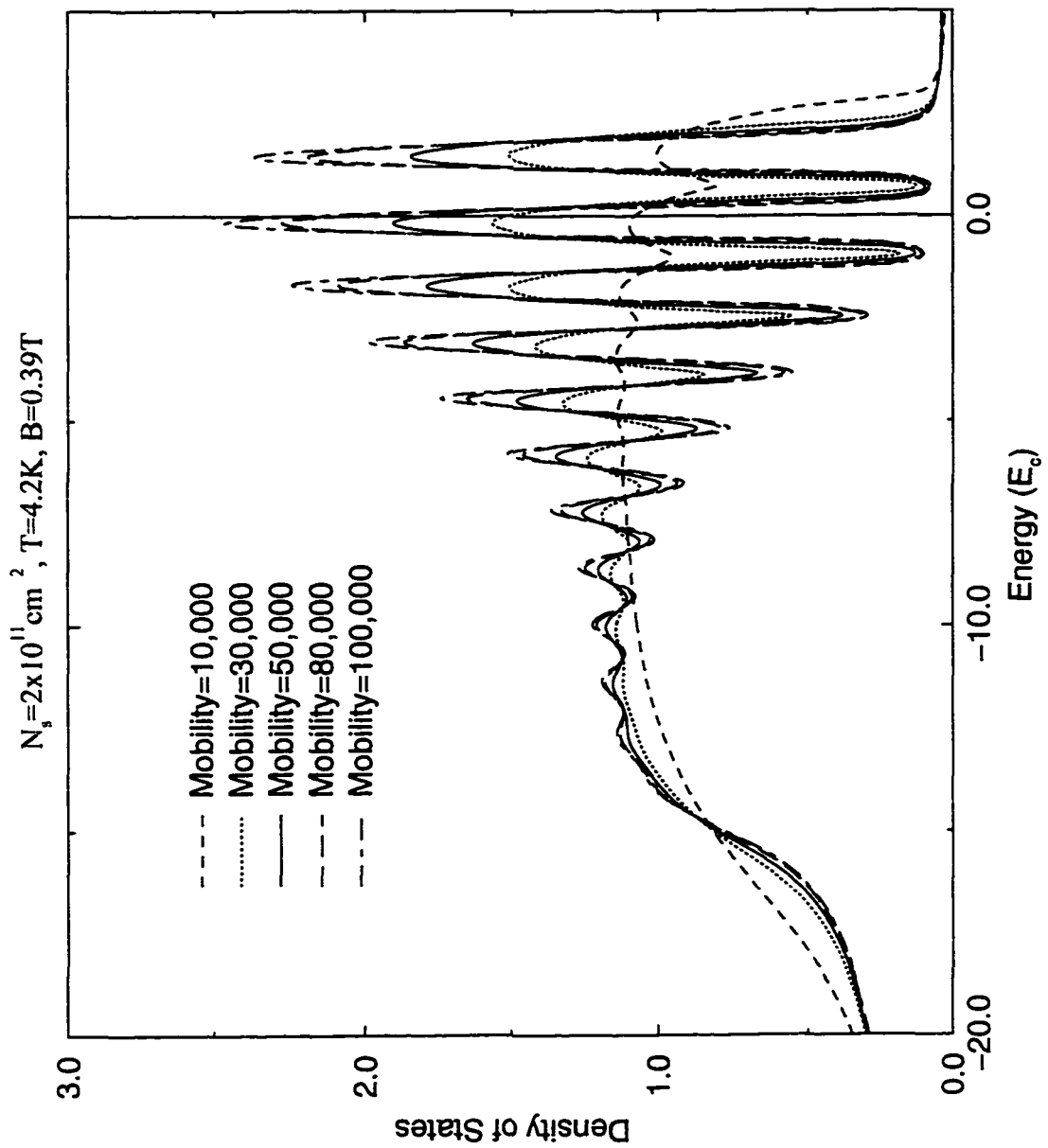


Figure 7.24: Increasing the mobility produces well defined levels in the density of states. Here all Fermi Energies are aligned at $E = 0$.

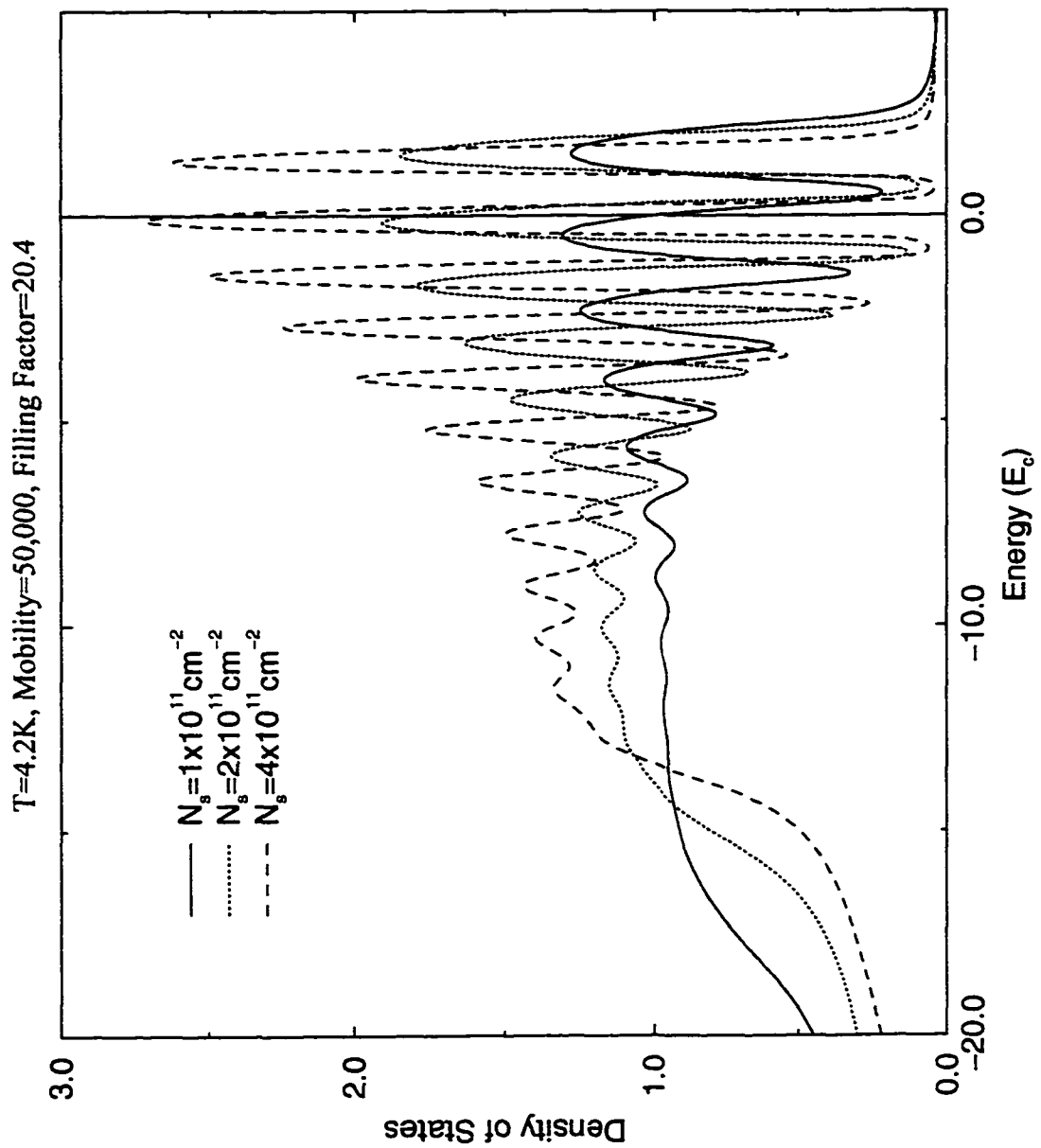


Figure 7.25: The density of states plotted for different electron sheet densities. (Again all Fermi energies are aligned at $E = 0$.)

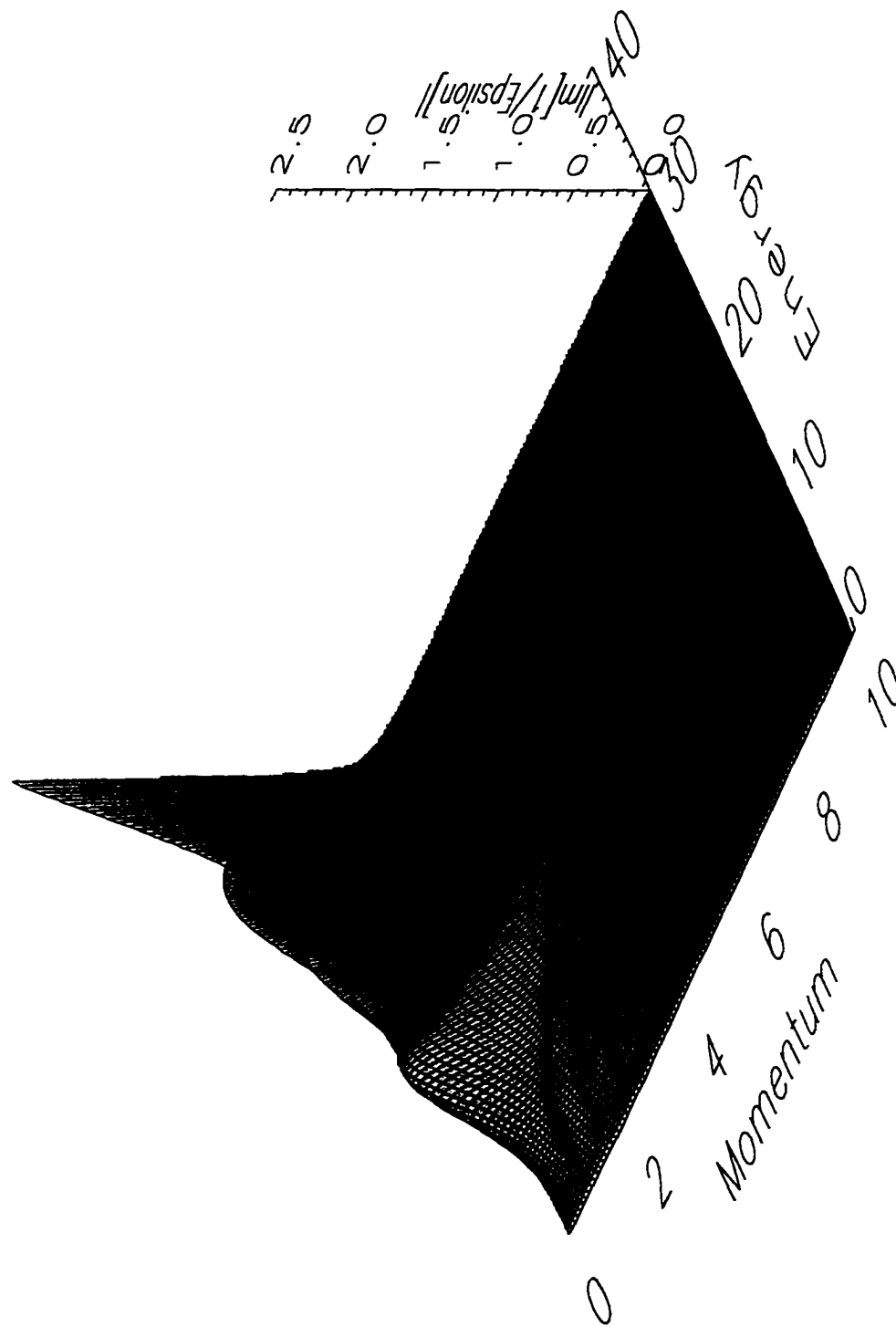


Figure 7.26: The dielectric response function for $N_s = 2 \times 10^{11} \text{cm}^{-2}$, $T = 4.2 \text{K}$, $\mu = 10,000 \text{cm}^2/\text{Vs}$, $a = 50 \text{\AA}$, $B = 0.390 \text{T}$

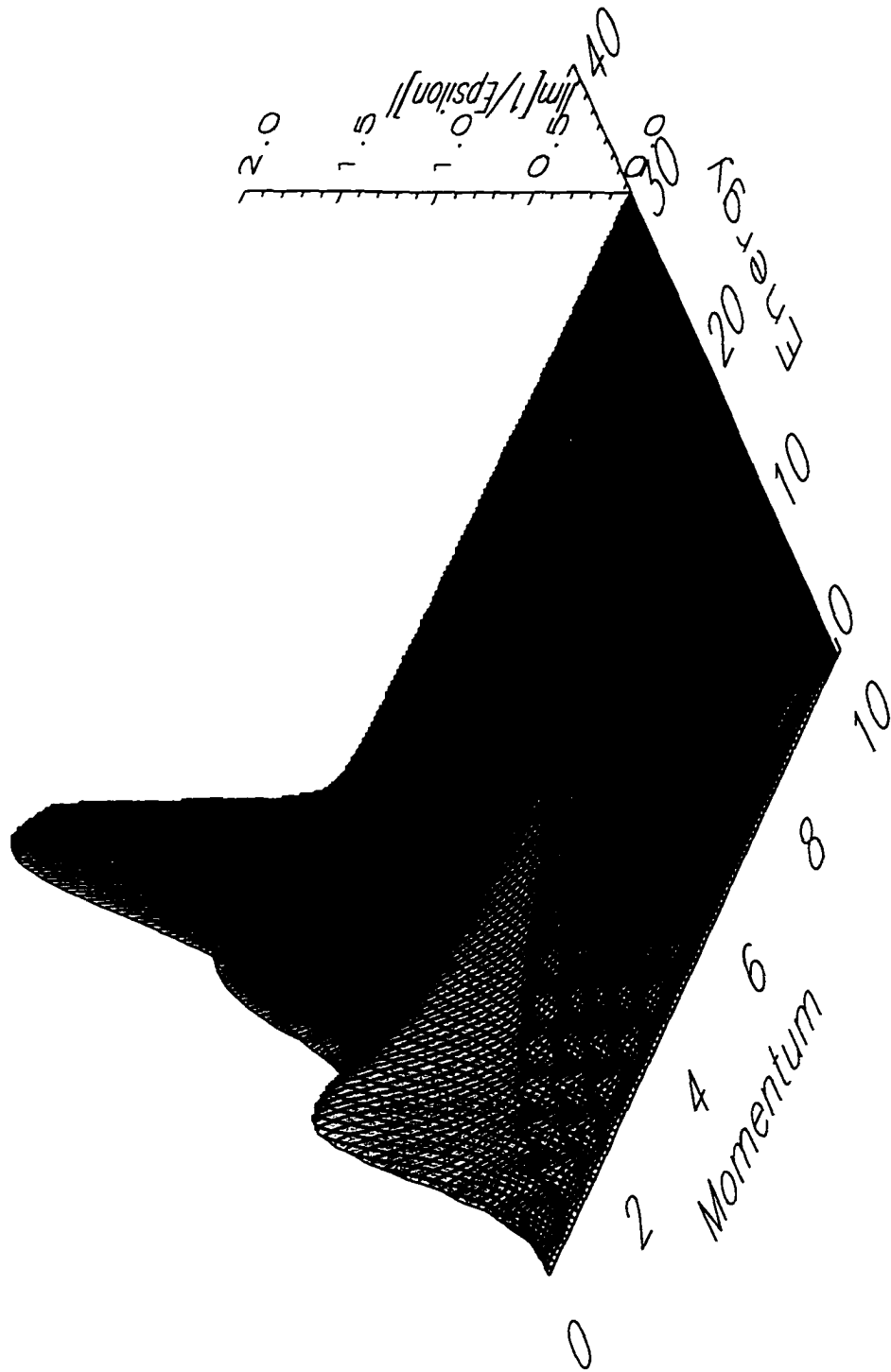


Figure 7.27: The dielectric response function for $N_s = 2 \times 10^{11} \text{cm}^{-2}$, $T = 4.2 \text{K}$, $\mu = 30,000 \text{cm}^2/\text{Vs}$, $a = 50 \text{\AA}$, $B = 0.390 \text{T}$

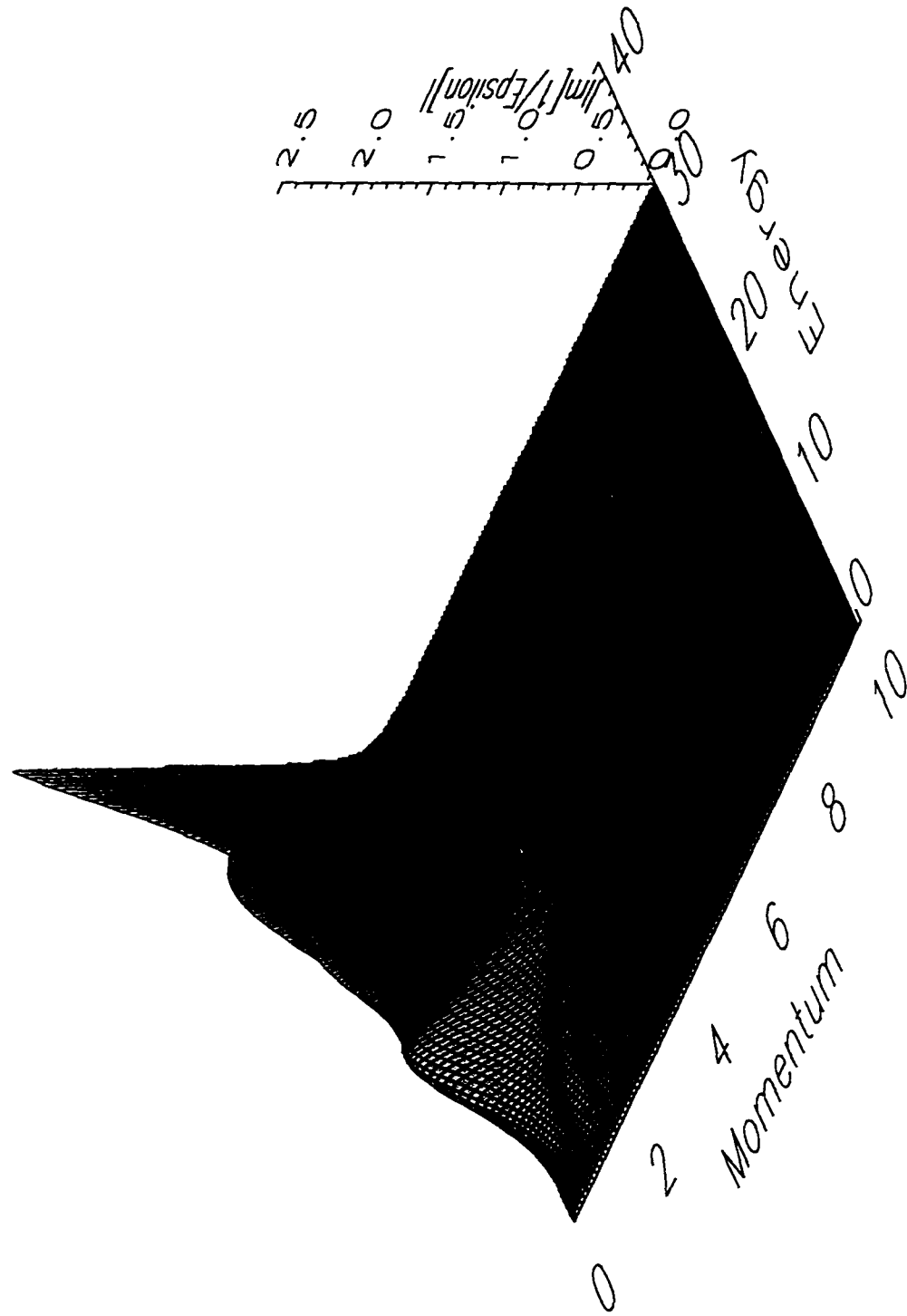


Figure 7.28: The dielectric response function for $N_s = 2 \times 10^{11} \text{cm}^{-2}$, $T = 4.2 \text{K}$, $\mu = 80,000 \text{cm}^2/\text{Vs}$, $a = 50 \text{\AA}$, $B = 0.390 \text{T}$

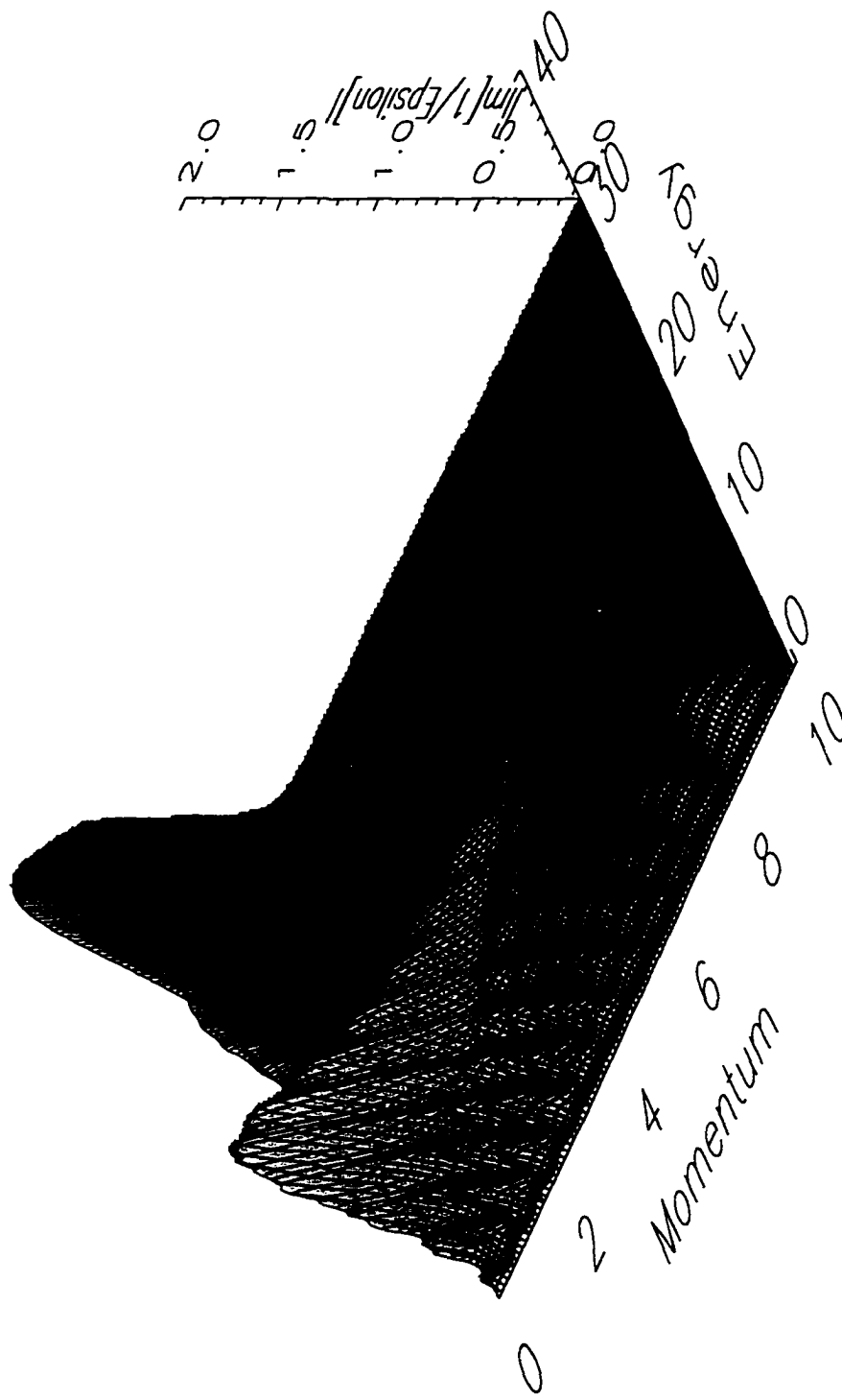


Figure 7.29: The dielectric response function for $N_s = 2 \times 10^{11} \text{cm}^{-2}$, $T = 4.2 \text{K}$, $\mu = 100,000 \text{cm}^2/\text{Vs}$, $a = 50 \text{\AA}$, $B = 0.390 \text{T}$

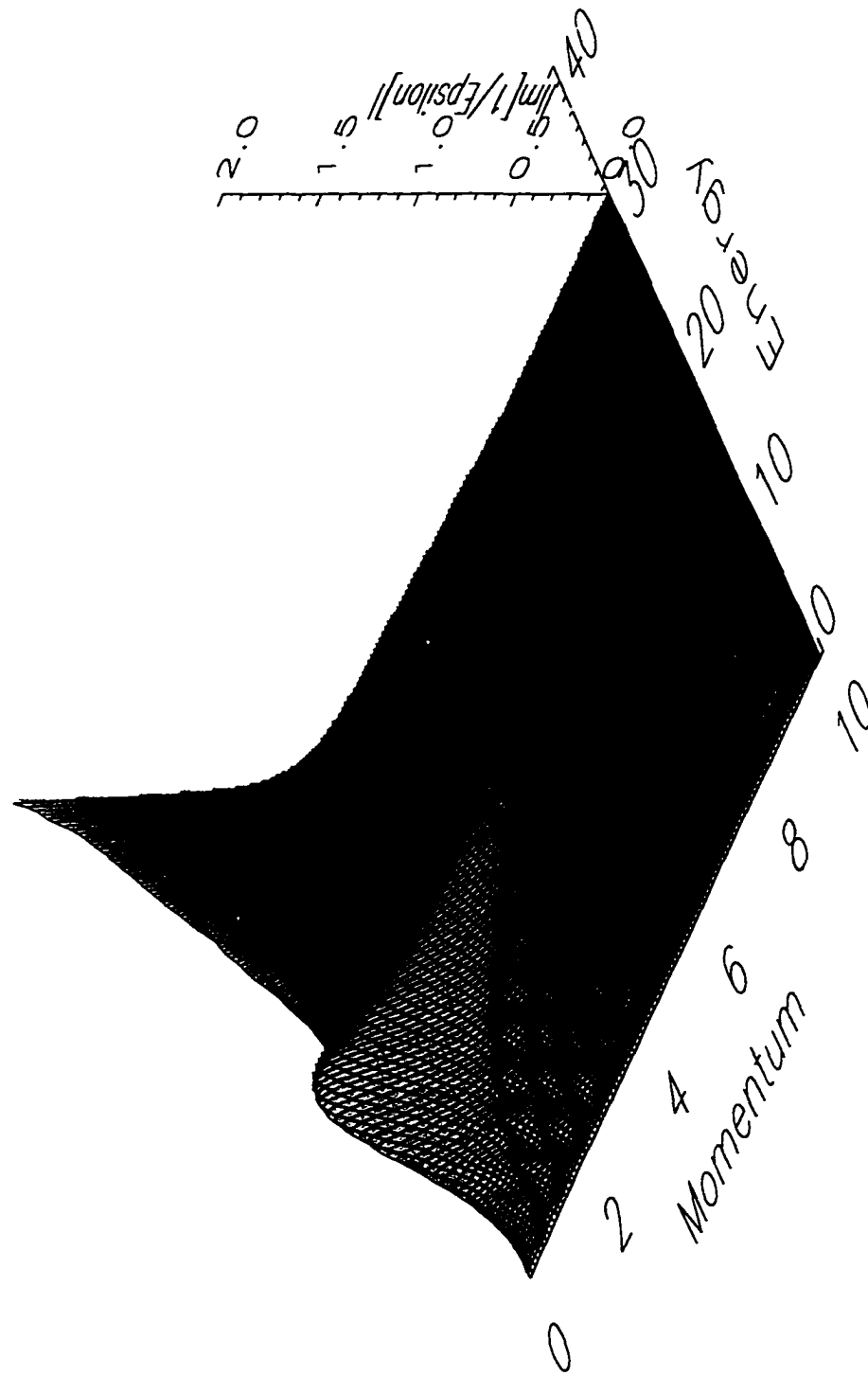


Figure 7.30: The dielectric response function for $N_s = 1 \times 10^{11} \text{cm}^{-2}$, $T = 4.2 \text{K}$, $\mu = 50,000 \text{cm}^2/\text{Vs}$, $a = 50 \text{\AA}$, $B = 0.195 \text{T}$

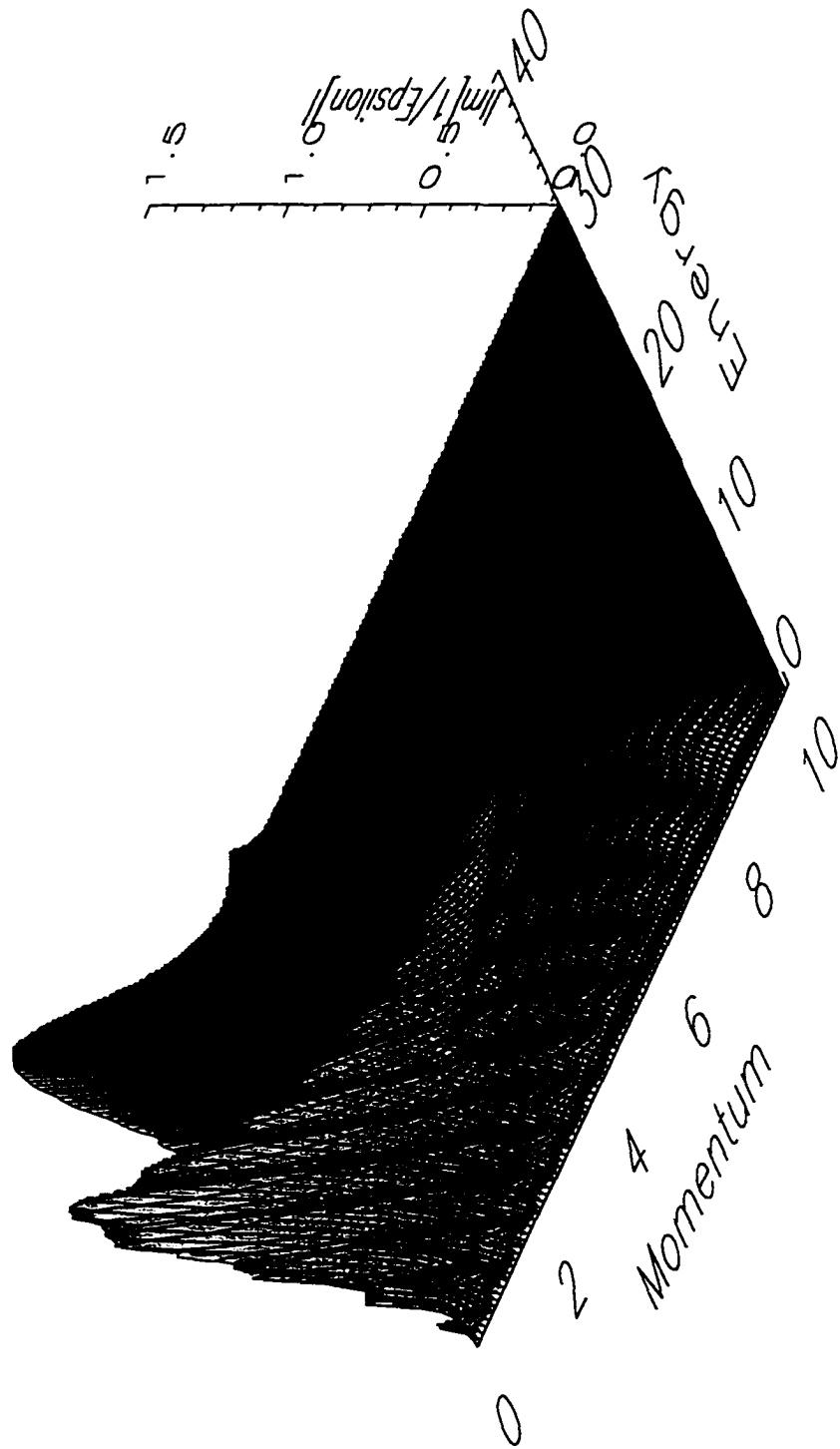


Figure 7.31: The dielectric response function for $N_s = 4 \times 10^{11} \text{cm}^{-2}$, $T = 4.2 \text{K}$, $\mu = 50,000 \text{cm}^2/\text{Vs}$, $a = 50 \text{\AA}$, $B = 0.780 \text{T}$

become strongly truncated and how a “gap” opens up at the Fermi energy which agrees well with experiment.

The polarizability at these higher magnetic fields also displays some interesting features. Here in figure 7.34 we can see three distinct ridges which represent three collective modes which correspond to the three filled spin split levels. We can also see that magnetic field damps out these modes at larger momenta. In figure 7.35, we see

Finally, as a bit of a test, we ran the model with the same parameters at $\nu = \frac{3}{2}$ which is shown in figure 7.36. Here we can see how the Fermi energy divides the the fully filled spin level and fully empty spin level while the half filled spin-split level has a sharp symmetric peak centered on the Fermi energy with smooth tails.

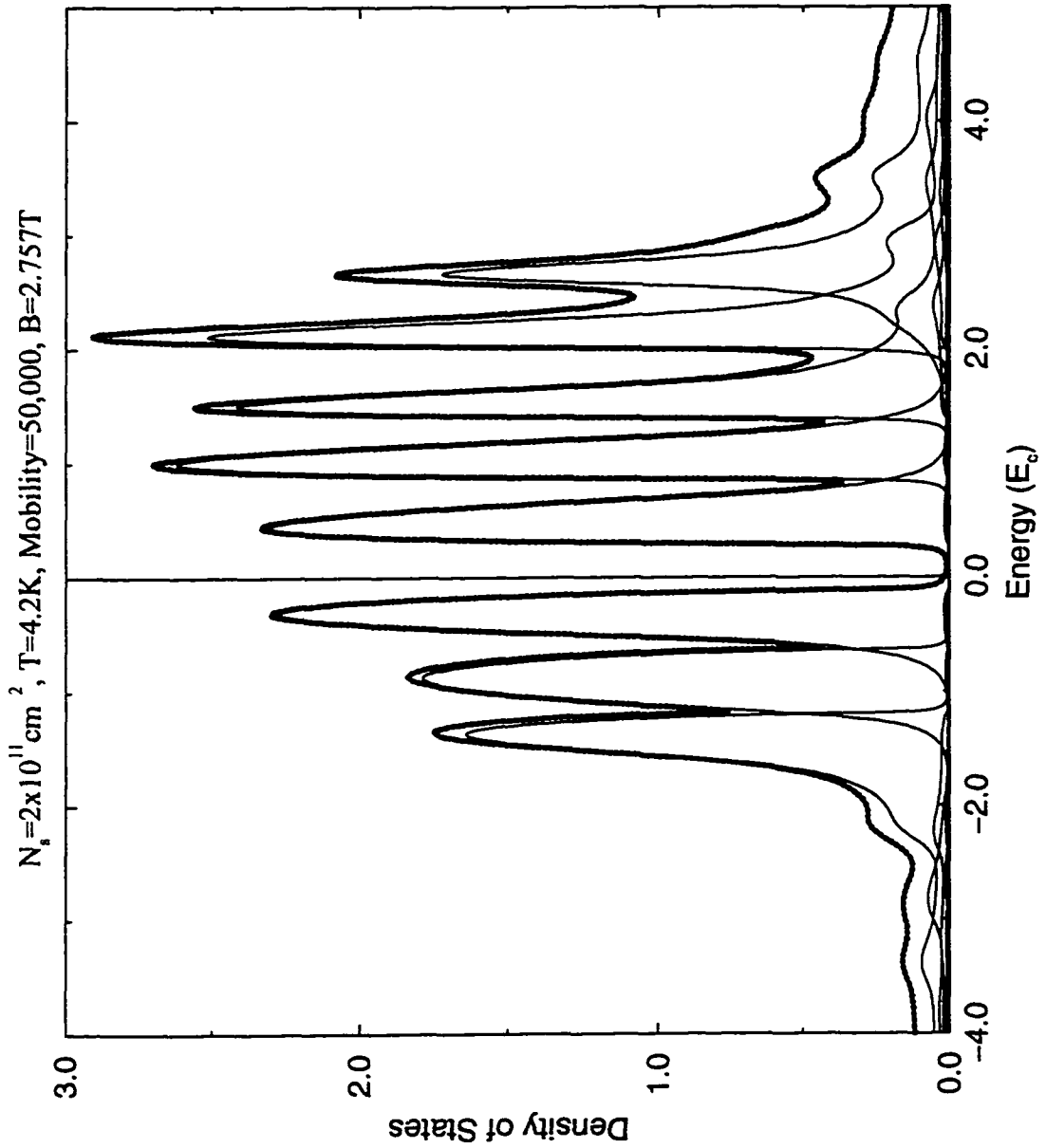


Figure 7.32: The density of states at $\nu = 3$. ($N_s = 2 \times 10^{11} \text{ cm}^{-2}$, $\mu = 50,000 \text{ cm}^2/\text{Vs}$, $T = 4.2\text{K}$, $a = 50\text{\AA}$, $B = 2.757\text{T}$)

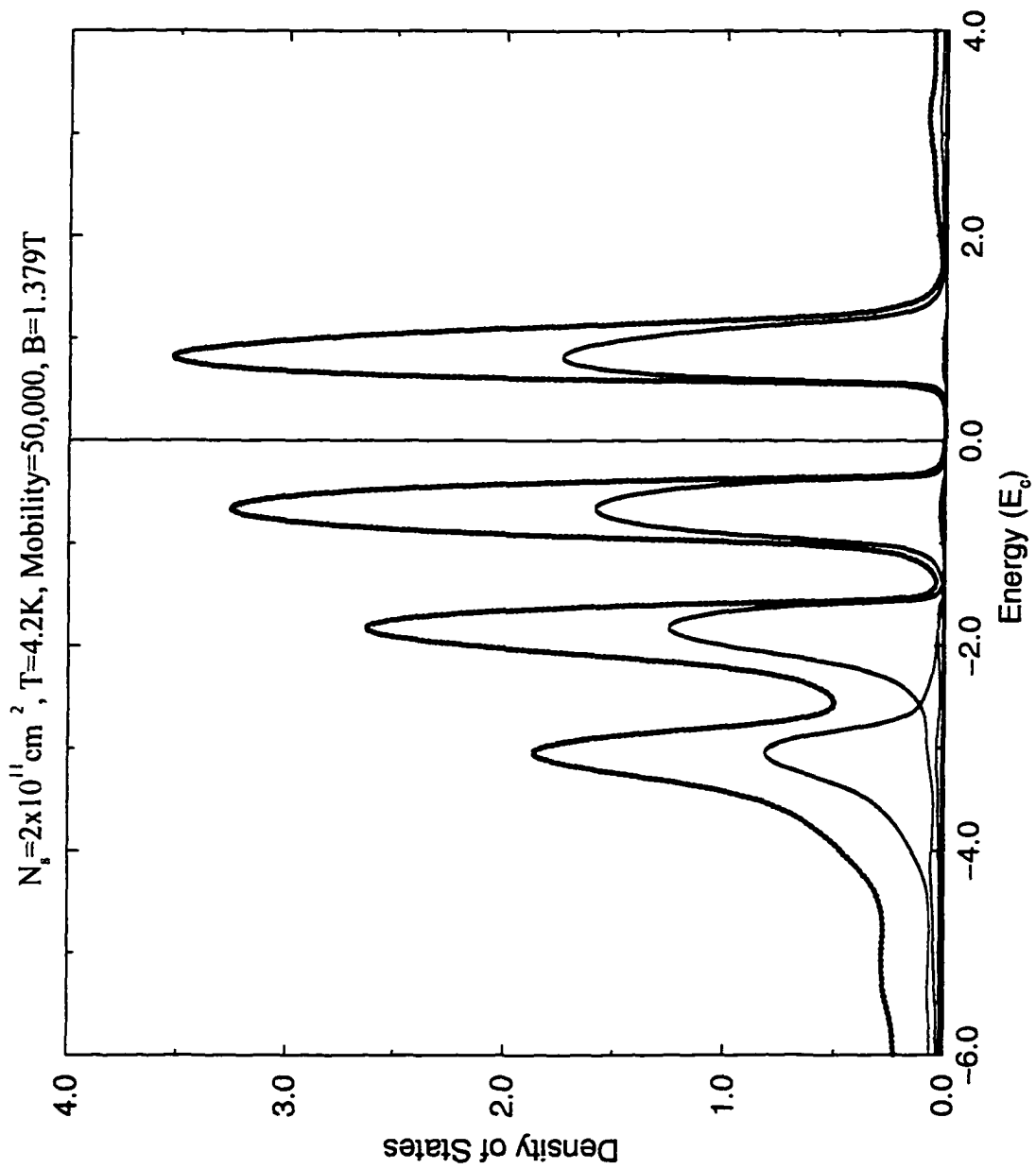


Figure 7.33: The density of states at $\nu = 6$. ($N_s = 2 \times 10^{11} \text{ cm}^{-2}$, $\mu = 50,000 \text{ cm}^2/\text{Vs}$, $T = 4.2\text{K}$, $a = 50\text{\AA}$, $B = 1.378\text{T}$)

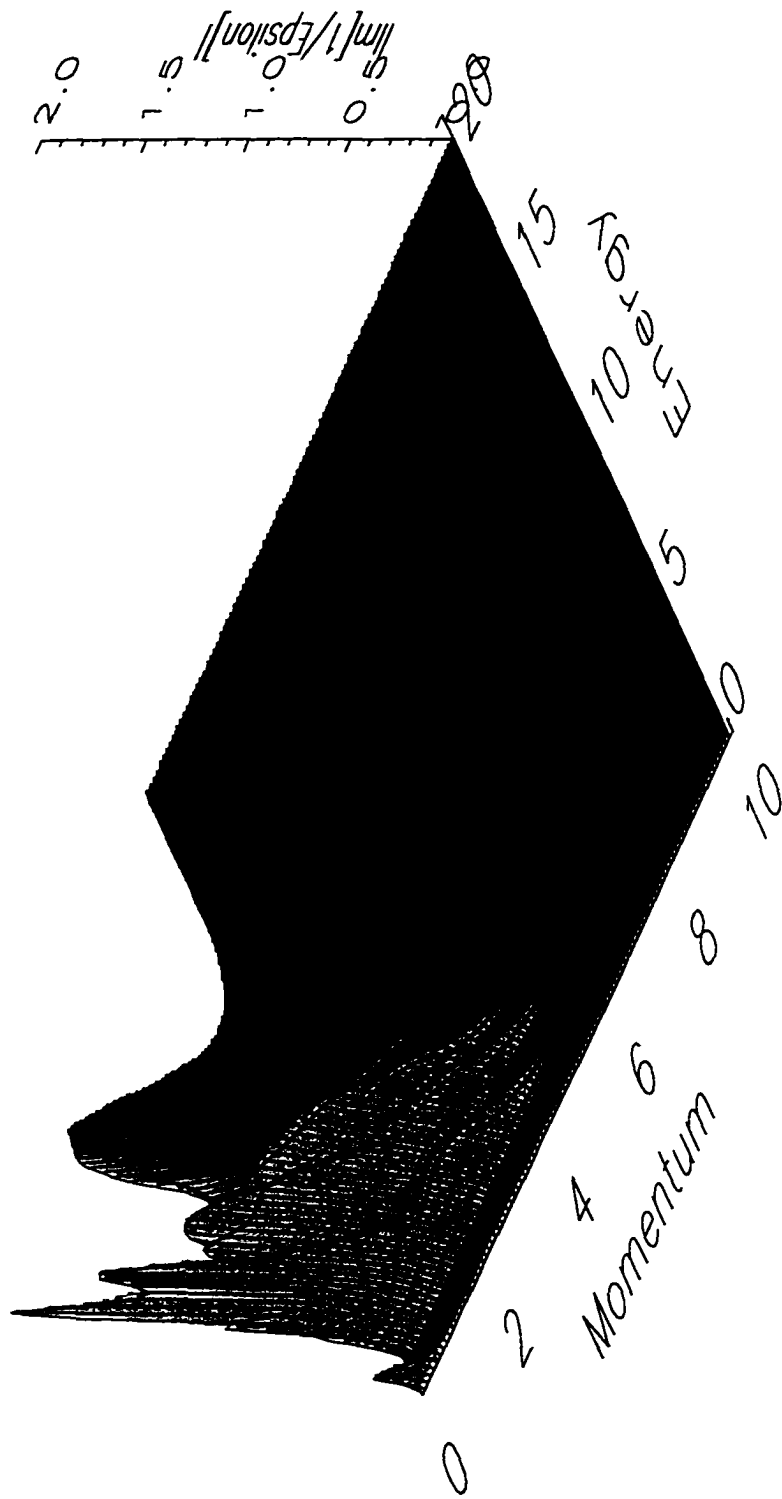


Figure 7.34: The dielectric response function at $\nu = 3$. ($N_s = 2 \times 10^{11} \text{cm}^{-2}$, $T = 4.2 \text{K}$, $\mu = 50,000 \text{cm}^2/\text{Vs}$, $a = 50 \text{\AA}$, $B = 1.378 \text{T}$)

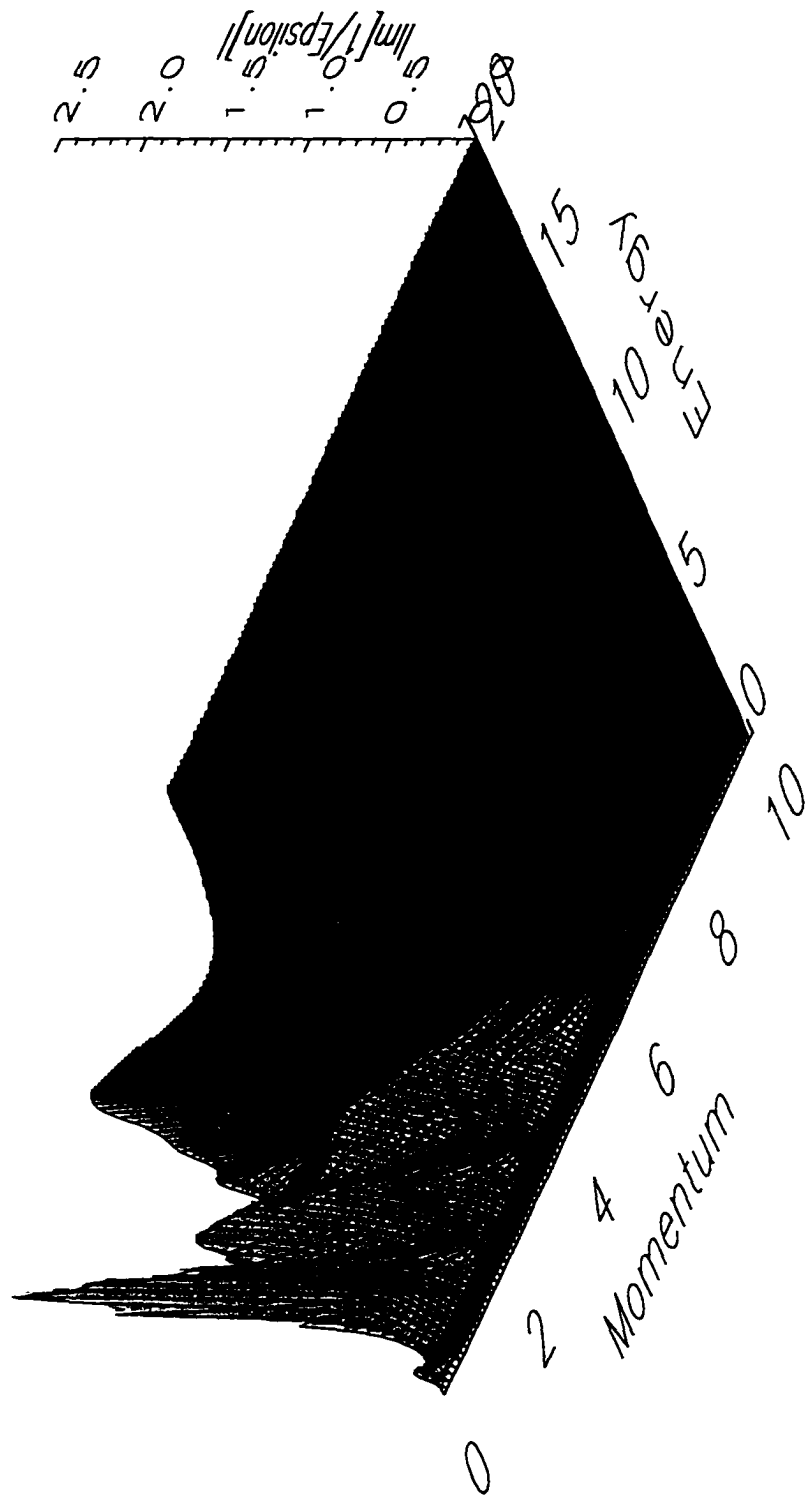


Figure 7.35: The dielectric response function at $\nu = 6$. ($N_s = 2 \times 10^{11} cm^{-2}$, $\mu = 50,000 cm^2/Vs$, $T = 4.2K$, $a = 50\text{\AA}$, $B = 2.757T$)

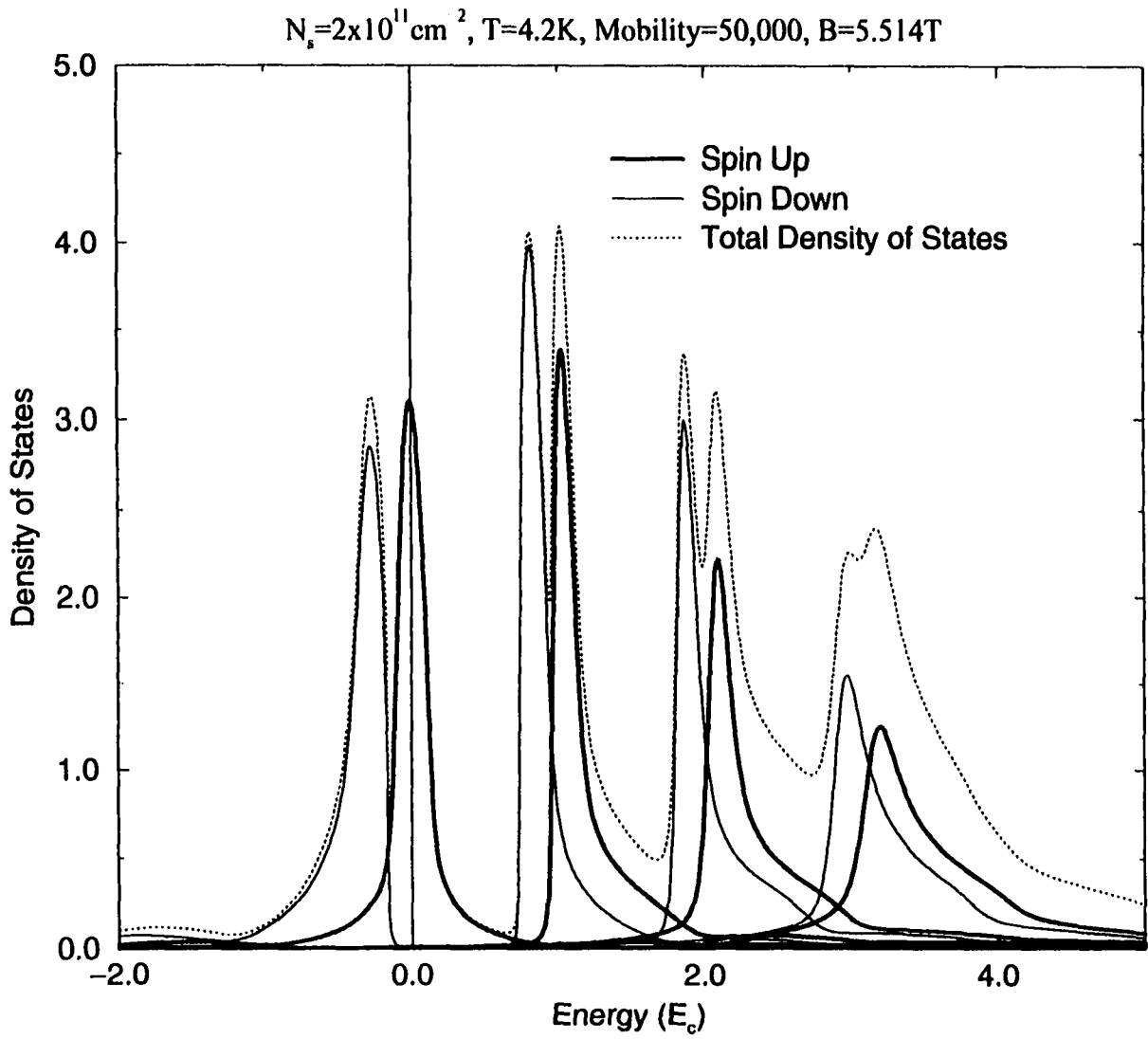


Figure 7.36: The density of states at $\nu = \frac{3}{2}$. ($N_s = 2 \times 10^{11} \text{ cm}^{-2}$, $\mu = 50,000 \text{ cm}^2/\text{Vs}$, $T = 4.2 \text{ K}$, $a = 50 \text{ \AA}$, $B = 5.514 \text{ T}$)

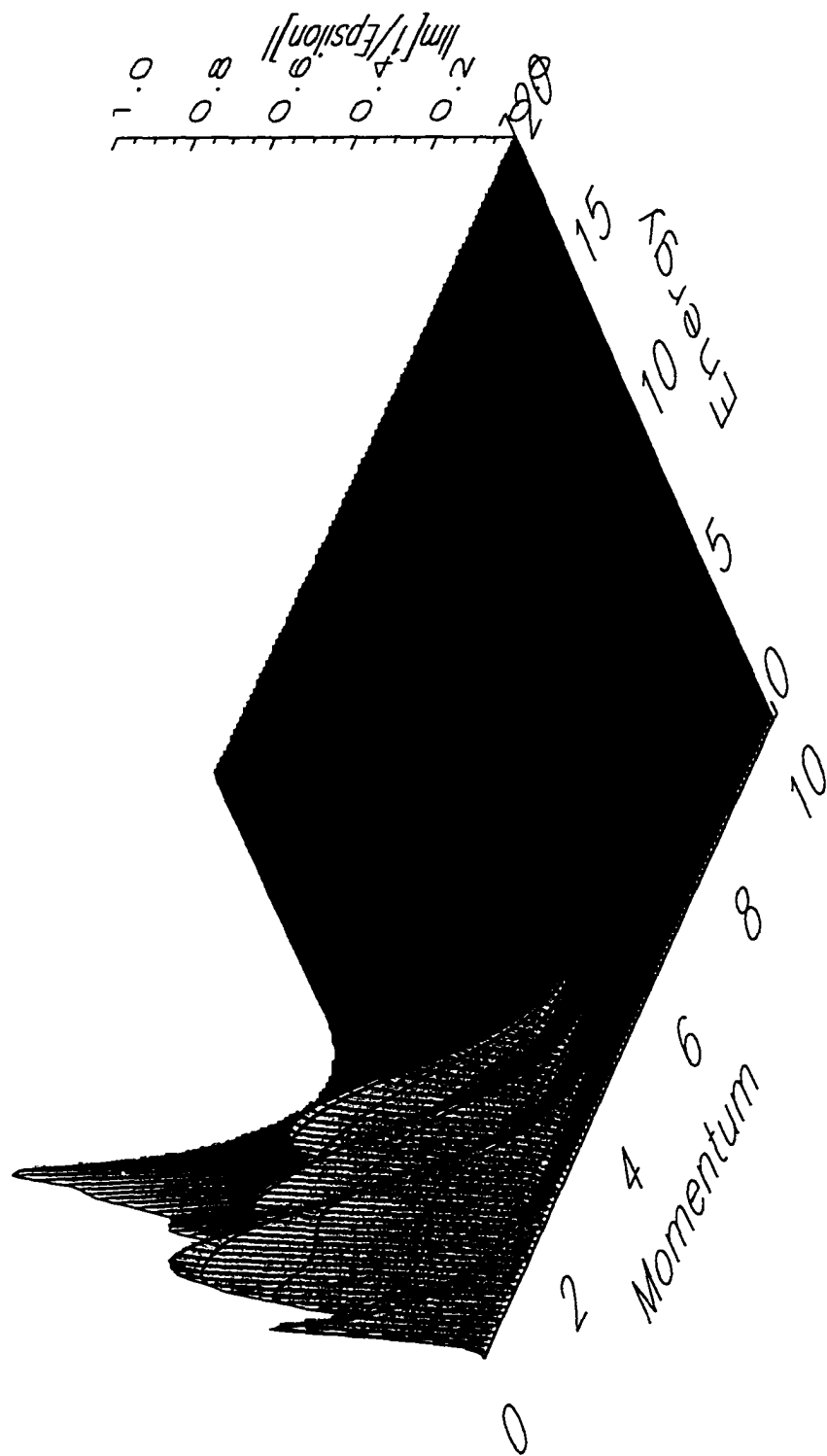


Figure 7.37: The dielectric response function at $\nu = \frac{3}{2}$. ($N_s = 2 \times 10^{11} \text{cm}^{-2}$, $\mu = 50,000 \text{cm}^2/\text{Vs}$, $T = 4.2 \text{K}$, $a = 50 \text{\AA}$, $B = 5.514 \text{T}$)

Chapter 8

Conclusions

8.1 Conclusions

We have performed several numerical calculations which have helped us look into the structure of the density of states of a two-dimensional electron gas as affected by impurities in an applied perpendicular magnetic field. We have looked at impurity scattering in terms of the self-consistent random phase approximation with and without an approximation of the "vertex correction". We have also extended these models by including the self-consistent electron-electron interaction. In doing this, we have calculated the dynamic dielectric response function at large range of filling factors. In this journey we have found:

- Static impurity screening produces models which have a semi-elliptic Landau level shape especially in the high field, high mobility limit.
- When the simplest inter-Landau level interactions are included, the widths of the energy levels are strongly influenced by the filling factor. Landau level widths grow as the system approaches integer filling factors as fewer electron states are available for screening.
- Adding a vertex correction which includes inter-Landau level interaction but not inter-Landau level exchange over-estimates the reduction in screening (a smaller magnitude of the polarizability) and produces instabilities when Landau levels cease to overlap.
- Spin is ignorable in the static impurity scattering models.

- Adding dynamic electron-electron interactions to the standard impurity scattering picture, produces a density of states which is more consistent with low to intermediate magnetic field results. At low magnetic fields the density of states takes on a more Lorentzian shape which has been shown to work well to predict the behavior of Schubnikov-de Haas oscillations. [18]
- At higher magnetic fields, the dynamically screened model produces results which are consistent with the self-consistent Born and many-site approximations.
- The electron exchange terms in the dynamic model provide a mechanism to predict the large Landé g -factor enhancement which is seen at odd filling factors in high magnetic fields. (Electron spin is not ignorable in the non-static model.) The exchange term is driven by the relative populations of the electron spins providing a positive feedback which serves to enhance the spin-splitting of the Landau levels.

8.2 Extensions and Enhancements

There is certainly much more that could be done with this calculation. Due to time constraints, we chose to only deal with the density of states. Once we have a good model for the density of states, the path to many more “physical” calculations has been opened. Some of these include

- We have not generated magnetic field spectra for the non-static model.
- The mobility in these calculations is a model parameter based on a simple Thomas-Fermi screening at zero field. This could definitely be improved.
- Temperature dependence is also very important in these system, and there is a wealth of information to be gained from studying the temperature dependence.
- Adding the additional effects of a tilted magnetic field would also be interesting.
- Modeling of more “real world” systems could be achieved by including inter-subband interactions and more realistic impurity distributions.

- Calculation of the transport properties is a very exciting topic, considering the importance of the Quantum Hall Effect to the solid state physics world. It may be possible to reconstruct the Green's function from our calculation using the $G_N(E)$, the unperturbed wavefunctions, and careful treatment of the boundary conditions. This would then allow for the calculation of the Green's function for the current density which would then allow for the detailed investigation of the transport.

Appendix A

The Electron in a Magnetic Field

A.1 Landau Gauge

Consider an electron confined to a plane with a perpendicular magnetic field. The Hamiltonian for this situation is given by

$$H_0 = \frac{1}{2m} \left(\vec{p} + \frac{e}{c} \vec{A} \right)^2 \quad (\text{A.1})$$

where we shall choose \vec{A} to be in the Landau gauge $\vec{A} = B_z x \hat{j}$. Thus we have:

$$\begin{aligned} H_0 &= \frac{1}{2m} \left(i\hbar \nabla + \frac{e}{c} B_z x \hat{j} \right) \frac{1}{2m} \left(i\hbar \nabla + \frac{e}{c} B_z x \hat{j} \right) \quad (\text{A.2}) \\ &= \frac{1}{2m} \left(-\hbar^2 \nabla^2 + \frac{2e}{c} i\hbar B_z x \frac{\partial}{\partial y} + \left(\frac{eB}{c} \right)^2 x^2 \right) \\ &= \frac{-\hbar^2}{2m} \left(\frac{\partial^2}{\partial x^2} + \frac{\partial^2}{\partial y^2} \right) + i\hbar \omega_c x \frac{\partial}{\partial y} + \frac{1}{2} m \omega_c^2 x^2 \end{aligned}$$

where $\omega_c = \frac{eB_z}{mc}$ is the cyclotron frequency. Now we can see that the Schrödinger equation is separable and we can write the wave function as

$$\psi = \psi_x L^{\frac{1}{2}} e^{ipy} \quad (\text{A.3})$$

where L is the width of the sample in the y direction. After making this substitution we obtain

$$\left(\frac{-\hbar^2}{2m} \frac{\partial^2}{\partial x^2} + \frac{\hbar^2 p^2}{2m} - \hbar \omega_c p x + \frac{1}{2} m \omega_c^2 x^2 \right) \psi_x = E \psi_x \quad (\text{A.4})$$

Now let us make a further substitution of

$$X = x - \frac{\hbar p}{\omega_c} = x - pl^2 \quad (\text{A.5})$$

We call $l = \sqrt{\frac{\hbar}{m\omega_c}} = \sqrt{\frac{\hbar c}{eB_c}}$ the magnetic length. Finally we get

$$\left(\frac{-\hbar^2}{2m} \frac{\partial^2}{\partial X^2} + \frac{1}{2} m \omega_c^2 X^2 \right) \psi_X = E \psi_X \quad (\text{A.6})$$

which we recognize as the Hamiltonian for the harmonic oscillator. We can now define two operators

$$a^\dagger = \frac{1}{\sqrt{2m}} \left(-\hbar \frac{\partial}{\partial X} + m \omega_c X \right) \quad (\text{A.7})$$

$$a = \frac{1}{\sqrt{2m}} \left(\hbar \frac{\partial}{\partial X} + m \omega_c X \right) \quad (\text{A.8})$$

$$(\text{A.9})$$

We can then see that we can write the Hamiltonian as

$$\begin{aligned} \left(\frac{-\hbar^2}{2m} \frac{\partial^2}{\partial X^2} + \frac{1}{2} m \omega_c^2 X^2 \right) &= a^\dagger a + \frac{\hbar \omega_c}{2} \\ &= a a^\dagger - \frac{\hbar \omega_c}{2} \end{aligned} \quad (\text{A.10})$$

Thus, we have the commutation relation

$$[a, a^\dagger] = \hbar \omega_c \quad (\text{A.11})$$

Now we see that if we apply a^\dagger to both sides of the above equation

$$\begin{aligned} a^\dagger \left(a^\dagger a + \frac{\hbar \omega_c}{2} \right) \psi_X &= E (a^\dagger \psi_X) \\ \left(a^\dagger a - \hbar \omega_c + \frac{\hbar \omega_c}{2} \right) (a^\dagger \psi_X) &= E (a^\dagger \psi_X) \\ \left(a^\dagger a + \frac{\hbar \omega_c}{2} \right) (a^\dagger \psi_X) &= (E + \hbar \omega_c) (a^\dagger \psi_X) \end{aligned} \quad (\text{A.12})$$

Therefore a^\dagger raises the energy state of the system. Correspondingly we can prove that a lowers the energy state. Since the ground state cannot be lowered then we expect that

$$av_{X_0} = 0 \quad (\text{A.13})$$

Expanding upon this idea:

$$\frac{1}{\sqrt{2m}} \left(\hbar \frac{\partial}{\partial X} + m\omega_c X \right) v_{X_0} = 0 \quad (\text{A.14})$$

This yields the solution

$$\begin{aligned} \ln v_{X_0} &= \frac{m\omega_c}{2\hbar} X^2 + \text{const.} \\ v_{X_0} &= Ae^{-\frac{X^2}{2l^2}} \end{aligned} \quad (\text{A.15})$$

Now that we have the ground state we may calculate all higher states by

$$\begin{aligned} v_{X_n} &= (a^\dagger)^n v_{X_0} \\ &= \left[\frac{1}{\sqrt{2m}} \left(-\hbar \frac{\partial}{\partial X} + m\omega_c X \right) \right]^n Ae^{-\frac{X^2}{2l^2}} \end{aligned} \quad (\text{A.16})$$

Rewriting this slightly

$$\begin{aligned} v_{X_n} &= A \left(\frac{1}{\sqrt{2m}} \right)^n e^{\frac{X^2}{2l^2}} \left[e^{-\frac{X^2}{2l^2}} \left(-\hbar \frac{\partial}{\partial X} + m\omega_c X \right) e^{\frac{X^2}{2l^2}} \right]^n e^{-\frac{X^2}{2l^2}} \\ &= A' e^{\frac{X^2}{2l^2}} \left[-\frac{\partial}{\partial (X/l)} \right]^n e^{-\frac{X^2}{2l^2}} \\ &= A' H_n(X/l) e^{-\frac{X^2}{2l^2}} \end{aligned} \quad (\text{A.17})$$

where we have made use of Rodrigues' formula for the Hermite polynomials to obtain the closed form. After normalizing we end up with the solutions

$$v_{X_n} = (\pi^{\frac{1}{2}} 2^n n! l)^{-\frac{1}{2}} H_n(X/l) e^{-\frac{X^2}{2l^2}} \quad (\text{A.18})$$

Which ultimately yields the answer

$$\psi_{N,p} = (L\pi^{\frac{1}{2}}2^n n!)^{-\frac{1}{2}} H_n(x/l - pl) e^{-\frac{x/l - pl}{2}} e^{ip_y} \quad (\text{A.19})$$

A.2 Symmetric Gauge

Let us now opt for the symmetric gauge. $\vec{A} = \frac{B_z}{2}(-y\hat{i} + x\hat{j})$. Now our Hamiltonian becomes

$$\begin{aligned} H_0 &= \frac{1}{2m} \left[\vec{p} + \frac{eB_z}{2c}(-y\hat{i} + x\hat{j}) \right]^2 \\ &= \frac{1}{2m} \left[p_x^2 + p_y^2 + \frac{eB_z}{c}(xp_y - yp_x) + \frac{e^2 B_z^2}{4c^2}(x^2 + y^2) \right] \\ &= \left(\frac{p_x^2}{2m} + \frac{m\omega_c^2}{8}x^2 \right) + \left(\frac{p_y^2}{2m} + \frac{m\omega_c^2}{8}y^2 \right) + \frac{1}{2}\omega_c L_z \end{aligned} \quad (\text{A.20})$$

Let us define some new operators:

$$a^\dagger = \frac{1}{\sqrt{2m}} \left(-ip_x + \frac{m\omega_c}{2}x \right) \quad (\text{A.21})$$

$$a = \frac{1}{\sqrt{2m}} \left(ip_x + \frac{m\omega_c}{2}x \right) \quad (\text{A.22})$$

$$b^\dagger = \frac{1}{\sqrt{2m}} \left(-ip_y + \frac{m\omega_c}{2}y \right) \quad (\text{A.23})$$

$$b = \frac{1}{\sqrt{2m}} \left(ip_y + \frac{m\omega_c}{2}y \right) \quad (\text{A.24})$$

Remembering that $[x, p_x] = i\hbar$ and $[y, p_y] = i\hbar$ we look at

$$\begin{aligned} a^\dagger a &= \frac{1}{2m} \left(-ip_x + \frac{m\omega_c}{2}x \right) \left(ip_x + \frac{m\omega_c}{2}x \right) \\ &= \frac{1}{2m} \left(p_x^2 - ip_x \frac{m\omega_c}{2}x + ip_x \frac{m\omega_c}{2}x p_x + \frac{m\omega_c^2}{4}x^2 \right) \\ &= \frac{1}{2m} \left(p_x^2 + i \frac{m\omega_c}{2} [x, p_x] + \frac{m\omega_c^2}{4}x^2 \right) \\ &= \frac{1}{2m} \left(p_x^2 + \frac{m\omega_c^2}{4}x^2 \right) - \frac{\hbar\omega_c}{4} \end{aligned} \quad (\text{A.25})$$

Additionally, we see that

$$aa^\dagger = \frac{1}{2m} \left(p_x^2 + \frac{m\omega_c^2}{4} x^2 \right) - \frac{\hbar\omega_c}{4} \quad (\text{A.26})$$

so that we can form the commutation relationships

$$[a, a^\dagger] = \frac{\hbar\omega_c}{2} \quad (\text{A.27})$$

$$[b, b^\dagger] = \frac{\hbar\omega_c}{2} \quad (\text{A.28})$$

Last, let us look at

$$\begin{aligned} a^\dagger b - b^\dagger a &= \frac{1}{2m} \left(-ip_x + \frac{m\omega_c}{2} x \right) \left(ip_y + \frac{m\omega_c}{2} y \right) \\ &\quad - \frac{1}{2m} \left(-ip_y + \frac{m\omega_c}{2} y \right) \left(ip_x + \frac{m\omega_c}{2} x \right) \\ &= \frac{1}{2m} \left(2i \frac{m\omega_c}{2} x p_y - 2i \frac{m\omega_c}{2} y p_x \right) \\ &= i \frac{\omega_c}{2} (x p_y - y p_x) \\ &= i \frac{\omega_c}{2} L_x \end{aligned} \quad (\text{A.29})$$

With these relationships we can now write

$$\begin{aligned} H_0 &= a^\dagger a + b^\dagger b + \frac{\omega_c}{2} L_z + \frac{\hbar\omega_c}{2} \\ &= a^\dagger a + b^\dagger b + i(b^\dagger a - a^\dagger b) + \frac{\hbar\omega_c}{2} \\ &= (a^\dagger + ib^\dagger)(a - ib) + \frac{\hbar\omega_c}{2} \\ &= u^\dagger u + \frac{\hbar\omega_c}{2} \end{aligned} \quad (\text{A.30})$$

where now we have again defined two new operators

$$u^\dagger = (a^\dagger + ib^\dagger) \quad (\text{A.31})$$

$$u = (a - ib) \quad (\text{A.32})$$

Before we continue let us look at the commutation relation

$$\begin{aligned}
\left[(a^\dagger a + b^\dagger b) \cdot i \frac{\hbar \omega_c}{2} L_z \right] &= \left[(a^\dagger a + b^\dagger b) \cdot (a^\dagger b - b^\dagger a) \right] & (A.33) \\
&= ab^\dagger [a^\dagger, a] + [b, b^\dagger] a^\dagger b - [a, a^\dagger] b^\dagger a - b^\dagger a [b^\dagger, b] \\
&= ab^\dagger \frac{\hbar \omega_c}{2} - \frac{\hbar \omega_c}{2} a^\dagger b - \frac{\hbar \omega_c}{2} b^\dagger a + b^\dagger a \frac{\hbar \omega_c}{2} \\
&= 0
\end{aligned}$$

Thus we have the result that the energy and the z-component of angular momentum are simultaneous observables. Continuing with our commutation relations, if we now look at

$$\begin{aligned}
uu^\dagger &= (a - ib)(a^\dagger + ib^\dagger) & (A.34) \\
&= aa^\dagger + i(ab^\dagger - ba^\dagger) + b^\dagger b \\
&= a^\dagger a + \frac{\hbar \omega_c}{2} + b^\dagger b + \frac{\hbar \omega_c}{2} + \frac{\omega_c}{2} L_z \\
&= a^\dagger a + b^\dagger b + \frac{\omega_c}{2} L_z + \hbar \omega_c \\
&= u^\dagger u + \hbar \omega_c
\end{aligned}$$

we see that

$$[u^\dagger, u] = \hbar \omega_c \quad (A.35)$$

Now,

$$\begin{aligned}
H_0 \psi &= E \psi & (A.36) \\
\left(u^\dagger u + \frac{\hbar \omega_c}{2} \right) \psi &= E \psi \\
u \left(u^\dagger u + \frac{\hbar \omega_c}{2} \right) \psi &= E u \psi \\
\left(uu^\dagger + \frac{\hbar \omega_c}{2} \right) u \psi &= E u \psi \\
\left(u^\dagger u + \frac{\hbar \omega_c}{2} \right) (u \psi) &= (E - \hbar \omega_c) (u \psi) \\
H_0 (u \psi) &= (E - \hbar \omega_c) (u \psi)
\end{aligned}$$

So we see that u is an operator that lowers the energy of the state by $\hbar\omega_c$. We can make a corresponding observation for u^\dagger which raises the energy of the state by $\hbar\omega_c$. Since the angular momentum is a good quantum number what do these operators do to effect the angular momentum of a state? We see

$$\begin{aligned}
L_z \psi &= l_z \psi & (A.37) \\
-\frac{2i}{\omega_c} (a^\dagger b - b^\dagger a) \psi &= l_z \psi \\
u \left[-\frac{2i}{\omega_c} (a^\dagger b - b^\dagger a) \right] \psi &= l_z u \psi \\
-\frac{2i}{\omega_c} (a - ib) (a^\dagger b - b^\dagger a) \psi &= l_z u \psi \\
-\frac{2i}{\omega_c} \left[(a^\dagger b - b^\dagger a) a - i (a^\dagger b - b^\dagger a) b + i \frac{\hbar\omega_c}{2} (a - ib) \right] \psi &= l_z (u \psi) \\
L_z (u \psi) &= (l_z - \hbar) (u \psi)
\end{aligned}$$

Thus we see that the u operator also lowers the angular momentum by \hbar . We can also see that u^\dagger raises the angular momentum by \hbar . Now to calculate the ground state of the system. Since we cannot lower the energy below the ground state then

$$u \psi_0 = 0 \quad (A.38)$$

so that

$$\begin{aligned}
(a - ib) \psi_0 &= 0 & (A.39) \\
\left[\frac{1}{\sqrt{2m}} \left(ip_x + \frac{m\omega_c}{2} x \right) - \frac{i}{\sqrt{2m}} \left(ip_y + \frac{m\omega_c}{2} y \right) \right] \psi_0 &= 0 \\
\frac{1}{\sqrt{2m}} \left[\hbar \left(\frac{\partial}{\partial x} x - i \frac{\partial}{\partial y} \right) + \frac{m\omega_c}{2} (x - iy) \right] \psi_0 &= 0 \\
\frac{1}{\sqrt{2m}} e^{-i\theta} \left[\hbar \left(\frac{\partial}{\partial r} - \frac{i}{r} \frac{\partial}{\partial \theta} \right) + \frac{m\omega_c}{2} r \right] \psi_0 &= 0
\end{aligned}$$

where we have now changed to cylindrical coordinates using

$$x = r \cos \theta \quad (A.40)$$

$$y = r \sin \theta \quad (A.41)$$

$$\frac{\partial}{\partial x} = \cos\theta \frac{\partial}{\partial r} - \frac{1}{r} \sin\theta \frac{\partial}{\partial \theta} \quad (\text{A.42})$$

$$\frac{\partial}{\partial y} = \sin\theta \frac{\partial}{\partial r} + \frac{1}{r} \cos\theta \frac{\partial}{\partial \theta} \quad (\text{A.43})$$

In cylindrical coordinates, we also see that

$$L_z = -i\hbar \left(x \frac{\partial}{\partial y} - y \frac{\partial}{\partial x} \right) = -i\hbar \frac{\partial}{\partial \theta} \quad (\text{A.44})$$

Thus we can decompose the wavefunction as $\psi_0 = \psi_\theta \psi_r$ so that

$$\begin{aligned} L_z \psi &= l_z \psi & (\text{A.45}) \\ L_z \psi_\theta \psi_r &= l_z \psi_\theta \psi_r \\ L_z \psi_\theta &= l_x \psi_\theta \\ -i\hbar \frac{\partial}{\partial \theta} \psi_\theta &= l_x \psi_\theta \end{aligned}$$

Therefore we have the solution for ψ_θ using the periodic boundary conditions that

$$\psi_\theta = e^{il_z \theta} \quad (\text{A.46})$$

with l_z an integer. Since the electron has a negative charge, the electron is counter-rotating with respect to the magnetic field. Thus, it is advantageous to talk about negative angular momentum. With this in mind, let us set $m_z = -l_z$ so that

$$\psi_\theta = e^{-im_z \theta} \quad (\text{A.47})$$

Now, substituting this result into the above equation we get

$$\begin{aligned} \frac{1}{\sqrt{2m}} e^{-i\theta} \left[\hbar \frac{\partial}{\partial r} - \frac{i\hbar}{r} \frac{\partial}{\partial \theta} + \frac{m\omega_c}{2} \right] \psi_{r0} e^{-im_z \theta} &= 0 & (\text{A.48}) \\ \left[\hbar \frac{\partial}{\partial r} - \frac{\hbar m_z}{r} + \frac{m\omega_c}{2} \right] \psi_{r0} &= 0 \end{aligned}$$

This equation now has the solution:

$$\ln \psi_{r0} = m_z \ln r - \frac{m\omega_c}{4\hbar} r^2 + \text{const.} \quad (\text{A.49})$$

$$\psi_{r0} = Ar^{m_z} e^{-\frac{m\omega_c}{4\hbar} r^2}$$

Thus the ground state solution for this system is

$$\psi_0 = Ar^{m_z} e^{-\frac{m\omega_c}{4\hbar} r^2} e^{-im_z\theta} \quad (\text{A.50})$$

Now let us use a form of the raising operator to generate the wave function in general. We could be tempted to use u^\dagger by itself, but as we saw this also increases the angular momentum. Hence, let us develop another related operator.

$$q = re^{-i\theta} \quad (\text{A.51})$$

Now, obviously

$$q\psi_{0,m_z} = \psi_{0,m_z+1} \quad (\text{A.52})$$

so that this operator lowers the angular momentum of the ground state wavefunction (and therefore increases m_z .) Let us proceed by considering the operator

$$(u^\dagger)^n q^n = \left[\frac{e^{i\theta}}{\sqrt{2m}} \left(-\hbar \frac{\partial}{\partial r} - \frac{i\hbar}{r} \frac{\partial}{\partial \theta} + \frac{m\omega_c}{2} r \right) \right]^n [re^{-i\theta}]^n \quad (\text{A.53})$$

Though let us first generate another related operator defined as

$$\bar{q} = r^{-1} e^{-i\theta} \quad (\text{A.54})$$

We find

$$\frac{e^{i\theta}}{\sqrt{2m}} \left(-\hbar \frac{\partial}{\partial r} - \frac{i\hbar}{r} \frac{\partial}{\partial \theta} + \frac{m\omega_c}{2} r \right) [r^{-1} e^{-i\theta}] = \quad (\text{A.55})$$

$$= \frac{1}{\sqrt{2m}} \left[-\hbar \left(-1 + \frac{1}{r} \frac{\partial}{\partial r} \right) - \frac{i\hbar}{r^2} \left(-i + \frac{\partial}{\partial \theta} \right) + \frac{m\omega_c}{2} \right]$$

$$= [r^{-1} e^{i\theta}] \left[\frac{e^{i\theta}}{\sqrt{2m}} \left(-\hbar \frac{\partial}{\partial r} - \frac{i\hbar}{r} \frac{\partial}{\partial \theta} + \frac{m\omega_c}{2} r \right) \right] \quad (\text{A.56})$$

Putting this another way

$$[u^\dagger, \bar{q}] = 0 \quad (\text{A.57})$$

Thus we can transform the operator:

$$(u^\dagger)^n = (u^\dagger \bar{q})^n (\bar{q})^{-n} \quad (\text{A.58})$$

with

$$u^\dagger \bar{q} = \tilde{u}^\dagger = \frac{1}{\sqrt{2m}} \left[-\frac{\hbar}{r} \frac{\partial}{\partial r} - \frac{i\hbar}{r^2} \frac{\partial}{\partial \theta} + \frac{m\omega_c}{2} \right] \quad (\text{A.59})$$

Now we may rewrite our newly constructed raising operator as

$$\begin{aligned} (u^\dagger)^n q^n &= (\tilde{u}^\dagger)^n q^n \bar{q}^{-n} \\ &= (\tilde{u}^\dagger)^n r^{2n} \end{aligned} \quad (\text{A.60})$$

All together we have

$$\begin{aligned} \mathcal{L}_{n,m_z} &= (\tilde{u}^\dagger)^n r^{2n} \mathcal{L}_{0,m_z} \\ &= (\tilde{u}^\dagger)^n A r^{(2n+m_z)} e^{-\frac{m\omega_c}{2\hbar} r^2} e^{-im_z \theta} \end{aligned} \quad (\text{A.61})$$

Our goal now becomes to simplify this expression to something that we know. To continue, let us make a variable substitution

$$s = \frac{m\omega_c}{2\hbar} r^2 \quad (\text{A.62})$$

Using the transformations

$$r = \sqrt{\frac{2\hbar}{m\omega_c}} s^{\frac{1}{2}} \quad (\text{A.63})$$

$$\frac{\partial}{\partial r} = 2\sqrt{\frac{m\omega_c}{2\hbar}} s^{\frac{1}{2}} \frac{\partial}{\partial s} \quad (\text{A.64})$$

we transform \tilde{u}^\dagger to become

$$\tilde{u}^\dagger = \sqrt{\frac{m\omega_c^2}{2}} \left(-\frac{\partial}{\partial s} - \frac{i}{2s} \frac{\partial}{\partial \theta} + \frac{1}{2} \right) \quad (\text{A.65})$$

so that now

$$\psi_{n,m_z}(s) = \left[\sqrt{\frac{m\omega_c^2}{2}} \left(-\frac{\partial}{\partial s} - \frac{i}{2s} \frac{\partial}{\partial \theta} + \frac{1}{2} \right) \right]^n A' s^{\frac{2n+m_z}{2}} e^{-\frac{s}{2}} e^{-im_z\theta} \quad (\text{A.66})$$

Now if we rewrite this slightly as

$$\begin{aligned} \psi_{n,m_z}(s) &= \quad (\text{A.67}) \\ &= s^{-\frac{m_z}{2}} e^{\frac{s}{2}} \left\{ s^{\frac{m_z}{2}} e^{-\frac{s}{2}} \left[\sqrt{\frac{m\omega_c^2}{2}} \left(-\frac{\partial}{\partial s} - \frac{i}{2s} \frac{\partial}{\partial \theta} + \frac{1}{2} \right) \right] s^{-\frac{m_z}{2}} e^{\frac{s}{2}} \right\}^n \\ &\quad \times A' s^{n+m_z} e^{-s} e^{-im_z\theta} \\ &= s^{-\frac{m_z}{2}} e^{\frac{s}{2}} \left\{ s^{\frac{m_z}{2}} e^{-\frac{s}{2}} \left[\sqrt{\frac{m\omega_c^2}{2}} \left(-\frac{\partial}{\partial s} - \frac{m_z}{2s} + \frac{1}{2} \right) \right] s^{-\frac{m_z}{2}} e^{\frac{s}{2}} \right\}^n \\ &\quad \times A' s^{n+m_z} e^{-s} e^{-im_z\theta} \\ &= s^{-\frac{m_z}{2}} e^{\frac{s}{2}} \left(-\frac{\partial}{\partial s} \right)^n A' s^{n+m_z} e^{-s} e^{-im_z\theta} \\ &= A' s^{-\frac{m_z}{2}} e^{\frac{s}{2}} (-1)^n n! s^{m_z} e^{-s} L_n^{m_z}(s) e^{-im_z\theta} \\ &= A' (-1)^n n! s^{\frac{m_z}{2}} e^{-\frac{s}{2}} L_n^{m_z}(s) e^{-im_z\theta} \end{aligned}$$

Where we have used Rodrigues' formula for the associated Laguerre polynomial to obtain the final result. Now, if we substitute s back into our result we get

$$\psi_{n,m_z}(r, \theta) = A_n \left(\frac{m\omega_c}{2\hbar} r^2 \right)^{\frac{m_z}{2}} e^{-\frac{m\omega_c}{4\hbar} r^2} L_n^{m_z} \left(\frac{m\omega_c}{2\hbar} r^2 \right) e^{-im_z\theta} \quad (\text{A.68})$$

Writing this in terms of the magnetic length $l_0 = \sqrt{\frac{\hbar}{m\omega_c}}$ and normalizing the wavefunction we finally obtain

$$\psi_{n,m_z}(r, \theta) = \left(\frac{n!}{2\pi l_0^2 (n+m_z)!} \right)^{\frac{1}{2}} \left(\frac{r^2}{2l_0^2} \right)^{\frac{m_z}{2}} L_n^{m_z} \left(\frac{r^2}{2l_0^2} \right) e^{-\frac{r^2}{4l_0^2}} e^{-im_z\theta} \quad (\text{A.69})$$

Appendix B

The Matrix Elements

B.1 Calculation of the Matrix Elements

In order to consider the interactions between Landau levels, we must consider the matrix elements $\langle Np|e^{i\vec{q}\cdot\vec{r}}|N'p'\rangle$ where

$$\psi_{Np}(x, y) = L^{-\frac{1}{2}} e^{ipy} (2^N N! \pi^{\frac{1}{2}} l)^{-\frac{1}{2}} e^{-\frac{(x-pl)^2 + y^2}{2l^2}} H_N(x/l - pl) \quad (\text{B.1})$$

and $H_N(x)$ is a Hermite polynomial of order N . Thus we have

$$\begin{aligned} M_{Np, N'p'} &= \langle Np|e^{i\vec{q}\cdot\vec{r}}|N'p'\rangle \quad (\text{B.2}) \\ &= \int_{-\infty}^{\infty} dx \int_0^L dy e^{i\vec{q}\cdot\vec{r}} \psi_{Np}(\vec{r}) \psi_{N'p'}(\vec{r}) \\ &= \int_{-\infty}^{\infty} dx \int_0^L dy e^{i(q_x x + q_y y)} \\ &\quad \times \left[L^{-\frac{1}{2}} e^{-ipy} (2^N N! \pi^{\frac{1}{2}} l)^{-\frac{1}{2}} e^{-\frac{(x-pl)^2 + y^2}{2l^2}} H_N(x/l - pl) \right] \\ &\quad \times \left[L^{-\frac{1}{2}} e^{ip'y} (2^{N'} N'! \pi^{\frac{1}{2}} l)^{-\frac{1}{2}} e^{-\frac{(x-p'l)^2 + y^2}{2l^2}} H_{N'}(x/l - p'l) \right] \\ &= \int_{-\infty}^{\infty} dx \int_0^L dy \frac{1}{L} (2^{N+N'} N! N'! \pi l^2)^{-\frac{1}{2}} e^{i(q_x x - q_y y - py - p'y)} \\ &\quad \times e^{-\frac{(x/l - pl)^2 - (x/l - p'l)^2}{2}} H_N(x/l - pl) H_{N'}(x/l - p'l) \\ &= (K/L) \int_0^L dy e^{i(q_y - p + p')y} \\ &\quad \times \int_{-\infty}^{\infty} dx e^{iq_x x} e^{-\frac{(x/l - pl)^2 - (x/l - p'l)^2}{2}} \\ &\quad \times H_N(x/l - pl) H_{N'}(x/l - p'l) \end{aligned}$$

where we will let $K = (2^{N+N'} N! N'! \pi l^2)^{-\frac{1}{2}}$. Now if we perform the integral over y , then we have

$$\begin{aligned}
M_{Np, N'p'} &= K \delta^*(q_y - p + p') \tag{B.3} \\
&\times \int_{-\infty}^{\infty} dx e^{\left[iq_x x - \frac{x^2}{l^2} + x(p+p') - \left(\frac{p'^2 l^2}{2} + \frac{p^2 l^2}{2} \right) \right]} \\
&\times H_N(x/l - pl) H_{N'}(x/l - p'l) \\
&= K \delta^*(q_y - p + p') \int_{-\infty}^{\infty} dx e^{\left(\frac{x}{l} - \frac{pl+p'l-iq_x l}{2} \right)^2} \\
&\times e^{\left(\frac{p+p'}{2} \right)^2} e^{iq_x \left(\frac{p+p'}{2} \right)} e^{-\frac{q_x^2 l^2}{4}} e^{-\frac{p'^2 - p^2}{2}} \\
&\times H_N(x/l - pl) H_{N'}(x/l - p'l) \\
&= K \delta^*(q_y - p + p') e^{iq_x l^2 \left(\frac{p+p'}{2} \right)} e^{-\frac{q_x^2}{4}} \\
&\times e^{-\left(\frac{pl-p'l}{2} \right)^2} e^{-\frac{p'^2 l^2 + p^2 l^2}{2}} \\
&\times \int_{-\infty}^{\infty} dx H_N(x/l - pl) H_{N'}(x/l - p'l)
\end{aligned}$$

Now let us make a change in variables letting $x \rightarrow x + \frac{pl^2+p'l^2-iq_x l^2}{2}$, so that now we have

$$\begin{aligned}
M_{Np, N'p'} &= K \delta^*(q_y - p + p') e^{-\frac{q_x^2 l^2}{4}} e^{iq_x l^2 \left(\frac{p+p'}{2} \right)} e^{-\left(\frac{pl-p'l}{2} \right)^2} \tag{B.4} \\
&\times \int_{-\infty}^{\infty} dx e^{-\frac{x^2}{l^2}} H_N\left(\frac{x}{l} + \frac{p'l - pl - iq_x l}{2} \right) \\
&\times H_{N'}\left(\frac{x}{l} + \frac{pl - p'l - iq_x l}{2} \right)
\end{aligned}$$

Now we see that the arguments of the Hermite polynomials may be rewritten so that

$$\begin{aligned}
M_{Np, N'p'} &= K \delta^*(q_y - p + p') e^{iq_x l^2 \left(\frac{p+p'}{2} \right)} e^{-\frac{q_x^2 l^2}{4}} e^{-\frac{q_x^2 l^2}{4}} \tag{B.5} \\
&\times \int_{-\infty}^{\infty} dx e^{-\frac{x^2}{l^2}} H_N(x/l - a^*) H_{N'}(x/l + a)
\end{aligned}$$

where $a = \frac{pl-p'l+iq_x l}{2} = \frac{q_y l + iq_x l}{2}$ taking into account the delta function. From a table of standard integrals we find that

$$\int_{-\infty}^{\infty} dX e^{-X^2} H_N(X + a) H_M(X + b) = \tag{B.6}$$

$$\pi^{\frac{1}{2}} 2^N a^{N-M} M! L_M^{(N-M)}(-2ab)$$

for $N \geq M$. Ultimately we obtain the result

$$M_{Np, N'p'} = \left(\frac{2^{n-m} m!}{n!} \right)^{\frac{1}{2}} \delta^*(q_y - p + p') e^{iq_x l^2 \left(\frac{p-p'}{2} \right)} e^{-\frac{q^2 l^2}{4}} \quad (\text{B.7})$$

$$\times \left(\frac{\text{sign}(N' - N) q_y l + i q_x l}{2} \right)^{n-m} L_m^{n-m} \left(\frac{q^2 l^2}{2} \right)$$

where $n = \max(N, N')$ and $m = \min(N, N')$. Furthermore, we can substitute $\frac{ql}{2} e^{i\phi}$ for $\frac{\text{sign}(N' - N) q_y l + i q_x l}{2}$, so that we have

$$M_{Np, N'p'} = \left(\frac{2^{n-m} m!}{n!} \right)^{\frac{1}{2}} \delta^*(q_y - p + p') e^{iq_x l^2 \left(\frac{p-p'}{2} \right)} e^{i(n-m)\phi} \quad (\text{B.8})$$

$$\times e^{-\frac{q^2 l^2}{4}} \left(\frac{ql}{2} \right)^{n-m} L_m^{n-m} \left(\frac{q^2 l^2}{2} \right)$$

$$= \left(\frac{m!}{n!} \right)^{\frac{1}{2}} \delta^*(q_y - p + p') e^{iq_x l^2 \left(\frac{p-p'}{2} \right)}$$

$$\times e^{i(n-m)\phi} e^{-\frac{q^2 l^2}{4}} \left(\frac{ql}{\sqrt{2}} \right)^{n-m} L_m^{n-m} \left(\frac{q^2 l^2}{2} \right)$$

with $\phi = \arctan\left(\frac{q_x}{q_y}\right) \text{sign}(N' - N)$.

B.2 A Look at $\delta^*(q - p)$

We have used the notation $\delta^*(q - p)$ for the delta functions in our calculation of the matrix elements. This is to indicate that they are not necessarily the function we are familiar with. Let us use the definition:

$$\delta^*(q - p) \equiv \frac{1}{L} \int_0^L dy e^{i(q-p)y} \quad (\text{B.9})$$

Let us examine some of the properties of this entity. First let us take the case where $p = \frac{2\pi n}{L}$ where n is an integer. In this case we have:

$$\delta^*(q - p) = \begin{cases} \frac{1}{L} \int_0^L dy = 1. & \text{if } q = p \\ \frac{e^{i(q-p)L} - 1}{i(q-p)} = 0. & \text{if } q = \frac{2\pi m}{L} \\ \frac{e^{i(q-p)L} - 1}{i(q-p)} = \frac{e^{iqL} - 1}{i(q-p)} & \text{otherwise} \end{cases} \quad (\text{B.10})$$

So, if p and q are multiples of $\frac{2\pi}{L}$,

$$\delta^*(q - p) = \delta_{qp} \quad (\text{B.11})$$

where δ is the Kronecker delta function. If q is between these values this does not hold true. However, if we look at

$$\begin{aligned} \int_{-\infty}^{\infty} dq \delta^*(q - p) f(q) &= \int_{-\infty}^{\infty} dq \frac{1}{L} \int_0^L dy e^{i(q-p)y} f(q) \\ &= \frac{2\pi}{L} \int_0^L dy F(y) e^{-ipy} \end{aligned} \quad (\text{B.12})$$

where $F(y)$ is just the inverse Fourier transform of $f(q)$. Notice that this essentially reconstructs the function f in a periodic manor as this represents the Fourier series for $f(q)$ over the region $[0, L]$. Then, if L get large, $\delta^*(q - p)$ approaches the behavior of the Dirac delta function except for the prefactor $\frac{2\pi}{L}$. This turns out not to be a problem, if there is another factor to essentially cancel this dependence. This happens quite frequently in our Green's functions calculations where there is are factors of $\frac{1}{L}$ which multiply the expression. The integrals over the y - momentum sums combined with the integrals over the x component of momentum are then responsible for the somewhat mysterious appearance of the factors of $\frac{2\pi}{L}$.

Before we end this discussion, let us look at two further properties of this delta function:

$$\begin{aligned} \int_{-\infty}^{\infty} dq_2 \delta^*(q_2 - p) \delta^*(q - q_2) &= \int_{-\infty}^{\infty} dq_2 \frac{1}{L} \int_0^L dy_1 e^{i(q_2-p)y_1} \frac{1}{L} \int_0^L dy_2 e^{i(q-q_2)y_2} \\ &= \frac{1}{L^2} \int_{-\infty}^{\infty} dq_2 \int_0^L dy_1 \int_0^L dy_2 e^{iq_2(y_2-y_1)} e^{-ipy_1} e^{iqy_2} \\ &= \frac{2\pi}{L^2} \int_0^L dy_1 \int_0^L dy_2 \delta(y_2 - y_1) e^{-ipy_1} e^{iqy_2} \end{aligned}$$

$$\begin{aligned}
&= \frac{2\pi}{L^2} \int_0^L dy_2 e^{i(q-p)y_2} \\
&= \frac{2\pi}{L} \delta^*(q_2 - p)
\end{aligned} \tag{B.13}$$

and

$$\begin{aligned}
\sum_p \delta^*(q-p) \delta^*(p-q_2) &= \sum_p \frac{1}{L} \int_0^L dy_1 e^{i(q-p)y_1} \frac{1}{L} \int_0^L dy_2 e^{i(p-q_2)y_2} \\
&= \frac{1}{L^2} \int_0^L dy_1 \int_0^L dy_2 e^{i(qy_1 - q_2 y_2)} \sum_p e^{ip(y_2 - y_1)} \\
&= \frac{1}{L} \int_0^L dy_1 \int_0^L dy_2 e^{i(qy_1 - q_2 y_2)} \delta(y_2 - y_1) \\
&= \frac{1}{L} \int_0^L dy_1 e^{i(q-q_2)y_1} \\
&= \delta^*(q - q_2)
\end{aligned} \tag{B.14}$$

where we have used the fact that

$$\frac{1}{L} \sum_p e^{ip(y_2 - y_1)} = \sum_{n=0}^{\infty} e^{i \frac{2\pi n}{L} (y_2 - y_1)} = \delta(y_2 - y_1) \tag{B.15}$$

is the Fourier series of a Dirac delta function.

Appendix D

Hermite Polynomials and Their Integrals

We will start with the Hermite polynomials as defined by Rodrigues' formula as

$$H_n(x) = (-1)^n e^{x^2} \frac{d^n}{dx^n} (e^{-x^2}) \quad (\text{D.1})$$

First we see that there is a parity to the Hermite polynomials:

$$\begin{aligned} H_n(-x) &= (-1)^n e^{(-x)^2} \frac{d^n}{d(-x)^n} (e^{-(-x)^2}) \\ &= (-1)^n e^{x^2} (-1)^n \frac{d^n}{dx^n} (e^{-x^2}) \\ &= (-1)^n H_n(x) \end{aligned} \quad (\text{D.2})$$

Now from our definition:

$$e^{-(-x)^2} H_n(x) = (-1)^n \frac{d^n}{d(-x)^n} (e^{-(-x)^2}) \quad (\text{D.3})$$

and using the fact that

$$\frac{d^n}{dx^n} (fg) = \sum_{k=0}^n \binom{n}{k} f^{(k)} g^{(n-k)} \quad (\text{D.4})$$

we see that

$$\begin{aligned} H_{m+n}(x) e^{-x^2} &= (-1)^n \frac{d^n}{dx^n} (e^{-x^2} H_m(x)) \\ &= (-1)^n \sum_{k=0}^n \binom{n}{k} \frac{d^k}{dx^k} (e^{-x^2}) H_m^{(n-k)}(x) \end{aligned} \quad (\text{D.5})$$

$$= (-1)^n \sum_{k=0}^n \binom{n}{k} (-1)^{-k} H_k(x) H_m^{(n-k)}(x) e^{-x^2}$$

so that we finally we end up with the identity:

$$H_{m+n}(x) = \sum_{k=0}^n \binom{n}{k} (-1)^{n-k} H_k(x) H_m^{(n-k)}(x) \quad (\text{D.6})$$

We now can use this formula along with $H_0(x) = 1$ and $H_1(x) = 2x$ to generate two important relations for the Hermite polynomials. The first is

$$\begin{aligned} H_{n+1}(x) &= \sum_{k=0}^n \binom{n}{k} (-1)^{n-k} H_k(x) H_1^{(n-k)}(x) \\ &= \sum_{k=n-1}^n \binom{n}{k} (-1)^{n-k} H_k(x) (2x)^{(n-k)} \\ &= 2xH_n(x) - 2nH_{n-1}(x) \end{aligned} \quad (\text{D.7})$$

and the second is

$$\begin{aligned} H_{1+m}(x) &= \sum_{k=0}^1 \binom{1}{k} (-1)^{1-k} H_k(x) H_1^{(1-k)}(x) \\ &= H_m(x)H_1(x) - H'_m(x)H_0(x) \\ &= 2xH_m(x) - H'_m(x) \end{aligned} \quad (\text{D.8})$$

Additionally we see that if we combine these two expressions we obtain

$$H'_n(x) = 2nH_{n-1}(x) \quad (\text{D.9})$$

Now using this equation recursively we obtain the relation

$$H_n^{(k)}(x) = \frac{2^k n!}{(n-k)!} H_{n-k}(x) \quad (\text{D.10})$$

and using our above equation with $x = 0$ we get

$$H_n(0) = -2(n-1)H_{n-2}(0) = (-2)^l \frac{(n-1)!!}{(n-2l-1)!!} H_{n-2l}(0) \quad (\text{D.11})$$

Substituting $H_0(0) = 1$ and $H_1(0) = 0$, we see

$$H_n(0) = \begin{cases} (-2)^{\frac{n}{2}} (\frac{n}{2} - 1)!! & n \text{ even} \\ 0, & n \text{ odd} \end{cases} \quad (\text{D.12})$$

Combining these results, we get

$$H_n^{(k)}(0) = \begin{cases} \frac{2^k n!}{(n-k)!} (-2)^{\frac{n-k}{2}} (\frac{n-k}{2} - 1)!! & (n-k) \text{ even} \\ 0, & (n-k) \text{ odd} \end{cases} \quad (\text{D.13})$$

Now we may write the Taylor expansion of $H_n(x)$ about $x = 0$ as

$$H_n(x) = \sum_{k=0}^n (-1)^{\frac{n-k}{2}} 2^{\frac{n-k}{2}} \frac{n!}{(n-k)! k!} (\frac{n-k}{2} - 1)!! \left(\frac{1 + (-1)^{n-k}}{2} \right) x^k \quad (\text{D.14})$$

which may alternately be written as

$$\begin{aligned} H_n(x) &= \sum_{l=0}^{\frac{n}{2}} (-1)^l 2^{n-l} \frac{n!(l-1)!!}{(2l)!(n-2l)!} x^{n-2l} \\ &= \sum_{l=0}^{\frac{n}{2}} (-1)^l \frac{n!}{l!(n-2l)!} (2x)^{n-2l} \end{aligned} \quad (\text{D.15})$$

Now that we have these few tidbits under our belt, let us take a look at integrals of the form

$$\begin{aligned} \int_{-\infty}^{\infty} dx e^{-x^2} H_n(x) &= \int_{-\infty}^{\infty} dx (-1)^n \frac{d^n}{dx^n} (e^{-x^2}) \\ &= \left[(-1)^n \frac{d^{n-1}}{dx^{n-1}} (e^{-x^2}) \right]_{-\infty}^{\infty} \\ &= \left[H_{n-1}(x) e^{-x^2} \right]_{-\infty}^{\infty} \\ &= \begin{cases} 0, & n > 0 \\ \sqrt{\pi}, & n = 0 \end{cases} \end{aligned} \quad (\text{D.16})$$

We can use this result to look at the orthogonality property of $H_n(x)$. Let us start with

$$I = \int_{-\infty}^{\infty} dx e^{-x^2} H_n(x) H_m(x) \quad (\text{D.17})$$

We proceed by again using Rodrigues' formula and then integrating by parts such that

$$\begin{aligned}
I &= \int_{-\infty}^{\infty} dx (-1)^n \frac{d^n}{dx^n} (e^{-x^2}) H_m(x) dx & (D.18) \\
&= \left[(-1)^n H_m(x) \frac{d^{n-1}}{dx^{n-1}} (e^{-x^2}) \right]_{-\infty}^{\infty} \\
&\quad + \int_{-\infty}^{\infty} dx (-1)^{n-1} \frac{d^{n-1}}{dx^{n-1}} (e^{-x^2}) H'_m(x) \\
&= \left[H_m(x) H_{n-1}(x) e^{-x^2} \right]_{-\infty}^{\infty} + \int_{-\infty}^{\infty} dx H_{n-1}(x) H'_m(x) \\
&= 2m \int_{-\infty}^{\infty} dx H_{n-1}(x) H_{m-1}(x)
\end{aligned}$$

If we continue this process we obtain

$$I = \frac{2^n m!}{(m-n)!} \int_{-\infty}^{\infty} dx H_{n-m}(x) \quad (D.19)$$

Now we use our previous result to obtain

$$\int_{-\infty}^{\infty} dx e^{-x^2} H_n(x) H_m(x) = \begin{cases} 2^n n! \sqrt{\pi} & n = m \\ 0 & n \neq m \end{cases} \quad (D.20)$$

Now let us try

$$I = \int_{-\infty}^{\infty} dx e^{-x^2} H_n(x+a) H_m(x) \quad (D.21)$$

Using the derivative properties of the Hermite polynomials

$$\begin{aligned}
\frac{\partial I}{\partial a} &= \int_{-\infty}^{\infty} dx e^{-x^2} \frac{\partial}{\partial a} (H_n(x+a) H_m(x)) & (D.22) \\
&= 2n \int_{-\infty}^{\infty} dx e^{-x^2} H_{n-1}(x+a) H_m(x)
\end{aligned}$$

$$\frac{\partial^k I}{\partial a^k} = \frac{2^k n!}{(n-k)!} \int_{-\infty}^{\infty} dx e^{-x^2} H_{n-k}(x+a) H_m(x) \quad (D.23)$$

Now let us use a Taylor expansion about $a = 0$ so that

$$I = \sum_{k=0}^{\infty} \frac{2^k n!}{k!(n-k)!} \int_{-\infty}^{\infty} dx e^{-x^2} H_{n-k}(x) H_m(x) a^k \quad (D.24)$$

The only non-zero term in this sum is when $n - k = m$ so that

$$\begin{aligned} \int_{-\infty}^{\infty} dx e^{-x^2} H_n(x+a) H_m(x) &= \frac{2^{n-m} n!}{(n-m)! m!} 2^m m! \sqrt{\pi} a^{n-m} \\ &= \frac{2^n n!}{(n-m)!} \sqrt{\pi} a^{n-m} \end{aligned} \quad (D.25)$$

with the condition that $n \geq m$. We come finally to the last integral which we use in calculating the matrix elements:

$$I = \int_{-\infty}^{\infty} dx e^{-x^2} H_n(x+a) H_m(x+b) \quad (D.26)$$

Again using the derivative properties of the Hermite polynomials we can write

$$\begin{aligned} \frac{\partial^l I}{\partial b^l} &= \frac{2^l m!}{(m-l)!} \int_{-\infty}^{\infty} dx e^{-x^2} H_n(x+a) H_{m-l}(x+b) \\ \left. \frac{\partial^l I}{\partial b^l} \right|_{b=0} &= \frac{2^l m!}{(m-l)!} \int_{-\infty}^{\infty} dx e^{-x^2} H_n(x+a) H_{m-l}(x) \\ &= \frac{2^l m!}{(m-l)!} \frac{2^n n!}{(n-(m-l))!} \sqrt{\pi} a^{n-(m-l)} \end{aligned} \quad (D.27)$$

Again expanding in a Taylor series this time about $b = 0$ we find

$$\begin{aligned} I &= \sum_{l=0}^m \frac{2^l m!}{(m-l)!} \frac{2^n n!}{(n-(m-l))!} \sqrt{\pi} a^{n-(m-l)} b^l \\ &= \sqrt{\pi} 2^n a^{n-m} \sum_{l=0}^m \frac{m! n!}{(m-l)! (n-(m-l))!} (2ab)^l \end{aligned} \quad (D.28)$$

$$= \sqrt{\pi} 2^n a^{n-m} m! \sum_{l=0}^m (-1)^l \frac{(n + (n - m))!}{(m - l)!(m + (n - m) - (m - l))! l!} (-2ab)^l$$

After comparing this sum to the standard table we find that it becomes a Generalized Laguerre polynomial so that

$$\int_{-\infty}^{\infty} dx e^{-x^2} H_n(x + a) H_m(x + b) = \sqrt{\pi} 2^n a^{n-m} m! L_m^{(n-m)}(-2ab) \quad (\text{D.29})$$

provided that $n \geq m$. In the case that $n < m$ we can exchange the roles of the two polynomials so that

$$\int_{-\infty}^{\infty} dx e^{-x^2} H_n(x + a) H_m(x + b) = \sqrt{\pi} 2^m b^{m-n} n! L_n^{(m-n)}(-2ab) \quad (\text{D.30})$$

Appendix E

Kramers–Krönig and $\Pi(\omega, q)$

Starting with the expression for $\Pi(i\omega, q)$

$$\Pi(i\omega, q) = \sum_{N, N'} \int_{-\infty}^{\infty} dx \int_{-\infty}^{\infty} dy A_{N', \sigma'}(x) A_{N, \sigma}(y) \frac{f(x) - f(y)}{x - y + i\omega} |M_{N, N'}(q)|^2 \quad (\text{E.1})$$

We can now rewrite this expression in term of the Greens' Functions as

$$\begin{aligned} \Pi(i\omega, q) &= \quad (\text{E.2}) \\ &= \sum_{N, N'} |M_{N, N'}(q)|^2 \left\{ \int_{-\infty}^{\infty} dx A_{N', \sigma'}(x) G_{N, \sigma}(x + i\omega) f(x) \right. \\ &\quad \left. + \int_{-\infty}^{\infty} dy A_{N, \sigma}(y) G_{N', \sigma'}(y - i\omega) f(y) \right\} \\ &= \sum_{N, N'} |M_{N, N'}(q)|^2 \int_{-\infty}^{\infty} dx f(x) \\ &\quad \times \{ A_{N', \sigma'}(x) G_{N, \sigma}(x + i\omega) + A_{N, \sigma}(x) G_{N', \sigma'}(x - i\omega) \} \end{aligned}$$

Now performing the analytic continuation, we let $i\omega \rightarrow \omega + i\delta$ with $\delta \rightarrow 0$ so that

$$\begin{aligned} \Pi(\omega, q) &= \sum_{N, N'} |M_{N, N'}(q)|^2 \int_{-\infty}^{\infty} dx f(x) \quad (\text{E.3}) \\ &\quad \times \{ A_{N', \sigma'}(x) G_{N, \sigma}^R(x + i\omega) A_{N, \sigma}(x) G_{N', \sigma'}^A(x - i\omega) \} \end{aligned}$$

Now from the Kramers–Krönig relations we have that

$$G^R(y) = -\frac{i}{\pi} \int_{-\infty}^{\infty} dx P \frac{G^R(x)}{x - y} \quad (\text{E.4})$$

$$G^A(y) = \frac{i}{\pi} \int_{-\infty}^{\infty} dx P \frac{G^A(x)}{x-y} \quad (\text{E.5})$$

If we apply these to our expression for $\Pi(\omega, q)$ we obtain

$$\begin{aligned}
& \int_{-\infty}^{\infty} d\omega P \frac{\Pi(\omega, q)}{\omega - y} = \quad (\text{E.6}) \\
& = \int_{-\infty}^{\infty} \frac{d\omega}{\omega - y} \sum_{N, N'} |M_{N, N'}(q)|^2 \int_{-\infty}^{\infty} dx f(x) \\
& \quad \times \left\{ A_{N', \sigma'}(x) G_{N, \sigma}^R(x + \omega) + A_{N, \sigma}(x) G_{N', \sigma'}^A(x - \omega) \right\} \\
& = \sum_{N, N'} |M_{N, N'}(q)|^2 \int_{-\infty}^{\infty} dx f(x) \\
& \quad \times \left\{ A_{N', \sigma'}(x) \int_{-\infty}^{\infty} d\omega P \frac{G_{N, \sigma}^R(x + \omega)}{\omega - y} \right. \\
& \quad \left. + A_{N, \sigma}(x) \int_{-\infty}^{\infty} d\omega P \frac{G_{N', \sigma'}^A(x - \omega)}{\omega - y} \right\} \\
& = \sum_{N, N'} |M_{N, N'}(q)|^2 \int_{-\infty}^{\infty} dx f(x) \\
& \quad \times \left\{ A_{N', \sigma'}(x) \int_{-\infty}^{\infty} d\omega' P \frac{G_{N, \sigma}^R(\omega')}{\omega' - x - y} \right. \\
& \quad \left. + A_{N, \sigma}(x) \int_{-\infty}^{\infty} d\omega' P \frac{G_{N', \sigma'}^A(\omega')}{-\omega' + x - y} \right\} \\
& = \sum_{N, N'} |M_{N, N'}(q)|^2 \int_{-\infty}^{\infty} dx f(x) \\
& \quad \times \left\{ A_{N', \sigma'}(x) \left(-\frac{\pi}{i} \right) G_{N, \sigma}^R(x + y) \right. \\
& \quad \left. - A_{N, \sigma}(x) \left(\frac{\pi}{i} \right) G_{N', \sigma'}^A(x - y) \right\} \\
& = \left(-\frac{\pi}{i} \right) \sum_{N, N'} |M_{N, N'}(q)|^2 \int_{-\infty}^{\infty} dx f(x) \\
& \quad \times \left\{ A_{N', \sigma'}(x) G_{N, \sigma}^R(x + y) + A_{N, \sigma}(x) G_{N', \sigma'}^A(x - y) \right\} \\
& = \left(-\frac{\pi}{i} \right) \Pi(y, q)
\end{aligned}$$

Thus we have our final result:

$$\Pi(y, q) = -\frac{\pi}{i} \int_{-\infty}^{\infty} d\omega P \frac{\Pi(\omega, q)}{\omega - y} \quad (\text{E.7})$$

By separating the real and imaginary parts we end up with the following two expressions

$$\text{Im}\Pi(y, q) = -\frac{1}{\pi} \int_{-\infty}^{\infty} d\omega P \frac{\text{Re}\Pi(\omega, q)}{\omega - y} \quad (\text{E.8})$$

$$\text{Re}\Pi(y, q) = \frac{1}{\pi} \int_{-\infty}^{\infty} d\omega P \frac{\text{Im}\Pi(\omega, q)}{\omega - y} \quad (\text{E.9})$$

Appendix F

Calculating the Fourier Potential

We have have a two dimensional potential that looks like

$$V(\vec{r}) = \frac{e^2}{\kappa} \frac{1}{\sqrt{r^2 + a^2}} \quad (\text{F.1})$$

Taking the Fourier transform we have

$$V(\vec{q}) = \frac{e^2}{\kappa} \int d\vec{r} \frac{e^{i\vec{q}\cdot\vec{r}}}{\sqrt{r^2 + a^2}} \quad (\text{F.2})$$

which we can express in cylindrical coordinates as

$$V(\vec{q}) = \frac{e^2}{\kappa} \int_0^{2\pi} d\theta \int_0^\infty r dr \frac{e^{iqr \cos \theta}}{\sqrt{r^2 + a^2}} \quad (\text{F.3})$$

Performing the θ integral first and using the identity

$$\int_0^{2\pi} d\theta e^{ib \cos \theta} = 2\pi J_0(b) \quad (\text{F.4})$$

where $J_0(b)$ is the zeroth order Bessel function we arrive at

$$V(\vec{q}) = \frac{2\pi e^2}{\kappa q} \int_0^\infty dr \frac{r J_0(qr)}{\sqrt{r^2 + a^2}} \quad (\text{F.5})$$

Proceeding, we make the substitution $x = qr$ yielding

$$V(\vec{q}) = \frac{2\pi e^2}{\kappa q} \int_0^\infty dx \frac{x J_0(x)}{\sqrt{x^2 + q^2 a^2}} \quad (\text{F.6})$$

Now using the fact that

$$\int_0^\infty dx \frac{x J_0(x)}{\sqrt{x^2 + b^2}} = e^{-b} \quad (\text{F.7})$$

we have

$$V(\vec{q}) = \frac{2\pi e^2}{\kappa q} e^{-qa} \quad (\text{F.8})$$

F.1 Proof of the Bessel function identity

We wish to prove the relation (F.4)

$$\int_0^{2\pi} d\theta e^{ib \cos \theta} = 2\pi J_0(b)$$

Using the series expansion for

$$e^x = \sum_{m=0}^{\infty} \frac{x^m}{m!} \quad (\text{F.9})$$

we find that our integral becomes

$$\int_0^{2\pi} d\theta e^{ib \cos \theta} = \int_0^{2\pi} d\theta \sum_{m=0}^{\infty} \frac{(ib \cos \theta)^m}{m!} \quad (\text{F.10})$$

Exchanging the sum and the integral we find:

$$\int_0^{2\pi} d\theta e^{ib \cos \theta} = \sum_{m=0}^{\infty} \frac{(ib)^m}{m!} \int_0^{2\pi} d\theta (\cos \theta)^m \quad (\text{F.11})$$

Now

$$\int_0^{2\pi} d\theta (\cos \theta)^m = \begin{cases} 2\pi \left(\frac{1}{2}\right)^m \binom{m}{m/2} & m \text{ even} \\ 0 & m \text{ odd} \end{cases} \quad (\text{F.12})$$

so that

$$\begin{aligned} \int_0^{2\pi} d\theta (\cos \theta)^m &= \sum_{n=0}^{\infty} \frac{(ib)^{2n}}{(2n)!} \left[2\pi \left(\frac{1}{2}\right)^{2n} \binom{2n}{n} \right] \\ &= 2\pi \sum_{n=0}^{\infty} \left(-\frac{b^2}{4}\right)^n \frac{1}{(n!)^2} \\ &= 2\pi J_0(b) \end{aligned} \quad (\text{F.13})$$

since we recognize the series for $J_0(b)$

$$J_0(b) = \sum_{n=0}^{\infty} \frac{1}{(n!)^2} \left(-\frac{b^2}{4}\right)^n \quad (\text{F.14})$$

F.2 The second integral

Deriving the second integral relation requires a bit more trickery. We begin by defining the following three functions as:

$$u(a) = \int_0^{\infty} \frac{x J_0(x) dx}{\sqrt{x^2 + a^2}} \quad (\text{F.15})$$

$$v(a) = \int_0^{\infty} \frac{J_0'(x) dx}{\sqrt{x^2 + a^2}} \quad (\text{F.16})$$

$$w(a) = \int_0^{\infty} \frac{x J_0''(x) dx}{\sqrt{x^2 + a^2}} \quad (\text{F.17})$$

The zeroth order Bessel equation may be written in the form

$$x J_0(x) + J_0'(x) + x J_0''(x) = 0 \quad (\text{F.18})$$

Therefore we find the first relationship that we are looking for, namely

$$\begin{aligned} u(a) + v(a) + w(a) &= \int_0^{\infty} \frac{x J_0(x) + J_0'(x) + x J_0''(x)}{\sqrt{x^2 + a^2}} dx \\ &= 0 \end{aligned} \quad (\text{F.19})$$

In addition we know that

$$\int_0^{\infty} J_0(x) dx = 1 \quad (\text{F.20})$$

so that we find our second relationship

$$\begin{aligned} \frac{\partial u}{\partial a} + av &= \int_0^{\infty} dx \left[\frac{-ax J_0(x)}{(x^2 + a^2)^{\frac{3}{2}}} + \frac{-a J_0'(x)}{(x^2 + a^2)^{\frac{1}{2}}} \right] \\ &= \int_0^{\infty} dx \frac{d}{dx} \left[\frac{a J_0(x)}{\sqrt{x^2 + a^2}} \right] \\ &= \left[\frac{a J_0(x)}{\sqrt{x^2 + a^2}} \right]_0^{\infty} \end{aligned} \quad (\text{F.21})$$

$$= -1$$

Last, we find that

$$\begin{aligned} a \frac{\partial v}{\partial a} - w &= \int_0^\infty dx \left[\frac{-a^2 J_0'(x)}{(x^2 + a^2)^{\frac{3}{2}}} - \frac{x^2 J_0''(x)}{(x^2 + a^2)^{\frac{1}{2}}} \right] & (F.22) \\ &= \int_0^\infty dx \frac{d}{dx} \left[\frac{x J_0'(x)}{\sqrt{x^2 + a^2}} \right] \\ &= \left[\frac{x J_0'(x)}{\sqrt{x^2 + a^2}} \right]_0^\infty \\ &= 0 \end{aligned}$$

since

$$J_i(x) = -J_0'(x) \quad (F.23)$$

$$J_1(0) = 0 \quad (F.24)$$

$$\lim_{x \rightarrow \infty} J_n(x) = 0 \quad (F.25)$$

All together we have the system of equations

$$u + v + w = 0 \quad (F.26)$$

$$\frac{du}{da} + av + 1 = 0 \quad (F.27)$$

$$a \frac{dv}{da} - w = 0 \quad (F.28)$$

Taking the derivative of (F.27) we have

$$\frac{d^2 u}{da^2} + a \frac{dv}{da} + v = 0 \quad (F.29)$$

Now substitution in (F.26) and (F.28) we have

$$\frac{d^2 u}{da^2} + w + v = \frac{d^2 u}{da^2} - u \quad (F.30)$$

$$= 0$$

$$(F.31)$$

The general solution to this equation is

$$u(a) = Ae^{-1} + Be^a \quad (\text{F.32})$$

with A and B as arbitrary constants. Now we realize that

$$u(0) = \int_0^\infty \frac{xJ_0(x)dx}{\sqrt{x^2 + 0^2}} = \int_0^\infty J_0(x)dx = 1 \quad (\text{F.33})$$

Also, we see that

$$\lim_{a \rightarrow \infty} u(a) = \lim_{a \rightarrow \infty} \frac{xJ_0(x)dx}{\sqrt{x^2 + a^2}} = 0 \quad (\text{F.34})$$

We find that the choice of $A = 1$ and $B = 0$ fulfill these boundary conditions, so that we are left with

$$u(a) = e^{-a} \quad (\text{F.35})$$

Thus we have proven

$$\int_0^\infty \frac{xJ_0(x)dx}{\sqrt{x^2 + a^2}} = e^{-a} \quad (\text{F.36})$$

Appendix G

Program Listings

The Fortran 90 code that follows is the result of a long history of revisions. It originally started as a Fortran 77 code. Therefore, it still shows a little bit of its history and has deliberately been left in somewhat raw form as various pieces are added and removed. This particular product is a merger of several versions which included different physics. This allowed for a more consistent treatment of the different models. This was made possible by moving to Fortran 90 which allows for modules that superseded the old common block methods. Along with the program, we have included the Makefile and a sample input parameter file.

G.1 `besselj0.f90`

```
! A function to calculate the 0th order Bessel function

! This function uses either a Taylor series or an asymptotic
! series depending upon the value of x. Note the optimal
! cutoff was determined empirically as approximately 12.7.
! These series were obtained from the CRC Mathematics Handbook

      FUNCTION j0(x)
! TOL is a local parameter
! ..
      USE scondo_consts
! ..
! .. Function Return Value ..
      REAL (wp) :: j0
! ..
```

```

! .. Parameters ..
      REAL (wp), PARAMETER :: tol = 1.0E-16_wp
! ..
! .. Scalar Arguments ..
      REAL (wp), INTENT(IN) :: x
! ..
! .. Local Scalars ..
      REAL (wp) :: ival, jval, kval, oldterm, psum, qsum, &
                  sum, term, val, z
! ..
! .. Intrinsic Functions ..
      INTRINSIC abs, cos, sqrt, sin
! ..
! Choose either the Taylor series or the asymptotic series
      IF (abs(x)<12.7E0_wp) THEN

! This is the Taylor series
      z = -0.25E0_wp*x*x
      ival = 0.0E0_wp
      term = 1.0E0_wp
      sum = 1.0E0_wp
! Calculate and sum terms until sum changes less than tolerance
      DO WHILE (abs(term)>tol*abs(sum))
          ival = ival + 1.0E0_wp
          term = term*z/(ival*ival)
          sum = sum + term
      END DO
      val = sum
    ELSE

! This is the asymptotic series
      z = -1.0E0_wp/(64.0E0_wp*x*x)
      ival = 0.0E0_wp
      jval = -1.0E0_wp
      term = 1.0E0_wp
      oldterm = 2.0E0_wp
      sum = 1.0E0_wp
! Calculate first asymptotic series until terms diverge
      DO WHILE (abs(term/oldterm)<1.0E0_wp)
          ival = ival + 2.0E0_wp
          jval = jval + 4.0E0_wp
          kval = jval - 2.0E0_wp

```

```

        oldterm = term
        term = term*z*kval*kval*jval*jval/(ival*(ival-1.0E0_wp))
        psum = sum
        sum = sum + term
    END DO

    ival = 1.0E0_wp
    jval = 1.0E0_wp
    term = -0.125E0_wp/x
    oldterm = 2.0E0_wp
    sum = term
! Calculate second asymptotic series until terms diverg
    DO WHILE (abs(term/oldterm)<1.0E0_wp)
        ival = ival + 2.0E0_wp
        jval = jval + 4.0E0_wp
        kval = jval - 2.0E0_wp
        oldterm = term
        term = term*z*kval*kval*jval*jval/(ival*(ival-1.0E0_wp))
        qsum = sum
        sum = sum + term
    END DO

! Combine series results with asymptotic expression
    z = x - 0.25E0_wp*pi
    val = sqrt(2.0E0_wp/(pi*x))
    val = val*(psum*cos(z)-qsum*sin(z))

    END IF

    j0 = val

    RETURN
END FUNCTION j0

```

G.2 besstab.f90

! Subroutine to store table of Bessel functions
! in order to save calculation time

```
      SUBROUTINE besstab(bessval,nqpts,qsize)
! ..
      USE scondo_consts
! ..
! .. Scalar Arguments ..
      REAL (wp), INTENT(IN) :: qsize
      INTEGER, INTENT(IN) :: nqpts
! ..
! .. Array Arguments
      REAL (wp), INTENT(OUT) :: bessval(:, :)
! ..
! .. Local Scalars ..
      REAL (wp) :: qs2, tmp
      INTEGER :: i, j
! ..
! .. External Functions ..
      REAL (wp), EXTERNAL :: j0
! ..
! .. Intrinsic Functions ..
      INTRINSIC float
! ..
      qs2 = qsize*qsize
      DO j = 1, nqpts
        tmp = float(j-1)*qs2
        DO i = 1, j
          bessval(i,j) = j0(float(i-1)*tmp)
        END DO
        DO i = 1, j
          bessval(j,i) = bessval(i,j)
        END DO
      END DO
      RETURN
END SUBROUTINE besstab
```

G.3 bigw.f90

```
! Subroutine to calculate W(N,L,N,L;q)
! which is the vertex coupling. Note that the
! approximation used here ignores inter-Landau
! coupling in the vertex correction

! Variables:
!   upotsq - The square of the potential as a function of q
!   bw - W(N,L,N,L;q)
!   nimp - The impurity density
!   qsize - The momentum spacing
!   nqpts - The number of momentum points
!   nllev - The number of Landau levels

SUBROUTINE bigw(bessval,bw,upotsq,pjelem,nqpts,qsize,nllev,nimp)
! ..
    USE scondo_consts
! ..
! .. Scalar Arguments ..
    REAL (wp), INTENT(IN) :: nimp, qsize
    INTEGER, INTENT(IN) :: nllev, nqpts
! ..
! .. Array Arguments ..
    REAL (wp), DIMENSION (:,:,), INTENT(OUT) :: bw
    REAL (wp), DIMENSION (:,:), INTENT(IN) :: bessval
    REAL (wp), DIMENSION (:,:,), INTENT(IN) :: pjelem
    REAL (wp), DIMENSION (:), INTENT(IN) :: upotsq
! ..
! .. Local Scalars ..
    REAL (wp) :: fact, jnl, p, val
    INTEGER :: i, j, l, n
! ..
! .. Local Arrays ..
    REAL (wp) :: jnl2(nllev,nllev)
! ..
! .. External Functions ..
    REAL (wp), EXTERNAL :: jelem, melem
! ..
! .. Intrinsic Functions ..
    INTRINSIC float
```

```

! ..
      bw(1:nqpts,1:nllev,1:nllev) = 0.0EO_wp

!MIC$ DO ALL AUTOSCOPE
      DO j = 1, nqpts

          p = float(j-1)*qsize
          val = p*upotsq(j)

          DO n = 1, nllev
              DO l = 1, n
                  jnl2(l,n) = pjelem(j,n,n)*pjelem(j,l,l)*val
                  jnl2(n,l) = jnl2(l,n)
              END DO !l
          END DO !ln

          DO l = 1, nllev
              DO n = 1, nllev
!MIC$ GUARD
                  bw(1:nqpts,n,l) = bw(1:nqpts,n,l) + &
                      bessval(1:nqpts,j)*jnl2(n,l)
!MIC$ END GUARD
              END DO !n
          END DO !l

      END DO !j

! Xie, Li and Das Sarma have an expression equiv. to
!           bw(n,l,i)=bw(n,l,i)*qsize/(2.0d0*pi)
! but it was determined that they missed a factor of
! the impurity density (here = nimp)

      fact = nimp*qsize/(2.0EO_wp*pi)
      bw(1:nqpts,1:nllev,1:nllev) = bw(1:nqpts,1:nllev,1:nllev)*fact

      RETURN
END SUBROUTINE bigw

```

G.4 chempot.f90

```
! A function to calculate the chemical potential
! (Fermi energy) by integrating the density of states
! and using a binary search

! Variables:
!     dstat - The density of states
!     esize - The energy spacing
!     ns - The 2-D density
!     lopot - Low potential estimate
!     cutoff - The cutoff value for sum
!     sum - The integral sum

      FUNCTION chempot(dstat,nepts,esize,ns,beta)
! ..
      USE scondo_consts
! ..
! .. Function Return Value ..
      REAL (wp) :: chempot
! ..
! .. Parameters ..
      REAL (wp), PARAMETER :: tol = 1E-10_wp
! ..
! .. Scalar Arguments ..
      REAL (wp), INTENT(IN) :: beta, esize, ns
      INTEGER, INTENT(IN) :: nepts
! ..
! .. Array Arguments
      REAL (wp), INTENT(IN) :: dstat(:)
! ..
! .. Local Scalars ..
      REAL (wp) :: besize, betae, cutoff, esfact, estima, &
        hipot, lopot, sum
      INTEGER :: i, nmax
! ..
! .. Intrinsic Functions ..
      INTRINSIC exp, float, int, min
! ..
      cutoff = ns/esize
      besize = esize*beta
```

```

lopot = 0E0_wp
hipot = float(nepts-1)*esize

DO WHILE ((hipot-lopot)>=tol)
  estima = 0.5E0_wp*(lopot+hipot)

  esfact = beta*estima
  sum = 0E0_wp
  nmax = min(nepts,int((80E0_wp/beta+estima)/esize))
  DO i = 1, nmax
    betae = float(i-1)*besize - esfact
    sum = sum + dstat(i)/(exp(betae)+1E0_wp)
  END DO

  IF (sum>cutoff) THEN
    hipot = estima
  ELSE
    lopot = estima
  END IF

END DO

chempot = estima

RETURN
END FUNCTION chempot

```

G.5 densos.f90

```
! A subroutine to calculate the density of states
! from the imaginary part of the Green's functions

! Variables
!     grnfi - Imaginary part of the Greens fcn
!     dstat - The density of states

      SUBROUTINE densos(dstat,grnfi,nepts,nllev)
! ..
      USE scondo_consts
      USE scondo_spin
! ..
! .. Scalar Arguments ..
      INTEGER, INTENT (IN) :: nepts, nllev
! ..
! .. Array Arguments
      REAL (wp), DIMENSION(:), INTENT(OUT) :: dstat
      REAL (wp), DIMENSION(:, :, :), INTENT (IN) :: grnfi
! ..
! .. Local Scalars ..
      REAL (wp) :: fact
      INTEGER :: i, j, sp
! ..

      fact = -0.5E0_wp*gs/(pi*pi)

      dstat(1:nepts) = 0E0_wp

      DO sp = 1, spinstates
        DO j = 1, nllev
          dstat(1:nepts) = dstat(1:nepts) + grnfi(1:nepts,j,sp)
        END DO !j
      END DO !sp

      dstat(1:nepts) = dstat(1:nepts)*fact

      RETURN
END SUBROUTINE densos
```

G.6 findener.f90

```
! A subroutine to find the energies of the levels
! from the Greens Functions using various methods

      SUBROUTINE greng(grnfr,grnfi,esize,eoff,nepts,nllev,magfield)
! ..
      USE scondo_consts
      USE scondo_spin
! ..
! .. Scalar Arguments ..
      REAL (wp), INTENT(IN) :: eoff, esize, magfield
      INTEGER, INTENT(IN) :: nepts, nllev
! ..
! .. Array Arguments
      REAL (wp), INTENT(IN) :: grnfr(:,:,:), grnfi(:,:,:)
! ..
! .. Local Scalars ..
      REAL (wp) :: cume, cume2, e, ecross, oldval, temp, vmax, cumesq
      INTEGER :: i, j, sp
! ..
! .. Intrinsic Functions ..
      INTRINSIC abs, sqrt
! ..
      WRITE (73,1) magfield
      DO i = 1, nllev
      DO sp = 1, spinstates
          ecross = OE0_wp
          vmax = OE0_wp
          oldval = grnfr(1,i,sp)
          cume = OE0_wp
          cumesq = OE0_wp
          cume2 = OE0_wp
          DO j = 1, nepts
              e = float(j-1)
! Zero crossing of the real part of the Green's function
              IF (oldval*grnfr(j,i,sp)<=OE0_wp) THEN
                  oldval = grnfr(j,i,sp)
                  temp = abs(grnfi(j,i,sp))
                  IF (vmax<temp) THEN
                      vmax = temp
                      ecross = e
```

```

        END IF
    END IF
! Calculate mean value of the energy and the RMS value
    cume = cume + e*grnfi(j,i,sp)
    cumesq = cumesq + e*e*grnfi(j,i,sp)
    cume2 = cume2 + grnfi(j,i,sp)
END DO
cume = cume*esize*esize
cume2 = cume2*esize
cumesq = cumesq*esize*esize
ecross = ecross*esize

WRITE (73,1) ecross - 0.5E0_wp*esize - eoff - 0.5E0_wp
WRITE (73,1) (cume/cume2) - eoff - 0.5E0_wp
WRITE (73,1) sqrt((cumesq/cume2)-(cume*cume)/(cume2*cume2))
END DO !sp
END DO !i

WRITE (73,*) ' '
1  FORMAT (1X,E12.6)

RETURN
END SUBROUTINE greng

```

G.7 findwidth.f90

```
! A routine to calculate the full width at half max
! of the individual Landau levels.

      SUBROUTINE findwidth(grnfi,magfield,esize,nepts,nllev)
! .. Include Lines ..
      USE scondo_consts
      USE scondo_spin
! ..
! .. Scalar Arguments ..
      REAL (wp), INTENT(IN) :: esize, magfield
      INTEGER, INTENT(IN) :: nepts, nllev
! ..
! .. Array Arguments ..
      REAL (wp), INTENT(IN) :: grnfi(:, :, :)
! ..
! .. Local Scalars ..
      REAL (wp) :: hmx, mx, wth
      INTEGER :: i, j, lin, rin, sp
! ..
! .. Intrinsic Functions ..
      INTRINSIC float, min
! ..
      WRITE (74,1) magfield
      DO i = 1, nllev
      DO sp=1, spinstates
          mx = 0E0_wp
! Use min since we are really looking for -Im(G(E))
          DO j = 1, nepts
              mx = min(mx,grnfi(j,i,sp))
          END DO
          hmx = 0.5E0_wp*mx

! Find left half max

          j = 1
          DO WHILE ((j<nepts) .AND. (hmx<grnfi(j,i,sp)))
              j = j + 1
          END DO
          lin = j
```

```

! Find right half max

      j = nepts
      DO WHILE ((j>1) .AND. (hmx<grnfi(j,i,sp)))
        j = j - 1
      END DO
      rin = j

      width = float(rin-lin)*esize

      WRITE (74,1) width
1      FORMAT (1X,E10.4)

      END DO !sp
      END DO !i

      WRITE (74,*) ' '

      RETURN
END SUBROUTINE findwidth

```

G.8 fourpot.f90

```
! A subroutine to calculate the Fourier transformed
! potential from the dielectric function. It also
! creates the absolute square of the dielectric fctn.
! tfflag signals that the Thomas-Fermi result be returned

! Variables:
!   upot - The potential
!   upotsq - The square of the potential
!   bigpi - The polarizability
!   aimp - The impurity plane distance
!   esqr - The E-M coupling constant (e**2)
!   dieconst - The dielectric constant
!   tfcnst - The Thomas-Fermi const for the polarizability
!   tfflag - Signals to use the TF approx for the potential
!   qsize - The momentum spacing
!   nqpts - The number of Momentum points

      SUBROUTINE fourpot(bigpi,upot,upotsq,aimp,nqpts,qsize, &
                        dieconst,esqr,tfflag,tfcnst)

! ..
      USE scondo_consts
! ..
! .. Scalar Arguments ..
      REAL (wp), INTENT(IN) :: aimp, dieconst, esqr, qsize, tfcnst
      INTEGER, INTENT(IN) :: nqpts, tfflag
! ..
! .. Array Arguments
      REAL (wp), INTENT(IN OUT) :: bigpi(:)
      REAL (wp), INTENT(OUT) :: upot(:), upotsq(:)
! ..
! .. Local Scalars ..
      REAL (wp) :: fact, q
      INTEGER :: i
! ..
! .. Intrinsic Functions ..
      INTRINSIC exp, float
! ..
! We set u(q=0)=0 which is just a constant energy offset so
! that all our equations are consistant
      upot(1) = 0EO_wp
```

```

upotsq(1) = OE0_wp

IF (tfflag==1) THEN
  fact = dieconst/(2.OE0_wp*pi*esqr)
  DO i = 2, nqpts
    q = float(i-1)*qsize
    upot(i) = exp(-q*aimp)/(fact*q+tfcnst)
  END DO
  upotsq(1:nqpts) = upot(1:nqpts)*upot(1:nqpts)
! This is the equivlent polarizablity in the TF approx
! Generate this here for use in possible admixturing
! of the polarizability
  bigpi(1:nqpts) = -tfcnst
ELSE
  fact = dieconst/(2.OE0_wp*pi*esqr)
  DO i = 2, nqpts
    q = float(i-1)*qsize
    upot(i) = exp(-q*aimp)/(fact*q-bigpi(i))
    upotsq(i) = upot(i)*upot(i)
  END DO
END IF

RETURN
END SUBROUTINE fourpot

```

G.9 geneps.f90

```
! a subroutine to calculate the nonstatic Polarization
! and 1/epsilon

      SUBROUTINE geneps(epsr,epsi,grnfr,grnfi,pjelem,nllev,nqpts, &
                      nepts,qsize,esize,fermieng,beta,esqr,dieconst)
      USE scondo_consts
      USE scondo_spin
! ..
! .. Scalar Arguments ..
      REAL (wp) :: beta, esize, fermieng, qsize, esqr, dieconst
      INTEGER :: nepts, nllev, nqpts
! ..
! .. Array Arguments ..
      REAL (wp), DIMENSION(:,,:),INTENT(OUT) :: epsr,epsi
      REAL (wp), DIMENSION(:,::,:),INTENT(IN) :: grnfi, grnfr
      REAL (wp), DIMENSION(:,::,:),INTENT(IN) :: pjelem
! ..
! .. Local Scalars ..
      REAL (wp) :: cksum, e, fact, fct2, mnq, nv1, nv2, &
                q, sum, sum2, f
      REAL (wp) :: srule
      INTEGER :: i, j, k, l, nmax, nmaxb, sp
! ..
! .. Local Arrays ..
      REAL (wp) :: bot(nepts), frmi(nepts)
      REAL (wp) :: bbr(nepts,nllev,nllev), bbi(nepts,nllev,nllev)
      REAL (wp) :: bppr(nepts,nqpts), bppi(nepts,nqpts)
! ..
! .. Intrinsic Functions ..
      INTRINSIC exp, float, int, min, sqrt
! ..

PRINT *, "Entering NSPOLAR"
! Generate Fermi distribution
      nmax = min(nepts,int(((80E0_wp/beta)+fermieng)/esize))
      DO i = 1, nmax
         e = float(i-1)*esize - fermieng
         frmi(i) = 1E0_wp/(exp(beta*e)+1E0_wp)
      END DO
      DO i = nmax + 1, nepts
```

```

        frmi(i) = OEO_wp
    END DO

! Generate the entity B_{NN'}(E) which is used
! to generate the polarizability

PRINT *, "Epsilon step 1"
    fct2=1E0_wp/pi
    bbr(1:nepts,1:nllev,1:nllev) = OEO_wp
    bbi(1:nepts,1:nllev,1:nllev) = OEO_wp

PRINT *, "Epsilon step 2"
    DO i = 1, nmax
        DO sp = 1, spinstates
!MIC$ DO ALL AUTOSCOPE
            DO l=1,nllev
                DO k=1,nllev
                    DO j = 0, nepts-i
!
                        bbr(j+1,k,l)=bbr(j+1,k,l)+frmi(i) &
!
                            *grnfi(i,l,sp)*grnfr(i+j,k,sp)
                        bbi(j+1,k,l)=bbi(j+1,k,l)+frmi(i) &
                            *grnfi(i,l,sp)*grnfi(i+j,k,sp)
                    END DO !j
                    DO j = 0, i-1
!
                        bbr(j+1,k,l)=bbr(j+1,k,l)+frmi(i)&
!
                            *grnfi(i,l,sp)*grnfr(i-j,k,sp)
                        bbi(j+1,k,l)=bbi(j+1,k,l)-frmi(i) &
                            *grnfi(i,l,sp)*grnfi(i-j,k,sp)
                    END DO !j
                END DO !k
            END DO !l
        END DO !sp
    END DO !i

!Generate real part by Kramers-Kronig relation and using fact that
! this function is odd
    DO i=1,nepts
!MIC$ DO ALL AUTOSCOPE
        DO l=1,nllev
            DO k=1,nllev

```

```

        DO j=1,nepts
          IF (i /= j) THEN
            bbr(j,k,l)=bbr(j,k,l)+bbi(i,k,l)/float(i-j)
          END IF
        END DO !j
      END DO !k
    END DO !l
  END DO !i
  DO i=2,nepts
!MIC$ DO ALL AUTOSCOPE
    DO l=1,nllev
      DO k=1,nllev
        DO j=1,nepts
          bbr(j,k,l)=bbr(j,k,l)+bbi(i,k,l)/float(i+j-2)
        END DO !j
      END DO !k
    END DO !l
  END DO !i
!MIC$ DO ALL AUTOSCOPE
  DO l=1,nllev
  DO k=1,nllev
    DO i=1,nepts
      bbr(i,k,l)=bbr(i,k,l)*fct2
    END DO !i
  END DO !k
  END DO !l

```

! Generate polarizability from $B_{\{NN'\}}(E)$ and $|M_{\{NN'\}}|^{-2}$

```

PRINT *, "Epsilon step 3"
  bppr(1:nepts,1:nqpts)=0E0_wp
  bppi(1:nepts,1:nqpts)=0E0_wp

PRINT *, "Epsilon step 4"
  DO l=1,nllev
  DO k=1,nllev
!MIC$ DO ALL AUTOSCOPE
    DO j=1,nqpts
      bppr(1:nepts,j)=bppr(1:nepts,j) &
        +pjelem(j,k,l)*pjelem(j,k,l)*bbr(1:nepts,k,l)
      bppi(1:nepts,j)=bppi(1:nepts,j) &

```

```

                +pjelem(j,k,l)*pjelem(j,k,l)*bbi(1:nepts,k,l)
        END DO !j
    END DO !k
END DO !l

PRINT *, "Epsilon step 5"
! This factor = -gs*esize/(2*pi*pi)
fact = -gs*esize/(2E0_wp*pi*pi)
bppr(1:nepts,1:nqpts)=bppr(1:nepts,1:nqpts)*fact
bppi(1:nepts,1:nqpts)=bppi(1:nepts,1:nqpts)*fact

IF (1==0) THEN
PRINT *, "Writing Polarizability"
OPEN(unit=80,file='Polout.x',status='unknown')
DO j=1,nqpts,2
    DO i=1, nepts,5
        write(80,"(E12.4, E12.4, E12.4, E12.4)") &
            float(j-1)*qsize,float(i-1)*esize,bppr(i,j),bppi(i,j)
    END DO
END DO
CLOSE(80)
END IF

! This expression for 1/epsilon-1 has been simplified to remove the
! 1/q dependence

PRINT *, "Epsilon step 6"
fact=(dieconst*qsize)/(2.0E0_wp*pi*esqr) ! reusing fact
!MIC$ DO ALL AUTOSCOPE
DO j=1,nqpts
    f=fact*float(j-1)
    DO i=1, nepts
        bot(i)=(f-bppr(i,j))**2+bppi(i,j)*bppi(i,j)
    END DO !i
    DO i=1, nepts
        epsr(i,j)=((f-bppr(i,j))*bppr(i,j) &
            -bppi(i,j)*bppi(i,j))/bot(i)
        epsi(i,j)= f*bppi(i,j)/bot(i)
    END DO !i
END DO !j

```

```

! A Quick sum rule test ---

      srule=OE0_wp
      DO i=2,nepts
        srule = srule+epsi(i,2)/float(i-1)
      END DO

PRINT *, 'Sum rule yields --->',srule

      IF (i==0) THEN
PRINT *, "Writing Epsilon"
      OPEN(unit=80,file='nspolout.x',status='unknown')
      DO j=1,nqpts,2
        DO i=1, nepts,5
          write(80,"(E12.4, E12.4, E12.4, E12.4)") &
            float(j-1)*qsize,float(i-1)*esize,epsr(i,j),epsi(i,j)
        END DO
      END DO
      CLOSE(80)
      END IF

      RETURN
END SUBROUTINE geneps

```

G.10 greens.f90

```
! A subroutine to calculate the Green's functions for
! each landau level from the self energy

! Greens returns a value indicating the state of
! convergence which is the average absolute deviation
! between the old and new imaginary parts.
! Additionally it calculates the maximum deviation
! between old and new imaginary parts which
! it returns as a maximum admixturing value.
! This is used in order to avoid large transient
! spikes in the greens functions which arise due
! to quantization error.
! New greens functions are stored temporarily to
! be used later in admixturing.

! Variables:

! grnfr,grnfi - The old greens functions (real and imag)
! selfr,selfi - The self energy (real and imag)
! ngr,ngi      - New greens functions
! nepts        - Size of energy grid
! eoff         - Position of 0th Landau level minus one
! esize        - Energy spacing
! nllev        - Number of Landau levels
! conchk       - Measure of convergence
!             hgmub      - Spin split energy

      FUNCTION greens(ngr,ngi,grnfr,grnfi,selfr,selfi,nepts,eoff, &
                     esize,nllev,hgmub)
! ..
      USE scondo_consts
      USE scondo_spin
! ..
! .. Function Return Value ..
      REAL (wp) :: greens
! ..
! .. Scalar Arguments ..
      REAL (wp), INTENT(IN) :: eoff, esize, hgmub
      INTEGER, INTENT(IN) :: nepts, nllev
! ..
```

```

! .. Arrays Arguments ..
  REAL (wp), INTENT(IN) :: grnfi(:,:,:), grnfr(:,:,:)
  REAL (wp), INTENT(OUT) :: ngi(:,:,:), ngr(:,:,:)
  REAL (wp), INTENT(IN) :: selfi(:,:,:), selfr(:,:,:)
! ..
! .. Local Scalars ..
  REAL (wp) :: conchk, nv1, nv2
  INTEGER :: i, j, sp
! ..
! .. Local Arrays ..
  REAL (wp) :: bot(nepts,nllev,spinstates), &
              dnmr(nepts,nllev,spinstates)
  REAL (wp) :: spen(spinstates)
! ..
! .. Intrinsic Functions ..
  INTRINSIC float, sqrt
! ..

  IF (spinstates == 2) THEN
    spen(1) = -hgmub
    spen(2) = hgmub
  ELSE
    spen = OE0_wp
  END IF

  DO sp = 1, spinstates
  DO j = 1, nllev
    DO i = 1, nepts
      dnmr(i,j,sp) = (float(i)*esize-(float(j) &
        +eoff+spen(sp))-selfr(i,j,sp))
      bot(i,j,sp) = 1.OE0_wp/(dnmr(i,j,sp)*dnmr(i,j,sp) &
        +selfi(i,j,sp)*selfi(i,j,sp))

    END DO !i
  END DO !j
  END DO !sp
  ngr(1:nepts,1:nllev,1:spinstates) = &
    dnmr(1:nepts,1:nllev,1:spinstates) &
    *bot(1:nepts,1:nllev,1:spinstates)
  ngi(1:nepts,1:nllev,1:spinstates) = &
    selfi(1:nepts,1:nllev,1:spinstates) &
    *bot(1:nepts,1:nllev,1:spinstates)

```

```

conchk = OEO_wp
nv1 = OEO_wp
nv2 = OEO_wp
DO sp = 1, spinstates
DO j = 1, nllev
  DO i = 1, nepts
    conchk=max(abs(ngi(i,j,sp)-grnfi(i,j,sp)),conchk)
    nv1=max(abs(ngi(i,j,sp)),nv1)
    nv2=max(abs(grnfi(i,j,sp)),nv2)
  END DO !i
END DO !j
END DO !sp

greens = conchk/sqrt(nv1*nv2)

RETURN
END FUNCTION greens

```

G.11 greens2.f90

```
! A subroutine to calculate the Green's functions for
! each landau level from the self energy

! This version takes both the static and non-static self energies
! to calculate the greens functions

! Greens returns a value indicating the state of
! convergence which is the average absolute deviation
! between the old and new imaginary parts.
! Additionally it calculates the maximum deviation
! between old and new imaginary parts which
! it returns as a maximum admixturing value.
! This is used in order to avoid large transient
! spikes in the greens functions which arise due
! to quantization error.
! New greens functions are stored temporarily to
! be used later in admixturing.

! Variables:

! grnfr,grnfi - The old greens functions (real and imag)
! selfr,selfi - The self energy (real and imag)
! ngr,ngi      - New greens functions
! nepts        - Size of energy grid
! eoff         - Position of 0th Landau level minus one
! esize        - Energy spacing
! nllev        - Number of Landau levels
! conchk       - Measure of convergence
!             hgmub          - Spin split energy

      FUNCTION greens2(ngr,ngi,grnfr,grnfi,selfr,selfi,nsr,nsi, &
                     nepts,eoff,esize,nllev,hgmub)
! ..
      USE scondo_consts
      USE scondo_spin
! ..
! .. Function Return Value ..
      REAL (wp) :: greens2
! ..
! .. Scalar Arguments ..
```

```

REAL (wp), INTENT(IN) :: eoff, esize, hgmub
INTEGER, INTENT(IN) :: nepts, nllev
! ..
! .. Arrays Arguments ..
REAL (wp), INTENT(IN) :: grnfi(:,:,:), grnfr(:,:,:)
REAL (wp), INTENT(OUT) :: ngi(:,:,:), ngr(:,:,:)
REAL (wp), INTENT(IN) :: selfi(:,:,:), selfr(:,:,:)
REAL (wp), INTENT(IN) :: nsi(:,:,:), nsr(:,:,:)
! ..
! .. Local Scalars ..
REAL (wp) :: conchk, nv1, nv2
INTEGER :: i, j, sp
! ..
! .. Local Arrays ..
REAL (wp) :: bot(nepts,nllev,spinstates), spen(spinstates)
REAL (wp) :: dnmr(nepts,nllev,spinstates), &
             dnmi(nepts,nllev,spinstates)
! ..
! .. Intrinsic Functions ..
INTRINSIC float, sqrt
! ..

IF (spinstates == 2) THEN
    spen(1) = -hgmub
    spen(2) = hgmub
ELSE
    spen=0E0_wp
END IF

DO sp = 1, spinstates
DO j = 1, nllev
    DO i = 1, nepts
        dnmr(i,j,sp) = (float(i)*esize-(float(j)+eoff+spen(sp)) &
            -selfr(i,j,sp) -nsr(i,j,sp))
        dnmi(i,j,sp) = selfi(i,j,sp) + nsi(i,j,sp)
        bot(i,j,sp) = 1.0E0_wp/(dnmr(i,j,sp)*dnmr(i,j,sp) &
            +dnmi(i,j,sp)*dnmi(i,j,sp))

    END DO !i
END DO !j
END DO !sp
ngr(1:nepts,1:nllev,1:spinstates) = &
    dnmr(1:nepts,1:nllev,1:spinstates) &

```

```

                                *bot(1:nepts,1:nllev,1:spinstates)
ngi(1:nepts,1:nllev,1:spinstates) = &
                                dnmi(1:nepts,1:nllev,1:spinstates) &
                                *bot(1:nepts,1:nllev,1:spinstates)

conchk = OEO_wp
nv1 = OEO_wp
nv2 = OEO_wp
DO sp = 1, spinstates
DO j = 1, nllev
  DO i = 1, nepts
    conchk=max(abs(ngi(i,j,sp)-grnfi(i,j,sp)),conchk)
    nv1=max(abs(ngi(i,j,sp)),nv1)
    nv2=max(abs(grnfi(i,j,sp)),nv2)
  END DO !i
END DO !j
END DO !sp

greens2 = conchk/sqrt(nv1*nv2)

RETURN
END FUNCTION greens2

```

G.12 jelem.f90

```
! A function to generate the matrix element Jnn'

! Variables:
!     n - Landau level n
!     np - Landau level n'
!     novmfact - n!/m!

      FUNCTION jelem(n,np,ql)
! ..
      USE scondo_consts

! .. Function Return Value ..
      REAL (wp) :: jelem

! ..
! .. Scalar Arguments ..
      REAL (wp), INTENT(IN) :: ql
      INTEGER, INTENT(IN) :: n, np

! ..
! .. Local Scalars ..
      REAL (wp) :: ff, novmfact, val, x
      INTEGER :: i, mm, nn

! ..
! .. External Functions ..
      REAL (wp), EXTERNAL :: laguerre

! ..
! .. Intrinsic Functions ..
      INTRINSIC exp, sqrt, float

! ..
      IF (np>n) THEN
          nn = np
          mm = n
      ELSE
          nn = n
          mm = np
      END IF

      novmfact = 1.0E0_wp
      ff = float(nn)
      IF (mm/=nn) THEN
          DO i = mm, nn - 1
```

```

        novmfact = novmfact*ff
        ff = ff - 1E0_wp
    END DO
END IF

IF (mm/=nn) THEN
    x = ql*ql
    val = sqrt(1E0_wp/novmfact)*(ql/sqrt(2E0_wp))**(nn-mm)
!FPP$ EXPAND(laguerre)
    jelem = val*exp(-0.25E0_wp*x)*laguerre(nn-mm,mm,0.5E0_wp*x)
ELSE
    x = ql*ql
!FPP$ EXPAND(laguerre)
    jelem = sqrt(1E0_wp/novmfact)*exp(-0.25E0_wp*x) &
        *laguerre(0,mm,0.5E0_wp*x)
END IF
RETURN
END FUNCTION jelem

```

! A subroutine to pre-calculate the matrix elements
! which are stored in pjelem

```

SUBROUTINE jeltab(pjelem,nqpts,qsize,nllev)
! ..
    USE scondo_consts
! ..
! .. Scalar Arguments ..
    REAL (wp), INTENT(IN) :: qsize
    INTEGER, INTENT(IN) :: nllev, nqpts
! ..
! .. Array Arguments
    REAL (wp), INTENT(OUT) :: pjelem(:, :, :)
! ..
! .. Local Scalars ..
    INTEGER :: i, iq, j
! ..
! .. External Functions ..
    REAL (wp), EXTERNAL :: jelem
! ..

```

```

! .. Intrinsic Functions ..
      INTRINSIC float
! ..
!MIC$ DO ALL SHARED(pjelem,nqpts,nllev,qsize) PRIVATE(j,i,iq)
      DO j = 1, nllev
        DO i = 1, j
          DO iq = 1, nqpts
!FPP$ NEXPAND(jelem)
            pjelem(iq,i,j) = jelem(i-1,j-1,float(iq-1)*qsize)
            pjelem(iq,j,i) = pjelem(iq,i,j)
          END DO
        END DO
      END DO

      RETURN
END SUBROUTINE jeltab

```

G.13 laguerre.f90

```
! Function to return the value of the associated laguerre
! polynomial
```

```
! Variables:
```

```
      FUNCTION laguerre(alpha,n,x)
! ..
      USE scondo_consts
! .. Function Return Value ..
      REAL (wp) :: laguerre
! ..
! .. Scalar Arguments ..
      REAL (wp), INTENT(IN) :: x
      INTEGER, INTENT(IN) :: alpha, n
! ..
! .. Local Scalars ..
      REAL (wp) :: aval, ival, naval, tot, trm
      INTEGER :: i
! ..
! .. Intrinsic Functions ..
      INTRINSIC float
! ..
! Calculate m=0 term (n+alpha)!/n!alpha!
      trm = 1.0E0_wp
      IF (alpha>0) THEN
          ival = 1.0E0_wp
          naval = float(n+alpha)
          DO i = 1, alpha
              trm = trm*naval/ival
              ival = ival + 1.0E0_wp
              naval = naval - 1.0E0_wp
          END DO
      END IF

! Calculate and add the rest of the terms using:
! Tm= [x(m-n-1)/m(m+alpha)] Tm-1

      tot = trm
      IF (n>0) THEN
```

```
    ival = 1.0E0_wp
    naval = float(n+1)
    aval = float(alpha)
    DO i = 1, n
        trm = trm*x*(ival-naval)/(ival*(ival+aval))
        tot = tot + trm
        ival = ival + 1.0E0_wp
    END DO
END IF

laguerre = tot
RETURN
END FUNCTION laguerre
```

G.14 llcouple.f90

```
! Subroutine to calculate the Landau level coupling

! Variables:
!   upotsq - The potential squared
!   oqgamma - The Landau level coupling
!   nimp - The impurity density
!   nllev - The number of Landau levels
!   qsize - The momentum spacing
!   nqpts - The number of momentum points

SUBROUTINE llcouple(oqgamma,pjelem,upotsq,nqpts,qsize,nllev,nimp)
! ..
    USE scondo_consts
! ..
! .. Scalar Arguments ..
    REAL (wp), INTENT(IN) :: nimp, qsize
    INTEGER, INTENT(IN) :: nllev, nqpts
! ..
! .. Arrays Arguments ..
    REAL (wp), INTENT(OUT) :: oqgamma(:, :)
    REAL (wp), INTENT(IN) :: pjelem(:, :, :)
    REAL (wp), INTENT(IN) :: upotsq(:)
! ..
! .. Local Scalars ..
    REAL (wp) :: fact, q, qupot2
    INTEGER :: j, k
! ..
! .. Intrinsic Functions ..
    INTRINSIC float
! ..
    fact = nimp*qsize*qsize/(2E0_wp*pi)

    oqgamma(1:nllev,1:nllev) = OE0_wp

    DO k = 1, nqpts
        q = float(k-1)
        qupot2 = q*upotsq(k)
        DO j = 1, nllev
            oqgamma(1:nllev,j) = oqgamma(1:nllev,j) &
                + qupot2*pjelem(k,1:nllev,j) &
```

```
                                *pjelem(k,1:nlev,j)
      END DO
    END DO

    DO j = 1, nlev
      oqgamma(1:nlev,j) = oqgamma(1:nlev,j)*fact
    END DO

    RETURN
  END SUBROUTINE llcouple
```

G.15 main.f90

! This is a unified version of the set of programs used
! to calculate the density of states of a 2DEG under several
! approximations.

```
PROGRAM scondo
! ..
    USE scondo_consts
    USE scondo_interfaces
    USE scondo_control
    USE scondo_spin
! ..
! .. Local Scalars ..
    REAL (wp) :: adfac, adfacmax, adfacmin, aimp, beta, &
        bot, cong, converg, ctol, d1, d2, de, &
        dieconst, e, econc, eoff, esize, esqr, &
        fermieng, impconc, impdist, mage, magfield, &
        maglen, magstep, mfact, mobil, nimp, ns, &
        oldcon, oldcong, omegac, q, qsize, refef, &
        tau, tauc, temp, tfcnst, val, val2, zef
    REAL (wp) :: gstar, hgmub, eupper, rng
    INTEGER :: i, it, itmax, j, k, l, nbpts, nepts, nllev, &
        nsitmax, nqpts, sp
! ..
! .. External Functions ..
    REAL (wp), EXTERNAL :: tauconst
! ..
! .. Intrinsic Functions ..
    INTRINSIC aint, float, int, min, sqrt
! ..
! .. Arrays

    REAL (wp), ALLOCATABLE :: grnfr(:,:,:), grnfi(:,:,:)
    REAL (wp), ALLOCATABLE :: selfr(:,:,:), selfi(:,:,:)
    REAL (wp), ALLOCATABLE :: ngr(:,:,:), ngi(:,:,:)
    REAL (wp), ALLOCATABLE :: upot(:), upotsq(:)
    REAL (wp), ALLOCATABLE :: bessval(:,:)
    REAL (wp), ALLOCATABLE :: bigpi(:), newbpi(:)
    REAL (wp), ALLOCATABLE :: dstat(:)
    REAL (wp), ALLOCATABLE :: pjelem(:,:,:)
    REAL (wp), ALLOCATABLE :: oqgamma(:,:)
```

```

REAL (wp), ALLOCATABLE :: epsr(:,,:), epsi(:,:)
REAL (wp), ALLOCATABLE :: nsr(:,,:,:), nsi(:,,:,:)
REAL (wp), ALLOCATABLE :: spen(:)
REAL (wp), ALLOCATABLE :: bw(:,,:,:)

! ..
! .. Namelists ..
  NAMELIST /material/dieconst, mfact, gstar
  NAMELIST /sample/mobil, econc, impdist
  NAMELIST /run/temp, magfield, magstep, nbpts
  NAMELIST /energy_mom/esize, eoff, eupper, qsize, &
            nepts, nqpts, nllev
  NAMELIST /converge/ctol, itmax, nsitmax
  NAMELIST /calcctrl/include_non_static, include_spin, &
            include_static_vertex
  NAMELIST /writectrl/write_static_polar, write_ns_polar, &
            write_static_greens, write_ns_greens, &
            write_epsilon
  NAMELIST /files/diagfile,dosfile,elevelfile,ewidthfile, &
            greensfile, specfile, staticpolarfile, &
            nsgreensfile, nsspecfile, nspolarfile, &
            epsilonfile

! ..

! These have since been deprecated but give a good idea what type
! of parameters we are using.
! Material parameters (hard coded)
  dieconst = 12.8E0_wp
  mfact = 0.067E0_wp
  gstar = -0.44E0_wp

! Sample parameters
  mobil = 40000_wp
  econc = 2.0E11_wp
  impdist = 50E-8_wp

! Test case parameters (hard coded)
  temp = 1.2E0_wp
  magfield = 1.653E4_wp
  magstep = 1.653E3_wp
  nbpts = 1

```

```

! Energy and momentum parameters
  esize = .006E0_wp
  eoff = 1.5E0_wp
  qsize = .025E0_wp
  nepts = 2000
  nqpts = 400
  nllev = 8

! Tolerances
  ctol = 1E-10_wp

! Iteration maximums
! itmax=30
  itmax = 20

! param.in now has all of the configuration info
! Read parameter file
  OPEN (unit=5,file='runparam.in')
  READ (unit=5,nml=material)
  READ (unit=5,nml=sample)
  READ (unit=5,nml=run)
  READ (unit=5,nml=energy_mom)
  READ (unit=5,nml=converge)
  READ (unit=5,nml=calcctrl)
  READ (unit=5,nml=writectl)
  READ (unit=5,nml=files)
  CLOSE (5)

! Handle spin cases
  IF (include_spin) THEN
    spinstates=2
    gs=1E0_wp
  ELSE
    spinstates=1
    gs=2E0_wp
  END IF

!   specfile = 'spcout.x'
!   dosfile = 'dosout.x'

```

```

!     staticpolarfile = 'bpiout.x'
!     greensfile = 'grnout.x'
!     diagfile = 'diaout.x'
!     elevelfile = 'elvout.x'
!     ewidthfile = 'wthout.x'

OPEN (unit=8,file=specfile,status='unknown')
OPEN (unit=9,file=dosfile,status='unknown')
OPEN (unit=70,file=staticpolarfile,status='unknown')
OPEN (unit=71,file=greensfile,status='unknown')
OPEN (unit=72,file=diagfile,status='unknown')
OPEN (unit=73,file=elevelfile,status='unknown')
OPEN (unit=74,file=ewidthfile,status='unknown')
OPEN (unit=75,file=nsspecfile,status='unknown')

! Set up allocatable arrays
ALLOCATE(grnfr(1:nepts,1:nllev,1:spinstates))
ALLOCATE(grnfi(1:nepts,1:nllev,1:spinstates))
ALLOCATE(selfr(1:nepts,1:nllev,1:spinstates))
ALLOCATE(selfi(1:nepts,1:nllev,1:spinstates))
ALLOCATE(ngr(1:nepts,1:nllev,1:spinstates))
ALLOCATE(ngi(1:nepts,1:nllev,1:spinstates))
ALLOCATE(upot(1:nqpts))
ALLOCATE(upotsq(1:nqpts))
ALLOCATE(bessval(1:nqpts,1:nqpts))
ALLOCATE(bigpi(1:nqpts))
ALLOCATE(newbpi(1:nqpts))
ALLOCATE(dstat(1:nepts))
ALLOCATE(oqgamma(1:nllev,1:nllev))
ALLOCATE(pjelem(1:nqpts,1:nllev,1:nllev))
ALLOCATE(epsr(1:nepts,1:nqpts))
ALLOCATE(epsi(1:nepts,1:nqpts))
ALLOCATE(nsr(1:nepts,1:nllev,1:spinstates))
ALLOCATE(nsi(1:nepts,1:nllev,1:spinstates))
ALLOCATE(spen(1:spinstates))
IF (include_static_vertex) THEN
    ALLOCATE(bw(1:nqpts,1:nllev,1:nllev))
END IF

```

```

! Calculate the scattering parameters
  tau = 1E-7_wp*mobil*mfact*emass/emks
  tauc = tauconst(econc,dieconst,mfact,impdist)
  impconc = 1.0E0_wp/(tau*tauc)
  PRINT *, 'Tau=', tau
  PRINT *, 'Ni=', impconc

! Initialize bessel table
  CALL besstab(bessval,nqpts,qsize)

! Initialize matrix element table
  CALL jeltab(pjelem,nqpts,qsize,nlev)

DO k = 1, nbpts

PRINT *, 'Magnetic Field (Tesla) =', (magfield*1E-4_wp)

! Calculate scaling
  maglen = sqrt(hbar*cspeed/(echg*magfield))
  omegac = echg*magfield/(emass*mfact*cspeed)
  mage = hbar*omegac

  beta = mage/(boltz*temp)

  zef = 2E0_wp*pi*hbar*hbar*econc/(gs*emass*mfact)
  esize = (float(nllev+1)+eoff+eupper)/float(nepts)
  PRINT *, zef, nllev, esize

  hgmub=.25E0_wp*gstar*mfact
  PRINT *, 'Spin split energy=', hgmub

! Generate starting point Greens functions
  IF (spinstates == 2) THEN
    spen(1)= -hgmub
    spen(2)=  hgmub
  ELSE
    spen=0E0_wp
  END IF

  val = -0.5E0_wp*hbar/(tau*mage)
  PRINT *, 'val=', val

```

```

DO sp = 1, spinstates
DO i = 1, nllev
  DO j = 1, nepts
    val2 = float(j)*esize - (float(i)+eoff + spen(sp))
    bot = 1.0E0_wp/(val2*val2+val*val)
    grnfr(j,i,sp) = val2*bot
    grnfi(j,i,sp) = val*bot
  END DO !j
END DO !i
END DO !sp

! Scale parameters
ns = econc*(maglen*maglen)
nimp = impconc*(maglen*maglen)
aimp = impdist/maglen
esqr = echg*echg/(maglen*mage)
PRINT *, 'l=', maglen
PRINT *, 'Ec=', mage
tfcnst = (maglen/hbar)
tfcnst = gs*tfcnst*tfcnst*emass*mfact*mage/pi

PRINT *, 'Scaled parameters:'
PRINT *, 'Sheet Density      = ', ns
PRINT *, 'Impurity Density   = ', nimp
PRINT *, 'Impurity Distance = ', aimp
PRINT *, 'E-M Coupling       = ', esqr
PRINT *, 'T-F Constant        = ', tfcnst

CALL densos(dstat,grnfi,nepts,nllev)

adfamax = 1E0_wp
adfamin = 1E-2_wp
adfacs = 1E0_wp
rng = 1E0_wp

! Calculate the Fourier potential using
! Thomas-Fermi as initial potential
CALL fourpot(bigpi,upot,upotsq,aimp,nqpts, &
             qsize,dieconst,esqr,1,tfcnst)

CALL llcouple(oqgamma,pjelem,upotsq,nqpts,qsize,nllev,nimp)

```

```

! Give a starting point selfenergy
  selfr(1:nepts,1:nllev,1:spinstates)=0
  selfi(1:nepts,1:nllev,1:spinstates)=1E-5_wp
  DO sp = 1, spinstates
  DO l = 1, nllev
    DO j = 1, nllev
      selfr(1:nepts,j,sp) = selfr(1:nepts,j,sp) &
        + oqgamma(j,l)*grnfr(1:nepts,l,sp)
      selfi(1:nepts,j,sp) = selfi(1:nepts,j,sp) &
        + oqgamma(j,l)*grnfi(1:nepts,l,sp)
    END DO !j
  END DO !l
  END DO !sp

! From now on we have got a starting point

  CALL selfenergy(oqgamma,selfr,selfi,nepts,nllev, &
    esize,eoff,hgmub)
  converg = greens(ngr,ngi,grnfr,grnfi,selfr,selfi, &
    nepts,eoff,esize,nllev,hgmub)
  oldcon = converg
  CALL mix(ngr,ngi,grnfr,grnfi,nepts,nllev,1E0_wp)
  CALL densos(dstat,grnfi,nepts,nllev)
  fermieng = chempot(dstat,nepts,esize,ns,beta)
  PRINT *, 'Fermi Energy=', fermieng-0.5E0_wp-eoff

  IF (include_static_vertex) THEN
    CALL bigw(bessval,bw,upotsq,pjelem,nqpts,qsize,nllev,nimp)
    cong = vertpol(bw,grnfr,grnfi,pjelem,bigpi,newbpi,nllev, &
      fermieng,nqpts,nepts,qsize,esize,beta)
  ELSE
    cong = polarize(grnfr,grnfi,pjelem,bigpi,newbpi,nllev, &
      fermieng,nqpts,nepts,qsize,esize,beta)
  END IF
  CALL pmix(bigpi,newbpi,nqpts,1E0_wp)

! The big self consistent loop
  it = 1
  DO WHILE ((converg>ctol) .AND. (it<=itmax))
    CALL fourpot(bigpi,upot,upotsq,aimp,nqpts,qsize, &

```

```

                                dieconst,esqr,0,tfcnst)
CALL llcouple(oqgamma,pjelem,upotsq,nqpts,qsize,nllev,nimp)

CALL selfenergy(oqgamma,selfr,selfi,nepts,nllev, &
                esize,eoff,hgmub)
oldcon = converg
converg = greens(ngr,ngi,grnfr,grnfi,selfr,selfi,nepts, &
                eoff,esize,nllev,hgmub)
!   CALL mix(ngr,ngi,grnfr,grnfi,nepts,nllev,adfac)
CALL mix(ngr,ngi,grnfr,grnfi,nepts,nllev,1E0_wp)

CALL densos(dstat,grnfi,nepts,nllev)
fermieng = chempot(dstat,nepts,esize,ns,beta)
oldcong = cong
IF (include_static_vertex) THEN
    CALL bigw(bessval,bw,upotsq,pjelem,nqpts,qsize, &
            nllev,nimp)
    cong = vertpol(bw,grnfr,grnfi,pjelem,bigpi,newbpi, &
            nllev,fermieng,nqpts,nepts,qsize,esize,beta)
ELSE
    cong = polarize(grnfr,grnfi,pjelem,bigpi,newbpi,nllev, &
            fermieng,nqpts,nepts,qsize,esize,beta)
END IF
IF (cong >= oldcong) THEN
!   adfac = max(5E-3_wp,.5E0_wp*adfacs)
    adfac = adfac/(1.0_wp + (cong/oldcong))
    rng=max(rng*.95_wp,adfacsmin)
ELSE
!   adfac = min(1.7E0_wp*adfacs,1E0_wp)
    adfac = adfac/(1.0_wp - (cong/oldcong))
    adfac = min(adfac,rng)
    rng=min(rng*1.5_wp,adfacsmax)
END IF
CALL pmix(bigpi,newbpi,nqpts,adfacs)
!   CALL pmix(bigpi,newbpi,nqpts,1E0_wp)

PRINT *, 'Iteration', it
PRINT *, 'Fermi Energy=', fermieng-0.5E0_wp-eoff
PRINT *, 'Convergence----->', cong
PRINT *, 'Greens =====', converg
PRINT *, 'Adfacs=', adfacs

```

```

        WRITE (72,2) it, cong, converg
        it = it + 1
        PRINT *, ' '
    END DO

    CALL greng(grnfr,grnfi,esize,eoff,nepts,nllev,magfield)
    CALL findwidth(grnfi,magfield,esize,nepts,nllev)

    DO i = 1, nepts
        e = float(i-1)*esize
        WRITE (9,1) e - .5E0_wp - eoff, dstat(i)*2E0_wp*pi/gs
    END DO
    WRITE (9,*) '&'

IF (write_static_greens) THEN
    DO j = 1, nllev
        DO sp = 1, spinstates
            DO i = 1, nepts
                e = float(i-1)*esize
                WRITE (71,1) e - .5E0_wp - eoff, -grnfi(i,j,sp)/pi
            END DO !i
            WRITE (71,*) '&'
        END DO !sp
    END DO !j
END IF

IF (write_static_polar) THEN
    DO i = 1, nqpts
        q = float(i-1)*qsize
        WRITE (70,1) q, bigpi(i)
    END DO
    WRITE (70,*) '&'
END IF

! Estimate density of states at the Fermi energy
d1 = dstat(int(fermieng/esize))

```

```

d2 = dstat(int(fermieng/esize)+1)
de = fermieng - aint(fermieng/esize)*esize
refef = refineef(oqgamma,fermieng,nllev,esize,eoff,hgmub)
WRITE (8,3) magfield, fermieng-0.5E0_wp-eoff, &
          d1 + (d2-d1)*de, refef
magfield = magfield + magstep

! If we want epsilon from the nonstatic calculation
IF (write_epsilon .AND. .NOT. include_non_static) THEN
  CALL geneeps(epsr,epsi,grnfr,grnfi,pjelem,nllev,nqpts, &
              nepts,qsize,esize,fermieng,beta,esqr,dieconst)
PRINT *, "Writing Epsilon"
OPEN(unit=80,file=epsilonfile,status='unknown')
DO j=1,nqpts,2
  DO i=1, nepts,5
    write(80,"(E12.4, E12.4, E12.4, E12.4)") &
      float(j-1)*qsize,float(i-1)*esize,epsr(i,j), &
      epsi(i,j)
  END DO
END DO
CLOSE(80)
END IF

IF (include_non_static) THEN
! Do the nonstatic calculation

  adfac=1E0_wp
  it = 1
! The nonstatic self consistant loop
! Use a constant number of iterations for now
  DO WHILE (it <= nsitmax)

    CALL geneeps(epsr,epsi,grnfr,grnfi,pjelem,nllev,nqpts, &
                nepts,qsize,esize,fermieng,beta,esqr, &
                dieconst)

    CALL selfe_corr(grnfr,grnfi,selfr,selfi,nsr,nsi,epsi, &
                  epsr,pjelem,nepts,nqpts,nllev,qsize, &
                  esize,fermieng,beta,esqr, &
                  dieconst,eoff,hgmub)
  END DO

```

```

CALL selfenergy2(oqgamma,selfr,selfi,nsr,nsi,nepts, &
                nllev,esize,eoff,hgmub)

! Police the imaginary part of the selfenergy
! Probably not necessary anymore
selfi=min(selfi,0E0_wp)
grnfi=min(grnfi,0E0_wp)

! Convergence logic -- needs work
oldcon = converg
converg = greens2(ngr,ngi,grnfr,grnfi,selfr,selfi, &
                 nsr,nsi,nepts,eoff,esize,nllev,hgmub)
IF (it > 1) THEN
  IF (converg>oldcon) THEN
    adfac = max(1E-1_wp,.9E0_wp*adfacs)
  ELSE
    adfac = min(1.5E0_wp*adfacs,.97E0_wp)
  END IF
END IF

! CALL mix(ngr,ngi,grnfr,grnfi,nepts,nllev,1.0_wp)
CALL mix(ngr,ngi,grnfr,grnfi,nepts,nllev,adfacs)
CALL densos(dstat,grnfi,nepts,nllev)

IF (write_ns_greens) THEN
  OPEN(UNIT=90, FILE=nsgreensfile, STATUS='unknown')
  DO j = 1, nllev
  DO sp = 1, spinstates
    DO i = 1, nepts
      e = float(i-1)*esize
      WRITE (90,'(2E12.4)') e - .5E0_wp - eoff, &
        -grnfi(i,j,sp)/pi
    END DO !i
    WRITE (90,*) '&'
  END DO !sp
  END DO !j
  CLOSE(90)
END IF

fermieng = chempot(dstat,nepts,esize,ns,beta)
PRINT *, 'Iteration', it
PRINT *, 'Fermi Energy=', fermieng-0.5E0_wp-eoff

```

```

PRINT *, 'Greens =====', converg
PRINT *, 'Adfac=', adfac

cong = polarize(grnfr,grnfi,pjelem,bigpi,newbpi,nllev, &
               fermieng,nqpts,nepts,qsize,esize,beta)
CALL pmix(bigpi,newbpi,nqpts,1E0_wp)
CALL fourpot(bigpi,upot,upotsq,aimp,nqpts,qsize,dieconst, &
             esqr,1,tfcnst)
CALL llcouple(oqgamma,pjelem,upotsq,nqpts,qsize,nllev,nimp)

it = it+1
END DO

!Write out DOS
DO i = 1, nepts
  e = float(i-1)*esize
  WRITE (9,1) e - .5E0_wp - eoff, dstat(i)*2E0_wp*pi/gs
END DO
WRITE (9,*) '&'

IF (write_epsilon) THEN
PRINT *, "Writing Epsilon"
OPEN(unit=80,file=epsilonfile,status='unknown')
DO j=1,nqpts,2
  DO i=1, nepts,5
    write(80,"(E12.4, E12.4, E12.4, E12.4)" &
           float(j-1)*qsize,float(i-1)*esize, &
           epsr(i,j),epsi(i,j)
  END DO
END DO
CLOSE(80)
END IF

! Write out DOS at the Fermi energy
d1 = dstat(int(fermieng/esize))
d2 = dstat(int(fermieng/esize)+1)
de = fermieng - aint(fermieng/esize)*esize
WRITE (75,'(1X,3E17.8)') magfield, fermieng-0.5E0_wp-eoff, &
                        d1 + (d2-d1)*de
END IF !Do nonstatic

```

```
magfield = magfield + magstep
```

```
END DO ! End magnetic field loop
```

```
1  FORMAT (1X,2E18.8)  
2  FORMAT (1X,I6,1X,3E16.8)  
3  FORMAT (1X,4E17.8)
```

```
CLOSE (unit=75)
```

```
CLOSE (unit=74)
```

```
CLOSE (unit=73)
```

```
CLOSE (unit=72)
```

```
CLOSE (unit=71)
```

```
CLOSE (unit=70)
```

```
CLOSE (unit=9)
```

```
CLOSE (unit=8)
```

```
STOP
```

```
END PROGRAM scondo
```

G.16 melem.f90

```
! A function to generate the matrix element Mnn'  
! in our case n=n' so we simplify it to Mnn  
  
    FUNCTION melem(n,ql)  
! ..  
    USE scondo_consts  
! .. Function Return Value ..  
    REAL (wp) :: melem  
! ..  
! .. Scalar Arguments ..  
    REAL (wp), INTENT(IN) :: ql  
    INTEGER, INTENT(IN) :: n  
! ..  
! .. Local Scalars ..  
    REAL (wp) :: x  
! ..  
! .. External Functions ..  
    REAL (wp), EXTERNAL :: laguerre  
! ..  
! .. Intrinsic Functions ..  
    INTRINSIC exp  
! ..  
    x = ql*ql  
!FPP$ EXPAND(laguerre)  
    melem = exp(-0.25E0_wp*x)*laguerre(0,n,0.5E0_wp*x)  
    RETURN  
END FUNCTION melem
```

G.17 mix.f90

```
! A subroutine to admixture the new greens functions
! with the old

! Variables:
!     ngr,ngi - New real and imag greens functions
!     grnfr,grnfi - Real and imag greens functions
!     adfac - The admixturing factor
!     nepts - The number of energy points
!     nllev - The number of Landau levels

      SUBROUTINE mix(ngr,ngi,grnfr,grnfi,nepts,nllev,adfacs)
! ..
      USE scondo_consts
      USE scondo_spin
! ..
! .. Scalar Arguments ..
      REAL (wp), INTENT(IN) :: adfacs
      INTEGER, INTENT(IN) :: nepts, nllev
! ..
! .. Array Arguments ..
      REAL (wp), INTENT(IN OUT) :: grnfi(:,:,:), grnfr(:,:,:)
      REAL (wp), INTENT(IN) :: ngi(:,:,:), ngr(:,:,:)
! ..
! .. Local Scalars ..
      REAL (wp) :: adcaf
! ..
      adcaf = 1.0E0_wp - adfacs
      grnfr(1:nepts,1:nllev,1:spinstates) = &
          ngr(1:nepts,1:nllev,1:spinstates)*adfacs + &
          grnfr(1:nepts,1:nllev,1:spinstates)*adcaf
      grnfi(1:nepts,1:nllev,1:spinstates) = &
          ngi(1:nepts,1:nllev,1:spinstates)*adfacs + &
          grnfi(1:nepts,1:nllev,1:spinstates)*adcaf

      RETURN
END SUBROUTINE mix
```

G.18 pmix.f90

```
! A subroutine to admixture the new polarizability
! with the old

! Variables:
! bigpi - The polarizability
! newbpi - The new polarizability
!   adfac - The admixturing factor
!   nqpts - The number of momentum points

      SUBROUTINE pmix(bigpi,newbpi,nqpts,adfacs)
! ..
      USE scondc_consts
! ..
! .. Scalar Arguments ..
      REAL (wp), INTENT(IN) :: adfacs
      INTEGER, INTENT(IN) :: nqpts
! ..
! .. Array Arguments
      REAL (wp), INTENT(IN OUT) :: bigpi(:)
      REAL (wp), INTENT(IN) :: newbpi(:)
! ..
! .. Local Scalars ..
      REAL (wp) :: adcaf
      INTEGER :: i
! ..

      adcaf = 1.0E0_wp - adfacs
      bigpi(1:nqpts) = newbpi(1:nqpts)*adfacs + bigpi(1:nqpts)*adcaf

      RETURN
END SUBROUTINE pmix
```

G.19 polarize.f90

```
! A subroutine to calculate the Polarization

      FUNCTION polarize(grnfr,grnfi,pjelem,bigpi,newbpi,nllev, &
                     fermieng,nqpts,nepts,qsize,esize,beta)
! ..
      USE scond_constants
      USE scond_spin
! ..
! .. Function Return Value ..
      REAL (wp) :: polarize
! ..
! .. Scalar Arguments ..
      REAL (wp), INTENT(IN) :: beta, esize, fermieng, qsize
      INTEGER, INTENT(IN) :: nepts, nllev, nqpts
! ..
! .. Array Arguments ..
      REAL (wp), INTENT(IN) :: grnfr(:,:,:), grnfi(:,:,:)
      REAL (wp), INTENT(IN OUT) :: bigpi(:), newbpi(:)
      REAL (wp), INTENT(IN) :: pjelem(:,:,:)
! ..
! .. Local Scalars ..
      REAL (wp) :: cksum, e, fact, mnq, nv1, nv2, q, sum2
      INTEGER :: i, j, k, l, nmax, sp
! ..
! .. Local Automatic Arrays ..
      REAL (wp) :: frmi(nepts)
! ..
! .. Intrinsic Functions ..
      INTRINSIC exp, float, int, min, sqrt
! ..
! Generate Fermi distribution
      nmax = min(nepts,int(((80E0_wp/beta)+fermieng)/esize))
      DO i = 1, nmax
         e = float(i-1)*esize - fermieng
         frmi(i) = 1E0_wp/(exp(beta*e)+1E0_wp)
      END DO
      DO i = nmax + 1, nepts
         frmi(i) = 0E0_wp
      END DO
```

```

! The prefactor
fact = -gs*esize/(2.0E0_wp*pi*pi)

newbpi(1:nqpts) = OE0_wp

DO sp = 1, spinstates
!MIC$ DO ALL shared(nllev,frmi,grnfr,grnfi,newbpi,
!MIC$1          nmax,pjelem,nqpts,sp)
!MIC$2          private(j,k,l,sum2)
DO k = 1, nllev
DO l = 1, nllev
sum2 = OE0_wp
DO j = 1, nmax
sum2 = sum2 + frmi(j)*(grnfr(j,k,sp)*grnfi(j,l,sp) &
+grnfr(j,l,sp)*grnfi(j,k,sp))
END DO
!MIC$ GUARD
newbpi(1:nqpts) = newbpi(1:nqpts) + &
pjelem(1:nqpts,k,l)*pjelem(1:nqpts,k,l)*sum2
!MIC$ END GUARD
END DO !k
END DO !l
END DO !sp

newbpi(1:nqpts) = newbpi(1:nqpts)*fact

! Return Convergence check
cksum = OE0_wp
nv1 = OE0_wp
nv2 = OE0_wp
DO i = 1, nqpts
cksum=max(abs(newbpi(i)-bigpi(i)),cksum)
nv1 = max(abs(bigpi(i)),nv1)
nv2 = max(abs(newbpi(i)),nv2)
END DO

polarize = cksum/sqrt(nv1*nv2)
CLOSE (90)
RETURN
END FUNCTION polarize

```

G.20 refineef.f90

```
! A subroutine to refine the value of the density of states
! at the Fermi Energy

      FUNCTION refineef(oqgamma,ef,nllev,esize,eoff,hgmub)
! ..
      USE scondo_consts
      USE scondo_spin
! ..
! .. Function Return Value ..
      REAL (wp) :: refineef
! ..
! .. Scalar Arguments ..
      REAL (wp), INTENT(IN) :: ef, eoff, esize, hgmub
      INTEGER, INTENT(IN) :: nllev
! ..
! .. Array Arguments ..
      REAL (wp), INTENT(IN) :: oqgamma(:, :)
! ..
! .. Local Scalars ..
      REAL (wp) :: bi, bot, br, diff, dos, keval, sumi, sumr, xtol
      INTEGER :: i, it, j, k, maxit, sp
! ..
! .. Local Arrays ..
      REAL (wp) :: osli(nllev,spinstates), oslr(nllev,spinstates)
      REAL (wp) :: sli(nllev,spinstates), slr(nllev,spinstates)
      REAL (wp) :: spen(2)

! Take care of the spin energy
      IF (spinstates == 2) THEN
          spen(1) = -hgmub
          spen(2) = hgmub
      ELSE
          spen = OE0_wp
      END IF

! ..
! Recalculate the Self energies at this energy point
! using the coupling constants.
```

```

xtol = 1E-12_wp
maxit = 100000
oslr(1:nllev,1:spinstates) = 0E0_wp
osli(1:nllev,1:spinstates) = -1E-5_wp
diff = 1E0
it = 1
DO WHILE ((diff>=xtol) .AND. (it<=maxit))
  DO sp = 1, spinstates
    DO j = 1, nllev
      sumr = 0E0_wp
      sumi = -1E-5_wp
      keval = ef - eoff - spen(sp)
      DO k = 1, nllev
        keval = keval - 1E0
        br = keval - oslr(k,sp)
        bot = 1E0_wp/(br*br+osli(k,sp)*osli(k,sp))
        sumr = sumr + oqgamma(j,k)*br*bot
        sumi = sumi + oqgamma(j,k)*osli(k,sp)*bot
      END DO
      slr(j,sp) = sumr
      sli(j,sp) = sumi
    END DO !j
  END DO !sp
  diff = 0E0_wp
  DO sp = 1, spinstates
    DO j = 1, nllev
      br = oslr(j,sp) - slr(j,sp)
      bi = osli(j,sp) - sli(j,sp)
      diff = diff + br*br + bi*bi
      oslr(j,sp) = 0.5E0_wp*(slr(j,sp)+oslr(j,sp)) !Admixture
      osli(j,sp) = 0.5E0_wp*(sli(j,sp)+osli(j,sp))
    END DO !j
  END DO !sp
  it = it + 1
END DO

```

```

! Now sum the imaginary parts of the Green's functions to get the DOS
dos = 0E0_wp
keval = ef - eoff
DO sp = 1, spinstates
DO i = 1, nllev
  keval = keval - 1E0_wp

```

```
      br = keval - oslr(i,sp) - spen(sp)
      dos = dos + osli(i,sp)/(br*br+osli(i,sp)*osli(i,sp))
END DO !i
END DO !sp

refineef = -0.5E0_wp*gs*dos/(pi*pi)

RETURN
END FUNCTION refineef
```

G.21 scondo_consts.f90

! The Header file for the Self Consistent DOS

MODULE scondo_consts

IMPLICIT NONE

INTEGER, PARAMETER :: wp = kind(0.0D0)

! Array Size Parameters

INTEGER, PARAMETER :: esp = 3001, lsp = 17, qsp = 801

! System Parameters

! REAL (wp), PARAMETER :: gs = 1E0_wp

! Physical Parameters

REAL (wp), PARAMETER :: boltz = 1.38062E-16_wp

REAL (wp), PARAMETER :: cspeed = 2.997925E10_wp

REAL (wp), PARAMETER :: echg = 4.80325E-10_wp

REAL (wp), PARAMETER :: emass = 9.10956E-28_wp

REAL (wp), PARAMETER :: emks = 1.60219E-19_wp

REAL (wp), PARAMETER :: hbar = 1.05459E-27_wp

REAL (wp), PARAMETER :: oneev = 1.60219E-12_wp

REAL (wp), PARAMETER :: pi = 3.14159265358979E0_wp

! .. Intrinsic Functions ..

! INTRINSIC kind

END MODULE scondo_consts

G.22 scondo_control.f90

! The control module allows sharing of different control parameters
! which are read in via the name-list facility. The object here is
! to have a fully configurable program without recompilation

```
MODULE scondo_control

    LOGICAL :: include_non_static
    LOGICAL :: include_spin
    LOGICAL :: include_static_vertex

    LOGICAL :: write_static_polar
    LOGICAL :: write_ns_polar
    LOGICAL :: write_static_greens
    LOGICAL :: write_ns_greens
    LOGICAL :: write_epsilon

    CHARACTER(80) :: diagfile
    CHARACTER(80) :: dosfile
    CHARACTER(80) :: elevelfile
    CHARACTER(80) :: ewidthfile
    CHARACTER(80) :: greensfile
    CHARACTER(80) :: specfile
    CHARACTER(80) :: staticpolarfile

    CHARACTER(80) :: epsilonfile
    CHARACTER(80) :: nsgreensfile
    CHARACTER(80) :: nsspecfile
    CHARACTER(80) :: nspolarfile

END MODULE scondo_control
```

G.23 scondo_interfaces.f90

```
MODULE scondo_interfaces
  INTERFACE
    SUBROUTINE densos(dstat,grnfi,nepts,nllev)
      USE scondo_consts
      REAL (wp), DIMENSION(:), INTENT(OUT) :: dstat
      REAL (wp), DIMENSION(:,:,:),INTENT (IN) :: grnfi
      INTEGER, INTENT(IN) :: nepts, nllev
    END SUBROUTINE densos
  END INTERFACE

  INTERFACE
    SUBROUTINE besstab(bessval,nqpts,qsize)
      USE scondo_consts
      REAL (wp), DIMENSION(:,:), INTENT(OUT) :: bessval
      INTEGER, INTENT(IN) :: nqpts
      REAL (wp), INTENT(IN) :: qsize
    END SUBROUTINE besstab
  END INTERFACE

  INTERFACE
    SUBROUTINE selfenergy2(oqgamma,selfr,selfi,nsr,nsi,nepts, &
      nllev,esize,eoff,hgmub)
      USE scondo_consts
      REAL (wp), DIMENSION(:,:), INTENT(IN) :: oqgamma
      REAL (wp), DIMENSION(:,:,:), INTENT(IN OUT) :: selfr, selfi
      REAL (wp), DIMENSION(:,:,:), INTENT(IN) :: nsr, nsi
      INTEGER, INTENT(IN) :: nepts
      INTEGER, INTENT(IN) :: nllev
      REAL (wp), INTENT(IN) :: esize,eoff,hgmub
    END SUBROUTINE selfenergy2
  END INTERFACE

  INTERFACE
    SUBROUTINE selfenergy(oqgamma,selfr,selfi,nepts,nllev, &
      esize,eoff,hgmub)
      USE scondo_consts
      REAL (wp), DIMENSION(:,:), INTENT(IN) :: oqgamma
      REAL (wp), DIMENSION(:,:,:), INTENT(IN OUT) :: selfr, selfi
      INTEGER, INTENT(IN) :: nepts
      INTEGER, INTENT(IN) :: nllev
    END SUBROUTINE selfenergy
  END INTERFACE
```

```

    REAL (wp), INTENT(IN) :: esize,eoff,hgmub
  END SUBROUTINE selfenergy
END INTERFACE

```

```

INTERFACE

```

```

  FUNCTION greens(ngr,ngi,grnfr,grnfi,selfr,selfi, &
                 nepts,eoff,esize,nllev,hgmub)

```

```

    USE scondo_consts

```

```

    REAL (wp), DIMENSION(:,:,:), INTENT(OUT) :: ngr, ngi

```

```

    REAL (wp), DIMENSION(:,:,:), INTENT(IN)  :: grnfr, grnfi

```

```

    REAL (wp), DIMENSION(:,:,:), INTENT(IN)  :: selfr, selfi

```

```

    INTEGER, INTENT(IN) :: nepts

```

```

    REAL (wp), INTENT(IN) :: esize,eoff

```

```

    INTEGER, INTENT(IN) :: nllev

```

```

    REAL (wp), INTENT(IN) :: hgmub

```

```

    REAL (wp) :: greens

```

```

  END FUNCTION greens

```

```

END INTERFACE

```

```

INTERFACE

```

```

  FUNCTION greens2(ngr,ngi,grnfr,grnfi,selfr,selfi, nsr, nsi, &
                  nepts,eoff,esize,nllev,hgmub)

```

```

    USE scondo_consts

```

```

    REAL (wp), DIMENSION(:,:,:), INTENT(OUT) :: ngr, ngi

```

```

    REAL (wp), DIMENSION(:,:,:), INTENT(IN)  :: grnfr, grnfi

```

```

    REAL (wp), DIMENSION(:,:,:), INTENT(IN)  :: selfr, selfi

```

```

    REAL (wp), DIMENSION(:,:,:), INTENT(IN)  :: nsr, nsi

```

```

    INTEGER, INTENT(IN) :: nepts

```

```

    REAL (wp), INTENT(IN) :: esize,eoff

```

```

    INTEGER, INTENT(IN) :: nllev

```

```

    REAL (wp), INTENT(IN) :: hgmub

```

```

    REAL (wp) :: greens

```

```

  END FUNCTION greens2

```

```

END INTERFACE

```

```

INTERFACE

```

```

  SUBROUTINE mix(ngr,ngi,grnfr,grnfi,nepts,nllev,adfacs)

```

```

    USE scondo_consts

```

```

    REAL (wp), DIMENSION(:,:,:), INTENT(IN)  :: ngr, ngi

```

```

    REAL (wp), DIMENSION(:,:,:), INTENT(IN OUT) :: grnfr, grnfi

```

```

    INTEGER, INTENT(IN) :: nepts, nllev

```

```

    REAL (wp), INTENT(IN) :: adfacs

```

```
END SUBROUTINE
END INTERFACE
```

```
INTERFACE
```

```
FUNCTION chempot(dstat,nepts,esize,ns,beta)
  USE scond_consts
  REAL (wp), DIMENSION(:), INTENT(IN) :: dstat
  INTEGER, INTENT(IN) :: nepts
  REAL (wp), INTENT(IN) :: esize,ns,beta
  REAL (wp) :: chempot
END FUNCTION chempot
END INTERFACE
```

```
INTERFACE
```

```
FUNCTION polarize(grnfr,grnfi,pjelem,bigpi,newbpi,nllev, &
  fermieng,nqpts,nepts,qsize,esize,beta)
  USE scond_consts
  REAL (wp), DIMENSION(:,:,:), INTENT(IN) :: grnfr, grnfi
  REAL (wp), DIMENSION(:,:,:), INTENT(IN) :: pjelem
  REAL (wp), DIMENSION(:), INTENT(IN OUT) :: bigpi
  REAL (wp), DIMENSION(:), INTENT(IN OUT) :: newbpi
  INTEGER, INTENT(IN) :: nllev
  REAL (wp), INTENT(IN) :: fermieng
  INTEGER, INTENT(IN) :: nqpts,nepts
  REAL (wp), INTENT(IN) :: qsize,esize,beta
  REAL (wp) :: polarize
END FUNCTION polarize
END INTERFACE
```

```
INTERFACE
```

```
FUNCTION vertpol(bw,grnfr,grnfi,pjelem,bigpi,newbpi,nllev, &
  fermieng,nqpts,nepts,qsize,esize,beta)
  USE scond_consts
  REAL (wp), DIMENSION(:,:,:), INTENT(IN) :: bw
  REAL (wp), DIMENSION(:,:,:), INTENT(IN) :: grnfr, grnfi
  REAL (wp), DIMENSION(:,:,:), INTENT(IN) :: pjelem
  REAL (wp), DIMENSION(:), INTENT(IN OUT) :: bigpi
  REAL (wp), DIMENSION(:), INTENT(IN OUT) :: newbpi
  INTEGER, INTENT(IN) :: nllev
  REAL (wp), INTENT(IN) :: fermieng
  INTEGER, INTENT(IN) :: nqpts,nepts
  REAL (wp), INTENT(IN) :: qsize,esize,beta
```

```
    REAL (wp) :: polarize
  END FUNCTION vertpol
END INTERFACE
```

```
INTERFACE
  SUBROUTINE jeltab(pjelem,nqpts,qsize,nllev)
    USE scond_constants
    REAL (wp), DIMENSION(:,:,:), INTENT(OUT) :: pjelem
    INTEGER, INTENT(IN) :: nqpts
    REAL (wp), INTENT(IN) :: qsize
    INTEGER, INTENT(IN) :: nllev
  END SUBROUTINE jeltab
END INTERFACE
```

```
INTERFACE
  SUBROUTINE llcouple(oqgamma,pjelem,upotsq,nqpts,qsize,nllev,nimp)
    USE scond_constants
    REAL (wp), DIMENSION(:,:), INTENT(OUT) :: oqgamma
    REAL (wp), DIMENSION(:,:,:), INTENT(OUT) :: pjelem
    REAL (wp), DIMENSION(:), INTENT(IN) :: upotsq
    INTEGER, INTENT(IN) :: nqpts
    REAL (wp), INTENT(IN) :: qsize
    INTEGER, INTENT(IN) :: nllev
    REAL (wp), INTENT(IN) :: nimp
  END SUBROUTINE llcouple
END INTERFACE
```

```
INTERFACE
  SUBROUTINE fourpot(bigpi,upot,upotsq,aimp,nqpts,qsize,dieconst, &
    esqr,tfflag,tfcnst)
    USE scond_constants
    REAL (wp), DIMENSION(:), INTENT(IN OUT) :: bigpi
    REAL (wp), DIMENSION(:), INTENT(OUT) :: upot,upotsq
    REAL (wp), INTENT(IN) :: aimp
    INTEGER, INTENT(IN) :: nqpts
    REAL (wp), INTENT(IN) :: qsize,dieconst,esqr
    INTEGER, INTENT(IN) :: tfflag
    REAL (wp), INTENT(IN) :: tfcnst
  END SUBROUTINE fourpot
END INTERFACE
```

```
INTERFACE
```

```

SUBROUTINE pmix(bigpi,newbpi,nqpts,adfacs)
  USE scondo_consts
  REAL (wp), DIMENSION(:), INTENT(IN OUT) :: bigpi
  REAL (wp), DIMENSION(:), INTENT(IN) :: newbpi
  INTEGER, INTENT(IN) :: nqpts
  REAL (wp), INTENT(IN) :: adfacs
END SUBROUTINE pmix
END INTERFACE

INTERFACE
  FUNCTION refineef(oqgamma,ef,nllev,esize,eoff,hgmub)
    USE scondo_consts
    REAL (wp), DIMENSION(:,:), INTENT(IN) :: oqgamma
    REAL (wp), INTENT(IN) :: ef
    INTEGER, INTENT(IN) :: nllev
    REAL (wp), INTENT(IN) :: eoff,esize,hgmub
    REAL (wp) :: refineef
  END FUNCTION refineef
END INTERFACE

INTERFACE
  SUBROUTINE findwdth(grnfi,magfield,esize,nepts,nllev)
    USE scondo_consts
    REAL (wp), DIMENSION(:,:,:), INTENT(IN) :: grnfi
    REAL (wp), INTENT(IN) :: magfield,esize
    INTEGER, INTENT(IN) :: nepts,nllev
  END SUBROUTINE findwdth
END INTERFACE

INTERFACE
  SUBROUTINE greng(grnfr,grnfi,esize,eoff,nepts,nllev,magfield)
    USE scondo_consts
    REAL (wp), DIMENSION(:,:,:), INTENT(IN) :: grnfr,grnfi
    REAL (wp), INTENT(IN) :: esize,eoff
    INTEGER, INTENT(IN) :: nepts,nllev
    REAL (wp), INTENT(IN) :: magfield
  END SUBROUTINE greng
END INTERFACE

INTERFACE
  SUBROUTINE geneps(epsr,epsi,grnfr,grnfi,pjelem,nllev, &

```

```

                                nqpts,nepts,qsize,esize,fermieng,beta, &
                                esqr,dieconst)
    USE scondo_consts
    REAL (wp), DIMENSION(:,,:),INTENT(OUT) :: epsr,epsi
    REAL (wp), DIMENSION(:,,,:),INTENT(IN) :: grnfi, grnfr
    REAL (wp), DIMENSION(:,,,:),INTENT(IN) :: pjelem
    INTEGER :: nepts, nllev, nqpts
    REAL (wp) :: qsize, esize, beta, fermieng, esqr, dieconst
END SUBROUTINE genepts
END INTERFACE

INTERFACE
    SUBROUTINE selfe_corr(grnfr,grnfi,selfr,selfi,nsr,nsi,epsi, &
                        epsr,pjelem,nepts,nqpts,nllev,qsize, &
                        esize,fermieng,beta,esqr, &
                        dieconst,eoff,hgmub)

    USE scondo_consts
    REAL (wp), DIMENSION(:,,,:),INTENT(IN) :: grnfi, grnfr
    REAL (wp), DIMENSION(:,,,:),INTENT(OUT) :: selfr, selfi
    REAL (wp), DIMENSION(:,,,:),INTENT(OUT) :: nsr, nsi
    REAL (wp), DIMENSION(:,,:),INTENT(IN) :: epsr,epsi
    REAL (wp), DIMENSION(:,,,:),INTENT(IN) :: pjelem
    INTEGER :: nepts, nllev, nqpts
    REAL (wp) :: qsize, esize, fermieng, beta, esqr, &
                dieconst, eoff, hgmub
END SUBROUTINE selfe_corr
END INTERFACE

INTERFACE
    SUBROUTINE bigw(bessval,bw,upotsq,pjelem,nqpts,qsize,nllev,nimp)
    USE scondo_consts
    REAL (wp), DIMENSION (:,:), INTENT(IN) :: bessval
    REAL (wp), DIMENSION (:,,:,:), INTENT(OUT) :: bw
    REAL (wp), DIMENSION (:), INTENT(IN) :: upotsq
    REAL (wp), DIMENSION (:,,:,:), INTENT(IN) :: pjelem
    INTEGER, INTENT(IN) :: nqpts
    REAL (wp), INTENT(IN) :: qsize
    INTEGER, INTENT(IN) :: nllev
    REAL (wp), INTENT(IN) :: nimp
END SUBROUTINE bigw
END INTERFACE

```

END MODULE scondo_interfaces

G.24 scondo_spin.f90

! Handles the uniform treatment of spin

```
MODULE scondo_spin
  USE scondo_consts

  REAL (wp) :: gs = 1E0_wp
  INTEGER :: spinstates

END MODULE scondo_spin
```

G.25 selfe_corr.f90

! A subroutine to calculate the electron-electron
! self energy correction

```
      SUBROUTINE selfe_corr(grnfr,grnfi,selfr,selfi,nsr,nsi,epsi, &
                           epsr,pjelem,nepts,nqpts,nllev,qsize, &
                           esize,fermieng,beta,esqr, &
                           dieconst,eoff,hgmub)
! ..
      USE scondo_consts
      USE scondo_control
      USE scondo_spin
! ..
! .. Scalar Arguments ..
      REAL (wp) :: beta, esize, fermieng, qsize, esqr, &
                 dieconst, eoff, hgmub
      INTEGER :: nepts, nllev, nqpts
! ...
! .. Array Arguments ..
      REAL (wp), DIMENSION(:,:,:),INTENT(IN) :: grnfi, grnfr
      REAL (wp), DIMENSION(:,:,:),INTENT(IN) :: selfr, selfi
      REAL (wp),DIMENSION(:,:,:), INTENT(OUT) :: nsr,nsi
      REAL (wp), DIMENSION(:,:,:),INTENT(IN) :: pjelem
      REAL (wp), DIMENSION(:,:),INTENT(IN) :: epsr,epsi
! ..
! .. Local Scalars ..
      REAL (wp) :: cksum, e, fact, mnq, nv1, nv2, q, sum, sum2, f
      REAL (wp) :: srule
      INTEGER :: i, j, k, l, nmax, nmaxb,sp
! ..
! .. Local Arrays ..
      REAL (wp) :: bot(nepts), frmi(nepts), bose(nepts), nbose(nepts)
      REAL (wp) :: dnmr(nepts), dnmi(nepts)
      REAL (wp) :: chi(nllev,nllev),xnt(nllev,spinstates), &
                 xchg(nllev,spinstates)
      REAL (wp) :: kr(nepts,nllev,nllev),ki(nepts,nllev,nllev)
      REAL (wp) :: spen(spinstates)
! ..
! .. Intrinsic Functions ..
      INTRINSIC exp, float, int, min, sqrt
! ..
```

```

PRINT *, "Entering New Self"
! Generate Fermi distribution
  nmax = min(nepts,int(((80E0_wp/beta)+fermieng)/esize))
  DO i = 1, nmax
    e = float(i-1)*esize - fermieng
    frmi(i) = 1E0_wp/(exp(beta*e)+1E0_wp)
  END DO
  DO i = nmax + 1, nepts
    frmi(i) = 0E0_wp
  END DO

! Generate Bose distribution
  nmaxb = min(nepts,int(((80E0_wp/beta))/esize))
  bose(1)=0E0_wp !fix for bad point at zero
  DO i = 2, nmaxb
    e = float(i-1)*esize
    bose(i) = 1E0_wp/(exp(beta*e)-1E0_wp)
  END DO
  DO i = nmaxb + 1, nepts
    bose(i) = 0E0_wp
  END DO

! Generate Negative Bose distribution
  nbose(1)=0E0_wp !fix for bad point at zero
  DO i = 2, nmaxb
    e = float(i-1)*esize
    nbose(i) = 1E0_wp/(exp(-beta*e)-1E0_wp)
  END DO
  DO i = nmaxb + 1, nepts
    nbose(i) = -1E0_wp
  END DO

!Now calculate the Self Energy Correction

  IF (spinstates == 2) THEN
    spen(1) = -hgmub
    spen(2) = hgmub
  ELSE
    spen = 0E0_wp
  END IF

```

```

! Create the complex entity K(x) where
!  $K_{NN_2}(x) = \int_0^{\infty} dq q$ 
!  $* |M_{NN_2}|^2 * V_e(q) / \epsilon(x,q)$ 

PRINT *, 'Calculating K s - step 1'
      kr(1:nepts,1:nllev,1:nllev)=OE0_wp
      ki(1:nepts,1:nllev,1:nllev)=OE0_wp

! Note that  $q * V_e(q) = \text{const}$ 

PRINT *, 'Calculating K s - step 2'
      DO j=1,nqpts
!MIC$ DO ALL shared(nllev,nepts,pjelem,epsr,epsi,kr,ki,j)
!MIC$1      private(1,k)
            DO l=1,nllev
            DO k=1,nllev
              kr(1:nepts,k,l)=kr(1:nepts,k,l) &
                + pjelem(j,k,l)*pjelem(j,k,l)*epsr(1:nepts,j)
              ki(1:nepts,k,l)=ki(1:nepts,k,l) &
                + pjelem(j,k,l)*pjelem(j,k,l)*epsi(1:nepts,j)
            END DO !k
            END DO !l
          END DO !j

PRINT *, 'Calculating New selfenergy'
      nsr(1:nepts,1:nllev,1:spinstates)=OE0_wp
      nsi(1:nepts,1:nllev,1:spinstates)=OE0_wp

PRINT *, 'Calculating New selfenergy stage 2'
! This is the positive energy interaction
      DO l=1,nllev
        DO j=1,nepts
          DO sp=1,spinstates
!MIC$ DO ALL shared(nllev,nepts,frmi,sp,j,l,nsi,frmi,grnfi,ki)
!MIC$1      private(k,i)
              DO k=1,nllev
                DO i=j+1,nepts
!
                  nsr(i,k,sp)=nsr(i,k,sp)+(1E0_wp-frmi(j)) &
                    *grnfi(j,l,sp)*kr(i-j+1,k,l)
                  nsi(i,k,sp)=nsi(i,k,sp)+(1E0_wp-frmi(j)) &

```

```

                                *grnfi(j,l,sp)*ki(i-j+1,k,l)
        END DO !i
        END DO !k
    END DO !sp
    END DO !j
END DO !l

PRINT *, 'Calculating New selfenergy stage 3'
DO l=1,nllev
    DO j=0,nepts-1
        DO sp=1,spinstates
!MIC$ DO ALL shared (nllev,nepts,nsr,nsi,bose,grnfr,grnfi,ki,sp,j,l)
!MIC$1     private (k,i)
            DO k=1,nllev
                DO i=j+1,nepts
!                    nsr(i,k,sp)=nsr(i,k,sp)+ &
!                        bose(j+1)*grnfr(i-j,l,sp)*ki(j+1,k,l)
                    nsi(i,k,sp)=nsi(i,k,sp)+ &
                        bose(j+1)*grnfi(i-j,l,sp)*ki(j+1,k,l)
                END DO !i
            END DO !k
        END DO !sp
    END DO !j
END DO !l

! This is the negative energy interaction
PRINT *, 'Calculating New selfenergy stage 4'
DO l=1,nllev
    DO j=1,nepts
        DO sp=1,spinstates
!MIC$ DO ALL shared(nllev,nepts,nsi,frmi,grnfi,ki,sp,j,l)
!MIC$1     private(k,i)
            DO k=1,nllev
                DO i=1,j
!                    nsr(i,k,sp)=nsr(i,k,sp) &
!                        +(1EO_wp-frmi(j))*grnfi(j,l,sp)*kr(i-j+1,k,l)
                    nsi(i,k,sp)=nsi(i,k,sp) &
                        -(1EO_wp-frmi(j))*grnfi(j,l,sp)*ki(j-i+1,k,l)
                END DO !i
            END DO !k
        END DO !sp
    END DO !j

```

```

        END DO !l

PRINT *, 'Calculating New selfenergy stage 5'
      DO l=1,nllev
        DO j=1,nepts-1
          DO sp=1,spinstates
!MIC$ DO ALL shared(nllev,nepts,nsr,nsi,nbose,grnfr,grnfi,ki,sp,j,l)
!MIC$1      private(k,i)
            DO k=1,nllev
              DO i=1,nepts-j
!              nsr(i,k,sp)=nsr(i,k,sp) &
!              -nbose(j+1)*grnfr(i+j,l,sp)*ki(j+1,k,l)
              nsi(i,k,sp)=nsi(i,k,sp) &
              -nbose(j+1)*grnfi(i+j,l,sp)*ki(j+1,k,l)
            END DO !i
          END DO !k
        END DO !sp
      END DO !j
    END DO !l

PRINT *, 'Calculating New selfenergy stage 6'
      fact=-esqr*qsize*esize/(dieconst*pi)

!      nsr(1:nepts,1:nllev,1:spinstates)= &
!      nsr(1:nepts,1:nllev,1:spinstates)*fact
      nsi(1:nepts,1:nllev,1:spinstates)= &
      nsi(1:nepts,1:nllev,1:spinstates)*fact

! Do a Kramers-Kronig on the self-energy -- what an improvement
      nsr=0.0_wp
      DO sp=1,spinstates
        DO k=1,nllev
          DO i=1,nepts
            DO j=1,i-1
              nsr(j,k,sp) = nsr(j,k,sp)+nsi(i,k,sp)/float(j-i)
            END DO
          DO j=i+1,nepts
            nsr(j,k,sp) = nsr(j,k,sp)+nsi(i,k,sp)/float(j-i)
          END DO
        END DO
      END DO
    END DO
  END DO

```

```

nsr= -nsr/pi

! This is the Exchange term
PRINT *, 'Calculating Exchange part of new selfenergy'
chi(1:nllev,1:nllev)=OE0_wp

DO j=1,nqpts
  DO k=1,nllev
    DO l=1,nllev
      chi(k,l)=chi(k,l)+pjelem(j,k,l)*pjelem(j,k,l)
    END DO
  END DO
END DO

xnt(1:nllev,1:spinstates)=OE0_wp
DO i=1,nepts
  DO sp=1,spinstates
    DO k=1,nllev
      xnt(k,sp)=xnt(k,sp)+frmi(i)*grnfi(i,k,sp)
    END DO !k
  END DO !sp
END DO !i

xchg(1:nllev,1:spinstates)=OE0_wp
DO sp=1,spinstates
  DO l=1,nllev
    xchg(1:nllev,sp)=xchg(1:nllev,sp)+chi(1:nllev,l)*xnt(l,sp)
  END DO !l
END DO !sp

fact=esqr*esize*qsize/(dieconst*pi)
xchg(1:nllev,1:spinstates)=xchg(1:nllev,1:spinstates)*fact

!Temporary
DO k=1,nllev
  IF (spinstates == 2) THEN
    PRINT *,k,xchg(k,1),xchg(k,2)
  ELSE
    PRINT *,k,xchg(k,1)
  END IF
END DO

```

```

! Add the exchange energy to the self energy correction
!MIC$ DO ALL AUTOSCOPE
  DO sp=1,spinstates
  DO k=1,nllev
    nsr(1:nepts,k,sp)=nsr(1:nepts,k,sp)+xchg(k,sp)
  END DO !k
  END DO !sp

  IF (1==0) THEN
PRINT *, 'Writing New selfenergy'
OPEN(unit=80,file='newself.x',status='unknown')
DO k=1,nllev
DO sp=1,spinstates
  DO i=1,nepts
    write(80,'(i3, e12.4, e12.4, e12.4)') k, &
      float(i-1)*esize, &
      nsr(i,k,sp), nsi(i,k,sp)

  END DO !i
END DO !sp
END DO !k
close(80)
END IF

PRINT *, "Exiting New Self"

RETURN
END SUBROUTINE selfe_corr

```

G.26 selfener.f90

```
! A subroutine to calculate the self energy

      SUBROUTINE selfenergy(oqgamma,selfr,selfi,nepts,nllev, &
                           esize,eoff,hgmub)
! ..
      USE scondo_consts
      USE scondo_spin
! ..
! .. Scalar Arguments ..
      REAL (wp), INTENT(IN) :: eoff, esize, hgmub
      INTEGER, INTENT(IN) :: nepts, nllev
! ..
! .. Array Arguments ..
      REAL (wp), INTENT(IN) :: oqgamma(:, :)
      REAL (wp), INTENT(IN OUT) :: selfi(:, :, :), selfr(:, :, :)
! ..
! .. Local Scalars ..
      REAL (wp) :: bis, brs, diff, e, keval, xtol
      INTEGER :: i, it, j, k, maxit, n, sp
! ..
! .. Local Arrays ..
      REAL (wp) :: bot(nllev,spinstates), br(nllev,spinstates), &
                  fbi(nepts,nllev,spinstates), &
                  fbot(nepts,nllev,spinstates), &
                  fbr(nepts,nllev,spinstates), &
                  fsli(nepts,nllev,spinstates), &
                  fslr(nepts,nllev,spinstates), &
                  sli(nllev,spinstates), slr(nllev,spinstates)
      REAL (wp) :: spen(spinstates)
! ..
! .. Intrinsic Functions ..
      INTRINSIC float
! ..
      xtol = 1E-14_wp
      maxit = 40000

      IF (spinstates == 2) THEN
         spen(1) = -hgmub
         spen(2) = hgmub
      ELSE
```

```

    spen = 0EO_wp
END IF

! Set the upper limit small for machines like workstations
! and about 80 for the Cray J90
DO n = 1, 40
    fslr(1:nepts,1:nllev,1:spinstates) = 0EO_wp
    fsli(1:nepts,1:nllev,1:spinstates) = -1E-5_wp

    DO sp = 1, spinstates
    DO j = 1, nllev
        keval = eoff + float(j) + spen(sp)
        DO i = 1, nepts
            fbr(i,j,sp) = float(i-1)*esize - keval - selfr(i,j,sp)
            fbot(i,j,sp) = 1EO_wp/(fbr(i,j,sp)*fbr(i,j,sp) &
                +selfi(i,j,sp)*selfi(i,j,sp))

            END DO !i
        END DO !j
    END DO !sp
    fbr(1:nepts,1:nllev,1:spinstates) = &
        fbr(1:nepts,1:nllev,1:spinstates) &
        *fbot(1:nepts,1:nllev,1:spinstates)
    fbi(1:nepts,1:nllev,1:spinstates) = &
        selfi(1:nepts,1:nllev,1:spinstates) &
        *fbot(1:nepts,1:nllev,1:spinstates)

    DO sp = 1, spinstates
    DO k = 1, nllev
        DO j = 1, nllev
            fslr(1:nepts,j,sp) = fslr(1:nepts,j,sp) &
                + oqgamma(j,k)*fbr(1:nepts,k,sp)
            fsli(1:nepts,j,sp) = fsli(1:nepts,j,sp) &
                + oqgamma(j,k)*fbi(1:nepts,k,sp)

            END DO !j
        END DO !k
    END DO !sp

    selfr(1:nepts,1:nllev,1:spinstates) = &
        0.8EO_wp*fslr(1:nepts,1:nllev,1:spinstates) + &
        0.2EO_wp*selfr(1:nepts,1:nllev,1:spinstates)
    selfi(1:nepts,1:nllev,1:spinstates) = &
        0.8EO_wp*fsli(1:nepts,1:nllev,1:spinstates) + &

```

0.2E0_wp*selfi(1:nepts,1:nllev,1:spinstates)

END DO

```
!MIC$ DO ALL
!MIC$1 SHARED(nepts,esize,eoff,oqgamma,selfr,selfi,
!MIC$2      maxit,nllev,xtol,spen,spinstates)
!MIC$3 PRIVATE(i,j,k,sp,keval,diff,it,br,bot,slr,sli,brs,bis,e)
  DO i = 1, nepts
    keval = float(i-1)*esize - eoff
    diff = 1E0_wp
    it = 1
    DO WHILE ((diff>=xtol) .AND. (it<=maxit))
      DO sp = 1, spinstates
        DO k = 1, nllev
          br(k,sp) = keval - float(k) - selfr(i,k,sp) - spen(sp)
          bot(k,sp) = 1E0_wp/(br(k,sp)*br(k,sp) &
            +selfi(i,k,sp)*selfi(i,k,sp))
          slr(k,sp) = 0E0_wp
          sli(k,sp) = -1E-5_wp
        END DO !k
      END DO !sp
      DO sp = 1, spinstates
        DO k = 1, nllev
          slr(1:nllev,sp) = slr(1:nllev,sp) &
            + oqgamma(1:nllev,k)*br(k,sp)*bot(k,sp)
          sli(1:nllev,sp) = sli(1:nllev,sp) &
            + oqgamma(1:nllev,k)*selfi(i,k,sp)*bot(k,sp)
        END DO !k
      END DO !sp

      diff = 0E0_wp
      DO sp = 1, spinstates
        DO j = 1, nllev
          brs = selfr(i,j,sp) - slr(j,sp)
          bis = selfi(i,j,sp) - sli(j,sp)
          diff = diff + brs*brs + bis*bis
          selfr(i,j,sp) = 0.8E0_wp*slr(j,sp) &
            + 0.2E0_wp*selfr(i,j,sp)
          selfi(i,j,sp) = 0.8E0_wp*sli(j,sp) &
```

```
                                + 0.2E0_wp*selfi(i,j,sp)
      END DO !j
      END DO !sp
      it = it + 1
    END DO
    IF (it>=maxit) THEN
      e = float(i-1)*esize
      PRINT *, 'Bad point at e=', e, diff
    END IF
  END DO

  RETURN
END SUBROUTINE selfenergy
```

G.27 selfener2.f90

```
! A subroutine to calculate the self energy
! In this case we are iterating including the non static part of the
! self energy.

      SUBROUTINE selfenergy2(oqgamma,selfr,selfi,nsr,nsi,nepts,nllev, &
                             esize,eoff,hgmub)
! ..
      USE scondo_consts
      USE scondo_spin
! ..
! .. Scalar Arguments ..
      REAL (wp), INTENT(IN) :: eoff, esize, hgmub
      INTEGER, INTENT(IN) :: nepts, nllev
! ..
! .. Array Arguments ..
      REAL (wp), INTENT(IN) :: oqgamma(:,,:)
      REAL (wp), INTENT(IN OUT) :: selfi(:,::,:), selfr(:,::,:)
      REAL (wp), INTENT(IN) :: nsi(:,::,:), nsr(:,::,:)
! ..
! .. Local Scalars ..
      REAL (wp) :: bis, brs, diff, e, keval, xtol
      INTEGER :: i, it, j, k, maxit, n, sp
! ..
! .. Local Arrays ..
      REAL (wp) :: bot(nllev,spinstates), br(nllev,spinstates), &
                  bi(nllev,spinstates), &
                  fbi(nepts,nllev,spinstates), &
                  fbot(nepts,nllev,spinstates), &
                  fbr(nepts,nllev,spinstates), &
                  fsli(nepts,nllev,spinstates), &
                  fslr(nepts,nllev,spinstates), &
                  sli(nllev,spinstates), slr(nllev,spinstates)
      REAL (wp) :: spen(spinstates)
! ..
! .. Intrinsic Functions ..
      INTRINSIC float
! ..
      xtol = 1E-14_wp
      maxit = 40000
```

```

    spen(1) = -hgmub
    spen(2) = hgmub

! Set the upper limit small for machines like workstations
! and about 80 for the Cray J90
DO n = 1, 40
    fslr(1:nepts,1:nllev,1:spinstates) = 0E0_wp
    fsli(1:nepts,1:nllev,1:spinstates) = -1E-5_wp

    DO sp = 1, spinstates
    DO j = 1, nllev
        keval = eoff + float(j) + spen(sp)
        DO i = 1, nepts
            fbr(i,j,sp) = float(i-1)*esize - keval &
                - selfr(i,j,sp) - nsr(i,j,sp)
            fbi(i,j,sp) = selfi(i,j,sp) + nsi(i,j,sp)
            fbot(i,j,sp) = 1E0_wp/(fbr(i,j,sp)*fbr(i,j,sp) &
                + fbi(i,j,sp)*fbi(i,j,sp))

            END DO !i
        END DO !j
    END DO !sp
    fbr(1:nepts,1:nllev,1:spinstates) = &
        fbr(1:nepts,1:nllev,1:spinstates) &
        *fbot(1:nepts,1:nllev,1:spinstates)
    fbi(1:nepts,1:nllev,1:spinstates) = &
        fbi(1:nepts,1:nllev,1:spinstates) &
        *fbot(1:nepts,1:nllev,1:spinstates)

    DO sp = 1, spinstates
    DO k = 1, nllev
        DO j = 1, nllev
            fslr(1:nepts,j,sp) = fslr(1:nepts,j,sp) &
                + oqgamma(j,k)*fbr(1:nepts,k,sp)
            fsli(1:nepts,j,sp) = fsli(1:nepts,j,sp) &
                + oqgamma(j,k)*fbi(1:nepts,k,sp)

            END DO !j
        END DO !k
    END DO !sp

    selfr(1:nepts,1:nllev,1:spinstates) = &
        0.8E0_wp*fslr(1:nepts,1:nllev,1:spinstates) + &
        0.2E0_wp*selfr(1:nepts,1:nllev,1:spinstates)

```

```

selfi(1:nepts,1:nllev,1:spinstates) = &
    0.8EO_wp*fsli(1:nepts,1:nllev,1:spinstates) + &
    0.2EO_wp*selfi(1:nepts,1:nllev,1:spinstates)

```

```

END DO

```

```

!MIC$ DO ALL
!MIC$1 SHARED(nepts,esize,eoff,oqgamma,selfr,selfi,
!MIC$2         maxit,nllev,xtol,spen,nsr,nsi,spinstates)
!MIC$3 PRIVATE(i,j,k,sp,keval,diff,it,br,bi,bot,slr,sli,brs,bis,e)
DO i = 1, nepts
    keval = float(i-1)*esize - eoff
    diff = 1EO_wp
    it = 1
DO WHILE ((diff>=xtol) .AND. (it<=maxit))
    DO sp = 1, spinstates
    DO k = 1, nllev
        br(k,sp) = keval - float(k) - selfr(i,k,sp) &
            - nsr(i,k,sp) - spen(sp)
        bi(k,sp) = selfi(i,k,sp) + nsi(i,k,sp)
        bot(k,sp) = 1EO_wp/(br(k,sp)*br(k,sp)+bi(k,sp)*bi(k,sp))
        slr(k,sp) = 0EO_wp
        sli(k,sp) = -1E-5_wp
    END DO !k
    END DO !sp
    DO sp = 1, spinstates
    DO k = 1, nllev
        slr(1:nllev,sp) = slr(1:nllev,sp) &
            + oqgamma(1:nllev,k)*br(k,sp)*bot(k,sp)
        sli(1:nllev,sp) = sli(1:nllev,sp) &
            + oqgamma(1:nllev,k)*bi(k,sp)*bot(k,sp)
    END DO !k
    END DO !sp

    diff = 0EO_wp
    DO sp = 1, spinstates
    DO j = 1, nllev
        brs = selfr(i,j,sp) - slr(j,sp)
        bis = selfi(i,j,sp) - sli(j,sp)
        diff = diff + brs*brs + bis*bis
        selfr(i,j,sp) = 0.8EO_wp*slr(j,sp) &

```

```
                + 0.2E0_wp*selfr(i,j,sp)
selfi(i,j,sp) = 0.8E0_wp*sli(j,sp) &
                + 0.2E0_wp*selfi(i,j,sp)
END DO !j
END DO !sp
it = it + 1
END DO
IF (it>=maxit) THEN
  e = float(i-1)*esize
  PRINT *, 'Bad point at e=', e, diff
END IF
END DO

RETURN
END SUBROUTINE selfenergy2
```

G.28 tauconst.f90

! A function to evaluate the integral which relates
! the quantum scattering time to the impurity density
! Using Thomas-Fermi

```
      FUNCTION tauconst(econc,dieconst,mfact,impdist)
! ..
      USE scondo_consts
! ..
! .. Function Return Value ..
      REAL (wp) :: tauconst
! ..
! .. Parameters ..
      REAL (wp), PARAMETER :: gss = 2E0_wp
! ..
! .. Scalar Arguments ..
      REAL (wp), INTENT(IN) :: dieconst, econc, impdist, mfact
! ..
! .. Local Scalars ..
      REAL (wp) :: bot, c1, c2, c3, c4, dx, f, kf, sn, sum, val, x
      INTEGER :: i, nsteps
! ..
! .. Intrinsic Functions ..
      INTRINSIC sqrt, exp, float, sin
! ..
      nsteps = 1000

      kf = sqrt(4.0E0_wp*pi*econc/gss)
      c1 = 4.0E0_wp*pi*hbar/(emass*mfact*gss*gss)
      c2 = -8.0E0_wp*kf*impdist
      c3 = 0.5E0_wp*dieconst*kf*hbar/echg
      c3 = c3*hbar/(emass*mfact*gss)/echg
      c4 = 1.0E0_wp
      dx = pi/float(nsteps)
      sum = 0.0E0_wp
      x = 0.0E0_wp
      f = 1.0E0_wp
      DO i = 1, nsteps
! f=1.0d0-cos(2.0E0_wp*x)
          sn = sin(x)
          bot = c3*sn + c4
```

```
    val = f*exp(c2*sn)/(bot*bot)
    sum = sum + val
    x = x + dx
END DO

tauconst = c1*sum*dx

RETURN
END FUNCTION tauconst
```

G.29 vertpol.f90

```
! A subroutine to calculate the Polarization
! This is with the vertex correction.

      FUNCTION vertpol(bw,grnfr,grnfi,pjelem,bigpi,newbpi,nllev, &
                     fermieng,nqpts,nepts,qsize,esize,beta)
! ..
      USE scondo_consts
      USE scondo_spin
! ..
! .. Function Return Value ..
      REAL (wp) :: vertpol
! ..
! .. Scalar Arguments ..
      REAL (wp), INTENT(IN) :: beta, esize, fermieng, qsize
      INTEGER, INTENT(IN) :: nepts, nllev, nqpts
! ..
! .. Array Arguments ..
      REAL (wp), INTENT(IN) :: bw(:,:,:)
      REAL (wp), INTENT(IN) :: grnfr(:,:,:), grnfi(:,:,:)
      REAL (wp), INTENT(IN OUT) :: bigpi(:), newbpi(:)
      REAL (wp), INTENT(IN) :: pjelem(:,:,:)
! ..
! .. Local Scalars ..
      REAL (wp) :: cksum, e, fact, mnq, nv1, nv2, q
      INTEGER :: i, j, k, l, nmax, sp
! ..
! .. Local Automatic Arrays ..
      REAL (wp) :: frmi(nepts)
      REAL (wp) :: br(nepts), bi(nepts)
      REAL (wp) :: g2r(nepts), g2i(nepts)
      REAL (wp) :: bot(nepts),res(nepts)
! ..
! .. Intrinsic Functions ..
      INTRINSIC exp, float, int, min, sqrt, sum
! ..
! Generate Fermi distribution
      nmax = min(nepts,int(((80E0_wp/beta)+fermieng)/esize))
      DO i = 1, nmax
         e = float(i-1)*esize - fermieng
         frmi(i) = 1E0_wp/(exp(beta*e)+1E0_wp)
```

```

END DO
DO i = nmax + 1, nepts
  frmi(i) = OEO_wp
END DO

fact = -gs*esize/(pi*pi)

newbpi(1:nqpts)=OEO_wp

!MIC$ DO ALL
!MIC$1 shared(nqpts,nllev,nepts,newbpi,bw,grnfr,grnfi,pjelem,
!MIC$2      frmi,nmax,spinstates)
!MIC$3      private(i,j,k,l,sp,g2r,g2i,br,bi,bot,res)
  DO i = 1, nqpts
    DO sp = 1, spinstates
      DO k = 1, nllev
        DO l = 1, nllev
! Cut Integral at nmax to save time
          g2r(1:nmax) = grnfr(1:nmax,k,sp)*grnfr(1:nmax,l,sp) &
                     - grnfi(1:nmax,k,sp)*grnfi(1:nmax,l,sp)
          g2i(1:nmax) = grnfr(1:nmax,k,sp)*grnfi(1:nmax,l,sp) &
                     + grnfr(1:nmax,l,sp)*grnfi(1:nmax,k,sp)
          br(1:nmax) = 1.OEO_wp - bw(i,k,l)*g2r(1:nmax)
          bi(1:nmax) = -bw(i,k,l)*g2i(1:nmax)
          bot(1:nmax) = br(1:nmax)*br(1:nmax) &
                     +bi(1:nmax)*bi(1:nmax)
          res(1:nmax) = (br(1:nmax)*grnfr(1:nmax,k,sp) &
                       +bi(1:nmax)*grnfi(1:nmax,k,sp)) &
                       *grnfi(1:nmax,l,sp)*frmi(1:nmax)/bot(1:nmax)

          newbpi(i) = newbpi(i) + pjelem(i,k,l) &
                     *pjelem(i,k,l)*sum(res(1:nmax))

          END DO !l
        END DO !k
      END DO !sp
    END DO !i

newbpi(1:nqpts) = newbpi(1:nqpts)*fact

```

```
! Return convergence information
  cksum = OEO_wp
  nv1 = OEO_wp
  nv2 = OEO_wp
  DO i = 1, nqpts
    cksum=max(abs(newbpi(i)-bigpi(i)),cksum)
    nv1 = max(abs(bigpi(i)),nv1)
    nv2 = max(abs(newbpi(i)),nv2)
  END DO

  vertpol = cksum/sqrt(nv1*nv2)
  RETURN
END FUNCTION vertpol
```

G.30 Makefile

```
.SUFFIXES: .f90 .o

# Choose the compiler
FORT = f90 -e i
#FORT = f90

# Set the optimization
#OPT = -O -byte_kinds -ccargs '-O6 -funroll-all-loops'
#OPT = -O4 -tune host
OPT = -Oscalar3,vector3,task3,inline3 -dp
#OPT = -O5 -qarch host -qtune host

# Uncomment these for systems without the Bessel functions
#BESSF = besselj0.f90
#BESS0 = besselj0.o

SRC = $(BESSF) densos.f90 jelem.f90 main.f90 polarize.f90 \
besstab.f90 fourpot.f90 laguerre.f90 melem.f90 selfener.f90 \
chempot.f90 greens.f90 llcouple.f90 mix.f90 \
    tauconst.f90 pmix.f90 \
findener.f90 refineef.f90 findwidth.f90 \
    geneps.f90 selfe_corr.f90 selfener2.f90 greens2.f90 \
    vertpol.f90 bigw.f90

OBJ = $(BESS0) densos.o jelem.o main.o polarize.o besstab.o \
fourpot.o laguerre.o melem.o selfener.o \
chempot.o greens.o llcouple.o mix.o tauconst.o pmix.o \
findener.o refineef.o findwidth.o \
    geneps.o selfe_corr.o selfener2.o greens2.o \
    vertpol.o bigw.o

MOD = scondo_consts.o scondo_interfaces.o scondo_control.o \
scondo_spin.o

scondo: $(OBJ) $(MOD)
$(FORT) -o scondo $(OBJ) $(MOD)

scondo_consts.o: scondo_consts.f90
```

```
$(FORT) $(OPT) -c scondo_consts.f90

scondo_interfaces.o: scondo_interfaces.f90 scondo_consts.o
$(FORT) $(OPT) -c scondo_interfaces.f90

scondo_control.o: scondo_control.f90
$(FORT) $(OPT) -c scondo_control.f90

scondo_spin.o: scondo_spin.f90 scondo_consts.o
$(FORT) $(OPT) -c scondo_spin.f90

# -lperf
$(OBJ): scondo_consts.o scondo_spin.o

main.o: scondo_interfaces.o scondo_control.o scondo_spin.o

selfe_corr.o: scondo_control.o scondo_spin.o

.f90.o: $(SRC)
$(FORT) $(OPT) -c $<

clean:
rm $(OBJ) scondo $(MOD) *.mod

print-source:
enscript -Gr2 $(SRC)
```

G.31 runparam.in

```
&material
  dieconst=12.8,
  mfact=0.067,
  gstar=-0.44 /
&sample
  mobil=50000,
  econc=2.0e11,
  impdist=50e-8 /
&run
  temp=4.2,
  magfield=2.068e4,
  magstep=2.000e2,
  nbpts=1 /
&energy_mom
  esize=0.006,
  eoff=15.5,
  eupper=1,
  qsize=0.025,
  nepts=6000,
  nqpts=400,
  nllev=4 /
&converge
  ctol=1e-5,
  itmax=20,
  nsitmax=20 /
&calcctrl
  include_non_static=T,
  include_spin=T,
  include_static_vertex=F /
&writectl
  write_static_polar=F,
  write_ns_polar=F,
  write_static_greens=F,
  write_ns_greens=T,
  write_epsilon=T /
&files
  diagfile="diaout.x",
  dosfile="dosout.x",
  elevelfile="elvout.x",
  ewidthfile="wthout.x",
```

```
greensfile="grnout.x",  
specfile="spcout.x",  
staticpolarfile="bpiout.x",  
nsgreensfile="nsgrnout.x",  
nsspecfile="nsspcout.x",  
nspolarfile="nspolout.x",  
epsilonfile="epsout.x" /
```

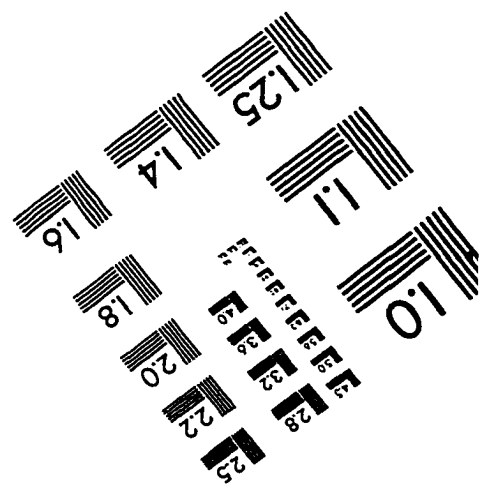
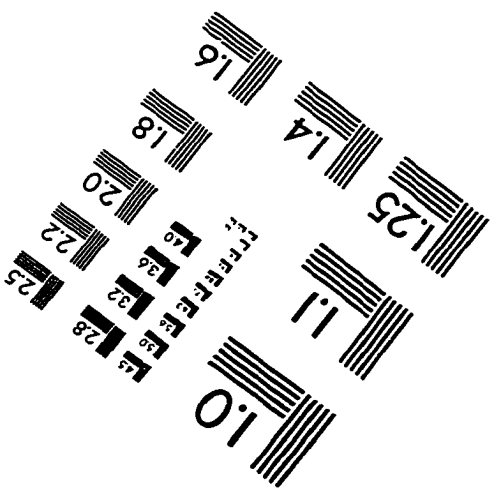
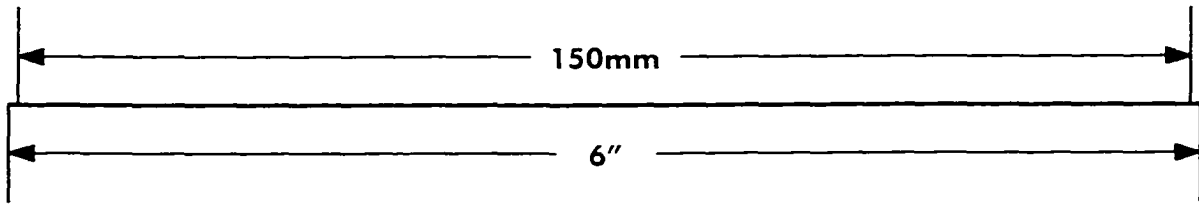
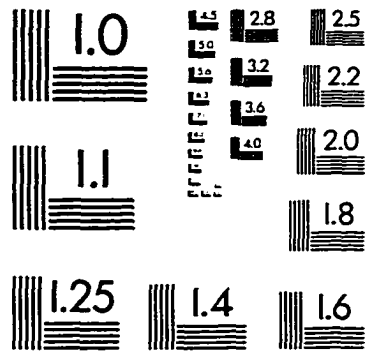
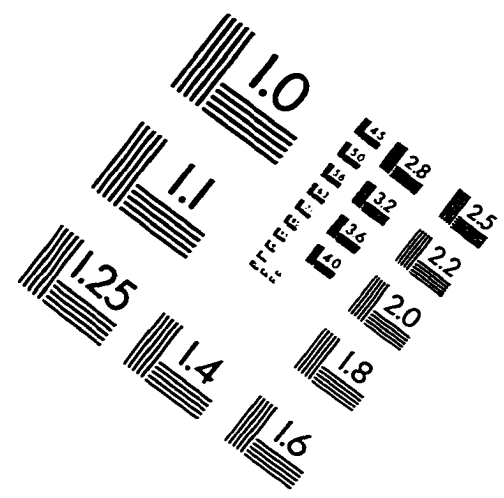
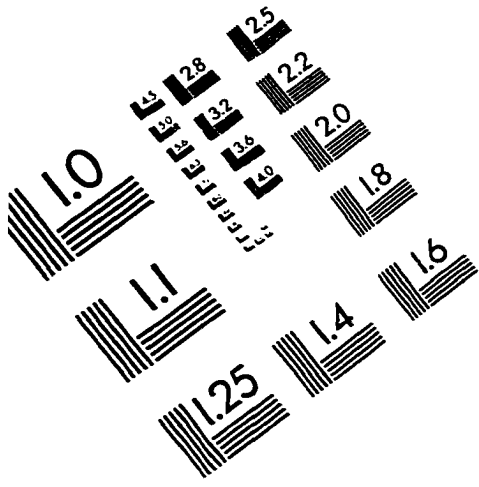
Reference List

- [1] Tsuneya Ando. Theory of quantum transport in a two-dimensional electron system under magnetic fields: Ii. single-site approximation under strong fields. *Journal of the Physical Society of Japan*. 36(6):1521–1529. June 1974.
- [2] Tsuneya Ando. Theory of quantum transport in a two-dimensional electron system under magnetic fields: Iii. many-site approximation. *Journal of the Physical Society of Japan*. 37(3):622–630. September 1974.
- [3] Tsuneya Ando. Theory of quantum transport in a two-dimensional electron system under magnetic fields: Iv. oscillatory conductivity. *Journal of the Physical Society of Japan*. 37(5):1233–1237. November 1974.
- [4] Tsuneya Ando, Alan B. Fowler, and Frank Stern. Electron properties of two-dimensional systems. *Reviews of Modern Physics*. 54(2):437–672. April 1982.
- [5] Tsuneya Ando, Yukio Matsumoto, and Yasutada Uemura. Theory of hall effect in a two-dimensional electron system. *Journal of the Physical Society of Japan*. 39(2):279–288. February 1975.
- [6] Tsuneya Ando and Yasutada Uemura. Theory of quantum transport in a two-dimensional electron system under magnetic fields: I. characteristics of level broadening and transport under strong fields. *Journal of the Physical Society of Japan*. 36(4):959–967. April 1974.
- [7] A. L. Efros, F. G. Pikus, and V. G. Burnett. Density of states of a two-dimensional electron gas in a long-range random potential. *Physical Review B*. 47(4):2233–2243. January 1993.

- [8] K. Ensslin, A. Wixforth, M. Sundaram, P. F. Hopkins, J. H. English, and A. C. Gossard. Single-particle subband spectroscopy in a parabolic quantum well via transport experiments. *Physical Review B*, 47(3):1366–1378, January 1993.
- [9] Vidar Gudmundsson and Juan José Palacios. Spin effects in a confined two-dimensional electron gas: Enhancement of the g factor, spin-inversion states, and their far-infrared absorption. *Physical Review B*, 52(15):11266–11272, October 1995.
- [10] R. J. Haug, K. v. Klitzing, and K. Ploog. Effect of exchange and correlation on the Fermi momenta of an electron liquid in a magnetic field. *Physical Review B*, 35(11):5933–5935, April 1987.
- [11] Akira Isihara and Ludvig Smrčka. Density and magnetic field dependences of the conductivity of two-dimensional electron systems. *J. Phys. C: Solid State Physics*, 19:6777–6789, May 1986.
- [12] A.H. MacDonald. Hartree-Fock approximation for response functions and collective excitations in a two-dimensional electron gas with filled Landau levels. *J. Phys. C: Solid State Physics*, 18:1003–1016, 1985.
- [13] Gerald D. Mahan. *Many-Particle Physics*. Plenum Press, New York, 1981.
- [14] N. H. March, W. H. Young, and S. Sampanthar. *The Many-Body Problem in Quantum Mechanics*. Cambridge University Press, 1967.
- [15] B. A. Mason. Personal communication.
- [16] K. Minakuchi and S. Hikami. Numerical study of localization in the two-state Landau level. *Physical Review B*, 53(16):10898–10905, April 1996.
- [17] G. Rickayzen. *Green's Functions and Condensed Matter*. Academic Press Limited, 1988.
- [18] D. G. Seiler. The Schubnikov-de Haas effect: A powerful tool for characterizing semiconductors. In G. Landwehr, editor, *Springer Series in Solid-State Sciences*, volume 87, pages 579–587. Springer-Verlag, 1989.

- [19] P. Skudlarski and G. Vignale. Effect of exchange and correlation on the fermi momenta of and electron liquid in a magnetic field. *Physical Review Letters*. 69(6):10898–10905. August 1992.
- [20] A. P. Smith, A. H. MacDonald, and G. Gumbs. Quasiparticle effective mass and enhanced g factor for a two-dimensional electron gas at intermediate magnetic fields. *Physical Review B*. 45(15):8829–8832. April 1992.
- [21] Frank Stern. Polarizability of a two-dimensional electron gas. *Physical Review Letters*. 18(14):546–548. April 1967.
- [22] B. Vinter. Many-body effects in n-type si inversion layers. i. effects in the lowest subband. *Physical Review B*. 13(10):4447–4456. May 1976.
- [23] L. Wendler and R. Pechstedt. Dynamical screenin, collective excitations, and electron-phonon interaction in heterostructures and semiconductor quantum wells. *Phys. Stat. Sol. (b)*. 138:197–217. April 1986.
- [24] X. C. Xie, Q. P. Li, and S. Das Sarma. Density of states and thermodynamic properties of a two-dimensional electron gas in a strong magnetic field. *Physical Review B*. 42(11):7132–7147, October 1990.
- [25] W. Xu and P. Vasilopoulos. Self-consistent density of states for heterostructures in strong magnetic fields. *Physical Review B*. 51(3):1694–1702. January 1995.

IMAGE EVALUATION TEST TARGET (QA-3)



APPLIED IMAGE . Inc
 1653 East Main Street
 Rochester, NY 14609 USA
 Phone: 716/482-0300
 Fax: 716/288-5989

© 1993, Applied Image, Inc., All Rights Reserved